THE HETEROGENEOUSLY CATALYSED SELECTIVE OXIDATION OF N-BUTANE TO MALEIC ANHYDRIDE.

by

Michael John Davies, B.Sc.

November, 1989

A thesis submitted for the degree of Doctor of Philosophy of the University of London.

Department of Chemical Engineering and Chemical Technology
Imperial College of Science, Technology and Medicine
London, SW7

ABSTRACT

The selective oxidation of n-butane to maleic anhydride was chosen as an instructive example of heterogeneous, catalytic, partial oxidation of hydrocarbons, as it exhibits many key steps:- paraffin activation, oxidative dehydrogenation, oxygen insertion and desorption of a partially oxidised product with the carbon chain intact. A catalytic flow microreactor was constructed for activity studies with product stream analysis being performed by a single injection into a gas chromatograph. Pre- and post-reaction surface and bulk characterisation of the catalytic materials being studied was performed using a variety of techniques, including X-ray diffraction, thermogravimetry, X-ray photoelectron spectroscopy and nitrogen physisorption.

The objective of this thesis was to study the palladium/copper system for the partial oxidation of n-butane to maleic anhydride, this system was chosen after studies of catalysis theories and the available literature had highlighted it as possibly being able to catalyse the desired reaction. From initial studies of this system, which proved that it was indeed active, it was discovered that the palladium component played no useful role and that chlorinated cupric oxide was the active component of the initial system. Detailed characterisation using a range of techniques and reaction studies identified the active phase and its precursor as copper (II) oxychloride (melanothallite) and copper (II) trihydroxychloride (atacamite) respectively. These two materials were found to reversibly interconvert by loss and gain of water, due to de- and re-hydroxylation of the lattice. The active phase was found to deactivate, and this was identified as a consequence of loss of chlorine and the subsequent formation of cupric oxide.

Catalytic activity studies were conducted using n-butane and C4 n-olefin feeds, and with the use of gas chromatography - mass spectroscopy, product distribution changes due to the different feeds were identified and correlated to maleic anhydride synthesis. This together with a study of the influence of oxygen content in the feedstock has enabled an insight to be gained into the reaction mechanism.

ACKNOWLEDGMENTS

I would like to thank the United Kingdom Atomic Energy Authority, Harwell for financial support and the opportunity to perform the following research, with special thanks to my industrial supervisors Dr. R. Smailes and Prof. J.A. Cairns and the other members of the Applied Chemistry Group, Materials Development Division. I am also grateful to Dr. A. Crossley and Dr. V. Moore for collection of the XPS spectra. I am extremely grateful to Dr. D. Chadwick of Imperial College, my University supervisor for the advice, stimulating discussion and close supervision of my work. Finally I would like to express my gratitude to my wife, Kathryn, for her patience and motivation she gave me, without whom this thesis would have taken much longer to produce.

CONTENTS

List of figures

List of tables

Chapter 1 Introduction 15

1.1 General Introduction

1.2 Maleic Anhydride Preparation Processes

1.3 Objectives and Structure of this Thesis

Chapter 2 Theoretical Considerations 25

2.1 Thermodynamics

2.2 Generalised Theories of Catalysis

2.2.1 The multiplet theory of catalysis

2.2.2 The electronic theory of catalysis

2.2.3 Crystal and ligand field models

2.2.4 The Mars - van Krevelen model for oxidation catalysis

Chapter 3 Literature Survey 39

3.1 Catalysts Active for n-Butane to Maleic Anhydride Conversion

3.1.1 Vanadium - phosphorus - oxides

3.1.2 Other active materials

3.2 Other Relevant Heterogeneous Partial Oxidation Processes

3.2.1 Oxidation of C2 hydrocarbons

3.2.2 Oxidation of C3 hydrocarbons

3.2.3 Oxidation of C4 hydrocarbons

3.2.4 Oxidation of C5 hydrocarbons

3.3 Homogeneous Catalysts for the Partial Oxidation of Hydrocarbons

Chapter 4 Experimental Techniques 60

4.1 Catalyst Characterisation

4.1.1 X-ray diffraction

4.1.2 Thermogravimetric analysis

4.1.3 Specific surface area

4.1.4 X-ray photoelectron spectroscopy

4.2 Catalytic Activity Measurements

4.2.1 Reactor system

4.2.2 Gas chromatograph analysis system

4.2.3 Gas chromatographic analysis methods

4.3 Initial Experiments

Chapter 5 Investigations of the Palladium/Copper System 76

5.1 Catalyst Preparation

5.1.1 2.6% palladium (from the chloride salt) on cupric oxide

5.1.2 0.45% palladium (fron the chloride salt) on cupric oxide

5.1.3 2.6% palladium (from the nitrate salt) on cupric oxide

5.2 Catalytic Activity

5.2.1 2.6% palladium chloride on cupric oxide, unreduced

5.2.2 2.6% palladium chloride on cupric oxide, reduced

5.2.3 0.45% palladium chloride on cupric oxide, reduced

5.2.4 2.6% palladium nitrate on cupric oxide, reduced

5.2.5 Cupric oxide

5.3 Catalyst Characterisation

5.3.1 2.6% palladium chloride on cupric oxide

5.3.2 0.45% palladium chloride on cupric oxide

5.3.3 2.6% palladium nitrate on cupric oxide

5.4 Discussion of Results and Conclusions

Chapter 6 Comparison of the Catalytic Activity of the Palladium/Copper System to Vanadium Phosphorus Oxides and Molybdate Catalysts 132

6.1 Catalyst Preparation and Characterisation

6.1.1 Vanadium phosphorus oxide - aqueous route

6.1.2 Vanadium phosphorus oxide - organic route

6.1.3 Bismuth molybdate

6.1.4 Bismuth molybdate plus 10% excess molybdenum trioxide

6.1.5 Nickel molybdate plus 15% excess molybdenum trioxide

6.1.6 Cobalt molybdate plus 15% excess molybdenum trioxide

6.1.7 Iron (II) molybdate

6.1.8 Iron (III) molybdate

6.2 Catalyst Activity Measurements

6.2.1 Vanadium phosphorus oxides

6.2.2 Bismuth molybdates

6.2.3 Nickel molybdate

6.2.3 Cobalt molybdate

6.2.4 Iron molybdates

6.2.5 Catalytic activity of other supported palladium catalysts

6.3 Discussion of Results

Chapter 7 Investigations of Copper Hydroxychloride Materials 144

7.1 Initial Activity Studies of the Support Material

7.2 Atacamite

7.2.1 Preparation

7.2.2 Characterisation

7.2.3 Catalytic activity studies

7.3 Deactivation of the Catalytically Active Species

Chapter 8 Mechanistic Investigations 179

8.1 Product Gases Analysis using Gas Chromatography - Mass Spectroscopy

8.2 Catalytic Activity with n-Butene Feeds

8.3 Catalytic Activity in the Absence of Oxygen in the Feed Gas

Chapter 9 Conclusions 199

9.1 Investigations of the Palladium/Copper System

9.2 Investigations of Copper Hydroxychloride Materials

9.3 Investigations of the Reaction Mechanism on Copper Oxychloride

References 207

Appendix A Gas chromatograph control and analysis methods.

Appendix B List of species detected by G.C. - M.S.

List of Figures

1 Diagramatic representation of the catalytic microreactor system.

2 Detail of reactor tube.

3 Typical stepwise temperature programme for the microreactor.

4 Gas chromatograph configuration for analysis method 2.

5 Example chromatogram using analysis method 2.

6 n-Butane conversion, carbon dioxide and maleic anhydride production curves for the unreduced 2.6% $PdCl_2$ on CuO catalyst.

7 Maleic anhydride yield and selectivity curves for the unreduced 2.6% $PdCl_2$ on CuO catalyst.

8 Chromatogram obtained from the unreduced 2.6% $PdCl_2$ on CuO catalyst at 350 Celsius.

9 n-Butane conversion, carbon dioxide and maleic anhydride production curves for the reduced 2.6% $PdCl_2$ on CuO catalyst.

10 Maleic anhydride yield and selectivity curves for the reduced 2.6% $PdCl_2$ on CuO catalyst.

11 Chromatogram obtained from the reduced 2.6% $PdCl_2$ on CuO catalyst at 350 Celsius.

12 n-Butane conversion, carbon dioxide and maleic anhydride production curves for the reduced 0.45% $PdCl_2$ on CuO catalyst.

13 Maleic anhydride yield and selectivity curves for the reduced 0.45% $PdCl_2$ on CuO catalyst.

14 Chromatogram obtained from the reduced 0.45% $PdCl_2$ on CuO catalyst at 325 Celsius.

15 n-Butane conversion and carbon dioxide production curves for the reduced 2.6% $Pd(NO_3)_2$ on CuO catalyst.

16 Chromatogram obtained from the reduced 2.6% $Pd(NO_3)_2$ on CuO catalyst at 250 Celsius.

17 Chromatogram obtained from the CuO catalyst at 275 Celsius.

18 n-Butane conversion and carbon dioxide production curves for the CuO catalyst.

19 Nitrogen physisorption isotherm for the CuO catalyst.

20 XRD pattern of the unreduced 2.6% $PdCl_2$ on CuO catalyst.

21 XPS spectrum of the Cu (2p) peaks of the unreduced 2.6% $PdCl_2$ on CuO catalyst.

22 XPS spectrum of the Pd (3d) peaks of the unreduced 2.6% $PdCl_2$ on CuO catalyst.

23 XPS spectrum of the Pd (3d) peaks of the reduced 2.6% $PdCl_2$ on CuO catalyst.

24 XPS spectrum of the Cl (2p) peak of the unreduced 2.6% $PdCl_2$ on CuO catalyst.

25 XPS spectrum of the Cl (2p) peak of the reduced 2.6% $PdCl_2$ on CuO catalyst.

26 XPS spectrum of the O (1s) peaks of the unreduced 2.6% $PdCl_2$ on CuO catalyst.

27 XPS spectrum of the O (1s) peaks of the reduced 2.6% $PdCl_2$ on CuO catalyst.

28 Thermogram of the unreduced 2.6% $PdCl_2$ on CuO catalyst in air.

29 Thermogram of the reduced 2.6% $PdCl_2$ on CuO catalyst in air.

30 XRD pattern of the unreduced 2.6% $PdCl_2$ on CuO catalyst after calcination at 550 Celsius.

31 XRD pattern of the reduced 0.45% $PdCl_2$ on CuO catalyst.

32 XPS spectrum of the Cu (2p) peaks of the unreduced 0.45% $PdCl_2$ on CuO catalyst.

33 XPS spectrum of the Pd (3d) peaks of the unreduced 0.45% $PdCl_2$ on CuO catalyst.

34 XPS spectrum of the Pd (3d) peaks of the reduced 0.45% $PdCl_2$ on CuO catalyst.

35 XPS spectrum of the Cl (2p) peak of the unreduced 0.45% $PdCl_2$ on CuO catalyst.

36 XPS spectrum of the Cl (2p) peak of the reduced 0.45% $PdCl_2$ on CuO catalyst.

37 XPS spectrum of the O (2p) peaks of the unreduced 0.45% $PdCl_2$ on CuO catalyst.

38 XPS spectrum of the O (2p) peaks of the reduced 0.45% $PdCl_2$ on CuO catalyst.

39 Thermogram of the unreduced 0.45% $PdCl_2$ on CuO catalyst in air.

40 Thermogram of the reduced 0.45% $PdCl_2$ on CuO catalyst in air.

41 XRD pattern of the unreduced 2.6% $Pd(NO_3)_2$ on CuO catalyst.

42 XRD pattern of the reduced 2.6% $Pd(NO_3)_2$ on CuO catalyst.

43 XPS spectrum of the Cu (2p) peaks of the unreduced 2.6% $Pd(NO_3)_2$ on CuO catalyst.

44 XPS spectrum of the Pd (3d) peaks of the unreduced 2.6% $Pd(NO_3)_2$ on CuO catalyst.

45 XPS spectrum of the Pd (3d) peaks of the reduced 2.6% $Pd(NO_3)_2$ on CuO catalyst.

46 XPS spectrum of the O (1s) peaks of the unreduced 2.6% $Pd(NO_3)_2$ on CuO catalyst.

47 XPS spectrum of the O (1s) peaks of the reduced 2.6% $Pd(NO_3)_2$ on CuO catalyst.

48 Thermogram of the unreduced 2.6% $Pd(NO_3)_2$ on CuO catalyst in air.

49 n-Butane conversion, carbon dioxide and maleic anhydride production curves for the mixed atacamite/CuO catalyst.

50 Maleic anhydride yield and production curves for the mixed atacamite/CuO catalyst.

51 Chromatogram obtained from the mixed atacamite/CuO catalyst at 350 Celsius.

52 XRD pattern of the pure atacamite catalyst as prepared.

53 XPS spectrum of the Cu (2p) peaks for the pure atacamite catalyst.

54 XPS spectrum of the Cl (2p) peak for the pure atacamite catalyst.

55 XPS spectrum of the O (1s) peak for the pure atacamite catalyst.

56 Thermogram of the mixed atacamite/CuO catalyst in air.

57 XRD pattern of the mixed atacamite/CuO catalyst after calcination at 550 Celsius.

58 Thermogram of the pure atacamite catalyst in air.

59 Thermogram of the pure atacamite catalyst after calcination at 325 Celsius.

60 XRD pattern of the pure atacamite catalyst after calcination at 325 Celsius.

61 n-Butane conversion, carbon dioxide and maleic anhydride production curves for the pure atacamite catalyst.

62 Maleic anhydride yield and selectivity curves for the pure atacamite catalyst.

63 Chromatogram obtained from the pure atacamite catalyst at 400 Celsius.

64 Chromatogram obtained from the $CuCl_2$ catalyst at 425 Celsius.

65 Chromatogram obtained from the CuCl catalyst at 450 Celsius.

66 n-Butane conversion curves for the catalyst deactivation experiment.

67 Chromatogram obtained from the pure atacamite catalyst after 10 minutes at 350 Celsius.

68 Chromatogram obtained from the pure atacamite catalyst after 2.5 hours at 350 Celsius.

69 Chromatogram obtained from the pure atacamite catalyst after 6 hours at 350 Celsius.

70 Isothermal thermogram of the pure atacamite catalyst in air at 350 Celsius.

71 Isothermal thermogram of the pure atacamite catalyst in argon at 350 Celsius.

72 Isothermal thermogram of the pure atacamite catalyst in 1% n-butane in air at 350 Celsius.

73 1-Butene conversion curve for the mixed atacamite/CuO catalyst.

74 Cis-2-butene conversion curve for the mixed atacamite/CuO catalyst.

75 1,3-Butadiene conversion curve for the mixed atacamite/CuO catalyst.

76 Chromatogram obtained from the mixed atacamite/CuO catalyst in a cis-2-butene/air feed at 250 Celsius.

77 Chromatogram obtained from the mixed atacamite/CuO catalyst in a cis-2-butene/air feed at 275 Celsius.

78 Chromatogram obtained from the mixed atacamite/CuO catalyst in a cis-2-butene/air feed at 300 Celsius.

79 Chromatogram obtained from the mixed atacamite/CuO catalyst in a n-butane/air feed at 350 Celsius.

80 Chromatogram obtained from the pure atacamite catalyst after 10 minutes at 250 Celsius in a cis-2-butene/helium feed.

81 Chromatogram obtained from the pure atacamite catalyst after 3 hours at 250 Celsius in a cis-2-butene/helium feed.

List of Tables

1.1 Principal commercial catalytic partial oxidation processes.

5.1 Palladium/copper system catalyst compositions.

5.2 Palladium/copper system catalytic activity results.

5.3a XPS results of the unreduced 2.6% $PdCl_2$ on CuO catalyst.

5.3b XPS results of the reduced 2.6% $PdCl_2$ on CuO catalyst.

5.4a XPS results of the unreduced 0.45% $PdCl_2$ on CuO catalyst.

5.4b XPS results of the reduced 0.45% $PdCl_2$ on CuO catalyst.

5.5a XPS results of the unreduced 2.6% $Pd(NO_3)_2$ on CuO catalyst.

5.5b XPS results of the reduced 2.6% $Pd(NO_3)_2$ on CuO catalyst.

6.1 Results of the catalytic activity studies performed on materials already known to be active for the n-butane to maleic anhydride conversion.

6.2 Catalytic activity results for various supported palladium chloride catalysts.

7.1 XPS results of the pure atacamite catalyst.

CHAPTER 1

INTRODUCTION

1.1 General Introduction.

The oxidation of hydrocarbons to produce oxygen-containing, or other heteroatom-containing derivatives is an important process in many industries, especially the chemical and petrochemical. These compounds, having a low natural abundance and a great usefulness as intermediates for production of consumer products, are more valuable than the parent hydrocarbon. Without a selective catalyst, the partial oxidation of hydrocarbons can be very complex, leading to the formation of a wide range of products, often as a consequence of branched or unbranched chain reactions. These products, all potentially valuable, would require elaborate separation processes.

In the presence of a catalytically active material, process costs can be significantly reduced by the catalyst being able to meet the following criteria[1]:

1) The catalyst must provide suitable sites on its surface (heterogeneous catalyst) for adsorption of the hydrocarbon molecules in a deformed, reactive state (chemisorption)[1].

2) The catalyst must "temper" the reactivity of the oxygen or other hetero-atom, in order to induce a reaction under mild, easily controllable conditions and, above all, it must induce selectivity, so only a small number of products are obtained. Loss of control of the oxidation process, producing water and carbon dioxide as the only products, is all too easy because of the large free energy and enthalpy changes involved. Hence the balance between a selective, partial oxidation process and a more complete oxidative degradation is a very fine one[2].

3) The catalyst must allow desorption of the desired partial oxidation product, without which the product might undergo further oxidation or the product could remain on the surface, blocking the active centres and therefore poisoning it.

Examples of catalytic reactions within the class of selective oxidation of hydrocarbons are given in Table 1.1. As can be seen from the world capacitity figures, our reliance on the products of such processes is very high. Therefore, more selective, more cost-effective processes are being continually sought, with emphasis on improved catalyst performance.

Table 1.1 subdivides this vast field into five types of reaction[2]:-

Type 1) The introduction of oxygen as a functional group.
e.g. ethylene → ethylene oxide

Type 2) The oxidative removal of hydrogen.
e.g. 1-butene → 1,3-butadiene

Type 3) The introduction of nitrogen as a functional group.
e.g. propylene → acrylonitrile

Type 4) The introduction of a halogen as a functional group.
e.g. ethylene → vinyl chloride

Type 5) Combustion to form carbon dioxide and water.

Since the subject of interest here is selective, partial oxidation, type 5 will be discussed only in the context of being an undesirable secondary reaction and therefore is not included in table 1.1. Table 1.1 shows that type 1 and type 2 are most important in terms of world capacity. It shows also that the vast majority of feedstocks are unsaturated hydrocarbons, however, there is significant usage of butane.

Table 1.1 **Principal Commercial Catalytic Partial Oxidation Processes.**

Reactants	Products	Catalysts	World capacity (1980 10^3 tpa)	Principal uses
Type 1.	**The introduction of oxygen as a functional group.**			
Ethylene	Ethylene oxide	Ag	7300	Ethylene glycol, polyols, polyester fibres.
Ethylene	Acetaldehyde	$Pd/V_2O_5/Al_2O_3$	2900	Acetic acid/anhydride,
		$Pd^{2+}/Cu^{+}/C$		crotonaldehyde
Propylene	Acrolein	Cu_2O/Al_2O_3		Animal foods, allyl alcohol
		Bi/Mo/O; Sn/Mo/O		
		Sn/Sb/O; Bi/Sb/O		
Propylene	Acrylic acid	Co/Bi/Mo/O		Polyacrylate
Propylene	Acetone	Sn/Mo/O; Co/Mo/O	3500	Paint, solvents, resins
		V,Ni,Cu,Zn/Mo/O		
Butenes	Crotonaldehyde	Sn/Mo/O; Co/Mo/O		
	Methyl vinyl ketone	Cu_2O		

Table 1.1(cont.)

Reactants	Products	Catalysts	World capacity (1980 10^3 tpa)	Principal uses
Butenes	Maleic Anhydride	V/P/O; V_2O_5	700	Resins, agricultural chemicals,
		P/Mo/O; V/Mo/O		unsaturated polyesters
		Co,Ni,Mn,Fe,Cd/Mo/O		(See type 2 also)
		P/Mo/Bi/O		
Isobutene	Methacrolein	Bi/Mo/O; Cu_2O		
Pentene	Pentanone(2&3)	Co/Mo/O; Sn/Mo/O		
Type 2.	**The oxidative removal of hydrogen.**			
Pentene	1,3-pentadiene	Bi/Mo/O		
Butenes	1,3-butadiene	Bi/Mo/O; Pb/Mo/O		
		Bi/W/O; Sb/Mn/O		
		Co/Al/W/O		
		Sn/P/O; Cr/Al/O		

Table 1.1(cont.)

Reactants	Products	Catalysts	World capacity (1980 10^3 tpa)	Principal uses
Butane	Maleic anhydride	V/P/O; V_2O_5	700	Resins, agricultural chemicals, unsaturated polyesters. (Type 1 also)
Type 3.	**The introduction of nitrogen as a functional group.**			
Propylene	Acrylonitrile	Bi/Mo/O(Sb)	4000	Acrylic fibres, synthetic
		U/Sb/O		rubbers, resins.
Isobutene	Methacrylonitrile	Fe/Te/Sb/Mo/O		
Type 4.	**The introduction of a halogen as a functional group.**			
Acetylene	Vinyl chloride	$FeCl_3$; $CuCl_2$	16500	P.V.C., manufacture of
Ethylene				trichloroethylene (solvent)

References 1,2,3,4,5,6,7,8.

It is predicted[3,4] that saturated hydrocarbon feedstocks such as butane are likely to grow in importance, because of their inherently higher natural abundance. However, due to the greater thermodynamic stability of paraffins, activation energies of oxidation processes are often higher than the olefin analogues. This results in harsher reaction conditions being necessary to obtain a comparable conversion and detrimental effects on the catalyst, such as rapid catalyst ageing and/or lowering of the selectivity achieved (see section 2.1 also). Despite this, the commercial and scientific interest in the selective partial oxidation of paraffins is high. Other processes, although commercially less important, do have great scientific potential in providing a fuller picture of partial oxidation catalysis, thereby allowing their principles to be applied to commercial processes to increase selectivity and yield. The oxidation of n-butane to maleic anhydride was chosen from those listed in table 1.1 as the reaction to study, as commercially it is very important at present and is probably set to become the major route to maleic anhydride (see section 1.2). It is also of scientific importance as an oxidation process requiring high selectivity combining paraffin activation, oxidative dehydrogenation, insertion of oxygen as a functional group and desorption of a partially oxidised product.

1.2 Maleic Anhydride Preparation Processes.

Maleic anhydride is an important chemical due to its versatility as an intermediate in a large number of chemical processes, especially the preparation of alkyd resins, unsaturated polyesters, and fumaric acid and other food additives, as well as insecticides, lubricating additives etc. The world consumption currently stands in excess of 700,000 tonnes per annum[9,10]. The continually

expanding role of maleic anhydride in the chemical industry has stimulated research efforts for more efficient and economical processes, with a requirement for catalysts which are more active, selective and stable. This is illustrated by the issuing of more than 70 patents relating to the n-butane route in the 1970's[3,9,10].

At least six possible maleic anhydride production processes have been evaluated, each having their pro s and con s. These are listed below, for purposes of comparison[11]:

a) The classical benzene process. Operated since 1933, this process gives selectivities of 50-60% and conversions of 85-95%, using V_2O_5-MoO_3 catalysts, in standard multitubular reactors. But in the 1970's benzene prices increased, due to its greater use in unleaded automobile fuel. This, together with higher oil prices and concern over benzene's toxicity, lead to other processes being adopted.

b) Oxidation of n-butenes. This process uses a vanadyl pyrophosphate catalyst (the vanadium ions in the +4 oxidation state and a P:V ratio of 1.6). The hydrocarbons from the C4 cut of naphtha cracking are used, although 1,3-butadiene is first removed due to its value in other processes as is isobutene. Dilution of the catalyst is necessary to avoid runaway, but over dilution results in low conversions. A dilution factor of 7.3 was calculated to give an olefin conversion of 87% with a selectivity in the range 50 to 60%[9].

c) Oxidation of all butenes. This process also uses a vanadyl pyrophosphate catalyst as in b) above. However, in this case isobutene is totally combusted, and in fact calculations show that reactor runaway is likely to occur if a standard multitubular reactor was used. For this reason a fluidised bed reactor is used to obtain isothermality and controllability, thus enabling higher hydrocarbon concentrations to be used (up to 10%). This process is

operated by Mitsubishi, utilising the fact that the hydrocarbon feed has the advantage of being very cheap in comparison to benzene. Calculations[9] show that high conversions (98%) are achievable with good selectivity towards maleic anhydride (48%).

d) Oxidation of n-butenes. Again a catalyst similar to that used in process b) is used. However, this process involves the separation of isobutenes in a prereactor to produce saleable methacrolein, tert-butylmethyl ether or tert-butanol before reaction of the n-butenes. Despite the production of these useful products, this process is more expensive overall.

e) Oxidation of n-butane. This hydrocarbon is recovered from refinery gas and is oxidised with the aid of a similar V-P-O catalyst to route b). Despite the more severe conditions required, the less expensive hydrocarbon feedstocks make this the favoured route. Commercial processes using a n-butane feed achieve 60 to 65% selectivity towards maleic anhydride with a n-butane conversion of 70 to 80%.

f) Oxidation of C5 hydrocarbons. Also using a vanadium phosphorus catalyst, uses the C5 cut from refinery gas, but the process is less selective, requiring rather harsh conditions and, therefore, its use is limited.

1.3 Objectives and Structure of this Thesis.

The subject of this thesis, the heterogeneously catalysed selective oxidation of n-butane to maleic anhydride, as already discussed in the previous sections is of great scientific and commercial interest. The reaction contains many important elements namely the activation and dehydrogenation of a readily available paraffin;

oxygen insertion into the adsorbed molecule to form a functional group; desorption of a partially oxidised product of great commercial value as the majority product before total oxidation has occurred. The objective of the research described in this thesis was to explore the properties of catalysts based on the palladium/copper system in relation to this partial oxidation reaction. These two elements in their various oxidation states have been highlighted in the succeeding chapters as possibly being able to catalyse the n-butane to maleic anhydride conversion either alone or in combination.

Chapter 2 contains relevant theoretical considerations for the reaction and a discussion of the theories of catalysis which are useful in understanding how materials may act as catalysts in selective oxidation reactions. The crystal and ligand field model identifies oxides of copper and also palladium as being possible primary components of an active catalyst. Chapter 3 is a literature survey of materials already known to be active for the selective oxidation of n-butane to maleic anhydride and materials active for other hydrocarbon partial oxidation reactions. In this chapter palladium metal as well as copper, cuprous oxide and cupric oxide are highlighted as being known to be active heterogenous catalysts for other hydrocarbon partial oxidation reactions. Partial hydrocarbon oxidation by homogeneous catalysts is also discussed and attention is given to the Wacker process for oxidation of ethylene to acetaldehyde which uses an aqueous solution of cupric chloride and palladium chloride.

Descriptions of the characterisation techniques used and the design, construction and use of a catalytic microreactor and its gas chromatographic analysis system are included in chapter 4. Chapter 5 contains the results and discussion of the palladium/copper system. Chapter 6 shows a comparison of the catalytic activity of the palladium/copper system with catalysts known as active materials for

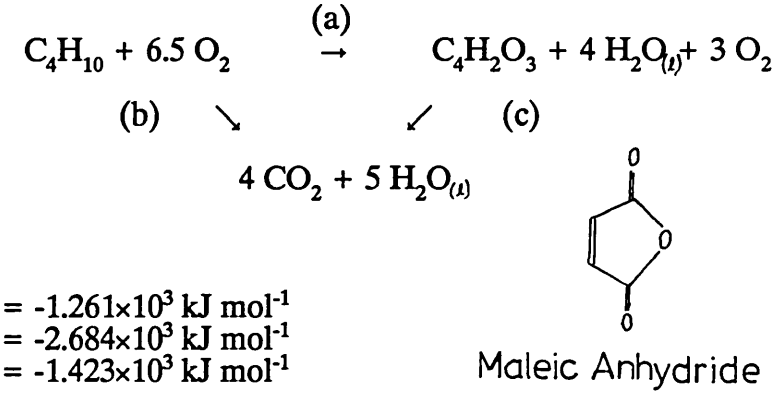
n-butane conversion to maleic anydride. Chapter 7 investigates the copper component of the system in more detail and identifies the palladium as having no active role in producing the partially oxidised products, and goes on to identify, characterise and study the active material, a copper oxychloride. Chapter 8 contains the results and discussion of some mechanistic studies performed on the active material. And finally chapter 9 comprises the final discussion of the experimental results obtained and concludes this thesis.

CHAPTER 2

THEORETICAL CONSIDERATIONS

2.1 Thermodynamics.

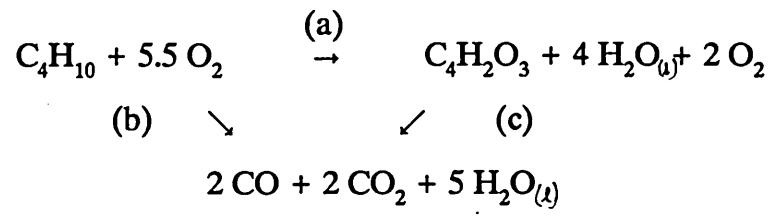
If the oxidation of hydrocarbons was controlled by the thermodynamics of the reactions alone the only products to be formed would be carbon dioxide and water, as these products are far more thermodynamically stable than any partially oxidised hydrocarbon. This can be seen from the reaction scheme below[11]:



(a) $\Delta H^{\ominus}_{R} = -1.261 \times 10^3$ kJ mol^{-1}
(b) $\Delta H^{\ominus}_{R} = -2.684 \times 10^3$ kJ mol^{-1}
(c) $\Delta H^{\ominus}_{R} = -1.423 \times 10^3$ kJ mol^{-1}

Maleic Anhydride

However, it must be noted that using the commercial V-P-O catalyst the combustion process does not yield carbon dioxide and water alone but gives carbon monoxide, carbon dioxide (in a 1:1 ratio) and water, the thermodynamic reaction cycle for which is shown below:



(a) $\Delta H^{\ominus}_{R} = -1.261\times10^{3}$ kJ mol^{-1}
(b) $\Delta H^{\ominus}_{R} = -2.091\times10^{3}$ kJ mol^{-1}
(c) $\Delta H^{\ominus}_{R} = -0.832\times10^{3}$ kJ mol^{-1}

The formation of a C-O bond or O-H bond by reaction of a hydrocarbon with molecular oxygen releases enough energy (approx. 360 and 465 kJ mol^{-1} respectively) to cause excessive fragmentation of the hydrocarbon molecule, leading to complete combustion. Therefore, once the catalyst surface has activated the hydrocarbon, its purpose is to oxidise the adsorbed molecule with oxygen of appropriate activity. For metal oxides the degree of "moderation" is related to the free energy of transition from a higher to lower oxide (e.g.. $V_2O_5 \rightarrow V_2O_4$), a value close to zero meaning that the catalyst has about the same oxidation potential as gas phase molecular oxygen, while a value near 400 kJ mol^{-1} suggests negligible reactivity towards a hydrocarbon.

2.2 Generalised Theories of Catalysis.

No one theory of catalysis alone enables predictions about partial oxidation activity to be made accurately, nor explains why certain materials are found to be active. The four main theories are (1) the "multiplet" theory of Balandin[12], (2) the electronic theory of Wolkenstein[13], (3) the "crystal field" theory of Dowden[14,15] and the Mars - van Krevelen Model[16].

2.2.1 The multiplet theory of catalysis.

This theory[5,12] supposes that only the part of a molecule undergoing catalytic conversion actually participates in the reaction. This particular group of atoms is termed the "index group" and may be considered analogous to the functional groups of organic chemistry. The theory also assumes that only certain atoms of the catalyst possess the necessary configuration for the reaction; these atoms are termed the "multiplet". These are the "active sites" proposed by Somorjai[17]. According to the theory, during catalysis, the index group of a reactant molecule is superimposed on the active atoms of the catalyst, thereby yielding an intermediate multiplet complex within which bond deformation and migration occurs. The multiplet complex, which is unstable, then either decomposes giving the products or reverts to the reactants depending on thermodynamic considerations. If the mechanism is a single step process e.g. dehydrogenation of amines to ketimines ($R_1R_2CHNH_2 \rightarrow R_1R_2C{=}NH + H_2$) obviously only one multiplet complex will be formed, but if it is a multistep mechanism e.g. n-butane to maleic anhydride, it is reasonable to assume that a number of multiplet complexes will be formed at each step; however, desorption of the products formed at each step may or may not occur.

Evidence for the index group (or active centre) comes from studies in which R_1 and R_2 of the amines (mentioned above) are varied; this was found to have little effect on the activation energies for the reaction on the catalyst. On account of the index group, certain restrictions, with respect to the catalyst are imposed on one's choice of catalyst by virtue of the stereochemistry of the reaction and of the interatomic distances within the index group. These restrictions are known as the "principle of structural correspondence", and from it predictions can be made,

particularly in the case of catalysis by metals (interatomic distances and crystal structures better known than oxides), as to which materials may be active for a particular conversion.

However, the principle of structural correspondence is insufficient to explain the products of certain catalytic reactions, e.g. ThO_2 and CaF_2 have similar interatomic distances, but thoria catalyses dehydration of alcohols, while calcium fluoride catalyses dehydrogenation. This difference, it was postulated, lay in the energetics of the reaction, the important energetic factors being heat of reaction (ΔH) and activation energy (E_a); ΔH and E_a may be derived from fundamental considerations of bond energies affected during the formation and decomposition of the multiplet complex. Values of the heat of reaction, the sum of energies involved in breaking and forming bonds (s); and of the adsorption potential of the catalyst (q) can be obtained similarly. Plotting values of the heat of formation of the multiplet complex (E) against q yields intersecting straight lines (volcano shaped curves), the point of intersection of these was found to have values of $q=0.5s$ and $E=0.5\Delta H$, and this is said to express the principle of energetic correspondence. Thus, for selections of an active catalyst for an endothermic reaction it is necessary for q to be as near to 0.5s as possible.

This theory runs into trouble in that it relies on taking bulk lattice parameters and applying them to a catalytic surfaces, where there is considerable disruption, so that bulk lattice parameters have little meaning with respect to the surface geometry.

2.2.2 The electronic theory of catalysis[5,13].

This theory mainly applied to semiconductors emphasises the fact that every catalytic process begins with the act of adsorption, and proposes that any generalised theory of catalysis should proceed from a consideration of the theory of adsorption. The theory uses, as a basis, the band theory of solids, and regards particles adsorbed on the surface of the catalyst as impurities or structural defects disturbing the strictly periodic nature of the surface. The concept of a chemisorbed particle as a structural defect allows one to regard the particle as a centre of localisation of either a free electron (an acceptor) or a free hole (a donor). The localisation of a free electron or hole near a chemisorbed particle, means that there is a possibility of their participation in the bonding of the particle to the surface, allowing a weakly adsorbed particle (physisorbed) to become strongly adsorbed (chemisorbed). As the particles approach the surface and become associated with a free electron or hole, the surface - particle bond strengthens and consequently results in a weakening of a intraparticle bond (as discussed in section 2.2.4 with oxygen chemisorption). Therefore, the position and presence of acceptor and donor energy levels in the band gap between the valence and conduction bands are important, as well as the position of the Fermi level, as this determines the concentration of the electron- and hole-gases on the surface of the crystal.

On the formation of a strongly chemisorbed particle on the surface, a charge appears on the surface and this causes a deformation of the energy bands at the surface, a negative surface charge causes a rise in the energy bands, and a surface positive charge causes a lowering. The Fermi level, however, once equilibrium has been established, is common to the surface and bulk, and thus is apparently shifted with respect to the valence and conduction bands. Reactions which proceed faster as

the Fermi level is apparently raised are accelerated by electrons and are known as *n*-type or acceptor reactions; opposite reactions are known as *p*-type or donor reactions. Catalytic activity is determined by the position of the Fermi level on the surface of the catalyst (ε_s^+) this, in turn, is determined by its position within the catalyst (ε_v^+). Factors altering the bulk Fermi level (and hence electrical conductivity) will also alter the surface Fermi level (and hence the catalytic activity). This gives rise to the parallelism between changes in electrical conductivity and catalytic activity often observed in catalysis. A notable success of the electronic theory has been to offer an explanation for the mechanism of promotion or poisoning by the apparently insignificant amounts of impurities added to semiconductors, remembering impurities need not be chemically foreign atoms, but include local disturbances in the strictly periodic nature of the lattice. Surface impurities directly affect ε_s^+ leaving ε_v^+ unchanged (seen as a change in catalytic activity but not electrical conductivity); bulk impurities alter ε_v^+ and hence ε_s^+, therefore both the electrical conductivity and catalytic activity are affected. Acceptor impurities lower the Fermi level whilst donor impurities raise the Fermi level.

2.2.3 Crystal and ligand field models.

In the opinion of Dowden and Wells[14], simple electronic theory was unable to explain certain changes in catalytic activity when proceeding across the fourth period of the periodic table, since the electronic levels of the cations (referred to vacuum) are approximately equal. These changes were observed for a number of catalytic reactions viz. H_2 - D_2 exchange, dehydrogenation and disproportionation of cyclohexane, hydrogenation of ethylene and decomposition of N_2O. The observed

changes were a rise in catalytic activity from d^0 (Ti^{4+}) to a maximum at d^3 (Cr_2O_3), falling to a minimum at d^5 (Fe_2O_3), and rising to a maximum again at d^{6-7} (Co_3O_4), and finally falling to a minimum again at d^{9-10} (CuO & ZnO). This double peak Dowden explained was due to crystal field stabilisation energy changes due to chemisorbing molecules increasing the coordination of the surface metal cations.

This theory can be applied to a number of catalytic systems with reasonable success for the design of a catalytically active material (see reference 18). Firstly, the active component of the catalyst has to be selected. In the case of n-butane to maleic anhydride, as already discussed, once the n-butane has been activated by loss of 2 hydrogen atoms to form a chemisorbed isomer of n-butene the reaction probably proceeds as if the reactant hydrocarbon were actually n-butene. Initial consideration must be made of the likely metal cations that will successfully adsorb, and therefore bond strongly butene and oxygen, and also butadiene, remembering for strong bonding good orbital overlap and available electrons on the right centres are necessary for electron donation and π-bonding back donation (see earlier). From these considerations, d - shell configurations of 1,2,3,8,9,10 should be suitable, and certain ions can be eliminated as they would (a) be unstable at the oxygen partial pressures used [Ti(III,II,I), Fe(0), Co(0,I), Ni(0) and Mn(V)] and (b) energetically unfavourable for π - complex formation [Zn(II)].

The most desirable groups are:

d^2 - d^3 : *n* - type semiconducting oxides

d^9 - d^{10}: *p* - type semiconducting oxides

the first group generally known to favour selective partial oxidation, the second group generally favouring total oxidation.

For the oxygen insertion step, the situation is complicated due to the fact that little is known about the mechanisms by which oxygen is inserted i.e. the active surface oxygen species, the mode of insertion and decomposition into the products.

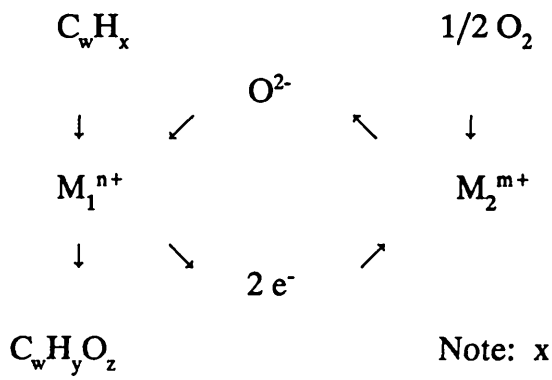
For the initial step of n-butane activation, it has already been discussed that very reactive oxygen surface species or acid sites are required. As *p* - type semiconducting oxides are more acidic than *n* - type and due to their greater propensity for combustion, they must have very reactive surface oxygen species, hence, their combustion efficiency must be controlled so that once the hydrocarbon has been activated only less reactive lattice oxygen is available for insertion into the dehydrogenated molecule.

This tempering of the combustion process is often achieved by the addition of a secondary component, which can act by causing the metal to bond to oxygen more strongly or can itself to bond to oxygen strongly. The secondary component must not effect the primary components activity too adversely, but should act by increasing the selectivity and possibly by helping the rate determining steps e.g. as in the effect of phosphorus in vanadium pentoxide. In addition, the secondary component must not be lost from the active, selective mixture at an appreciable rate.

From this design procedure suitable primary components might be oxides of vanadium and molybdenum (presently known to be active) also chromium, tungsten, copper, antimony, tin and possibly palladium. This is consistant with the findings of the literature survey of materials active for the partial oxidation of hydrocarbons (chapter 3).

2.2.4 The Mars - van Krevelen model for oxidation catalysis.

Most selective, partial hydrocarbon oxidations can be thought of as a redox cycle, known as the Mars and van Krevelen model[1,7,16]. The reactant hydrocarbon is adsorbed on a M_1^{n+} site to form a chemisorbed species (see later). This adsorbed species reacts with the lattice oxygen that is associated with the M_1^{n+} site, giving rise to a partially oxidised product, and a reduced M_1 site; concurrently electrons produced at M_1^{n+} are transported to a M_2^{m+} site. Molecular oxygen can be adsorbed on the M_2^{m+} site where it is converted into lattice oxygen and a consequential oxidation of the M_2 site. The transport of negative charges from M_1^{n+} to M_2^{m+} and of lattice oxygen from M_2^{m+} to M_1^{n+} (oxidation of the M_1^{n+} and reduction of the M_2^{m+} site) can be repeated indefinitely, or at least as long as the hydrocarbon is available to reduce the M_1 site, and the reactant oxygen is available to oxidise the M_2 site. Note M_1 and M_2 may or may not be the same element (see section 3.2.3 where both M_1 and M_2 are molybdenum ions in a bismuth molybdate lattice). At any particular instance, the steady state composition of the catalyst depends on the relative rates of reduction of the catalyst by the hydrocarbon and reoxidation by the gaseous oxygen. The long term stability of the catalyst depends on the fugacity of the oxygen in the gas phase, since the oxide must gradually attain a state that is in thermodynamically stable equilibrium with the gas.



This redox cycle depends on the ability of the catalyst surface sites to accept and/or donate electrons. In the formalism of molecular orbital theory, a redox reaction involves transfer of an electron to fill a bonding orbital of one reactant (to be reduced) from a partly filled antibonding orbital of the reactant to be oxidised. This is similar, but not equivalent, to an acid-base reaction in the Lewis sense, since a Lewis acid accepts electron pairs from a non-bonding orbital of a Lewis base. It is convenient, therefore, to treat the acidity and basicity of the catalyst together with the redox cycle. The overall conversion of n-butane to maleic anhydride is a base to acid conversion, that is, n-butane is more basic than maleic anhydride. However, the dehydrogenation steps in the mechanism are base to base conversions, and the oxygen insertion steps are base to acid conversions, and n-butane or maleic anhydride combustion is a base to acid conversion. Therefore, it is plain to see why an active material has to be amphoteric, and if it is largely acidic then dehydrogenation products would be desorbed, and if too basic then combustion processes would take over (see chapter 3).

The first step in the mechanistic process is uptake of reactants on the catalyst surface. Chemisorption of molecular, gaseous oxygen, as already stated, is very important to maintain the desired oxidation reaction, and thermodynamically relies on the eventual conversion of O_2 to $2O^{2-}$, this requires the donation of a total of four electrons to the dioxygen molecule leading to an oxygen-oxygen bond order of zero, and therefore dissociation of the molecule. Initial chemisorption of the dioxygen molecule therefore must occur on a reduced metal site, or in the Lewis sense a basic site. Using molecular orbital theory, and remembering the influence of the electrostatic field of a transition metal ion in a lattice causing a perturbation of the σ and π orbitals to form six sp^2-type hybrid orbitals, four hybrid π antibonding orbitals and a pair of π bonding orbitals, two $M\text{-}O_2$ structures can be envisaged. In one

structure the metal species is perpendicular to the O-O axis and overlap is between the filled π bonding orbital of the O_2 and the empty e_g atomic orbitals of the metal. The other structure involves the overlap of a filled sp^2 hybrid orbital on the O_2 to the empty e_g atomic orbital of the metal and gives a M-O-O bond angle of 120°, in this case we may have backbonding from the filled t_{2g} atomic orbitals on the metal to the empty π antibonding orbital of the O_2, resulting in strengthening of the M-O bond whilst weakening the O-O bond. This may facilitate the formation of single O species on the surface of the oxidation catalyst. This is in contrast to the former case where the empty π antibonding orbitals of the O_2 plays no role.

The formation of O^{2-} ions from adsorbed oxygen may be studied by considering the formation of O^{2-} ions from molecular oxygen (O_2) in the gas phase. Theoretically the reduction of molecular oxygen to O^{2-} ions can be thought to consist of three hypothetical steps. The dissociation of the molecular oxygen into atomic oxygen (an endothermic process), addition of the first electron to the neutral oxygen atom (exothermic) and finally the addition of a second electron to the oxygen anion (endothermic). The overall process being endothermic with the first and third steps of the hypothetical process being energy barriers in the conversion of gaseous oxygen into O^{2-}, however, it must be remembered that the presence of the metal will perturb the electron energy levels of the adsorbed oxygen species. However, it is likely that the addition of electrons to the molecular oxygen might occur prior to its dissociation following an alternative, perhaps lower energy route as follows. Addition of an electron to molecular oxygen to form O_2^-, then addition of a second electron to form O_2^{2-} followed finally by addition of a further two electrons to give an oxygen species with an oxygen-oxygen bond order of zero ($2O^{2-}$).

Chemisorption of the hydrocarbon would be similar if a carbon - carbon multiple bond existed (olefin), but if a saturated hydrocarbon was used as the

feedstock due to it s lack of lone pairs or π orbitals, bonding other than Lennard - Jones type (physisorption) is impossible unless a hydrogen is removed. This requires considerable energy, as seen in the difference in reactivities between paraffins and olefins (chapter 3). Therefore, the first step in activating a paraffin is the breaking of a C-H bond. (In catalysis by superacids, the first step is to protonate the hydrocarbon, followed by release of a hydrogen molecule to produce a carbenium ion; this will not be discussed). In considering the rate of this step, it is relevant to speculate whether the transition state resembles more closely a situation in which dissociation of the C-H bond is accompanied by a real charge separation to form H^+ and RCH_2^-; or whether it occurs without charge separation. In the gas phase, the homolytic process has a calculated heat of reaction of~400 kJ mol^{-1}, whilst the heterolytic process is about 1600 kJ mol^{-1}, as expected. The catalytic process would require less energy, as an energy gain would occur from formation of O-H bonds from the hydrogen atom or ion and hydrocarbon-metal bonds. These interactions should be so strong that this initial activation becomes thermodynamically favourable but obviously a process with a high energy barrier. Since paraffins are so inert the transition state is likely to resemble the reactants therefore, energetics of hydrogen abstraction are likely to parallel the gas phase processes making the heterolytic process appear much less favourable. Even taking into account energy gains for O-H bond formation and preferred attack at the weaker tertiary C-H bonds, thermodynamic considerations require the presence of a very reactive oxygen that is bound weakly to the solid. These highly reactive oxygen species, if at a high surface density would result in combustion of the hydrocarbon. Therefore, control of the number of sites where highly reactive oxygen chemisorbs is necessary. These sites are often defect sites on the surface of the lattice.

The next step is dehydrogenation, which again requires further C-H bond fission, again probably by lattice oxygen, but this time the oxygen doesn't need to be as reactive. The process probably goes via the stable intermediates of $p\pi$ - $d\pi$ bound olefins or π allyl species. The rate of this step would be enhanced if a) the cation to which the hydrocarbon is bound can readily undergo reduction, b) the surface oxygen is a strong Brønste d base and c) the cation is a soft acid. The first two points are obvious, while the third arises from the fact that dienes are softer bases than olefins.

Desorption of the surface bound olefin or diene, which in this study is undesirable, is facilitated by weak bonding of the hydrocarbon to the surface cation. If this cation is "hard", then desorption will probably occur, since the polarisable π - electrons in the olefin or diene are soft. Therefore a material active for further reaction by oxygen insertion requires, that the olefin or diene be adsorbed onto a soft cation.

Oxygen insertion, the next important step, requires only the correct number of oxygen atoms to be inserted. Excess incorporation, or incorporation at the wrong position in the carbon chain leads to undesirable combustion. There are at least two important oxide properties that affect the oxygen insertion step: geometric effect and metal - oxygen bond energy. The geometric effect is illustrated by the copper oxide catalysed oxidation of propylene to acrolein, where the extent of reduction of the catalyst is critical in determining the activity. Too few oxygens results in an inactive catalyst, while too many result in excessive oxidation. The metal - oxygen bond strength is also significant, since a weak bond results in nondiscriminative C-O bond formation, which leads to combustion eventually, while strong bonds lead to inactive oxygen for the insertion process. These two properties are interconnected,

as reducing the catalyst to optimise the geometric effect undoubtedly affects the M-O bond strength effect.

Finally, desorption of oxygenates is facilitated by weak Lewis acid sites and soft acid sites, as most oxygenates interact with the surface via the oxygen electron lone pair. These oxygenates are usually Lewis bases and hard bases.

One other process which must be considered is the combustion process, reduction in the rate of which would obviously lead to an increase in the selectivity of the catalyst. The extent of total oxidation can be minimised by decreasing (a) the surface residence time of the hydrocarbon reaction intermediates; (b) the strength of adsorption of the desired products relative to the reactants; (c) the amount of adsorbed oxygen active for combustion; and (d) the ratio of combustion to selective oxidation sites (remembering that for many catalytic systems separate sites have been identified - as in bismuth molybdate oxidation of butenes).

CHAPTER 3

LITERATURE SURVEY

3.1 Catalysts Active for n-Butane to Maleic Anhydride.

3.1.1 Vanadium - phosphorus - oxides.

This catalyst is widely used commercially for the conversion of n-butane to maleic anhydride. Vanadium pentoxide alone shows reasonable activity for n-butane conversion with a reasonable selectivity. However, on adding phosphorus in increasing concentration up to a P:V ratio of 1.6, the n-butane conversion dropped significantly, but the selectivity towards maleic anhydride was much improved. It was found that increasing the phosphorus solid solution concentration caused a change in three significant properties[10].

a) The oxygen mobility in the lattice was lowered, thereby causing a reduction in oxygen availability and a consequential decrease in the production of carbon oxides.

b) The vanadium (V^{IV}) oxidation state was stabilised. It should be appreciated that under normal reaction conditions the vanadium would tend to adopt the +5 oxidation state. However, a dynamic equilibrium of the vanadium ($V^{IV} \rightleftharpoons V^{V}$) redox couple has been found to be necessary for the oxidation of n-butane to maleic anhydride[9,19,20].

c) There is an increase in acidity and decrease in basicity of the catalyst[10,21,22]. The addition of phosphorus greatly improves the selectivity of the n-butane reaction. This correlates with the formation of strong Lewis acid surface sites which can activate the hydrocarbon by hydrogen abstraction,

possibly as a hydride anion[21,23]. Such acidic sites are necessary for initial activation of the hydrocarbon, which has been shown to be the rate limiting step at butane concentrations of less than 1% (by volume). Above that, the rate limiting step has been identified as oxygen chemisorption. Commercial processes usually use n-butane feed concentrations of 1% or less. The same kinetics are true for butene oxidation[24,25].

Two very similar catalyst preparation techniques are used[9,10,19], both involving the reduction of a V (Ⅴ) species to V (Ⅳ) followed by the addition of the required amount of ortho-phosphoric acid to give the desired P:V ratio. The first method uses concentrated hydrochloric acid as the reductant, the phosphorus compound being added subsequently to the blue vanadium (Ⅳ) solution. The catalyst precursor is obtained either by evaporation to dryness or by precipitation with cold water. The second method uses an organic reductant[26], mainly oxalic acid, or a mixture of isobutyl and benzyl alcohol. The vanadium pentoxide, held in suspension, is reduced to vanadium (Ⅳ), before addition of phosphorus pentoxide. The resulting slurry is refluxed to ensure homogeneity and removal of the precursor is achieved by filtration.

The range of catalyst precursors capable of being formed by either process is large, many being hydrated vanadyl pyrophosphates, but recent work[10,20,27] indicates that the vanadyl hydrogen phosphate precursor, $(VO)_2H_4P_2O_9$, is the most desirable, because on heating it liberates water yielding $(VO)_2P_2O_7$, which readily forms the active β- or B-phase[10]. Other precursors, by a variety of calcination/preconditioning procedures can also produce this active phase. Exact phase relationships and decomposition/phase changes are unclear, but are

extremely important and very critical in producing an active, selective, catalytic material.

The organic method of preparation produces a material with a slightly higher specific rate of maleic anhydride production from either n-butane or 1-butene. This allows lower operating temperatures, which are also useful for lowering deactivation rates of the catalyst caused by loss of phosphorus. The increase in n-butane conversion is more pronounced than for 1-butene. Work has shown[27] that organic molecules trapped between the layers of the VPO precursor material, on heating, cause a layer separation and deformation of the crystalline structure, thus inducing local straining of the V-(O-P) bonds. As a result, the co-ordination requirements of the vanadium are not completely satisfied, with a consequent increase in Lewis acidity and the creation of more sites able to activate the paraffin. The presence on the surface of the vanadium phosphorus oxides of an oxidising function (V=O double bonds) together with the strong Lewis acid sites, modifies the successive steps leading to selective products (maleic anhydride), instead of isomerized or cracked products which occur on other super acid oxides.

This illustrates the bifunctionality required, viz., strong Lewis acids to activate the non-polar, very stable paraffin, and basic sites with an oxidising function to partially oxidise the hydrocarbon with high selectivity to maleic anhydride and not to CO or CO_2.

The principal problem with the vanadium-phosphorus material is that it deactivates due to loss of phosphorus, thus requiring recharging of the reactor periodically with fresh catalyst. This period of operation is lengthened by either introducing a small concentration of a phosphorus containing compound into the gas feed stream, or by the use of phosphorus stabilising promoters such as alkali

metals, principally lithium. Many other promoters have been introduced to produce a wide range of effects, although the actual function of these is often unclear.

A mechanism for n-butane oxidation to maleic anhydride has been proposed by a number of workers[3,9,10,21,28,29,30]. This involves an initial dehydrogenation of n-butane to a butene, the exact isomer or adsorption state being still unclear. Further dehydrogenation to 1,3-butadiene occurs before oxygen insertion to produce in one or more steps, furan or crotonaldehyde, and then finally further oxygen insertion to form maleic anhydride. Two important side reactions have been identified: parallel combustion of n-butane to form carbon oxides; or subsequent combustion of maleic anhydride. Incorporation of "excess" phosphorus reduces the latter combustion process, but not totally[29].

Work by T.P.Moser[3,31], using ^{18}O enriched β-$VOPO_4$, in-situ Raman spectroscopy, and post-reactor analysis of maleic anhydride, carbon dioxide and water for presence of ^{18}O, showed many interesting mechanistic features. Firstly, the identification of two different sites on the surface, one site being mainly responsible for combustion, and a second site showing higher activity and selectivity. The results show that initially the hydrocarbon interacts with a highly active oxygen to produce an activated dehydrogenated paraffin, this oxygen being situated on the combustion site. The intermediate then undergoes further oxidation, either on the same site to form combustion products or after migration to the second site to form maleic anhydride.

The commercial process, utilising vanadium phosphorus oxides, is mainly carried out in tubular flow reactors, although the use of fluidised bed reactors to minimise degradation of the catalyst by hot spots, and to allow higher hydrocarbon concentration feeds to be used, is developing. The catalyst is generally used pelletized and unsupported, having a low surface area (approximately 20 m^2/g). It

is fed with approximately 1% (by volume) of n-butane in air (other hydrocarbons in small quantities being included to increase yields). Space velocities of 1000 - 6000 hr^{-1} are used, with reactor pressures of just above atmospheric, and temperatures of 450 - 550 Celsius, although olefin feeds require less harsh conditions, and are oxidised at lower temperatures, commonly 400 Celsius [9,10].

3.1.2 Other active materials.

The development of a catalyst for the conversion of C4 hydrocarbons, principally n-butane, to maleic anhydride, caused by economic and legislative pressures being put on the benzene process, started with the catalyst which had been developed for benzene conversion. This catalyst, as mentioned previously in section 2.1, consists of V_2O_5-MoO_3, and was found to be active also for butene conversion to maleic anhydride. The optimum molybdenum concentration was identified as being between 25 and 30% MoO_3[32], and this composition also related to the highest activity of butene isomerisation in the absence of air at the same temperature, and the highest activation energy of ^{18}O exchange between the gas phase and the catalyst surface[33]. Use of 4-^{13}C-1-butene suggested a surface mechanism involving a cyclic intermediate, methylcyclopropane or cyclobutane[34,35].

Another material found to be active is a mixture of MoO_3 and P_2O_5, in approximately a 5:1 mix. The activity of this catalyst was found to be increased by the addition of a small amount of Bi_2O_3, up to a ratio of MoO_3:Bi_2O_3 of 1:0.1. This caused an increase in activity and selectivity of the catalyst, but further addition of Bi_2O_3 caused an increase in diene and CO_2 production[36,37].

Other transition metal molybdates have also been shown to be active[38-42] including Co, Ni, Fe^{II}, Fe^{III}, Mn and Cd. All these materials were found to become

even more active if a 10% excess of MoO_3 was used above the molybdate stoichiometric mix. Oxidation pathways seem to be similar to those identified as occurring on V-P-O catalysts.

3.2 Other Relevant Heterogeneous Partial Oxidation Processes.

In trying to understand the mechanism by which n-butane is oxidised to maleic anhydride, it is useful to consider the many other heterogeneous catalytic processes by which n-butane is selectively, partially oxidized. It is quite reasonable to use the vast amount of information available on the conversion of other members of the homologous series, in that each has to be initially activated by hydrogen atom abstraction followed by chemisorption and further dehydrogenation and/or oxygen insertion. The literature also shows that the mechanistic information and catalytic properties involved in olefin oxidation processes are useful, in that the adsorbed olefin is often similar, if not identical, to the adsorbed activated paraffin intermediate, it being formed by dehydrogenative chemisorption. Much use of the many recent reviews on this subject have been made[2,5,8]. Materials found to be catalytically active for the selective, partial oxidation of hydrocarbons are predominantly oxides. Very few metals are known to be of use, silver being probably of greatest importance.

3.2.1 Oxidation of C2 hydrocarbons.

Commercially the most important process in this area is silver-catalysed epoxidation of ethylene. This process has been performed for over 50 years on silver catalysts in fixed bed reactors, despite the expected advantages of fluidised bed

reactors due to the high reaction exothermicity, this is the general case throughout this field. The reaction mixture, ethylene (20-30%), oxygen (6-8%) and methane (to 100%), are fed at 10 bar through the reactor held at 250-300°C with a contact time of 1-4 seconds[5]. The catalyst usually consists of silver metal (up to 35%) supported on a low surface area carrier, usually silica, aluminosilicates or silicon carbide, and is prepared by impregnating the carrier with a silver salt. Salts with lower solubilities are favoured, as they result in a higher dispersions upon drying. Studies investigating silver loading[5] show that the silver exists as spherical particles, with the majority of the support surface left uncovered. Hence, increasing the silver content results in only a small increase in catalytic activity for a large change in loading and results in an actual decrease in the specific rate of reaction. Increasing the surface area of the support actually causes the ratio of silver to support surface area s to decrease and, therefore, results in an increase in support reactions and a consequential decrease in selectivity towards ethylene oxide.

The mechanism of both the primary and secondary reactions have been much studied. The main advances in elucidating the surface mechanism have been made using nitrogen oxides as the oxidant to identify the oxygen species responsible for ethylene conversion, and the effect of promoters (namely chlorine and caesium). The use of nitrous oxide to give a surface of silver on which only one type of oxygen is adsorbed has been reported by a number of workers[43,44,45]. The results have indicated that atomic oxygen is responsible for the formation of ethylene oxide. However, the conclusions from the experiments may be ambiguous, since it has been shown[43] that the surface decomposition of nitrous oxide yields both molecular and atomic oxygen species although in variable ratios depending on the partial and total pressure. It has been found that adsorbed atomic chlorine and dissolved atomic oxygen both promote the selective oxidation process[45]. The dependence of

catalytic activity upon chlorine coverage suggests that adsorbed atomic oxygen is responsible for both the partial and complete oxidation of ethylene, increasing chlorine surface coverage increasing selectivity, but decreasing overall activity. Some workers have suggested, as a result of using nitrous oxide, that di-oxygen species are responsible[46], but this theory is inconsistent with the effects of chlorine predosing on the deuterium kinetic isotope effect[47]. Atomically clean silver surfaces were found to be completely unselective towards ethylene oxide formation, but after preconditioning, so that the silver contained a significant amount of dissolved oxygen, ethylene oxide was formed with reasonable selectivity.

The promotional action of both chlorine and dissolved oxygen[44], it is argued, is an electronic promotion and the principal effect is a positive influence on the selectivity of the primary chemistry. The promotion is caused by the electronegativity of chlorine, or dissolved atomic oxygen, lowering the electronic charge state of the adsorbed atomic oxygen. This favours nucleophilic attack by ethylene, rather than nucleophilic attack by the oxygen which would result in hydrogen stripping and thus fragmentation of the hydrocarbon molecule. The latter process is favoured by the other major commercial promoter in use, caesium. Caesium, being an electron donor, has a negative effect upon selectivity, and caesium promoted surfaces increase carbon dioxide production by further oxidation of ethylene oxide. This supports the hypothesis that the promotional effects of chlorine, dissolved oxygen and caesium are largely electronic. The usefulness of caesium becomes apparent when the secondary chemistry is studied. Addition of carbon dioxide to the gas stream is known to have a weak selective poisoning effect on total oxidation, due to the formation of surface carbonate species, removing adsorbed atomic oxygen. Silver carbonate, at the reaction temperatures in use, is unstable and, therefore, its surface concentration is low, but caesium forms a much

more stable carbonate species and thus a higher steady state coverage, resulting in a greater concomitant depletion of adsorbed atomic oxygen, and, therefore, an increase in selectivity, but a decrease in overall activity.

A major undesirable secondary reaction is the isomerisation of ethylene oxide to acetaldehyde. Chlorine accelerates the rate of isomerisation, in contradistinction to the effects of caesium, confirming the hypothesis that these promoters act by electronic perturbation of the system.

The only other metal based catalyst to have shown selectivity in the partial oxidation of hydrocarbons is palladium[5], which is used to convert ethylene to acetaldehyde, acetic anhydride and acetic acid. The palladium catalyst has been studied and used in a large number of forms, including films and sponge, but more usefully supported on high surface area alumina or silica, with vanadia often present, and sometimes as gold or silver/palladium alloys. Low temperatures (<280°C) and long contact times are generally used and as acetic acid has been shown to adsorb strongly, thus poisoning the surface of the catalyst, when used with recirculating reactors efficient stripping of the products must be employed. Use of ^{14}C tracers[48] with acetaldehyde feeds confirmed the following mechanism, which had been previously postulated[49], but was difficult to prove, due to the rapid further oxidation of acetaldehyde.

$$C_2H_4 + O_2 \begin{cases} \nearrow & CO_2 + H_2O \\ \searrow & CH_3CHO \rightarrow (CH_3CO)_2O \rightarrow CH_3CO_2H \end{cases}$$

Investigations to study other noble metals[50] highlighted a good correlation between specific activity and % d-character and metal atomic radius, in increasing order Pt>Pd>Ir>Ru>Rh, but selectivity lay in the order Pd>Ir>Rh>Pt>Ru, showing palladium to be both selective and active. A catalyst of palladous and cuprous chlorides on active carbon has also been shown to be active[51], as have alumina-molybdena materials[52].

3.2.2 Oxidation of C3 hydrocarbons.

Just like ethylene oxide, propylene oxide is a very important industrial intermediate, but until recently a highly selective process by which it could be formed had not been found. Work on silver catalysts has proven unsuccessful because although conversion to non-combustion products could be achieved a wide range of other products are also obtained, thereby adversely affecting the economic yield, by causing high separation and purification costs. A process using hydroperoxides by Halcon International has, however, solved the problem recently. This is a homogeneous system, using a variety of soluble compounds of molybdenum, vanadium, titanium, niobium, tantalum, tungsten, and rhenium as catalysts.

Another industrially important propylene conversion process is the formation of acrolein. The discovery that cuprous oxide could selectively catalyse the reaction marked the beginning of many olefin to aldehyde processes[6,53,54]. However, recently a great movement forward started with the discovery that bismuth molybdate was highly selective for this reaction[55].

The cuprous oxide, often supported on high surface area alumina, has been investigated thoroughly and the active phase has been identified as copper-rich

cuprous oxide, oxygen rich Cu(I)O favouring complete oxidation. Two modes of chemisorption have been identified[56] each leading to different intermediates on the surface and giving different products: a π-bonded allyl surface intermediate leads to the formation of acrolein; while a surface Cu(I) acetate species decomposes to give carbon dioxide. The oxygen content of the active phase has been interpreted as having different oxygen species present, leading to a theory that in low oxygen content cuprous oxide O^{2-} in the lattice dominates and is responsible for selective partial oxidation, whereas, surface oxygen atoms which are dominant in oxygen rich phases lead to combustion. Investigations of methyl bromide promoter action[57] has highlighted its usefulness in increasing acrolein selectivity and minimising the effect of varying oxygen partial pressures, this being attributed to the presence of surface bromine removing excess surface oxide ions to form $BrO^-(s)$, seen as an anchoring of the Fermi level. Excess surface bromine leads to surface bromide and total loss of activity.

A bismuth oxide and molybdenum oxide combination, the basic component of the famous Sohio catalyst[55,58], displays extremely high activity and selectivity towards acrolein, even in the absence of oxygen. Gross kinetic features have shown propylene to acrolein oxidation to be first order in propylene and zeroth order in oxygen, with the rate constants of the parallel and consecutive combustion reactions being much lower. By use of isotopic tracers it is clear that the reaction proceeds by hydrogen abstraction and formation of a π-allyl surface species[59]. Further isotope tracer studies using deuterated propylene have shown that abstraction of a second hydrogen occurs before oxygen insertion[60,61].

The presence of minor products, acetaldehyde, propylene oxide and propionaldehyde, was investigated using variations in oxygen concentrations and post-reactor volumes[62], which cause variations in the minor product concentrations.

A surface initiated homogeneous gas phase reaction had been identified[63], initiated by desorption of free allyl radicals followed by reaction with surface or gas phase oxygen leading to a free, or more likely, a surface bound allyl peroxide or hydroperoxide. This could then desorb and act as a chain initiator, reacting with more propylene to yield propylene oxide, or undergo surface decomposition to form acrolein.

Conflicting evidence for the formation of carbon oxides by competitive and/or consecutive reactions has been put forward as the conclusions of ^{14}C labelled propylene and acrolein studies[5].

A number of other mixed oxides have been found to be active in the production of acrolein. These include mixtures of SnO_2-MoO_3, SnO_2-Sb_2O_5, Sb_2O_5-VO_2 and Bi_2O_3-Sb_2O_5[5]. The activities of these catalysts tend to be low, and at best only 50% selectivity towards acrolein has been achieved, this being with mixed oxides of tin and molybdenum. Water vapour in the feed stream is necessary to form surface molybdenum hydroxides onto which the propylene chemisorb s as a π-allyl complex. However, combinations of the oxides of bismuth, tin, antimony and uranium, sometimes with other oxides, have been shown to be active and highly selective for the partial oxidation of a wide range of hydrocarbons, as will be discussed later.

Commercial processes to oxidise propylene to acrylic acid use two stage reactors, the first stage being the formation of acrolein. W.R.Grace & Co.[64] use a Bi-Mo-O catalyst, whilst BASF[65] use a bed of Mo-W-Te oxide on steatite. The second reactor converts the acrolein to acrylic acid, the Grace process using a Co-Mo-Bi oxide and the BASF a Mo-W-V-Fe oxide on steatite. Few studies of these systems have been reported, but materials which directly convert propylene to acrylic acid have been investigated including oxides of Sn-Mo and Co-Mo-Bi[5].

These however, give low selectivity and also produce large amounts of acrolein. Molybdenum oxide with oxides of arsenic and niobium or tantalum give only traces of acrolein, but acetic acid is a significant by-product.

Oxidation of propylene to acetone is another potentially important process. It has been shown[66] that a wide range of molybdenum trioxide-containing materials are active, but only if the reaction temperature is kept low (100-300°C). The presence of steam in the feed is also essential otherwise allylic oxidation leading to C-C bond fission occurs. The molybdenum oxide materials found to be active included tin, cobalt, titanium, iron and chromium. Other oxides found to be active, but less selective, were vanadium, nickel, copper and zinc. The most effective material was SnO_2-MoO_3, with a Sn:Mo ratio of 9:1.

Mechanistic work using D_2O together with exchange rate measurements and infra-red spectroscopy[67] showed not only that SnO_2-MoO_3 gave a higher exchange rate than either SnO_2 or MoO_3, but that the deuterium appeared preferentially on the central carbon. This was explained by the reaction between the propylene and an acidic, surface OH group, giving a surface bonded isopropoxy group. Work with propylene-2-D confirmed this, and using H_2O^{18} [67] proved that the inserted oxygen atom comes from water, and not from molecular oxygen.

3.2.3 Oxidation of C4 hydrocarbons.

The preparation of 1,3-butadiene is a very important process due to the usefulness of the product in many manufacturing processes. The most effective catalyst for the conversion of straight chain C4 hydrocarbons to butadiene is bismuth molybdate, however cobalt and nickel ferrite; antimony, lead and cobalt molybdate, and bismuth or aluminium tungstate are also active, and show good

selectivity. Some of these materials showed increased selectivity with the addition of steam to the feed, or if the degree of crystallinity or macroporosity was changed. These factors provided an example of diffusional control of selectivity[68].

The production of diolefins from saturated hydrocarbons is not generally successful, due to the low reactivity of these compounds. However, in the presence of halogens and their compounds, the dehydrogenation of n-butane to butadiene is achieveable in good yields. Hydrogen iodide is the most efficient halogen species, other halogens or halo-compounds giving lower yields, the reactions usually being carried out over calcium oxide/iodide, alumina - sodium chloride or metal oxide impregnated silica gel. Studies in which the latter are used[69] showed little variation in butadiene yields over a wide range of metal oxides and halides, thereby confirming the idea that the reactions are not actually heterogeneous but are gas-phase.

Oxidation of butenes over bismuth molybdate is not only commercially important, but is also fundamentally significant as it exhibits some mechanistic features which can be applied to many reactions in the vast field of oxidation catalysis. Very high selectivities for 1-butene are achievable over bismuth molybdates commonly 90-95% at conversions of up to 80%. Reaction by-products include cis and trans-2-butene and carbon oxides, 1-butene having been shown to be the most reactive straight chain C4 olefin. Parallel and consecutive routes to carbon oxides have been identified, but these are well suppressed on bismuth molybdate surfaces. Work[70] has shown the oxidation to be a good example of a Mars - van Krevelen mechanism[16] (see section 2.2):

$$C_4H_8 + \square + O^{2-} \rightleftharpoons C_4H_7^- + OH^- \quad (1)$$
$$Mo^{6+} + C_4H_7^- \rightarrow [Mo{=}C_4H_7]^{5+}$$

$$[Mo{=}C_4H_7]^{5+} + O^{2-} \rightarrow Mo^{4+} + \square + OH^- + C_4H_6 \quad (2)$$

$$2OH^- \rightleftharpoons O^{2-} + \square + H_2O \quad (3)$$

$$O^2 + 2\square + 2Mo^{4+} \rightarrow 2O^{2-} + 2Mo^{6+} \quad (4)$$

□ - anion vacancy. $[Mo{=}C_4H_7]^{5+}$ - π allyl complex of Mo^{6+} & $(C_4H_7^-)$.

From the kinetics, found to be first order in 1-butene and zeroth order in oxygen, reduction steps (1 and 2) are rate determining and reoxidation (step 4) is fast. This is confirmed by comparing the rate of reduction of the catalyst to the rate of 1-butene oxidation, which as predicted is identical[71]. Studies of adsorption equilibria of butenes, butadiene, water etc. on bismuth molybdates[72] showed oxygen adsorption occurred only on partially reduced catalysts, and in contrast to the behaviour of hydrocarbons, increased with the degree of catalyst reduction. Hydrocarbon adsorption isotherms[72] were found to follow simple Langmuir type adsorption equations, and two adsorption sites were identified. The A-sites were single sites, able to adsorb butadiene slowly and irreversibly. Reduction increased A-site vacancies, which were also able to adsorb oxygen irreversibly and water weakly and reversibly. A-sites, it was concluded, were O^{2-} ions associated with a bismuth ion. B-sites, identified as dual sites, adsorb butadiene fast and reversibly (therefore weakly), and from full surface coverage values it was concluded that there existed two B-sites for every A-site, and that the B-sites were anion vacancies on a Mo^{6+} ion surrounded by corner shared O^{2-} ions. The active site for butene was

therefore concluded to be one A-site and two B-sites. Using this information a reaction pathway could be envisaged as adsorption of the butene onto a B-site and abstraction of a hydrogen atom to leave a B-site bonded π-allyl complex, this complex then undergoes abstraction of a second hydrogen atom leaving a weakly bonded butadiene molecule which could desorb. Two hydrogen atoms could then migrate to the A-site and desorb as a water molecule. However, if the butadiene becomes strongly attached to the A-site O^{2-} ion it would undergo further oxidation to produce carbon oxides via furan.

Antimony-oxide containing materials are also catalytically active for the production of 1,3-butadiene. The range of antimonates found to be active include vanadium, iron, chromium, tin, nickel, manganese, cobalt and copper. Vanadium antimonate was found to be the most active but least selective, while iron antimonate was both active and selective. Work on this range of materials, in particular iron antimonate[73], showed the catalytic behaviour to be attributable to the formation of the antimonate phase. Studies of pulse oxidation of 1-butene and the reduction - oxidation of the catalyst surfaces[74] showed the fully oxidised catalyst to be relatively unselective towards butadiene, but when up to 40% of an oxygen monolayer had been removed by reduction the selectivity increased to 90%, and the reaction proceeded by alternating reduction and oxidation of the already partially reduced surface. It was concluded that in the oxidation of butene two types of oxygen participate. One type (strongly bound to the catalyst) was thought to yield the diene, whilst the other (weakly bound) was thought to yield carbon oxides. The main partial oxidation by-products were isomerised olefins, and it was found[75] that the addition of alkali metals to tin - antimony catalysts reduced this isomerisation, this being attributed to neutralisation of Lewis acid - type sites. A third type of materials found to be active for butene to butadiene conversion is mixed metal

oxides with a spinel structure, mainly ferrites. This range of materials also exhibits a redox cycle mechanism for oxidative dehydrogenation. Dehydrogenation of straight chain alkanes was found to be much more difficult, as expected, but was found to occur over chromia - alumina catalysts, and work using ^{14}C labelled C4 hydrocarbons indicated a mechanism involving initial dehydrogenation at the 1- and 4-position to form a surface bound cyclobutene.

Oxidation of butenes over copper (I) oxide has been shown to produce a wide range of carbonyl compounds and other oxygenated hydrocarbons. Copper (I) oxide however is more effective for the oxidation of isobutene to methacrolein. It has been shown that the rate determining step in this process is the reaction between adsorbed isobutene and gaseous or weakly adsorbed oxygen. An improvement in the selectivity is achieved by the addition of halogens to the gas stream. This phenomenon has long been known to increase the specificity of propylene oxidation. These additives include halogen-containing compounds and selenium or sulphur dioxide, which have a greater electron affinity than the skeleton catalyst, and in the case of halogen modifiers, owing their beneficial effect on selectivity to suppression of the undesirable further oxidation of methacrolein.

3.2.4 Oxidation of C5 hydrocarbons.

The majority of work carried out in this field is in the dehydrogenation of C5 olefins to produce the respective diene. The motivation stems from the industrial importance of isoprene, and less so piperylene, which are used in the production of polymers with superior properties to natural rubber, and if copolymerised with isobutene, produce a product which can be vulcanised. Synthetic elastomers such as

cis-1,4-polyisoprene rubber often are more homogeneous and resistant to cold and ageing than natural rubbers.

Modern catalyst technology has enabled selective oxidative dehydrogenation of isopentene in the presence of other C5 olefins or paraffins to be carried out without any effect on the latter. Such a catalyst is a mixed oxide of iron, phosphorus and rhenium[76].

The oxidation of straight chain C5 olefins is generally unselective: for example over cuprous oxide, unlike the oxidation of propylene, the oxidation of 1- or 2-pentene is unselective giving a wide range of partial oxidation products, including saturated C1 to C5 carbonyl compounds, as well as carbon dioxide[77]. Bismuth molybdate shows high selectivity at low conversions of 1-pentene to 1,3-pentadiene (88%), but as the conversion rises above 5% the selectivity drops so that at 15% conversion the selectivity is 79%. In contast, the same material gives a selectivity of >90% for 1-butene to 1,3-butadiene over a conversion range of 20-80%. Investigations into this phenomenon[78] have shown that the reaction products interfere with the oxygen chemisorption. As kinetics have indicated a mechanism[78] which involves a rate determining step of abstraction of an allylic hydrogen atom from a gas phase or physisorbed olefin molecule by oxygen chemisorbed on the surface, oxygen chemisorption inhibition would have a dramatic effect. This seems to be confirmed by investigations of pumice-supported V_2O_5 catalysts for the oxidation of 1-pentene and cis or trans-2-pentene[79]. After 5 hours the catalyst showed vastly different behaviour from the fresh material. The fresh catalyst shows reasonable selectivity and produces mainly acetaldehyde and propionaldehyde, whereas the aged material gives a wide range of products, including CO_2.

Oxidation of branched chain C5 hydrocarbons has been shown to be much more selective, although conversion of isopentane is naturally much more difficult than is isopentenes, and generally requires the use of halogen selectivity promoters. Iodine is the most effective promoter with catalysts such as MnO_2, $CaO/CaCO_3$ and NaOH on alumina, since these are good hydrogen iodide acceptor materials.

Isopentenes, having greater inherent reactivities, can be dehydrogenated to produce isoprene with good selectivities at reasonable conversions. Cuprous oxide gives acceptable selectivity, but also produces a wide range of by-products caused by oxygen insertion, these being C1 - C5 carbonyls, as well as combustion products. A number of studies of cuprous oxide-catalysed oxidative dehydrogenation of C5 and C4 olefins has yielded the expected trend in hydrogen abstraction, ie. attack of a tertiary carbon being more likely than of a secondary, etc., as expected, since a surface bound π-allyl species would probably be formed.

Bismuth molybdate catalysts also produce a reasonable range of products, and as with straight chain pentenes, oxidative dehydrogenation, although initially fairly selective, declines rapidly in selectivity at higher conversions, due to surface poisoning. Studies[80] relating inhibition to the possible reaction products, identified by allylic hydrogen abstraction, show that if the olefin has a vinylic methyl group, unsaturated aldehydes can be formed, and these strongly inhibit the reaction. Dienes, being the favoured product, are only weakly adsorbed and therefore result in a weak poisoning effect. However, even when 3-methyl-1-butene is used, which produces isoprene as the major product, the conversion should not be allowed to become too high, as a diene-aldehyde is produced which results in a consequential onset of severe poisoning.

Cobalt and tin molybdate materials give a range of saturated ketones primarily, but also produce isomerised olefins and combustion products.

3.3 Homogeneous Catalysts for the Partial Oxidation of Hydrocarbons.[81-85]

Homogeneous catalysts although able to partially oxidise hydrocabons, often with very high selectivity under mild reaction conditions, are very different to any heterogeneous analogues, the "active centres" of a solid catalyst are closely associated, electronically, with other identical surface active sites and the very similar bulk material. Whereas homogeneous catalysts although having "active centres", known as the active species, are often surrounded by a coordination sphere of ligands and/or solvent, so that close association with any other active species or bulk material able to act as an oxygen and/or electron transportation or storage medium does not exist. However, the elements and their oxidation states are often the same and there exists, in some cases, an analogy between the solid surface active centres and the solvated active species, so a brief survey of active materials, but in this case not the mechanism as it will probably be vastly different, follows.

Ethylene conversion to acetaldehyde[81], known as the Wacker process, is catalysed by an aqueous solution of cupric chloride containing trace amounts of palladium chloride. The ethylene oxidation to acetaldehyde occurring on the palladium chloride, which causes a reduction to elemental palladium, which in turn is reoxidised by cupric chloride. The redox cycle being completed by reoxidation of cuprous chloride by oxygen.

An extension of the Wacker process has allowed the conversion of propylene to acetone and methyl ethyl ketone from butenes, the catalyst being nearly identical, but process conditions being modified to allow for the different reactants and products.

Conversion of ethylene to vinyl acetate resembles the acetaldehyde process except the redox catalyst system is dissolved in acetic acid instead of water, the

system must be accurately buffered and the chloride ion concentration is also very critical, and as chloro byproducts are formed it must be continually replaced. An interesting heterogeneous analogy exists for this process (see section 3.2.1). The catalyst, palladium on carbon or alumina, is fed with an ethylene, acetic acid, oxygen mix. The catalyst is supported on heat exchanger tubes, and rapid product cooling is necessary to separate the liquid products from the unreacted acetic acid.

The oxidation of saturated hydrocarbons to alcohols, is as already stated, obviously difficult as often the result is chain fission. However, the higher n-paraffins can be oxidised in the presence of boric oxide to yield a mixture of secondary alkyl borates without chain fission. These borates, if kept at low concentration, can be hydrolysed to give alcohols, but if the conversion is allowed to get too high ketone formation increases.

Other organic oxidation processes are catalysed, usually, by elements that can change valence fairly readily, e.g. Co,Cu,Mn. Often they are combined with a fairly large organic fragment either as a salt or chelate to make them soluble in the organic substance to be oxidised.

CHAPTER 4

EXPERIMENTAL TECHNIQUES

The first part of this chapter describes the characterisation techniques used, brief description of each technique will be included as they were performed on commercially available instruments using standard proceedures. The second section deals with the catalyst evaluation rig that was designed, built and optimised, and because it is a unique piece of apparatus it will be described in great detail.

4.1 Catalyst Characterisation.

4.1.1 X-ray diffraction. (XRD)

X-ray powder diffraction patterns were taken using a Phillips PW1050 goniometer on a Phillips PW1010 X-ray generator. Nickel filtered Cu Kα radiation was used with a proportional detector feeding to a 2000 series electronic counting chain, and a scan speed of two minutes per degree (2Θ). Identification of the phases present was performed using the JCPDS powder diffraction file of d - spacings.

4.1.2 Thermogravimetric analysis. (TGA)

TGA profiles were obtained using a Dupont 951 Thermogravimetric analyser module linked to a Dupont 1090 microcomputer thermal analysis system. Powder samples were analysed in an open platinum foil boat, the furnace chamber being continually purged at 40 ml /min. to provide the required dynamic atmosphere for

the experiment. Temperature profiles were recorded at a linear heating rate of 10 degrees per minute; isothermal runs were initially heated to the desired temperature at this rate then held at the same temperature for the desired time. Temperatures quoted are sample temperatures and were recorded using a type K thermocouple placed within a few millimetres of the sample boat.

4.1.3 Specific surface area. (SA)

Measurements of the surface area of the catalytic materials were made using a Micromeritics 2600 Digisorb, with nitrogen as the adsorbent. Surface area values were calculated using the Brunauer, Emmett and Teller (B.E.T.) method[86], using either three or five points between partial pressures 0.05 and 0.21 P_0. Pore volume and pore area distributions were calculated by an algorithm based on Faass's[87] implementation of the Barrett, Joyner and Halenda (B.J.H.)[88] method using twenty six point full isotherms.

4.1.4 X-ray photoelectron spectroscopy. (XPS)

Samples for XPS were pelletised using a 12 mm die at 5 tonnes without a binding agent, before attaching to stubs with silver dag. Spectra were taken with a V.G. Escalab II using aluminium Kα radiation. Wide spectra (kinetic energy 500 - 1500 eV) were initially taken at 1 second per point and 1 eV resolution. All narrow narrow range spectra were taken at 0.1 s/point at 0.1 eV resolution and spectra were summed 20 times, except for carbon and copper peaks which were scanned 5 times. Corrections for charging were made using advantitious carbon, which was

corrected to 1201.8 eV kinetic energy (284.8 eV binding energy). Species were identified using references 89, 90 and 91.

4.2 Catalyst Activity Measurements.

The partial oxidation of n-butane was performed using a continuous flow, fixed bed reactor, with a gas chromatograph analytical system.

4.2.1 Reactor system.

A reactor system (Figure 1) was built with the aid of designs from the available literature[3,42,92,93,94] and from the design of catalyst evaluation rigs already in use with the Applied Chemistry Group, Harwell Laboratory[95]. Gases are fed into the laboratory to MKS modified Tylan 360 mass flow sensors with Brooks solenoid valves controlled by a MKS 254 controller unit, calibrated for air at room temperature and pressure (21 Celsius and 101 kPa) and capable of delivering a constant accurate flow with variable downstream pressures. Three mass flow controller units were available, one with a selectable input of one of four gases. The output from the flow controllers was fed into a tortuous path mixing chamber, to ensure thorough mixing, and then through a solenoid valve (for instant shut off by the alarm monitoring system in the event of runaway or an accident) and past a Maywood Instruments capacitance pressure transducer, to measure and record gas input pressure. The reactant feed stream was then fed through a Valco gas injection valve to allow sampling of the reactant mixture, or in an alternative configuration to

Diagramatic representation of catalytic microreactor system

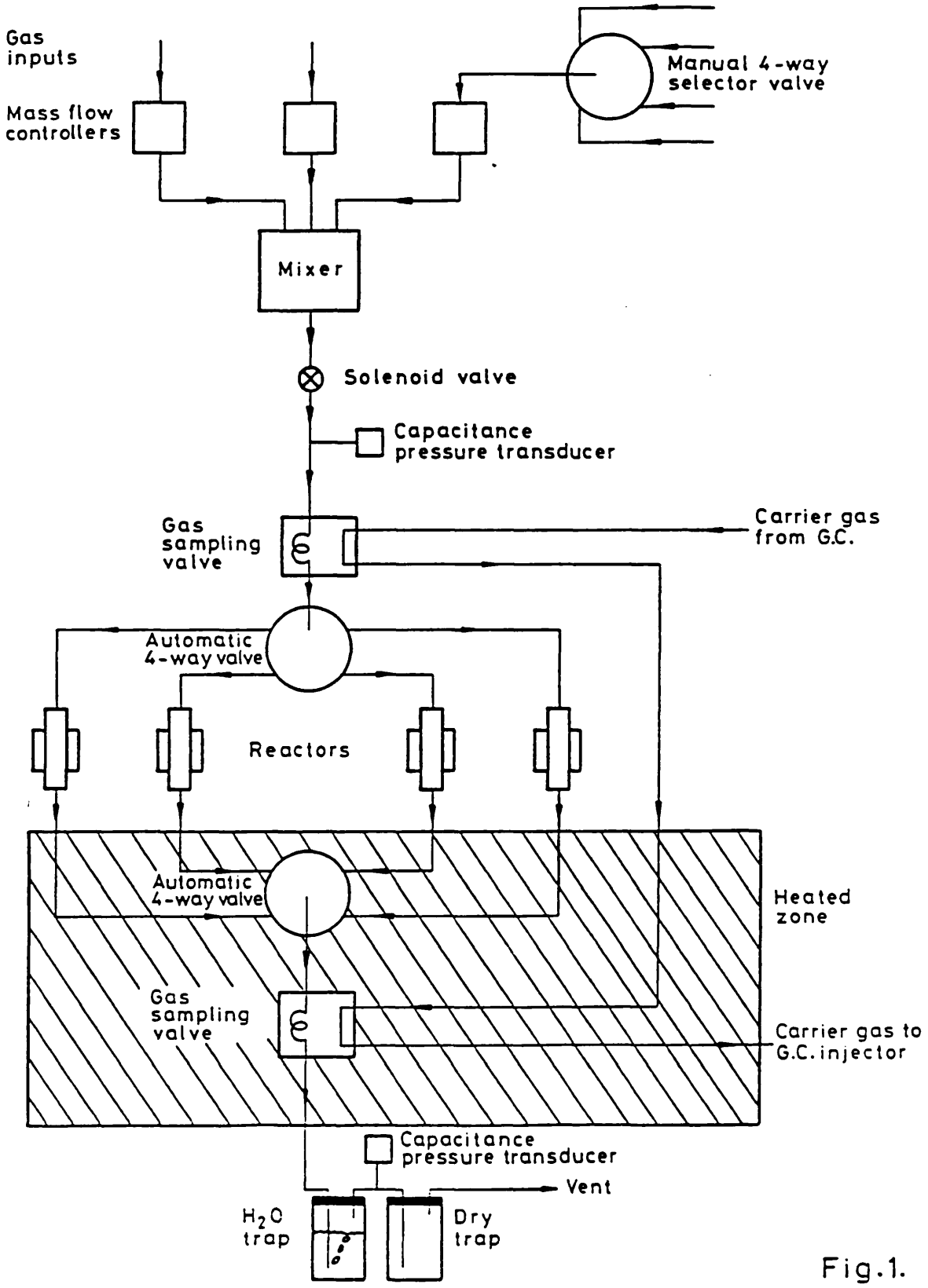
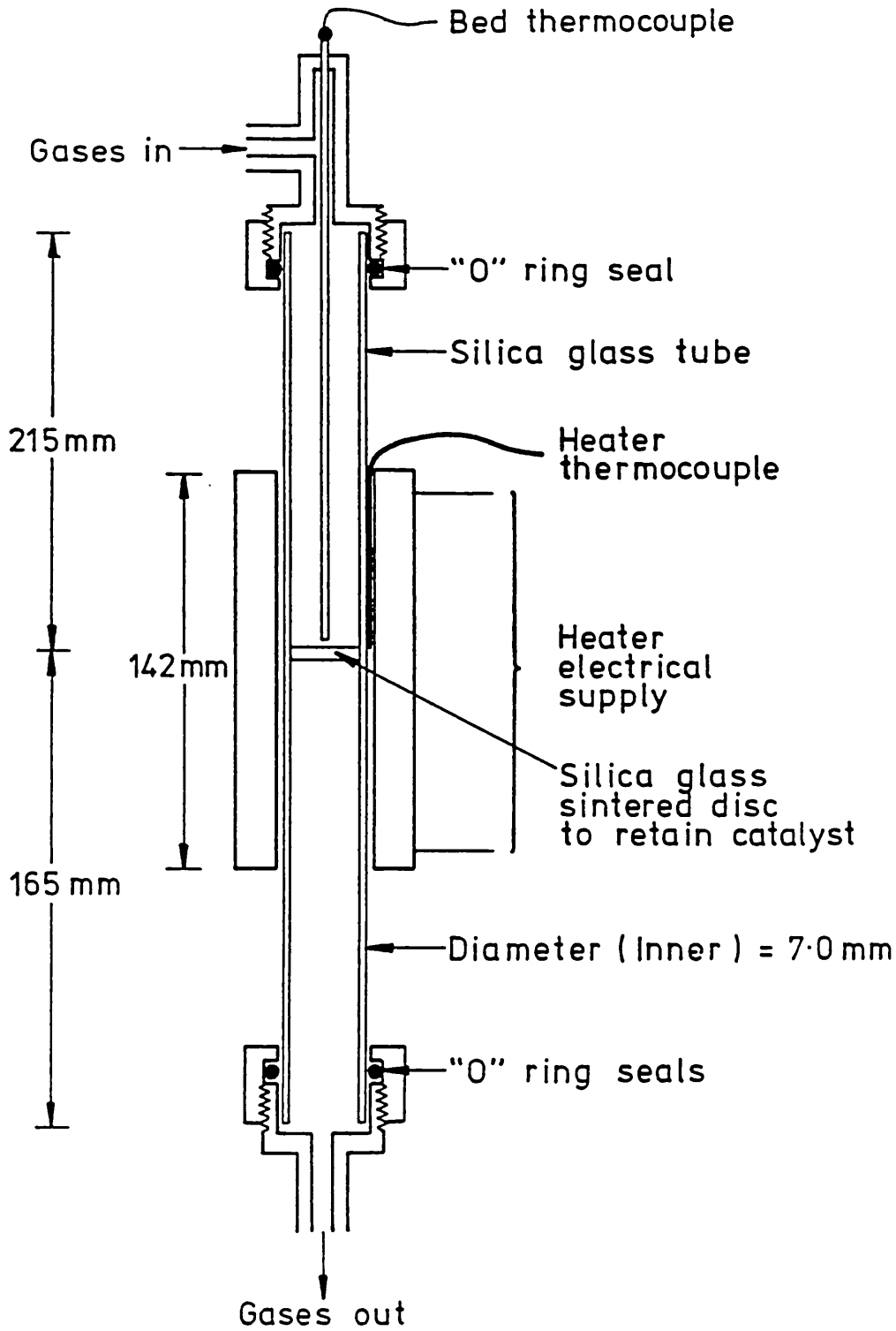


Fig.1.

allow slugs of reactant gas to be passed over the catalyst in an inert feed stream, usually the gas chromatograph carrier gas (helium).

The gas was then fed into the top of the reactor tube, a vertical silica glass tube (7.0 mm I.D. x 38 cm long)(Figure 2). The catalyst was supported as a powder, on a silica sintered glass frit to hold it in a reproducible position, and had a plug of silica glass wool on the gas input side. The reactor was resistively heated by a Nichrome wire coil in a pyropholite former; furnace temperature measurements and control feedback being provided by a type K thermocouple placed in the pyropholite furnace former. The catalyst bed temperatures were measured with a type K thermocouple placed in the catalyst bed. Approximately 0.5g of ungraded lightly ground catalyst powder was usually used, with a gas flow rate of approximately 20 ml /min giving an average gas hourly space velocity (G.H.S.V.) of approximately 1000 hr^{-1}. Negligible pressure drop across the catalyst bed was measured under these conditions.

The gases on exiting the reactor were fed along stainless steel lines heated by heating tapes fed from Variacs, the temperatures of which were monitored by type K thermocouples attached to the stainless steel lines. Typical temperatures were 160 - 200 Celsius, to stop any gases condensing out of the product stream. The gases were then fed through an oven-heated Valco gas sampling valve (heated to 220 Celsius), to allow samples for analysis to be taken. Finally the hot gases were fed through a room temperature glass "U" tube, past another Maywood Instruments pressure transducer to monitor output gas pressure (placed after the "U" trap to stop contamination by condensables), and then through a cold water bubbling trap before being vented outside the laboratory. Facility was also available for up to four reactors to be run sequentially by the addition of a Valco 4 way selector valve



REACTOR

Fig.2.

above and below the reactors, should uninterrupted analysis of up to 4 catalysts be required at a later date.

Automatic control of the gas sampling valves, 4 way selector valves, and the catalyst temperature was achieved using a Honeywell Digital Process Controller DCP 7700, allowing accurate control and reproducible run conditions to be made with simple programmes. Temperatures up to 1000 Celsius, at carefully controlled temperature ramp rates of up to 100 degrees per minute, and total flows of up to 300 ml /min were achievable (corresponding to a G.H.S.V. of 18000 hr^{-1} for 1 ml of catalyst).

Temperatures, pressures and flow rates were monitored by a Rosemount Alarm monitoring system and recorded by a Chessell 6 pen plotter. Any alarm conditions, e.g. temperature, pressure or flow, or gas leaks sensed by gas detectors over user adjustable levels shut the rig down safely, cutting off gas supplies with the inlet solenoid valve and cut power to the furnace immediately. This high level of automation and monitoring allowed the rig to be run 24 hours per day.

A typical stepwise programme is shown in Figure 3. An initial sample is taken by the product stream injector with the reactor flushed out, and at room temperature. The reactor was then ramped at 20°/min. to 250 Celsius, and held at that temperature for 2 hours and towards the end of which an injection was taken from the product stream. The reactor was then ramped to 275 Celsius, held for 2 hours and another injection taken of the product stream. This stepping continued at 25° steps up to 500 Celsius to build up a temperature profile of catalyst activity. After 2 hours at 500 Celsius a final injection was taken, the programme ended and the reactor allowed to cool naturally to room temperature, ready for the replacement of the catalyst with another sample, after which the programme could be restarted after the reactor system has been thoroughly flushed out.

Typical Stepwise Temperature Programme

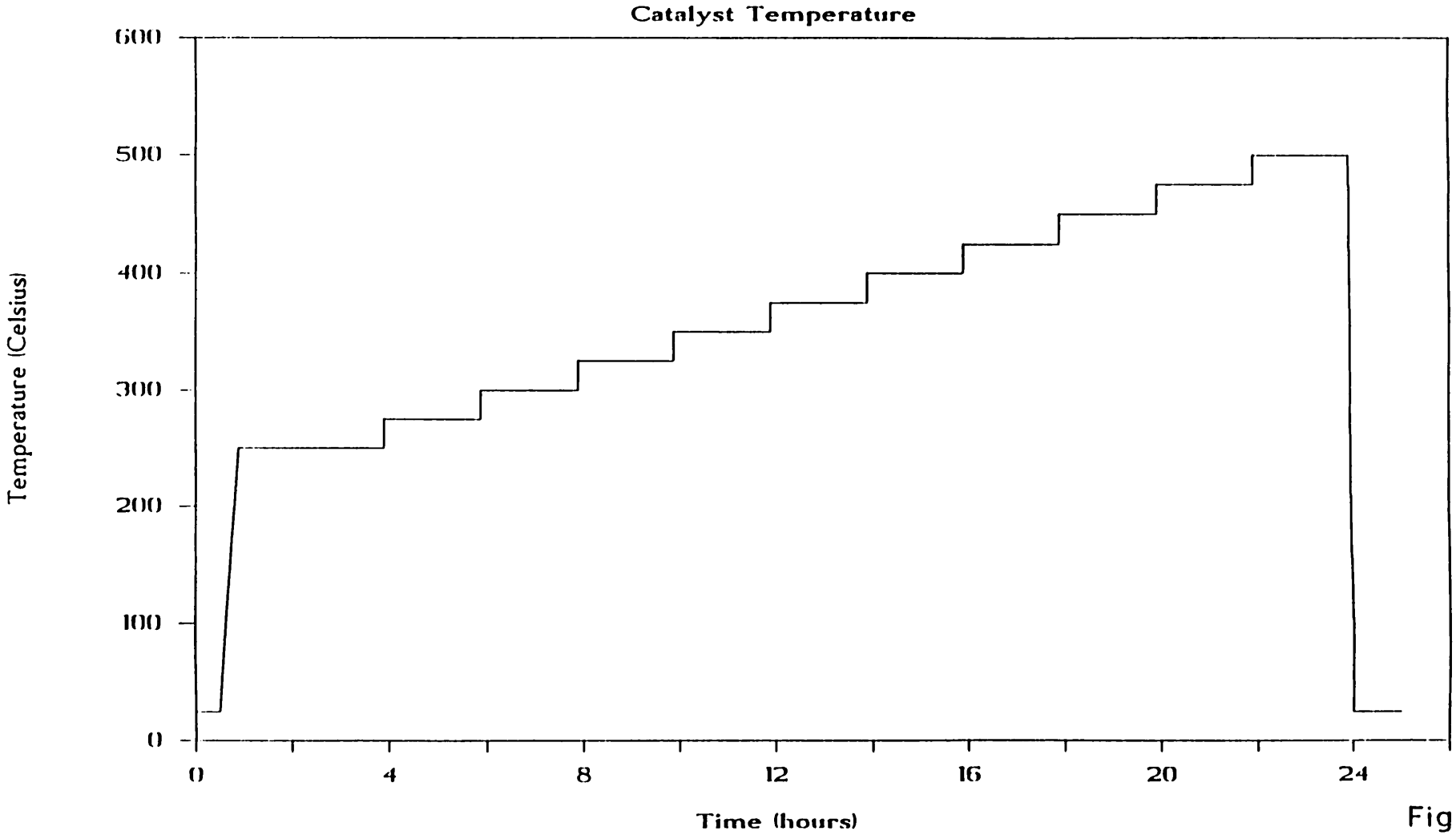


Fig.3.

4.2.2 Gas Chromatograph analysis system. (G.C.)

With the initial use of the available literature (ref. 3,42,92,93,94) and then by experimentation with bottled gas mixtures and injected standard samples, a pair of analysis methods was identified and perfected to give full product stream analysis from a single hot sample. All previous work reported in the literature on this reaction required at least two injections into separate gas chromatograph systems. The motivation for developing a single injection system was to allow analysis of the product stream at a single instant in time to be obtained. The first method developed achieved full product analysis from a single hot sample, but did not separate many of the product stream species, although it was much quicker than the second for full product elution from the column and therefore was used for the rapid testing of materials identified from the literature survey and theoretical considerations as of possible interest. The second method gave a much better product separation and, therefore, was used for the more detailed activity studies.

A Perkin - Elmer Sigma 1 Gas Chromatograph controlled by a P-E Sigma 1 Data Station was used with helium carrier gas and series connected thermal conductivity (TCD) and flame ionisation detectors (FID). The FID was optimised for hydrogen/air ratio using high temperature bleed from a porapak Q column. The detector outputs were fed through a P-E LCI100 analogue to digital converter into a Perkin-Elmer 3203 minicomputer with a LIMS database (Laboratory Information Management System) running a CLAS software package (Chromatography Laboratory Automation System). The minicomputer was used to collect and analyse all raw chromatography data outputted by all the gas chromatographs in use. The CLAS software integrates the chromatogram using a user inputted method and automatically outputs an analysis report. It also allows full reintegration and curve

arithmetic, as well as LIMS data base searching of many chromatography runs to get trend analysis etc. The helium carrier gas is first metered by the G.C. through the two Valco injector valves, which when actuated automatically send a start signal to the G.C. The carrier gas then returns to the G.C. along heated lines (200 Celsius) where it is fed onto the column. A reference helium supply is also metered and fed through an empty stainless steel tube in the G.C. oven to the reference side of the TCD.

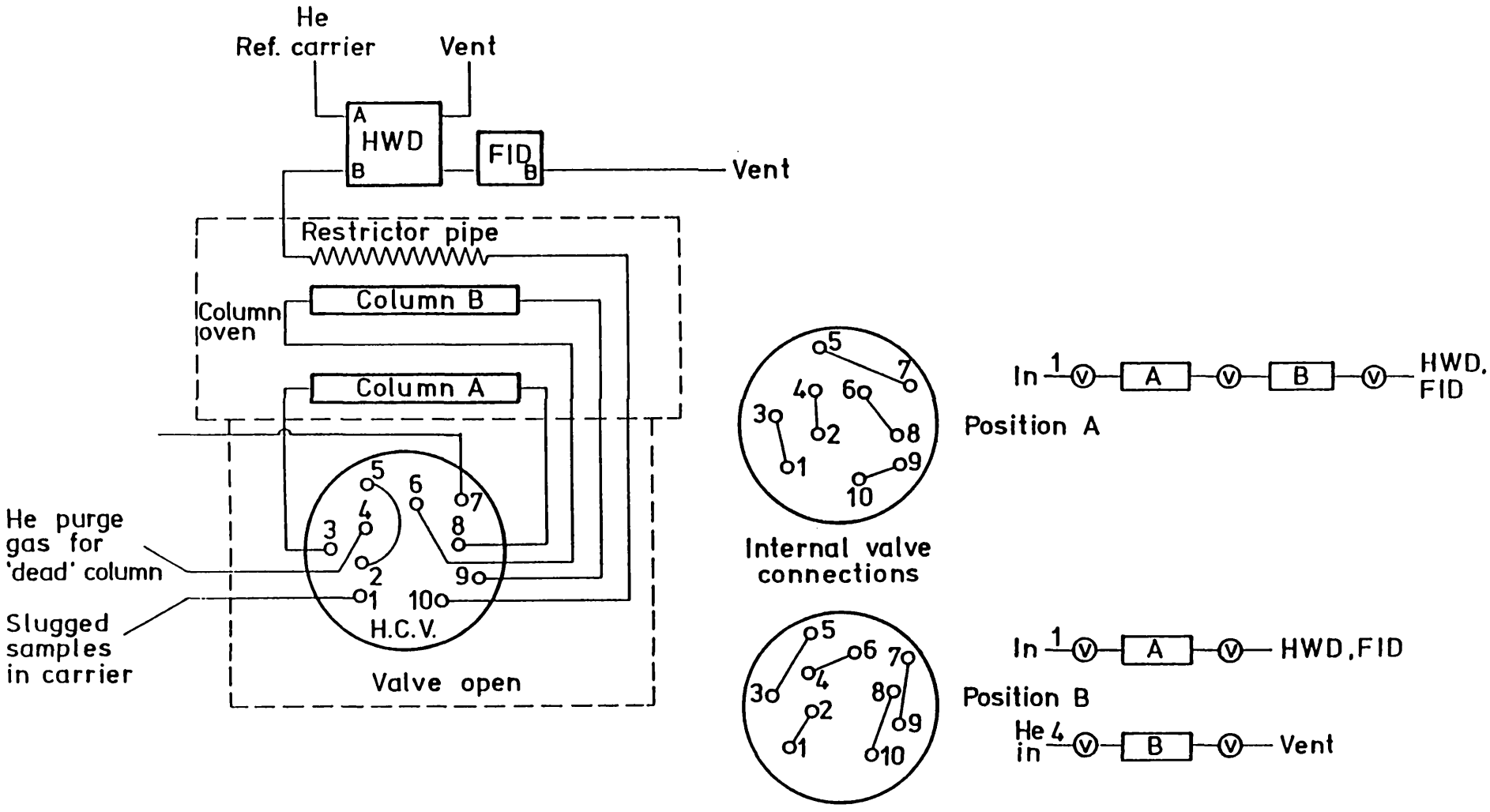
4.2.3 Gas Chromatographic analysis methods.

The first method used a single porapak QS column (0.25 inch O.D. × 0.5 m long). The hot sample was injected onto the front of the column, the G.C. oven was held at 180 Celsius for 4 minutes then ramped at 40°/min. to 200 Celsius (maximum column temperature) and held for 30 minutes, at a helium carrier gas flow rate of 60 ml /min. Air, carbon monoxide and carbon dioxide were essentially eluted together after 0.5 minutes and detected with the TCD. Carbon dioxide, if in reasonable concentration, appeared as a shoulder on the trailing edge of the peak, but quantitative integration was not possible. The n-butane peak appeared at a retention time of 2.85 minutes, and was detected using the FID and quantitatively integrated to give, on calibration, a response factor of 2.50×10^6 area units / % (vol.). The maleic anhydride peak was detected by the FID after a retention time of 25.0 minutes, having been calibrated using known amounts of maleic anhydride injected onto the column with a pyroprobe set at 500 Celsius, and gave a response factor of 3.833×10^3 area units / μmol.

The second method was developed to separate the peaks seen in the chromatogram with greater efficiency, and therefore enable quantitative analysis of

more of the product steam species to be achieved. A system that was found to give the desired separations was as follows, also depicted in Figures 4 and 5. Two columns were used with an automatic Valco 10 port - 2 way valve (heated to 220 Celsius) under the control of the P-E Sigma Data station. The first column (A) was a 1 metre × 1/4 inch O.D. glass porapak QS, the second a 1 metre × 1/8 inch O.D. stainless steel spherocarb. The use of a glass porapak QS column was found to be necessary during the course of this work, since when a stainless steel column was used the maleic anhydride was found to adsorb strongly to the walls of the column giving unreliable responses. After initial experiments were carried out to identify suitable columns, carrier gas flow rate and oven temperatures had to be optimised so that the carbon dioxide eluted sufficiently long after the air for peak integration but leaving a long enough gap before the hydrocarbons to allow switching of the 10 port valve before the butane eluted. Also total analysis time, time for elution of the maleic anhydride, had to be kept reasonably short. From these optimisation trials the following method was finalised.

The two columns were held initially in series at an oven temperature of 70 celsius for 5 minutes, the sample being loaded onto the front of the porapak column. The permanent gases (air, carbon monoxide and carbon dioxide) passed practically unhindered through and were separated by the spherocarb column. Air and carbon monoxide eluted after 3.80 and 4.46 minutes respectively and were detected using the TCD. The oven temperature was then ramped at 30°/min. to 160 Celsius where it was held for 4 minutes. Carbon dioxide was detected by the TCD eluting after a retention time of 10.40 minutes. As all the permanent gases had eluted and all the organics had been retained on the porapak column, the 10 port Valco valve was switched so that the species coming off the porapak were sent straight to the detector, and the spherocarb was switched out of "circuit", and purged with an



GAS CHROMATOGRAPH

Fig.4.

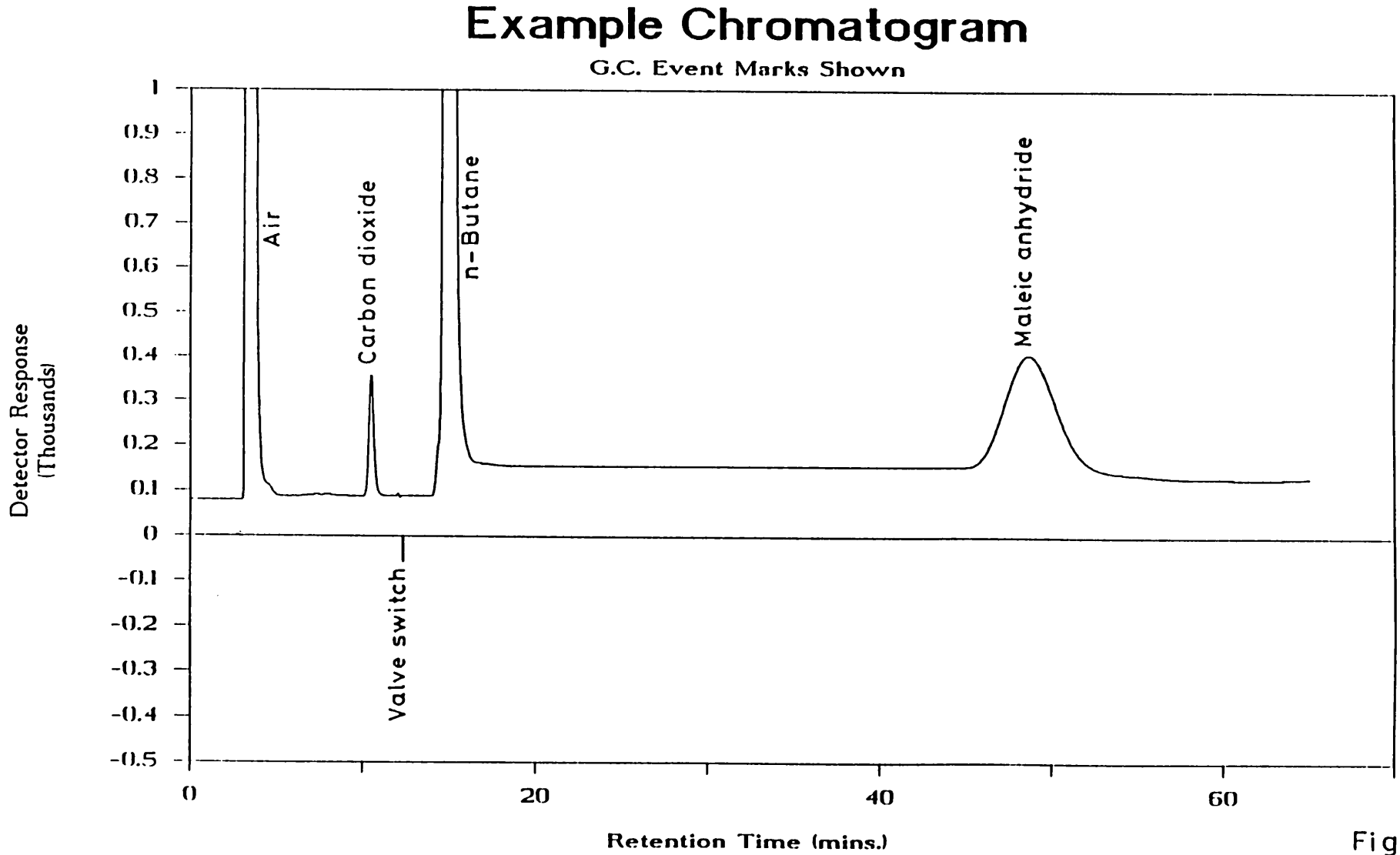

Example Chromatogram
G.C. Event Marks Shown
Detector Response (Thousands)
1
0.9
0.8
0.7
0.6
0.5
0.4
0.3
0.2
0.1
0
-0.1
-0.2
-0.3
-0.4
-0.5
Air
Carbon dioxide
n-Butane
Maleic anhydride
Valve switch
0
20
40
60
Retention Time (mins.)

Fig.5.

auxiliary supply of helium to stop any high temperature damage to the packing material. The data was also switched from being collected from the TCD to being collected from the FID. The oven temperature was then ramped at 40°/min. to 200 Celsius, and held for the remainder of the chromatographic run (55 minutes). In front of the detectors a restrictor pipe was placed to stop the FID flame being blown out when switching of the valve caused a momentary interruption followed by a surge of helium.

At a retention time of 14.80 minutes n-butane was eluted and detected by the FID, maleic anhydride being detected as eluting by the FID at a retention time of 48.80 minutes. A listing of the G.C. control programme and the data analysis method is included in appendix A. Response factors for carbon monoxide, carbon dioxide, n-butane and maleic anhydride are shown in the data analysis method listing. It was found by injecting mixtures of n-butane, 1-butene, cis- and trans-2-butene, and 1,3-butadiene that separation of these C4 hydrocarbons did not occur on this porapak column under the conditions used. However, by reducing the oven temperature and/or lengthening the column this separation could probably be achieved, but this would result in a great increase in the retention time for maleic anhydride, and, therefore, was considered undesirable. Use of a different column could also achieve this separation but would affect the retention times of other peaks.

4.3 Initial Experiments.

A few initial experiments were carried out to determine the inertness of the reactor system, and assess diluent materials that at a later stage might be necessary in reducing the probability of hot spots or nonisothermal behaviour of the catalyst bed due to the high exothermicity of the reaction under study.

Firstly, a complete stepwise run from 250 to 500 Celsius was performed as described in section 4.2.1 and figure 3, with an empty reactor, but with the catalyst bed thermocouple and silica wool plugs in the reactor, to confirm that the reactor system did not catalyse any reactions (combustion or partial oxidation). G.C. method 2 was used to analyse for product stream species for extra sensitivity. The results from this experiment showed that at each of the temperature values tested between 250 and 500 Celsius no conversion of the n-butane was detectable, nor was any other species detected except the feed gas of 1% n-butane in synthetic air. Therefore, for the purposes of this study the materials used to construct the reactor system were concluded to be inert, and, therefore, suitable for study of the chosen reaction. This experiment was conducted again at the end of the experiments using the reactor system, to re-check that the reactor materials were not partaking in any catalysis; and at each instance no reaction could be detected. This experiment also was useful in that it showed that the sample size at each reactor temperature was constant, and that no anomalous effects were occurring.

The second experiment was designed to check the inertness of silica granules. The reactor was packed with 5 grams of silica granules (Fluka chemicals, 0.2 - 0.7 mm diameter, 99.9 % purity, coating quality), together with the silica wool plug and thermocouple. An identical experiment was carried out as above, but in this case it was found that at 450 celsius and above, carbon dioxide and a few other unidentified

species were detected, with a slight decrease in n-butane concentration. The use of these silica granules was, therefore, deemed unsuitable.

The third experiment was designed to check the inertness of silicon carbide as a diluent material. The reactor was packed with 5 grams of silicon carbide (Sohio Electrominerals, 24 grit - 0.7 mm diameter, green grade 99.99 % purity), together with the silica wool plug and the catalyst bed thermocouple. The experiment was re-run, but again at 450 celsius and above carbon dioxide and other unidentified species were detected with a small decrease in n-butane conversion. Therefore, the use of these silicon carbide granules was also deemed unsuitable if isothermal runs above 400 Celsius were to be carried out, and if a diluent was found to be necessary at a later date (e.g. to investigate kinetic parameters) a higher grade silica or silicon carbide or alternative materials would have to found and tested.

CHAPTER 5

INVESTIGATIONS OF THE PALLADIUM / COPPER SYSTEM

As stated in chapter 1 the objective of the research was to explore the properties of catalysts based upon the palladium/copper system in relation to the selective oxidation of n-butane to maleic anhydride. In carrying out these objectives careful consideration was taken of the results of the literature survey of materials found to be catalytically active for hydrocarbon partial oxidation. Section 3.3 which discusses homogeneous catalysts used currently for the partial oxidation of hydrocarbons shows the usefulness of the palladium/copper couple in the Wacker process. It was therefore decided to investigate a heterogeneous analogue to this catalyst for the oxidation of n-butane to maleic anhydride. Heterogeneous analogues to the Wacker catalyst have been reported in the literature[96], however, the catalyst used was an alumina supported palladium/vanadate and not a palladium/copper material. Therefore, an initial investigation of palladium salts on a cupric oxide lattice was performed and is described below.

5.1 Catalyst Preparation.

The basic preparation method used for the catalysts described in this chapter was to dissolve the palladium salt (Johnson Matthey Chemicals) in water and then

to add the cupric oxide (Fisons AR grade) whilst stirring, and evaporate to dryness in an oven at 80 Celsius. Catalyst compositions are outlined in table 5.1 below.

Table 5.1

Catalyst	Support	Palladium salt (loading)	Preconditioning
1	CuO	$PdCl_2$ (2.6%)	Dried
2	CuO	$PdCl_2$ (2.6%)	Dried and reduced
3	CuO	$PdCl_2$ (0.45%)	Dried
4	CuO	$PdCl_2$ (0.45%)	Dried and reduced
5	CuO	$Pd(NO_3)_2$ (2.6%)	Dried
6	CuO	$Pd(NO_3)_2$ (2.6%)	Dried and reduced
7	CuO	-	Dried

5.1.1 2.6% palladium (from the chloride salt) on cupric oxide. (N°'s 1 and 2).

To a solution of palladium chloride in dilute hydrochloric acid, giving a solution of $PdCl_4^{2-}$ ions, was added, whilst stirring, cupric oxide to give a loading of 2.6% (by weight) of palladium. This palladium loading was empirically calculated to give, on reduction of the palladium, a monolayer of palladium atoms on the surface of the cupric oxide. The suspension was then evaporated to dryness in an oven overnight at 80 Celsius in air. Part of the material (catalyst 2) was then reduced, in a tubular furnace, at 200 Celsius in a flowing atmosphere of 5% hydrogen in argon, the temperature at which pure palladium chloride was found to decompose to

elemental palladium in a study carried out using the thermogravimetric analyser. The second portion (catalyst 1) was retained in the dried state.

5.1.2 0.45% palladium (from the chloride salt) on cupric oxide. (N°'s 3 and 4).

These materials were prepared in the same way as the 2.6% material, but this particular palladium loading was calculated as that required to cover the surface of the cupric oxide (measured by nitrogen physisorption as 9.33 m^2/g) with exactly one monolayer of square planar $PdCl_4^{2-}$ anions. Therefore in the dried, unreduced, form (catalyst 3) the material should be approximately a monolayer of palladium chloride anions on the surface of the cupric oxide. On adding the cupric oxide to the solution of palladium chloride anions the mixture was thoroughly stirred to release any trapped air, and it appeared on visual inspection that the solution wetted the surface of the cupric oxide well. Again a portion of the dried material was reduced using the same conditions as before to produce catalyst 4.

5.1.3 2.6% palladium (from the nitrate salt) on cupric oxide. (N°'s 5 and 6).

In order that any effects of any chloride could be determined a batch of material was made, using the same method as before, with palladium nitrate instead of palladium chloride. The palladium nitrate, sufficient to give an elemental palladium loading of 2.6% (by weight), was dissolved in the same amount of distilled water that had been used previously for the chloride preparations and cupric oxide was added to this solution whilst stirring. The suspension was evaporated to dryness overnight at 80 Celsius. A portion of the material was retained as catalyst 5 and the other portion was reduced in 5% hydrogen in argon at 200 Celsius for 3 hours

(catalyst 6), a temperature sufficiently high for full reduction of pure palladium nitrate determined by thermogravimetric analysis.

5.2 Catalytic Activity.

The catalytic performance of the materials described above was studied for the conversion of n-butane using the microreactor apparatus described in chapter 4. 0.5g of the catalytic materials and a flow rate of 20 ml /min (at STP) of 1% (by volume) of n-butane in synthetic air (21% oxygen, balance nitrogen) were used as the standard conditions, this gave a gas hourly space velocity of approximately 1300 hr^{-1} which is within the range of space velocities that the commercial vanadyl pyrophosphate catalysts are used. The temperature programme of the reactor was 25° steps from 250 to 500 Celsius, taking sample injections 10 minutes before the end of each isothermal period. However, as the longer gas chromatographic method was used (method 2) each isothermal step had to be held for 2 hours. All other reactor and gas chromatographic parameters were as described in sections 4.2.1 and 4.2.2 and as listed in appendix A.

For the purposes of this thesis total conversion is defined as the percentage of the key limiting reactant (n-butane) which is consumed to generate all the reaction products. Yield is defined as the percentage of the particular product generated per amount of initial key reactant, and finally, selectivity is defined as the percentage of the particular product produced per amount of key reactant consumed. These three parameters are calculated from the results obtained from the gas chromatograph.

With all the following experiments any products that were trapped out in the "U" trap were collected and if in sufficient quantity were analysed, as a "nujol mull" between potassium bromide discs, by infrared spectroscopy. A Perkin-Elmer 983 continuous beam infrared spectrometer was used, scanning between 3000 and 400 cm^{-1} with comparisons being made to standard reference maleic anhydride and maleic acid spectra[97]. Also the contents of both traps was dissolved in distilled water and analysed for acidity, using universal indicator solution, and for the presence of unsaturated organics, using potassium permanganate solution, both tests should show a positive result if maleic anhydride was present.

5.2.1 2.6% palladium chloride on cupric oxide, unreduced (catalyst 1).

The material as prepared in section 5.1.1 was oven dried at 80 Celsius (without reduction) and run to determine its catalytic activity, with respect to n-butane conversion, in a powdered undiluted form. The material showed reasonable activity towards the production of maleic anhydride with a maxima in the yield obtained of 1.2% at a catalyst temperature of 350 Celsius. This corresponded to a n-butane conversion of 14% and therefore a selectivity towards maleic anhydride of 8.7%. Table 5.2 summarises the maximum yield and selectivity of maleic anhydride and the corresponding n-butane conversion and associated temperature for the range of catalysts studied in this chapter. The temperature at which 50% of the n-butane had been converted was found to be 390 Celsius (Figure 6). Figure 7 shows the variation of maleic anhydride yield and selectivity with respect to temperature, and Figure 6 shows the variation of n-butane conversion and maleic anhydride and carbon dioxide production versus temperature. Examination of the chromatograms obtained shows the presence of unknown compounds in the

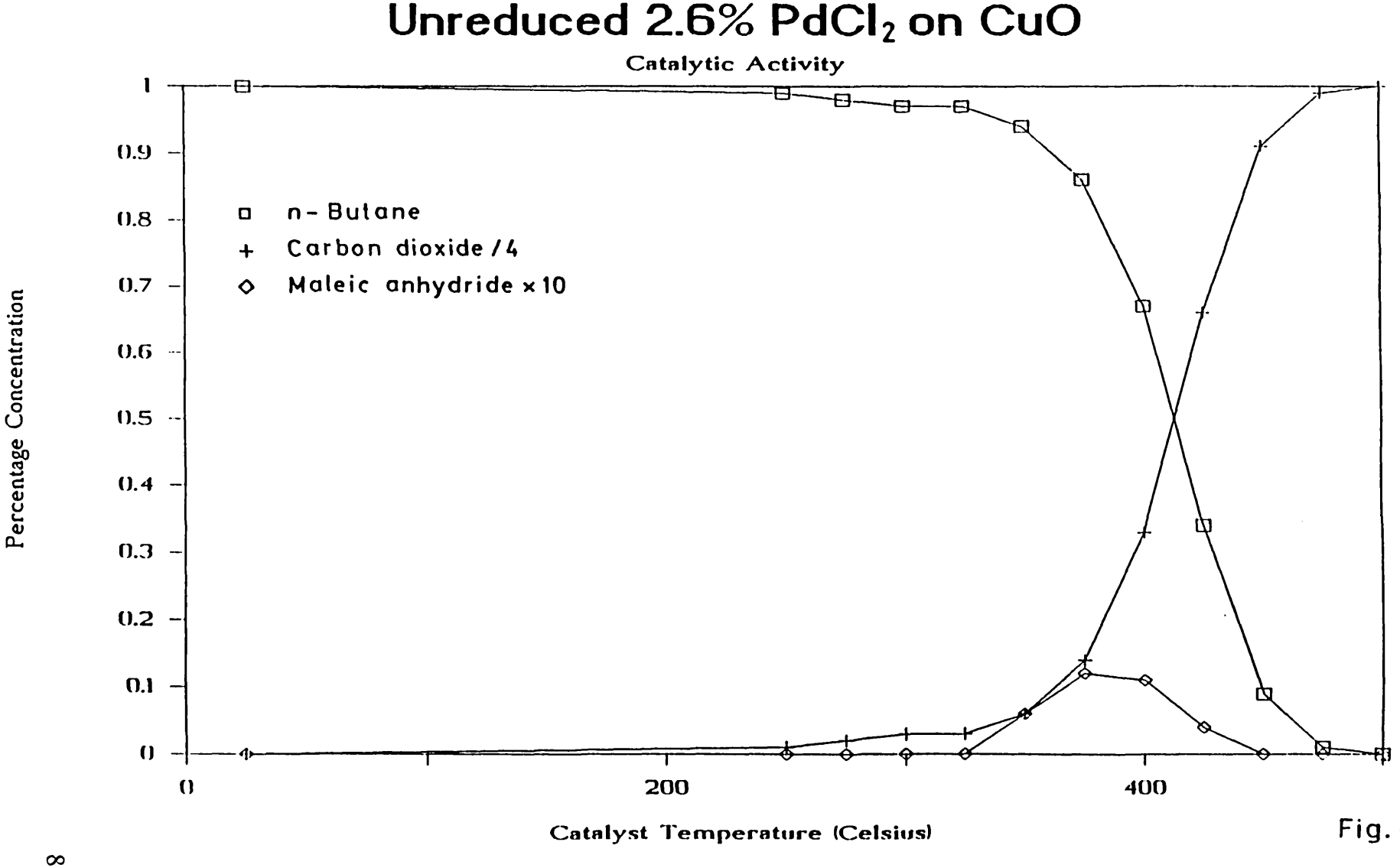

Unreduced 2.6% PdCl2 on CuO
Catalytic Activity
Percentage Concentration
1
0.9
0.8
0.7
0.6
0.5
0.4
0.3
0.2
0.1
0
n-Butane
Carbon dioxide /4
Maleic anhydride x10
0
200
400
Catalyst Temperature (Celsius)

Fig. 6.

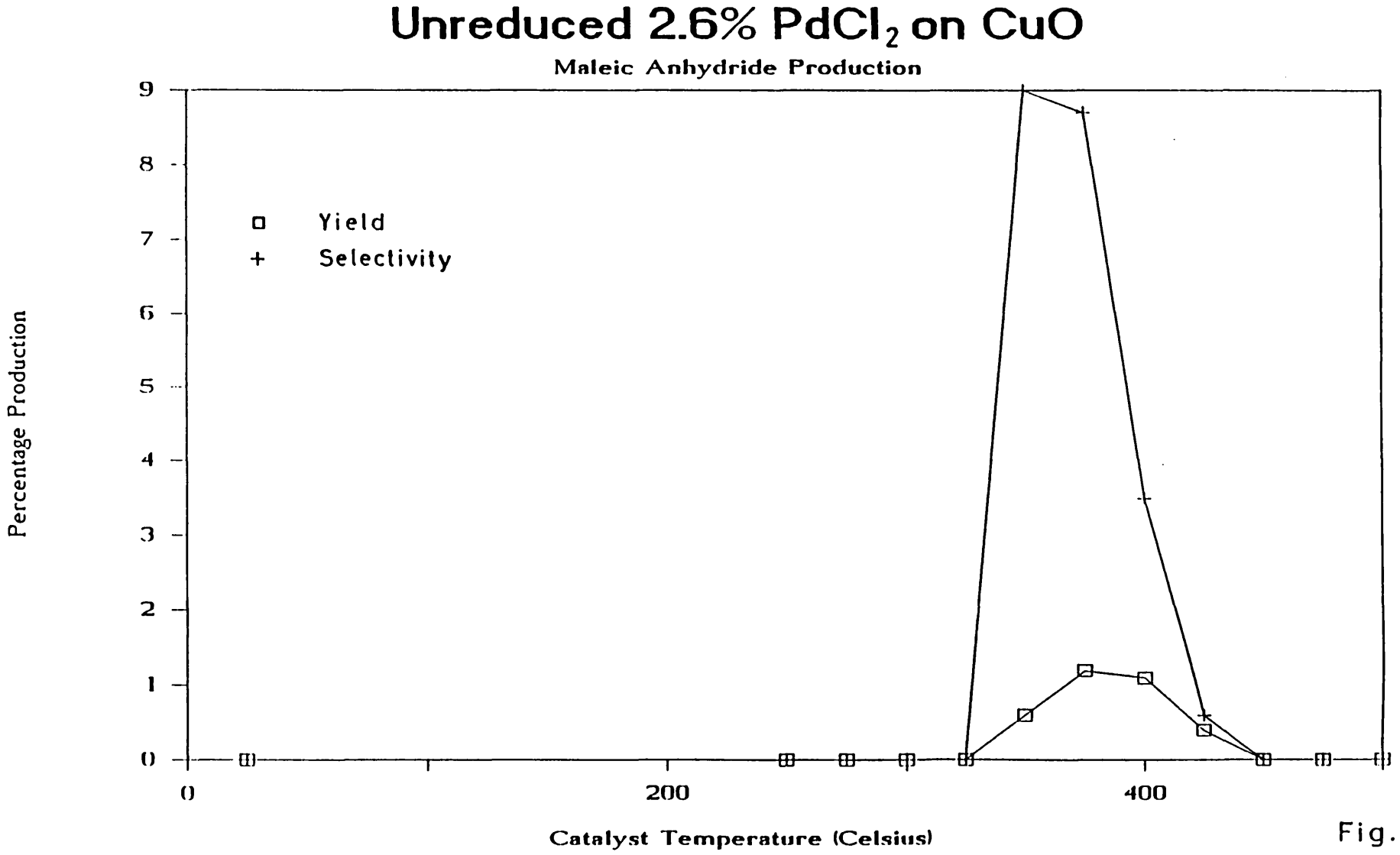

Unreduced 2.6% PdCl2 on CuO
Maleic Anhydride Production
Yield
Selectivity
Percentage Production
Catalyst Temperature (Celsius)
0
200
400
1
2
3
4
5
6
7
8
9

Fig.7.

product stream, Figure 8, and the way in which the concentration of these varies with temperature follows the same pattern as the maleic anhydride yield, Figure 6. The exact figure for the yield of these unidentified compounds was unobtainable as calibration of the gas chromatograph was not possible and calculation by assuming a 100% mass balance was impractical due to the figure being within experimental error of the other components. The assumption of a 100% mass balance, when calculating the selectivities was made by checking that the balance between n-butane and carbon dioxide was 100% when no other products were obtained, i.e. above 450 Celsius.

As this material had not been calcined before use, any decompositions occurring at the elevated temperatures used will obviously change the material under test. Results of characterisation of this material, including thermogravimetric analysis, show catalyst decompositions do occur in the temperature range under study and are given later in section 5.3.1. By inspection of the chromatograms obtained at each temperature it was also noticed that no carbon monoxide was produced. This could be due to two reasons, (i) that the reaction pathway which produced carbon dioxide did not go via carbon monoxide or (ii) that any carbon monoxide produced was immediately combusted to form carbon dioxide with or without prior desorption from the reaction site, the latter process seems the more likely as cupric oxide is well known as a catalyst for carbon monoxide removal from gas streams[98].

Analysis of the traps after this catalyst activity study gave a positive result for both wet chemical tests, but insufficient solid products were trapped for infrared analysis.

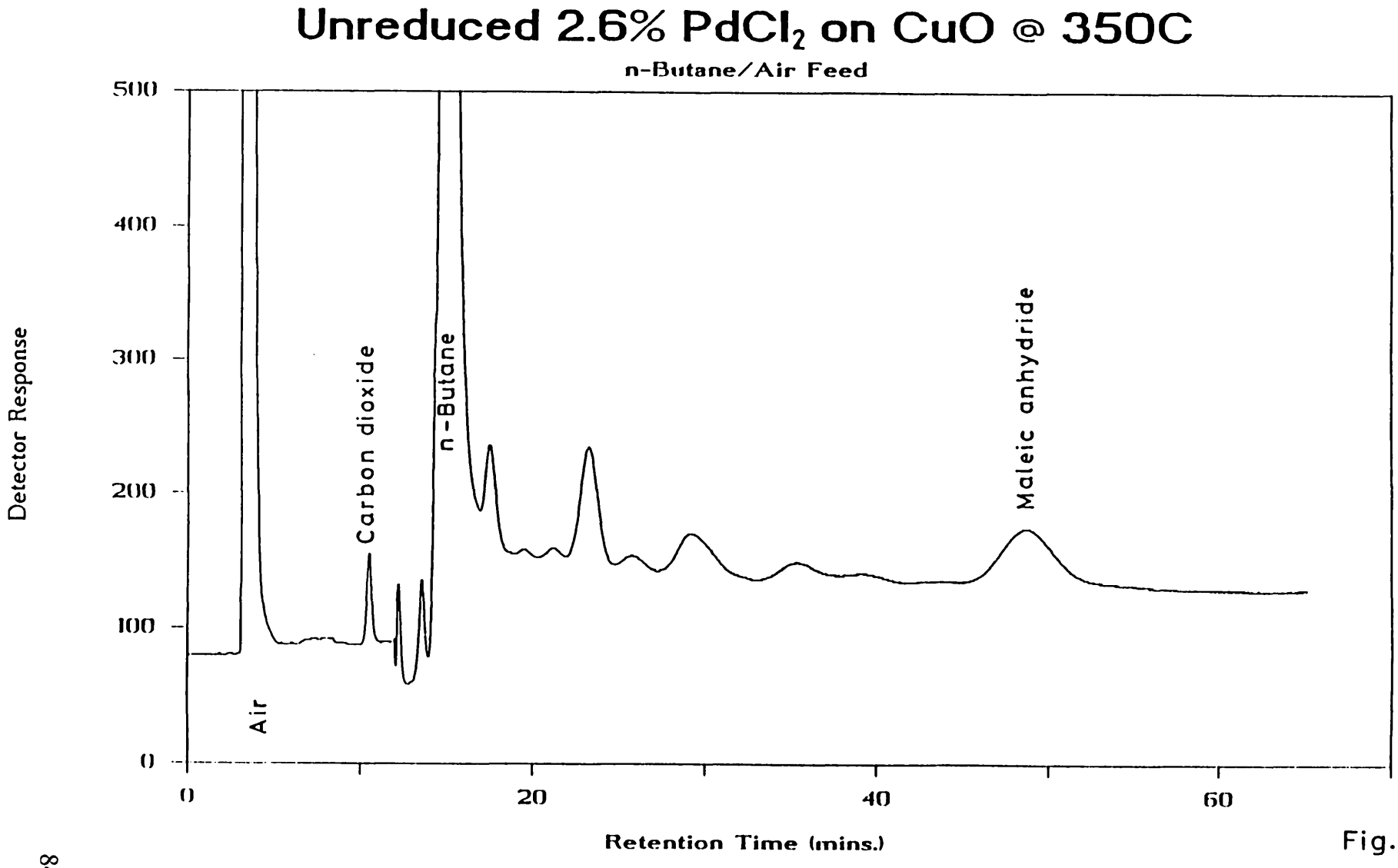

Unreduced 2.6% PdCl2 on CuO @ 350C
n-Butane/Air Feed
Detector Response
500
400
300
200
100
0
Air
Carbon dioxide
n-Butane
Maleic anhydride
0
20
40
60
Retention Time (mins.)

Fig. 8.

5.2.2 2.6% palladium chloride on cupric oxide, reduced (catalyst 2).

This material, prepared as described in section 5.1.1, was studied using an identical proceedure as that used for catalyst 1 for catalytic activity towards the conversion of n-butane to maleic anhydride. A maxima in the maleic anhydride yield was observed at 325 Celsius of 2.7%, compared with 1.2% at 350 Celsius for the unreduced material. This maxima corresponded to a n-butane conversion of 16% and therefore a selectivity towards maleic anhydride of 17%, see table 5.2. Figure 9 shows the n-butane conversion and maleic anhydride and carbon dioxide production curves versus catalyst temperature, and Figure 10 shows the variation with temperature of the maleic anhydride yield and selectivity. Unidentified peaks in the chromatograms were again detected, the retention times and shapes of these corresponded to those observed in the chromatograms from the unreduced material product stream, and the intensity of these peaks varied in the same way as with the unreduced material (Figure 11). The temperature for 50% conversion of the n-butane feed was found to be 380 Celsius compared with 390 Celsius for the unreduced material, see Figure 9. Therefore it seems that prereducing the catalyst has a positive effect upon the catalytic activity of the material, this effect being seen as an increase in maleic anhydride yield and selectivity and a reduction in the temperature required for optimum maleic anhydride yield and 50% conversion of the feed n-butane. As with catalyst 1 no peak for carbon monoxide was seen in the chromatograms obtained.

Analysis of the contents of the traps again gave a positive result for both wet chemical tests but insufficient solids were trapped for infrared spectroscopic analysis.

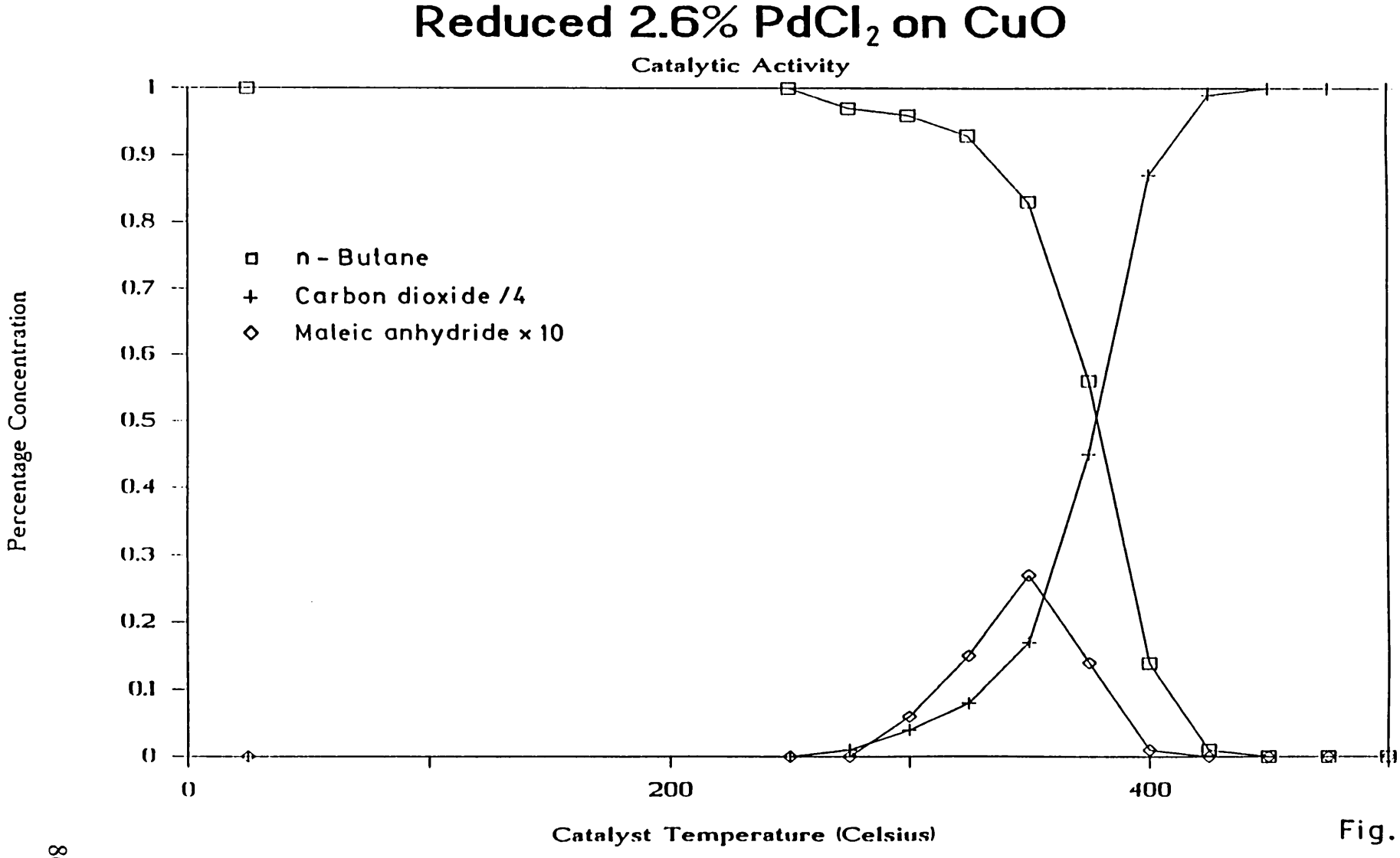

Reduced 2.6% PdCl2 on CuO
Catalytic Activity
Percentage Concentration
1
0.9
0.8
0.7
0.6
0.5
0.4
0.3
0.2
0.1
0
n - Butane
Carbon dioxide /4
Maleic anhydride x 10
0
200
400
Catalyst Temperature (Celsius)

Fig.9.

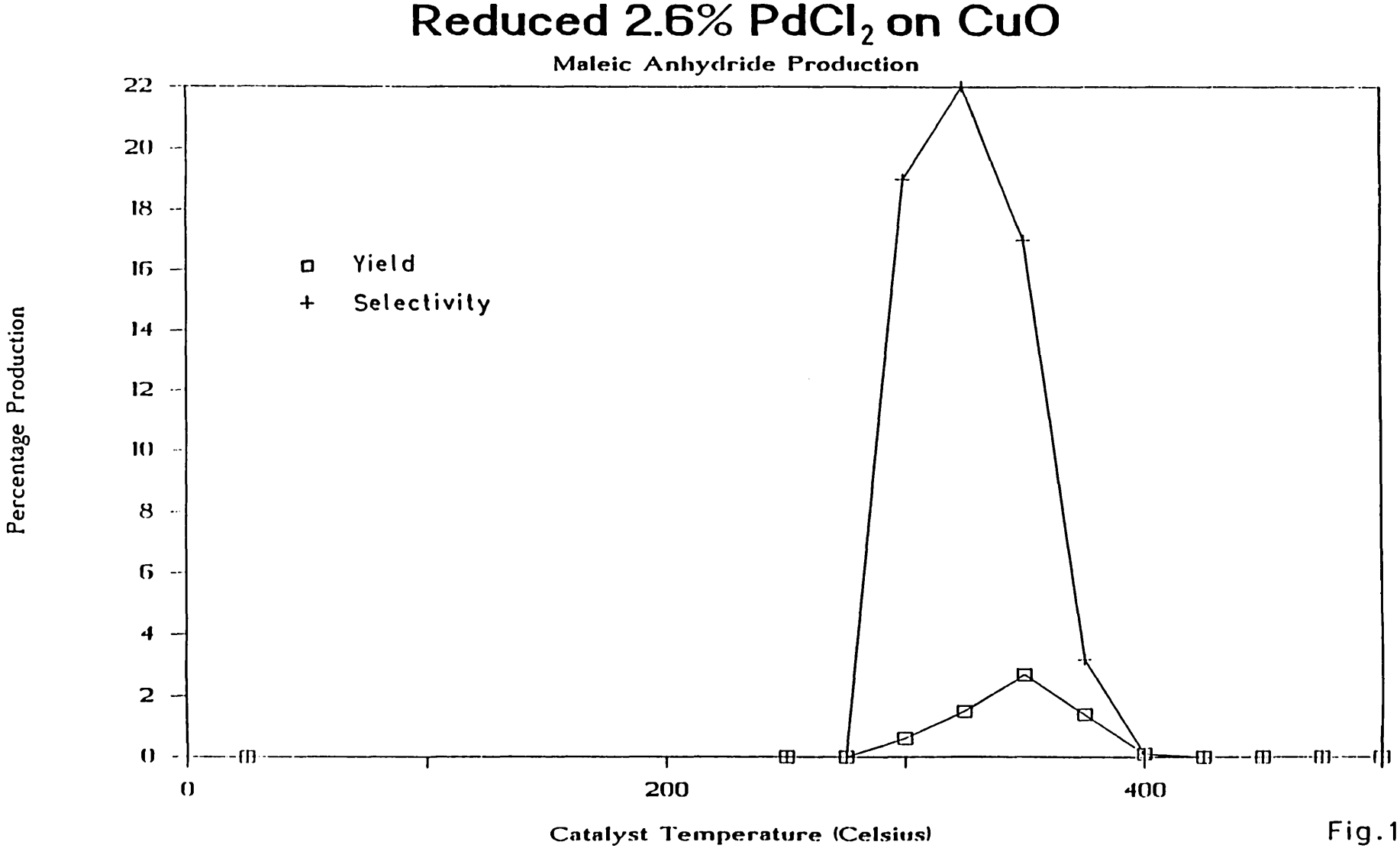

Reduced 2.6% PdCl2 on CuO
Maleic Anhydride Production
Percentage Production
22
20
18
16
14
12
10
8
6
4
2
0
Yield
Selectivity
0
200
400
Catalyst Temperature (Celsius)

Fig.10.

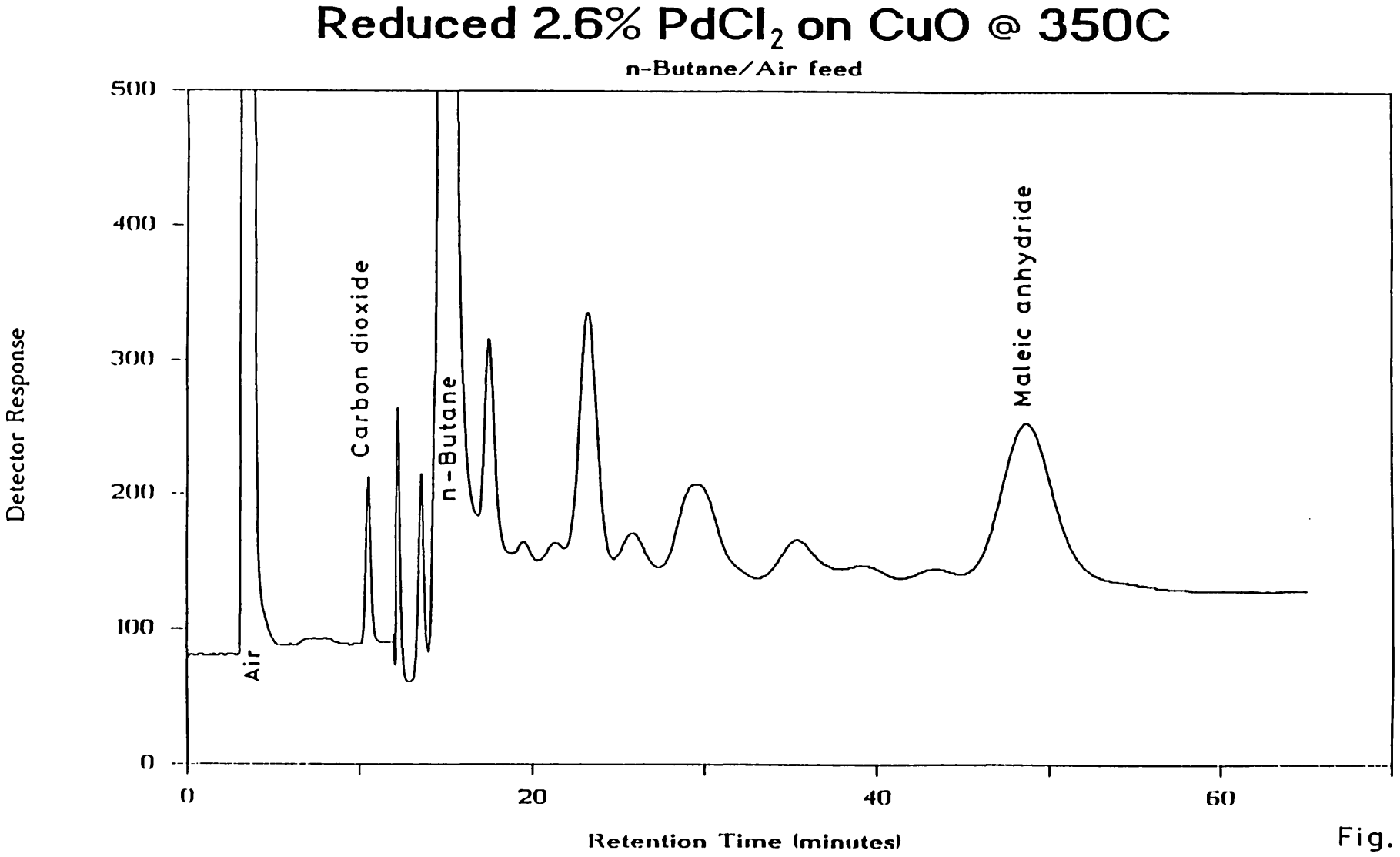

Reduced 2.6% PdCl2 on CuO @ 350C
n-Butane/Air feed
Detector Response
500
400
300
200
100
0
Air
Carbon dioxide
n-Butane
Maleic anhydride
0
20
40
60
Retention Time (minutes)

Fig.11.

5.2.3 0.45% palladium chloride on cupric oxide, reduced (catalyst 4).

A maximum in the yield and selectivity towards maleic anhydride was again found at approximately 325 Celsius, see Figure 13. However, the maximum yield detected was only 0.18%. This reduction in maleic anhydride yield was also matched in the unidentified peaks in the chromatogram. However, the unknowns were at the same retention times as for catalysts 1 and 2 and varied in area with respect to temperature in the same manner, see Figure 14. The n-butane conversions at each temperature studied are identical to those found for the material with a higher loading of palladium, the temperature for 50% conversion of n-butane being approximately 380 Celsius, see Figure 12. This result shows that the palladium probably has little effect upon the n-butane activation but may well be responsible for the production of partial oxidation products, as a reduction in maleic anhydride yield was seen without a reduction in n-butane conversions. Again it was noted that no carbon monoxide was produced.

Analysis of the contents of the postreactor traps gave a positive result for the acidity test and the aqueous washings slightly decolourised the permanganate solution, suggesting the presence of unsaturated products, but insufficient product was trapped for spectroscopic analysis.

5.2.4 2.6% of palladium nitrate on cupric oxide, reduced (catalyst 6).

This material showed no activity towards partial oxidation either in the production of maleic anhydride or any of the other unidentified peaks, which are assumed to be partially oxidised reaction intermediates or by-products, see Figure 16. Again no carbon monoxide was detected by gas chromatography. Also the

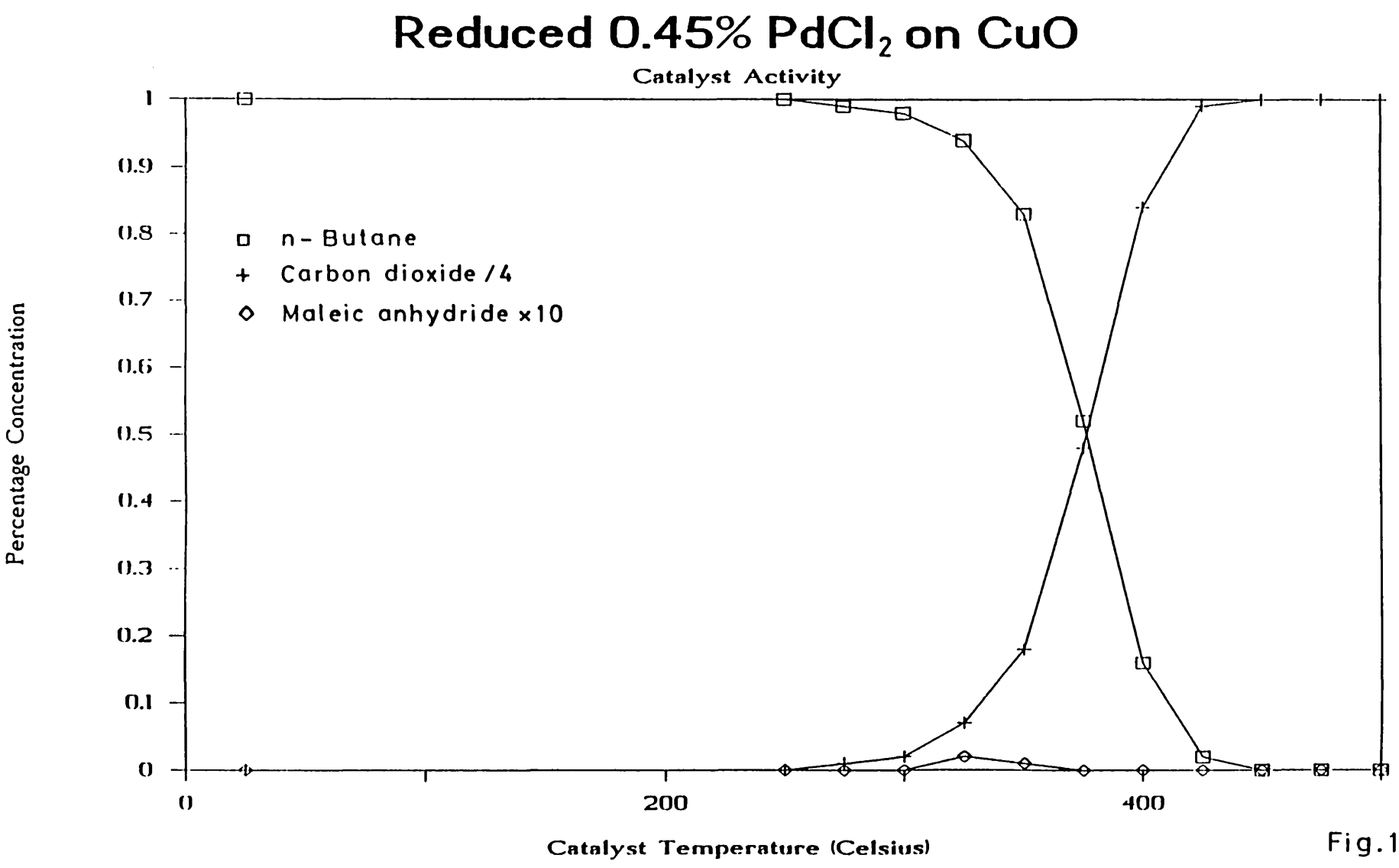

Reduced 0.45% $PdCl_2$ on CuO
Catalyst Activity
Percentage Concentration
1
0.9
0.8
0.7
0.6
0.5
0.4
0.3
0.2
0.1
0
n-Butane
Carbon dioxide /4
Maleic anhydride x10
0
200
400
Catalyst Temperature (Celsius)

Fig.12.

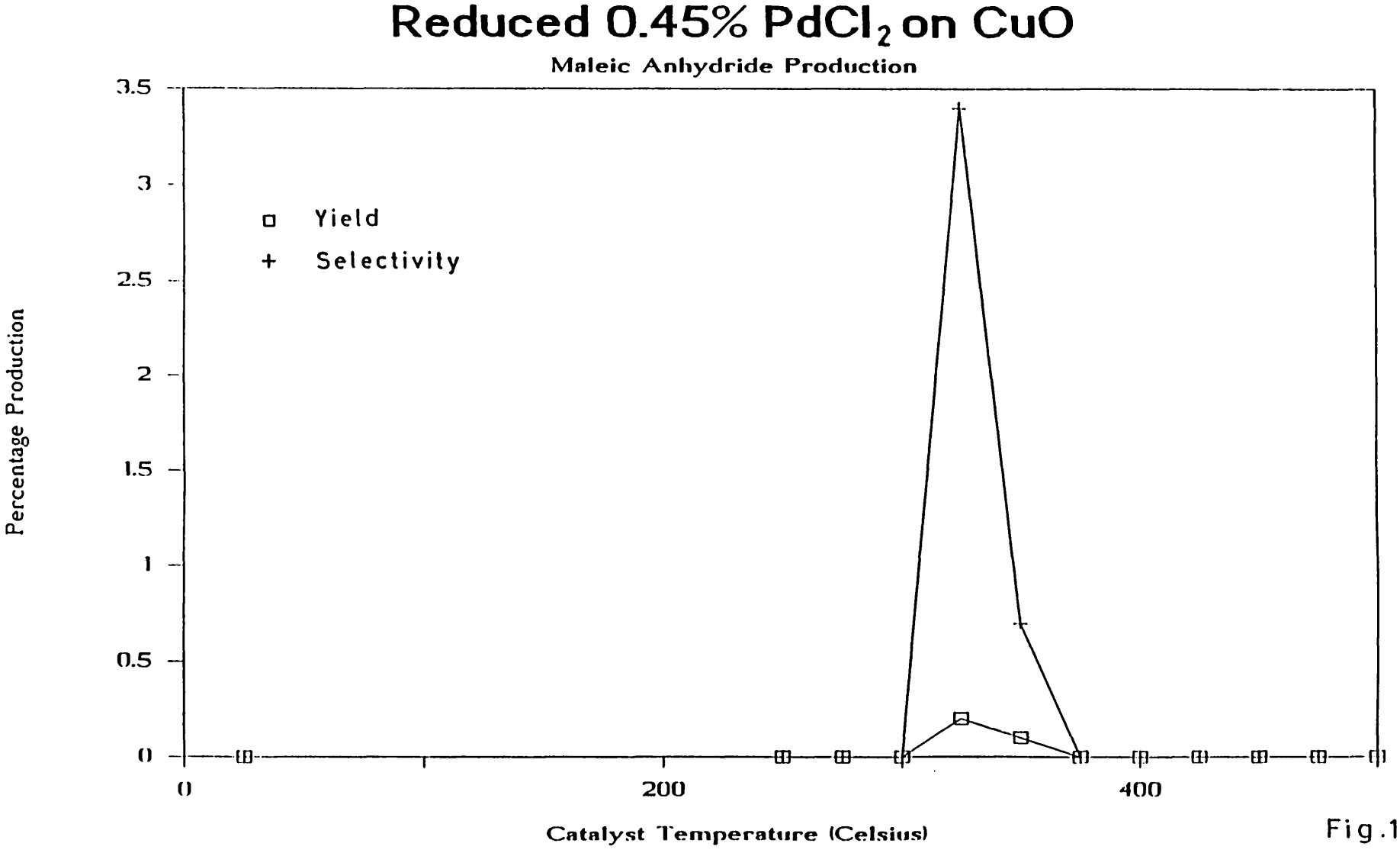

Reduced 0.45% PdCl2 on CuO
Maleic Anhydride Production
Yield
Selectivity
Percentage Production
Catalyst Temperature (Celsius)
3.5
3
2.5
2
1.5
1
0.5
0
0
200
400

Fig.13.

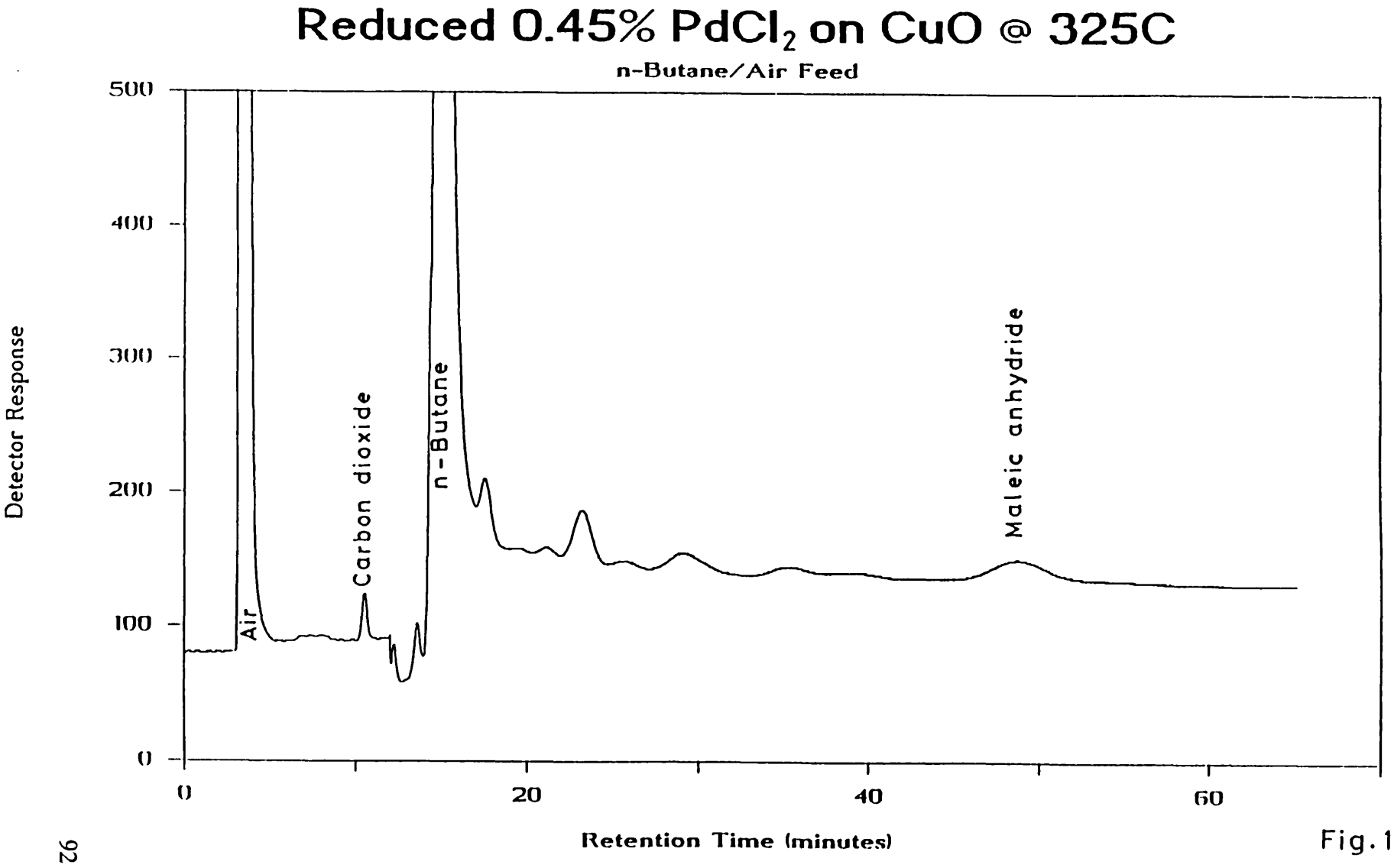

Reduced 0.45% PdCl2 on CuO @ 325C
n-Butane/Air Feed
Detector Response
500
400
300
200
100
0
Air
Carbon dioxide
n-Butane
Maleic anhydride
0
20
40
60
Retention Time (minutes)

Fig. 14.

conversion of n-butane and production of carbon dioxide curves were shifted to a much lower temperature, viz. 285 Celsius for 50% conversion of the n-butane, see Figure 15.

As the material was dried at 80 Celsius in air before being reduced in hydrogen/argon (5%) at 200 Celsius and then kept in air, the palladium would probably exist as elemental palladium and palladium (II) oxide. This was deduced using pure palladium nitrate and drying it at 80 Celsius before analysing it in a hydrogen/argon atmosphere by thermogravimetric analysis, where at 200 Celsius the palladium existed as the oxide and not until 650 Celsius did it reduce to yield palladium metal.

5.2.5 Cupric oxide.

The pure cupric oxide used to prepare the palladium / copper catalysts in section 5.1 was tested for catalytic activity towards n-butane oxidation to eliminate it as the active constituent in the materials so far studied. It was found that no maleic anhydride or other unidentified products, assumed to be partially oxidised organics produced by side reactions or intermediates desorbing, were detected, see Figure 17. The cupric oxide meerly combusted the n-butane to carbon dioxide, no carbon monoxide was detected in the product stream either. The temperature for 50% conversion of the n-butane feed was found to be only 320 Celsius, see Figure 18.

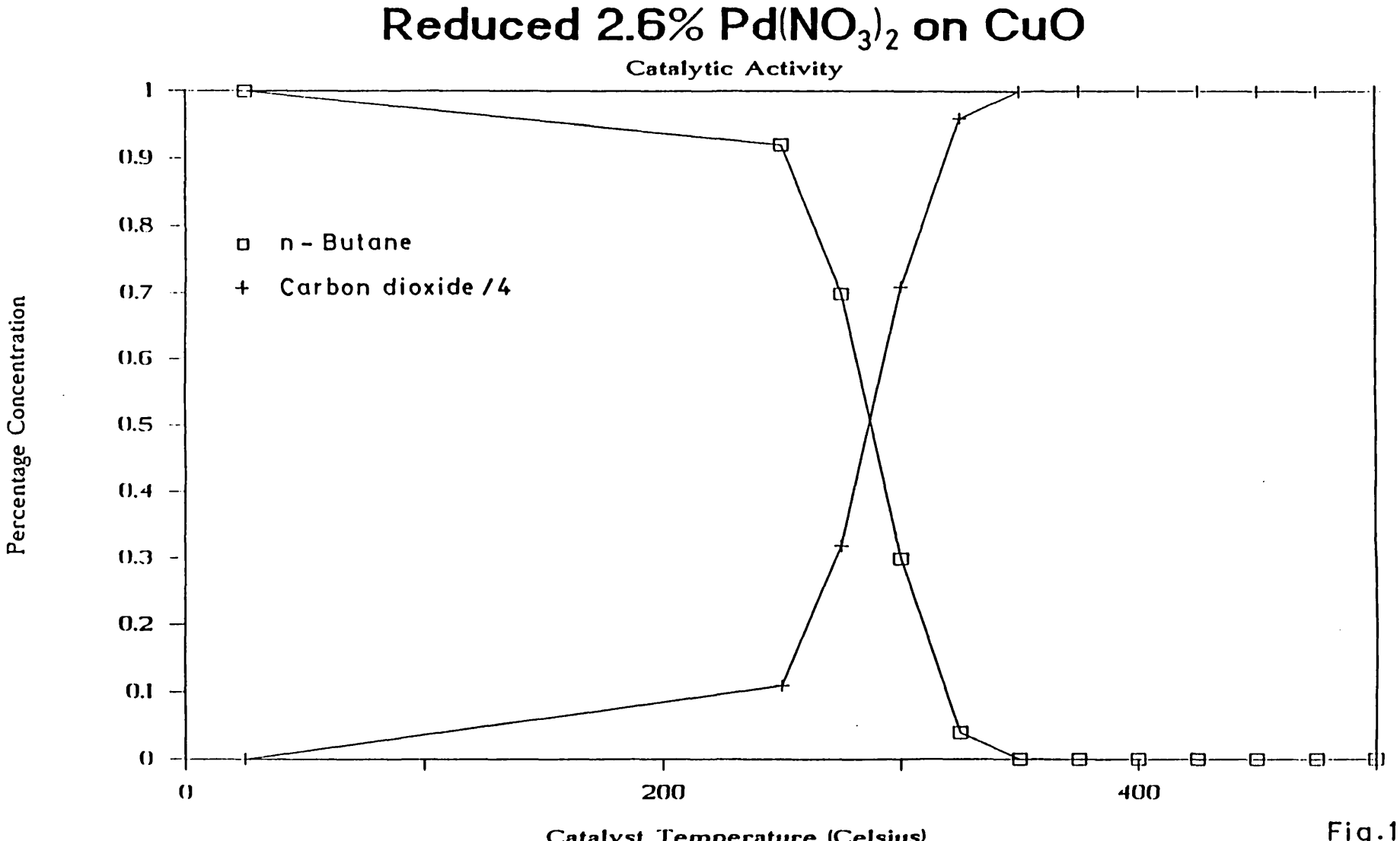

Reduced 2.6% Pd(NO3)2 on CuO
Catalytic Activity
Percentage Concentration
1
0.9
0.8
0.7
0.6
0.5
0.4
0.3
0.2
0.1
0
n - Butane
Carbon dioxide /4
0
200
400
Catalyst Temperature (Celsius)

Fig.15.

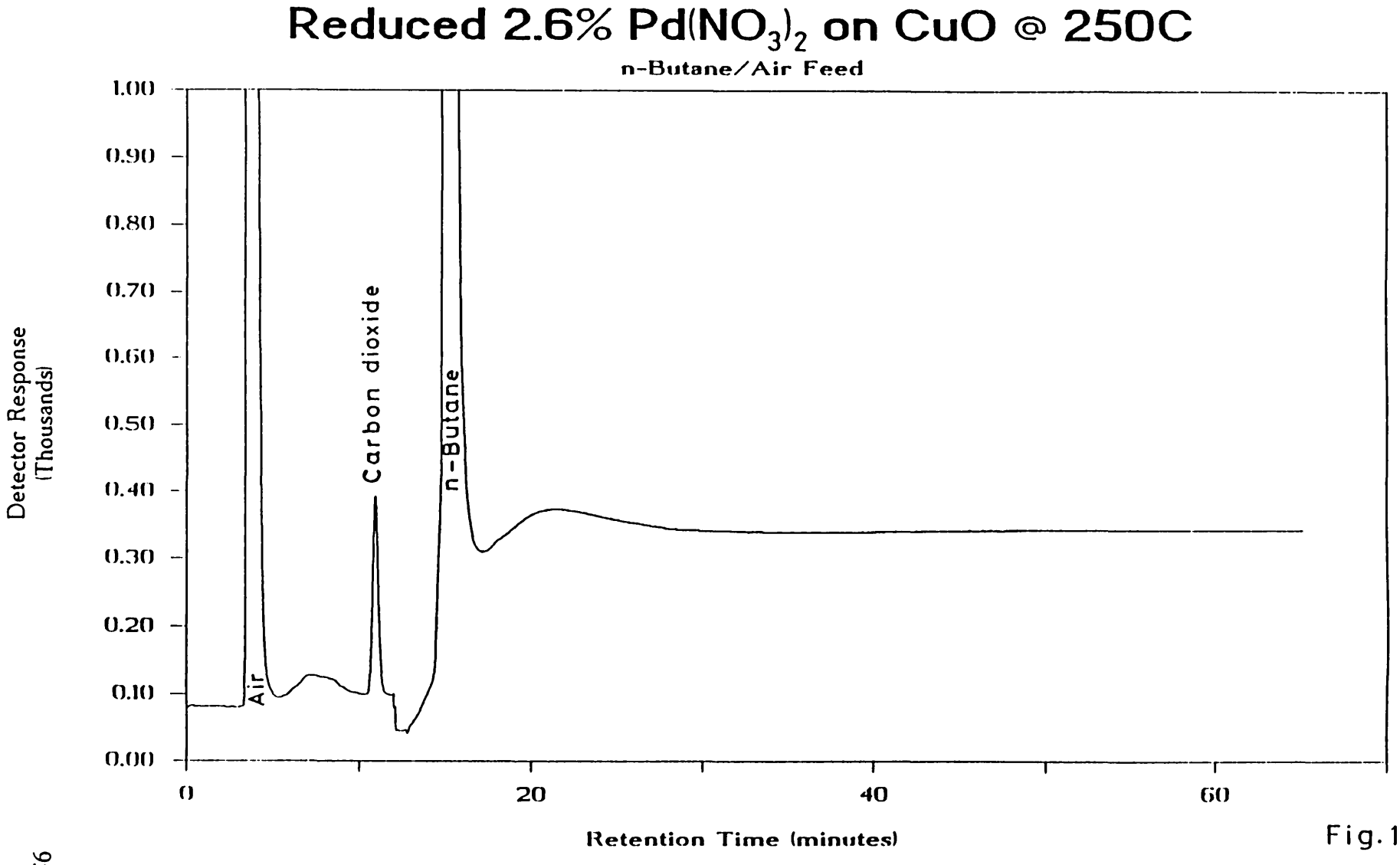

Reduced 2.6% Pd(NO3)2 on CuO @ 250C
n-Butane/Air Feed
Detector Response (Thousands)
1.00
0.90
0.80
0.70
0.60
0.50
0.40
0.30
0.20
0.10
0.00
Air
Carbon dioxide
n-Butane
0
20
40
60
Retention Time (minutes)

Fig. 16.

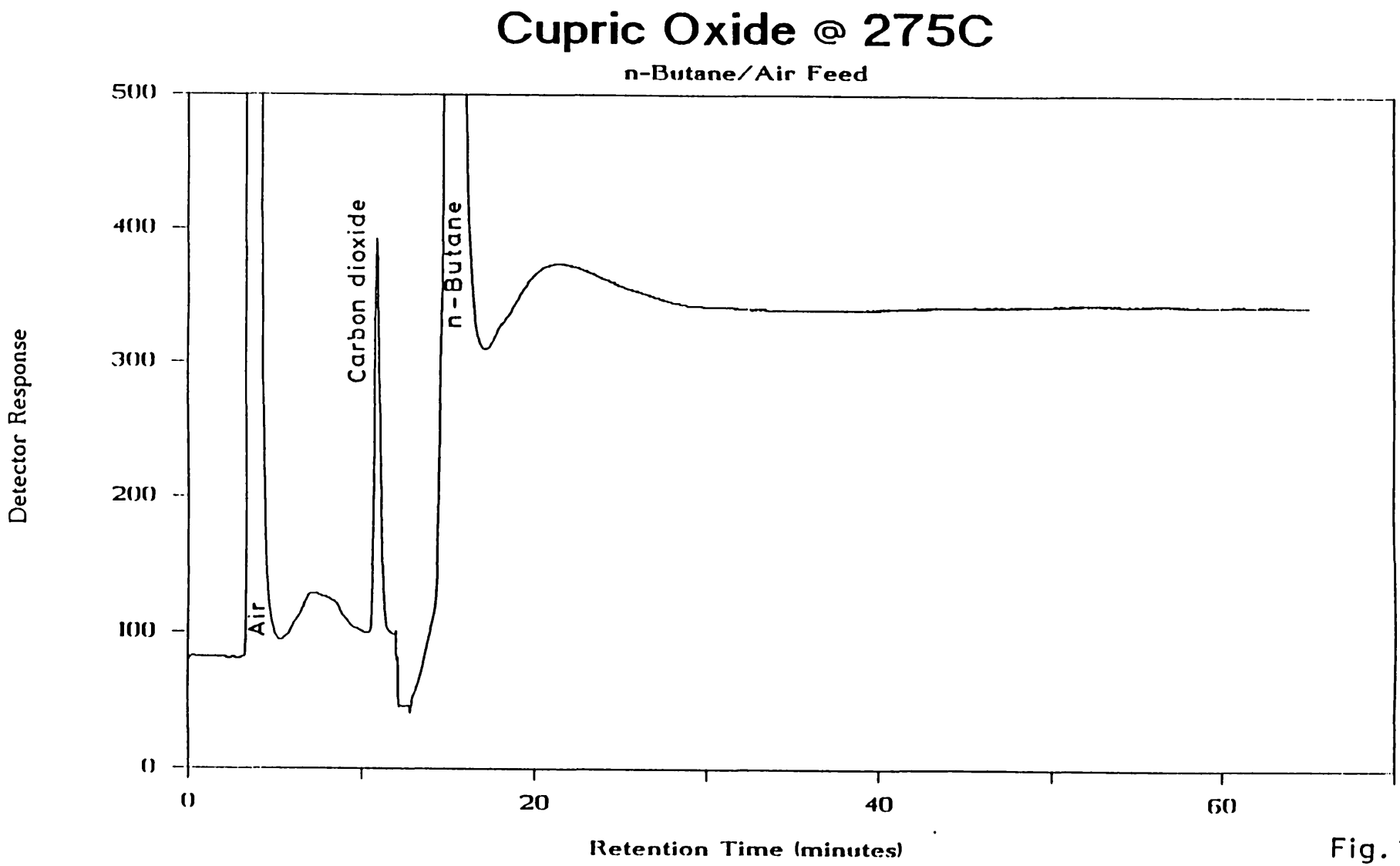

Cupric Oxide @ 275C
n-Butane/Air Feed
Detector Response
500
400
300
200
100
0
Air
Carbon dioxide
n-Butane
0
20
40
60
Retention Time (minutes)

Fig. 17.

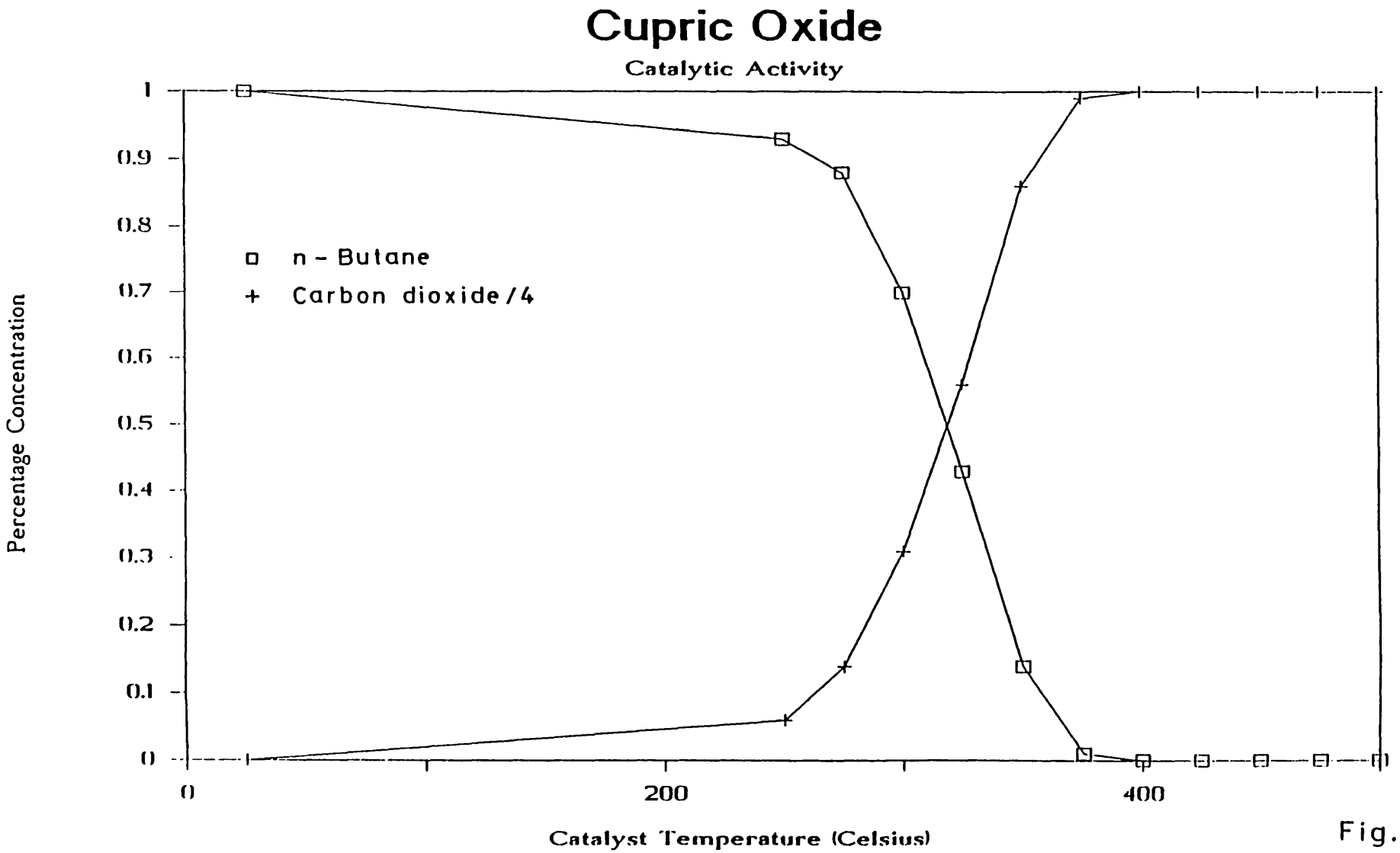

Cupric Oxide
Catalytic Activity
Percentage Concentration
1
0.9
0.8
0.7
0.6
0.5
0.4
0.3
0.2
0.1
0
n - Butane
+ Carbon dioxide/4
0
200
400
Catalyst Temperature (Celsius)

Fig.18.

Table 5.2

Pd/Cu System Catalytic Activity.

Catalyst	Max. Yield	Max. Selectivity	Butane Conversion	Temperature
2.6% $PdCl_2$ on CuO (unred.)	1.2%	8.7%	14%	350 Celsius
2.6% $PdCl_2$ on CuO (red.)	2.7%	17%	16%	325 Celsius
0.45% $PdCl_2$ on CuO (red.)	0.18%	3.4%	5.2%	325 Celsius
2.6% $Pd(NO_3)_2$ on CuO (red.)	-----	----	50%	285 Celsius
CuO (unred.)	-----	----	50%	320 Celsius

For those materials that showed no partial oxidation activity, temperatures for 50% n-butane conversions are given.

5.3 Catalyst Characterisation.

5.3.1 2.6% palladium chloride on cupric oxide.

Nitrogen physisorption gave the B.E.T. surface area values of the unreduced and reduced materials as 15.7 and 11.5 m^2/g respectively. This compared to a B.E.T. surface area of pure cupric oxide of 9.3 m^2/g. Full isotherm analysis of the pure cupric oxide showed the isotherm to be type 3 which is typical of a nonporous material, see Figure 19.

X-ray diffraction of the unreduced materials showed the presence of mainly cupric oxide, but also significant amounts of copper (II) trihydroxychloride in both the hydrated and anhydrous forms ($CuCl_2.3[Cu(OH)_2]$, atacamite phase) were detected. The reduced material showed less copper (II) trihydroxychloride as being present and the possible presence of cuprous oxide. This result was interesting as it shows that during preparation the acidic chloride solution does chlorinate the cupric oxide surface. Figure 20 shows the diffraction pattern obtained from the unreduced material. No palladium species were detected, probably due to their low concentration or the crystallite size was too small for detection.

X-ray photoelectron spectroscopy showed both the unreduced and reduced samples to be principally cupric oxide or chloride, see Tables 5.3 a) and b) and Figure 21 showing the copper spectrum of the unreduced sample. However, a difference was noticed in the palladium 3d peaks, both samples gave two $3d_{5/2}$ peaks but at different corrected binding energies. The unreduced sample showing the presence of a $[PdCl_4]^{2-}$ surface species along with $PdCl_2$, and the prereduced sample having a surface of predominantely $PdCl_2$ with a small amount of elemental palladium, see Figures 22 and 23 for the respective spectra. The chlorine 2p peaks

are characteristic of chloride in both catalysts, see Figures 24 and 25 for the spectra of the unreduced and reduced catalysts resectively. The oxygen 1s spectra, in both the unreduced and reduced materials, show the presence of two surface oxygen species which are in about a 1:1 ratio, these being identified as CuO and hydroxyl species probably from the atacamite see Figures 26 and 27.

Table 5.3 a)

X.P.S. results of the unreduced 2.6% palladium chloride on cupric oxide catalyst.

Peak	K.E. (eV)	B.E.* (eV)	Assignment	Concentration
Pd $3d_{5/2}$	1145.9	337.1	$PdCl_2$	0.9%
	1144.5	338.5	$[PdCl_4]^{2-}$	1.3%
Cu $2p_{3/2}$	549.9	933.1		
Cu $2p_{1/2}$	530.0	953.0	Cu^{2+}	32.7%
Cu LMM	917.5*			
O 1s	953.4	529.6	O^{2-}	22.8%
O 1s	951.3	531.7	OH^-	20.2%
Cl 2p	1285.0	198.0	Cl^-	3.9%

* *Binding energies corrected for charging using adventitious carbon (B.E. =284.4eV)*

Concentrations are given in atomic percent and are corrected for sensitivities.

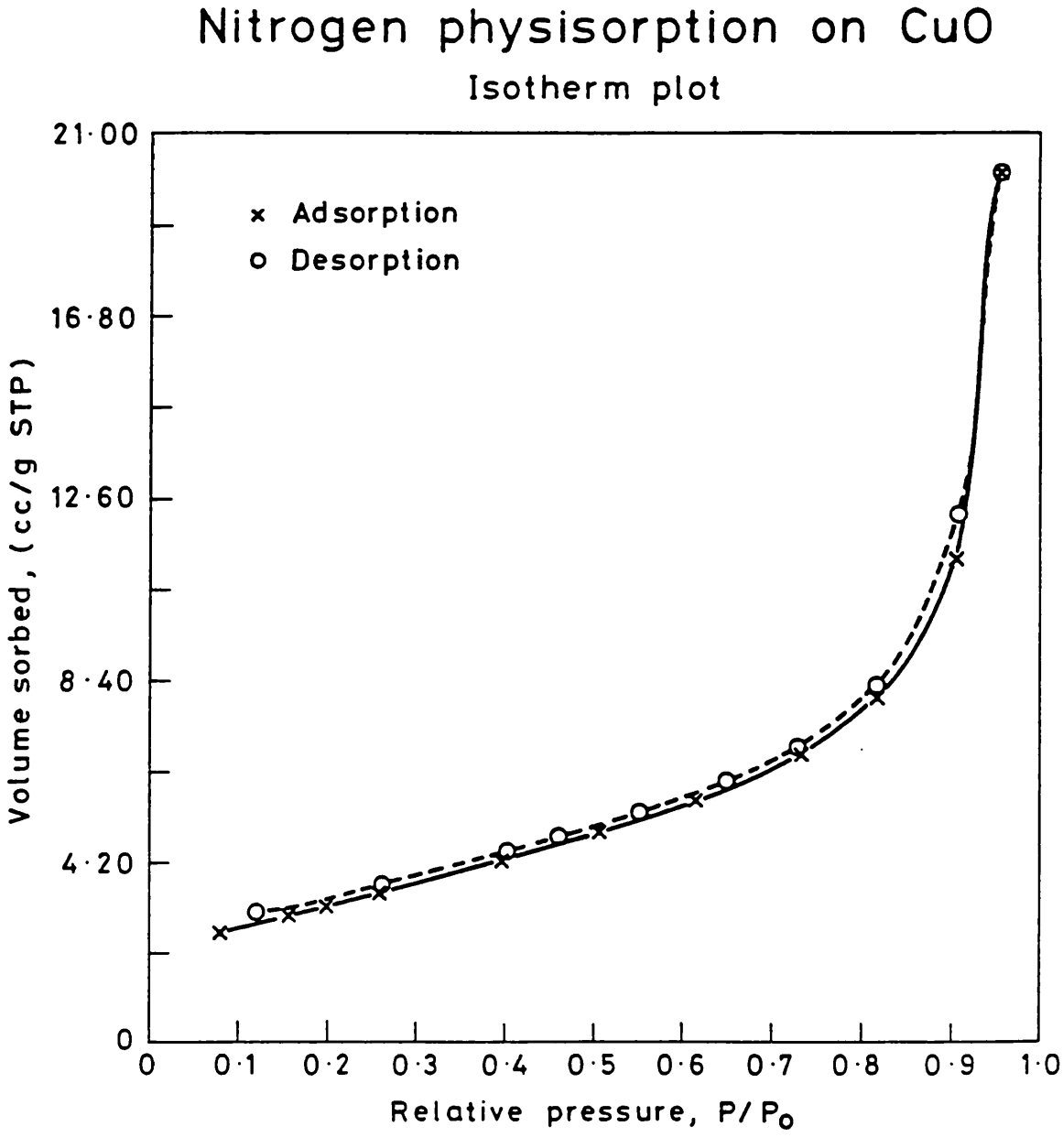

Nitrogen physisorption on CuO
Isotherm plot
× Adsorption
o Desorption
Volume sorbed, (cc/g STP)
21·00
16·80
12·60
8·40
4·20
0
0
0·1
0·2
0·3
0·4
0·5
0·6
0·7
0·8
0·9
1·0
Relative pressure, P/Po

Fig. 19

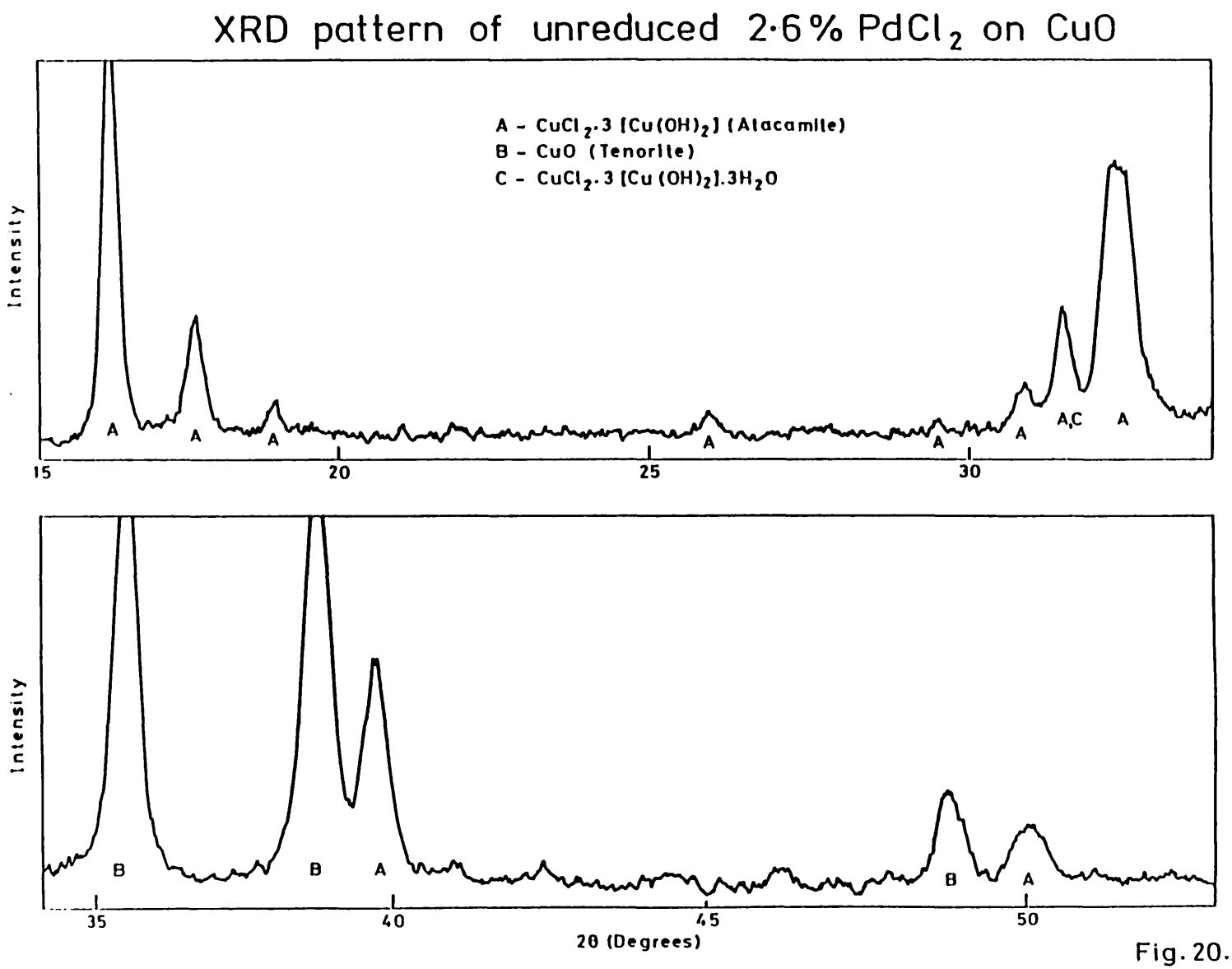

XRD pattern of unreduced 2·6% $PdCl_2$ on CuO
A - $CuCl_2 \cdot 3[Cu(OH)_2]$ (Atacamite)
B - CuO (Tenorite)
C - $CuCl_2 \cdot 3[Cu(OH)_2] \cdot 3H_2O$
Intensity
A
A
A
A
A
A
A,C
A
15
20
25
30
Intensity
B
B
A
B
A
35
40
45
50
2θ (Degrees)

Fig. 20.

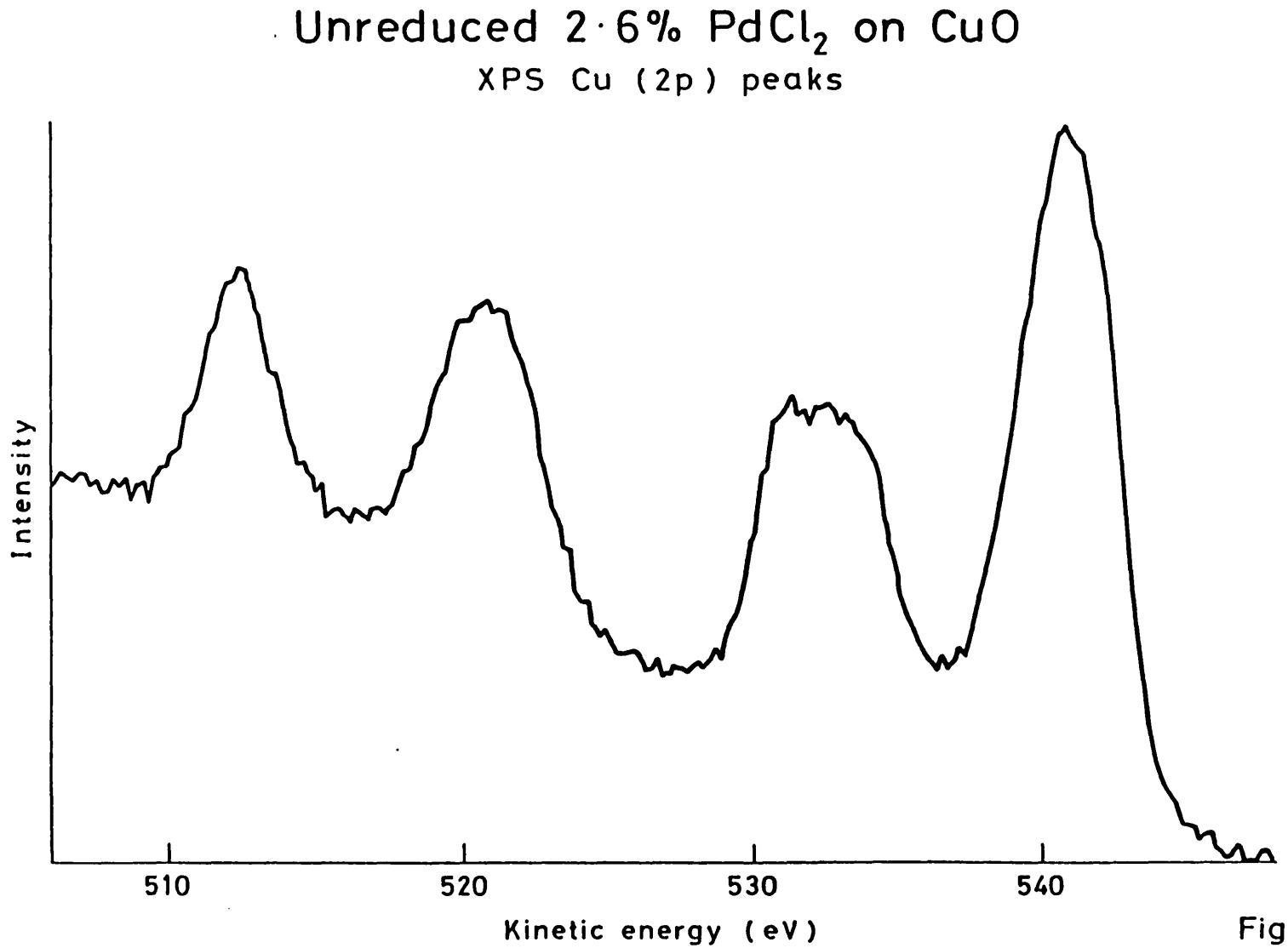

Unreduced 2·6% $PdCl_2$ on CuO
XPS Cu (2p) peaks
Intensity
510
520
530
540
Kinetic energy (eV)

Fig. 21

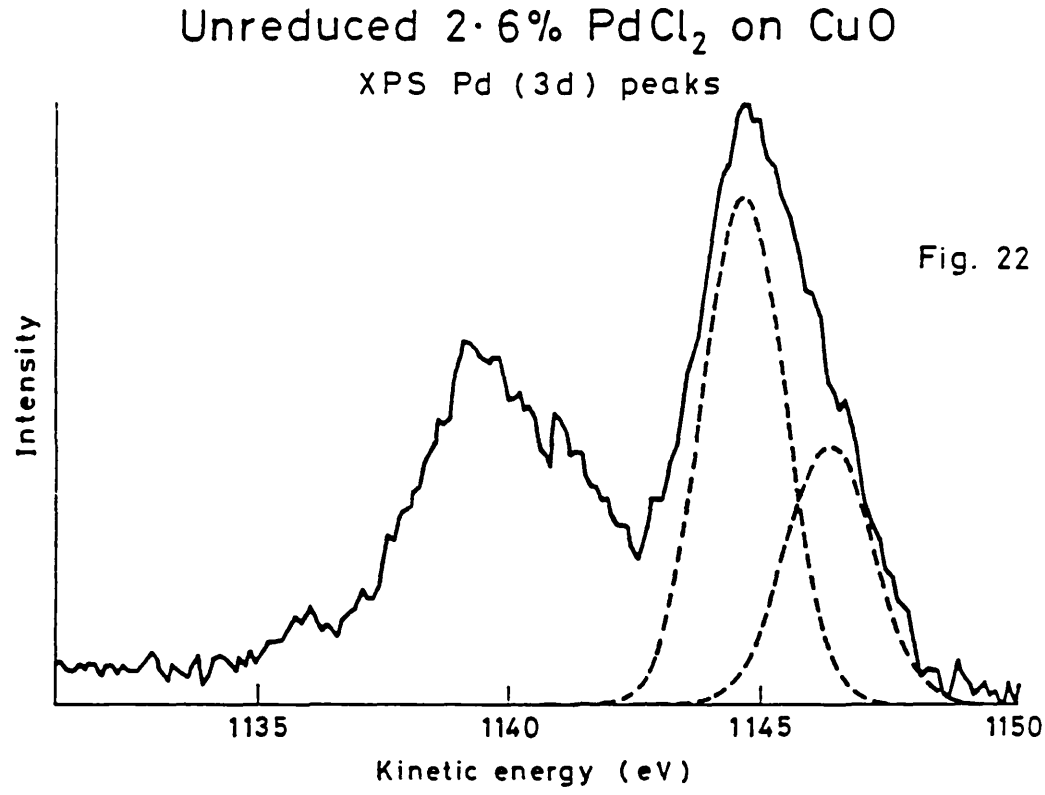

Unreduced 2·6% $PdCl_2$ on CuO
XPS Pd (3d) peaks
Intensity
1135
1140
1145
1150
Kinetic energy (eV)

Fig. 22

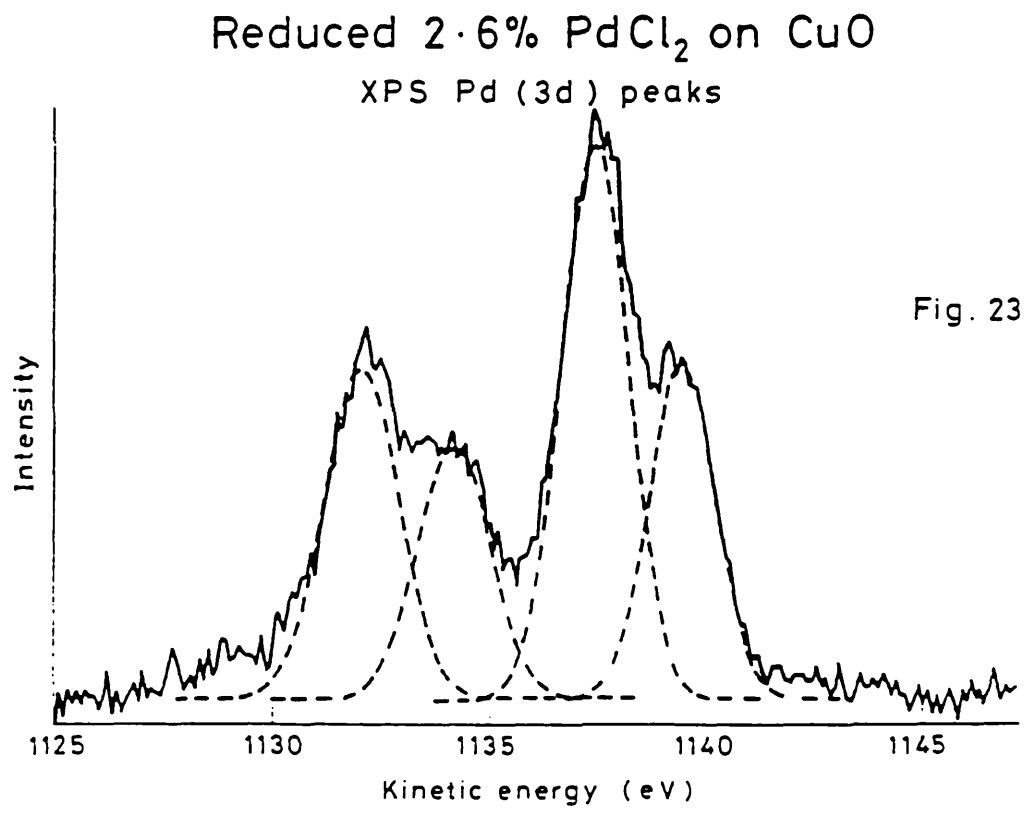

Reduced 2·6% $PdCl_2$ on CuO
XPS Pd (3d) peaks
Intensity
1125
1130
1135
1140
1145
Kinetic energy (eV)

Fig. 23

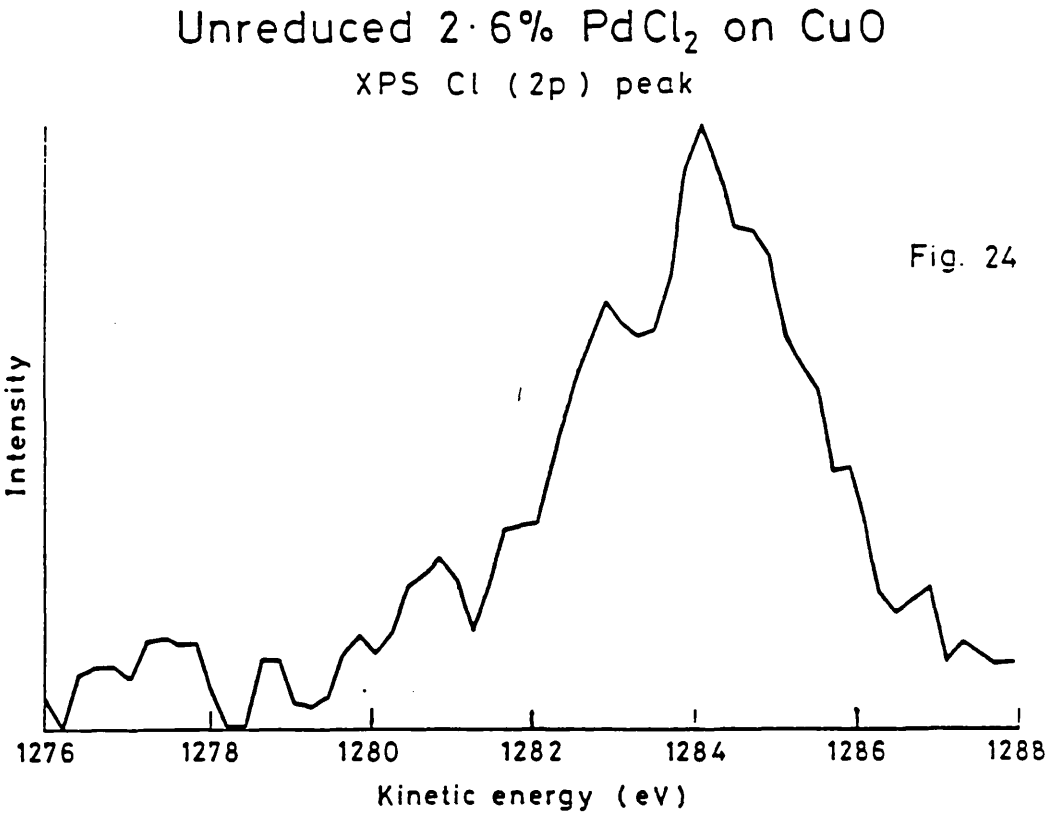

Unreduced 2·6% $PdCl_2$ on CuO
XPS Cl (2p) peak
Intensity
1276
1278
1280
1282
1284
1286
1288
Kinetic energy (eV)

Fig. 24

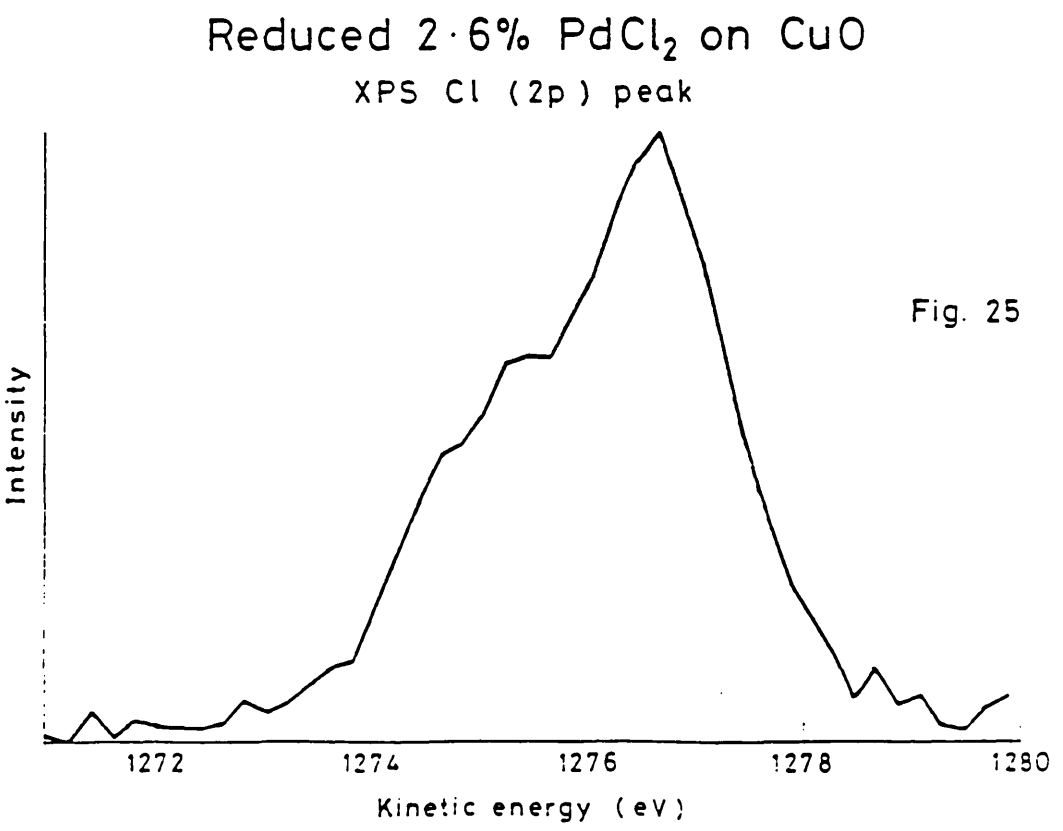

Reduced 2·6% $PdCl_2$ on CuO
XPS Cl (2p) peak
Intensity
1272
1274
1276
1278
1280
Kinetic energy (eV)

Fig. 25

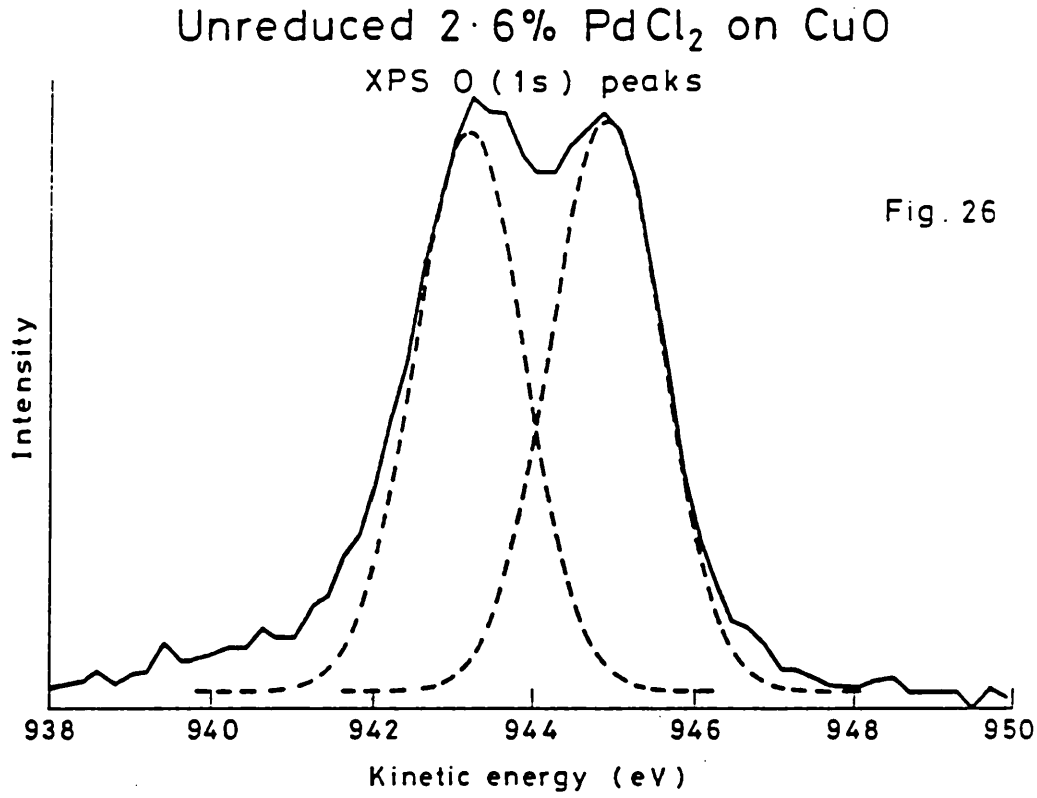

Unreduced 2·6% $PdCl_2$ on CuO
XPS O (1s) peaks
Intensity
938
940
942
944
946
948
950
Kinetic energy (eV)

Fig. 26

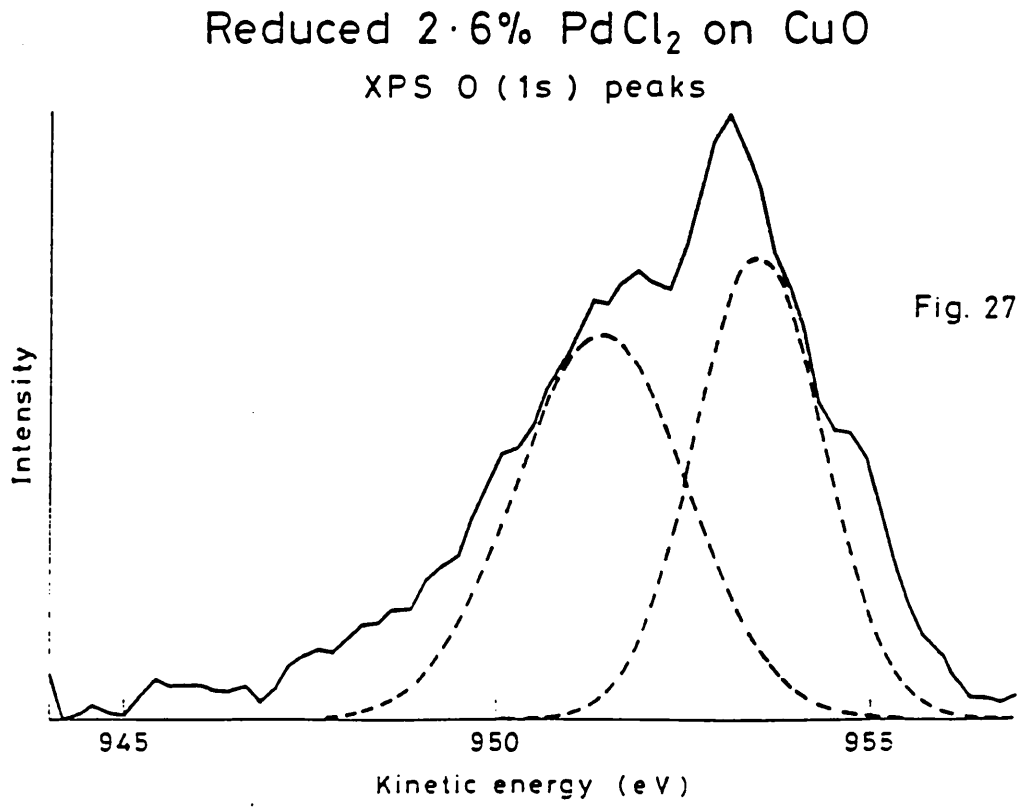

Reduced 2·6% $PdCl_2$ on CuO
XPS O (1s) peaks
Intensity
945
950
955
Kinetic energy (eV)

Fig. 27

Table 5.3 b)

X.P.S. results of the reduced 2.6% palladium chloride on cupric oxide catalyst.

Peak	K.E. (eV)	B.E.* (eV)	Assignment	Concentration
Pd $3d_{5/2}$	1139.3	334.6	Pd	0.5%
	1137.3	336.6	$PdCl_2$	0.8%
Cu $2p_{3/2}$	540.6	933.3		
Cu $2p_{1/2}$	520.8	953.2	Cu^{2+}	41.5%
Cu LMM	917.3*			
O 1s	944.8	529.1	O^{2-}	21.2%
O 1s	943.2	530.8	OH^-	21.2%
Cl 2p	1276.6	197.4	Cl^-	7.5%

* *Binding energies corrected for charging using adventitious carbon (B.E. =284.4eV)*

Thermogravimetric analysis, in a flowing atmosphere of air, gave two very similar weight loss curves for the unreduced and reduced material, each containing two distinct weight losses. The unreduced material gave a decomposition of 7% (weight) with a maximum decomposition rate at 300 Celsius, and a second decomposition at 440 Celsius of 6.5%, see Figure 28. The reduced material gave an

initial decomposition at 260 Celsius instead of 300 Celsius, see Figure 29. By calcining at 550 Celsius for 3 hours both materials, on analysis by X-ray diffraction, had decomposed to cupric oxide, see Figure 30.

5.3.2 0.45% palladium chloride on copper oxide.

B.E.T. surface area measurements of the unreduced and reduced materials gave values of 16.5 and 16.0 m^2/g respectively. The isotherm obtained was again type 3 or 5, and was very similar to that shown in Figure 19 for the 2.6% material.

X-ray diffraction of the unreduced material showed cupric oxide to be predominant with a small amount of copper (II) trihydroxychloride in the atacamite phase but much less than in the 2.6% material. The reduced material was predominantly cupric oxide, but it also contained atacamite, less than in the unreduced material, and a small amount of cuprous oxide was also detected, see Figure 31. The lower amount of atacamite may be due to less chloride being present in the preparation, see section 5.1.2.

X-ray photoelectron spectroscopy showed very similar results to those obtained for the 2.6% material, but as expected the intensity of the palladium and chlorine peaks were very much lower, so much so that exact identification by curve fitting would have been very unreliable if the higher palladium concentration material had not been analysed previously. Data from both the unreduced and reduced catalysts is shown in Tables 5.4 a) and b). The copper peaks are identical in both catalysts and the spectrum obtained from the unreduced catalyst is shown in Figure 32. The one important difference noted was in the palladium peaks where only one palladium species was detected and this was identified as $PdCl_2$, see Figures 33 and 34 for the unreduced and reduced catalysts respectively. The

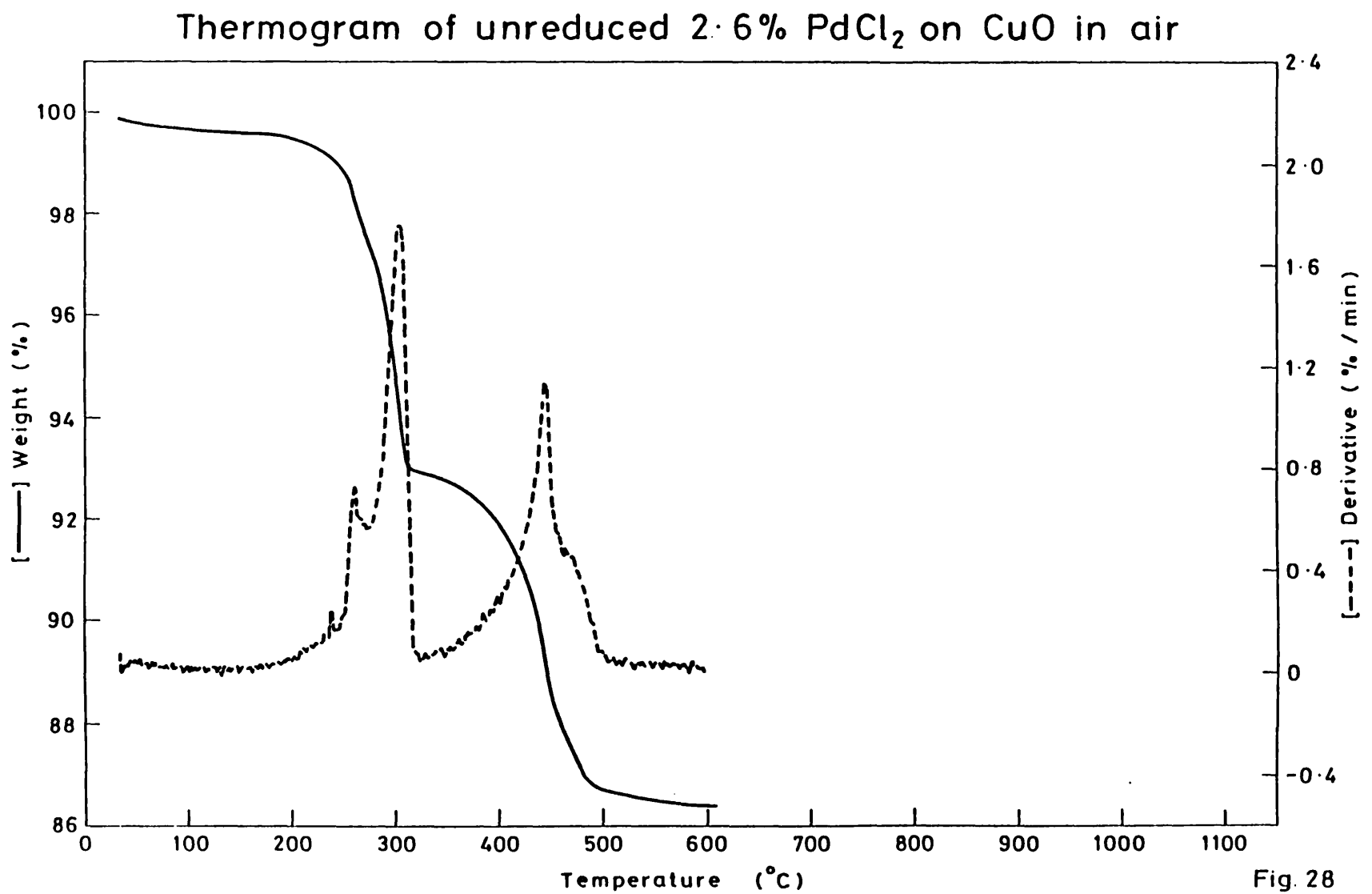

Thermogram of unreduced 2·6% $PdCl_2$ on CuO in air
[——] Weight (%)
[- - -] Derivative (% / min)
Temperature (°C)
100
98
96
94
92
90
88
86
2·4
2·0
1·6
1·2
0·8
0·4
0
-0·4
0
100
200
300
400
500
600
700
800
900
1000
1100

Fig. 28

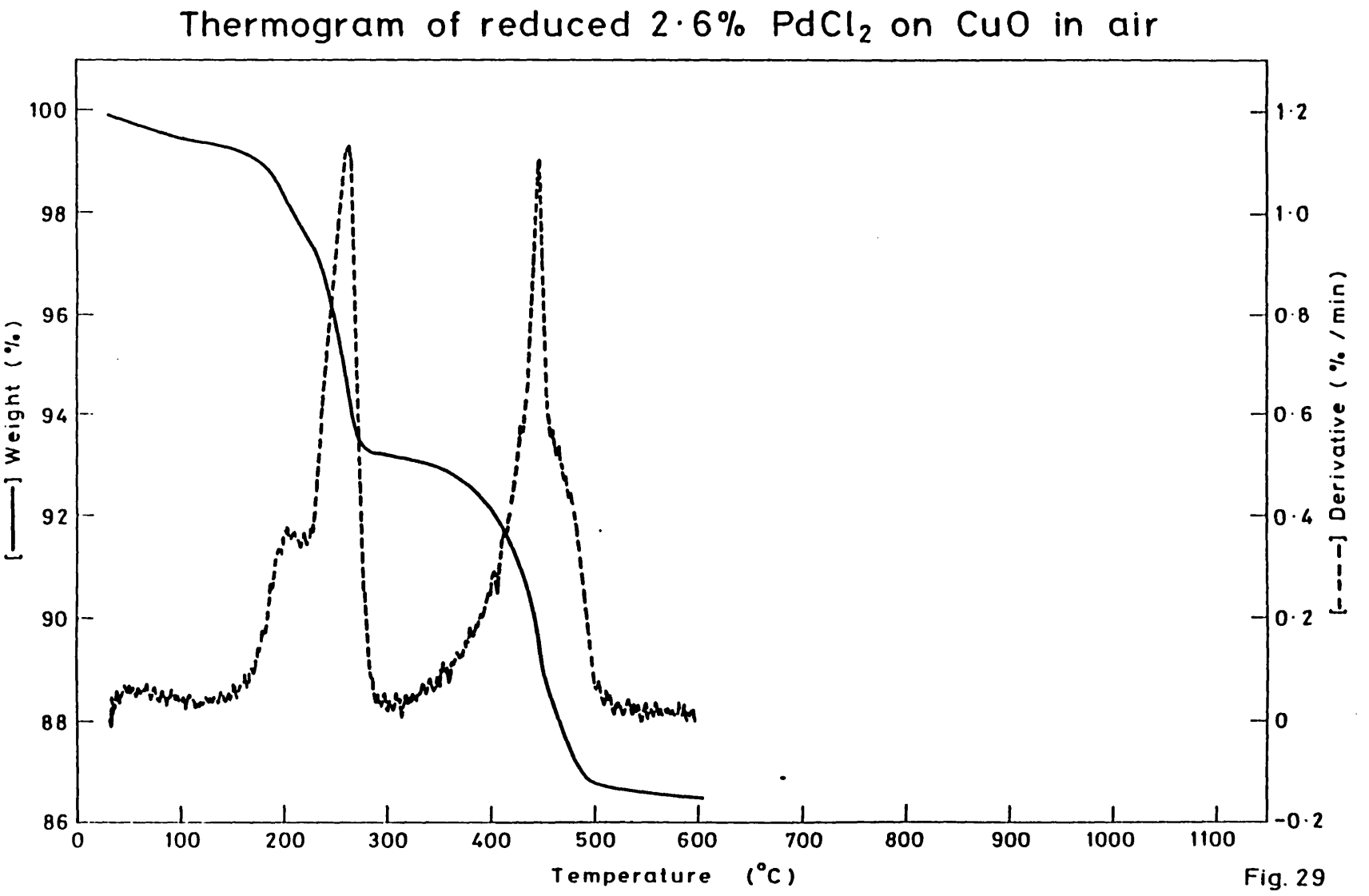

Thermogram of reduced 2·6% $PdCl_2$ on CuO in air
[——] Weight (%)
[- - - -] Derivative (% / min)
Temperature (°C)
100
98
96
94
92
90
88
86
1·2
1·0
0·8
0·6
0·4
0·2
0
-0·2
0
100
200
300
400
500
600
700
800
900
1000
1100

Fig. 29

XRD pattern of unreduced 2·6% $PdCl_2$ on CuO calcined at 550 Celsius

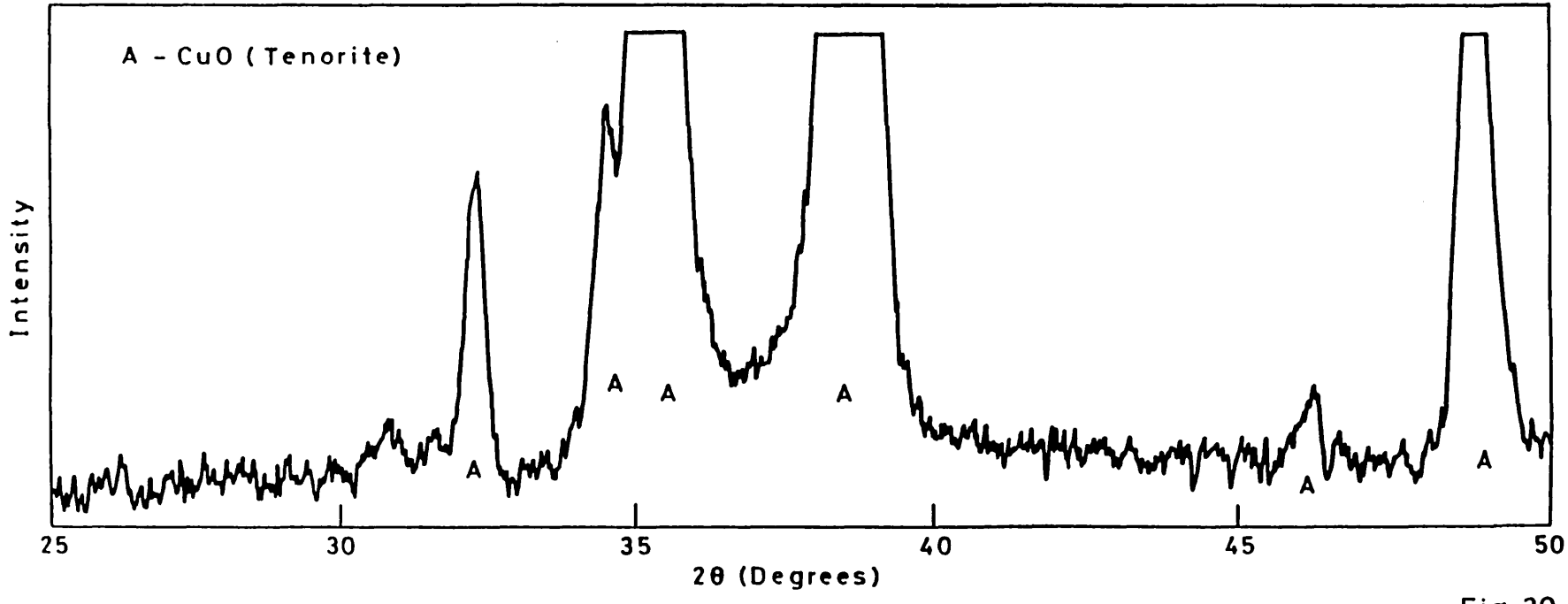


Fig.30.

XRD pattern of reduced 0·45% $PdCl_2$ on CuO

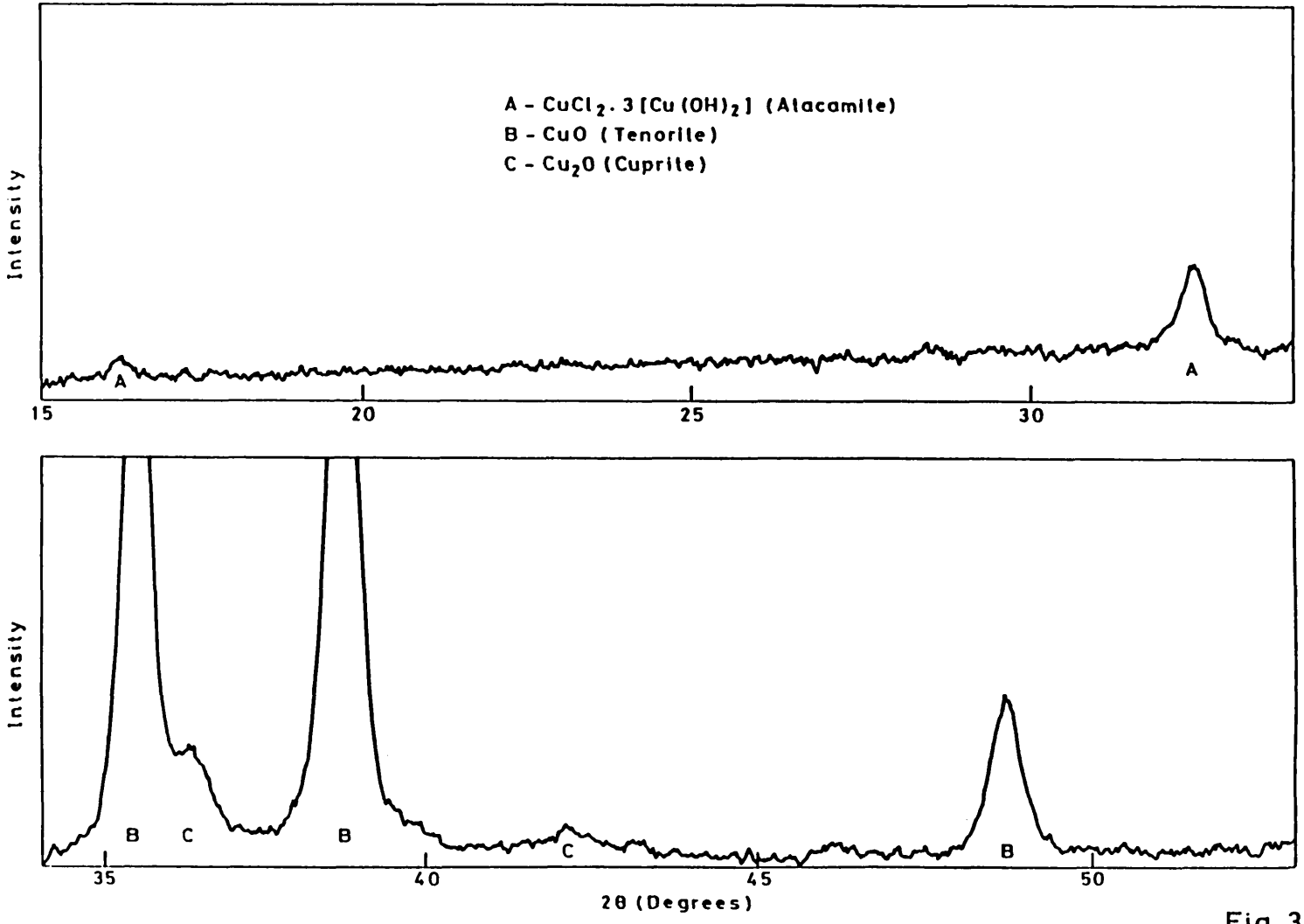


Fig. 31.

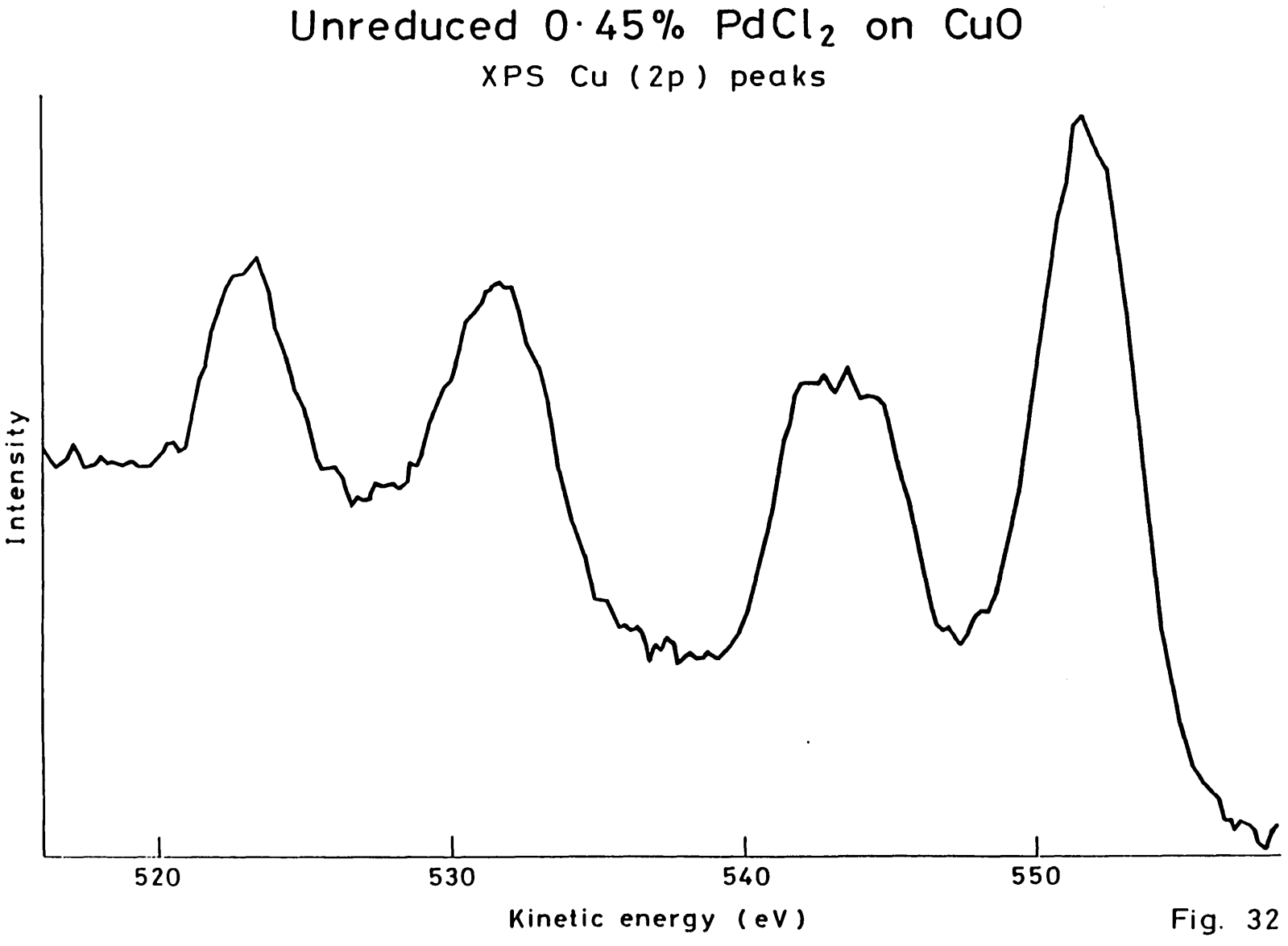

Unreduced 0·45% $PdCl_2$ on CuO
XPS Cu (2p) peaks
Intensity
520
530
540
550
Kinetic energy (eV)

Fig. 32

chlorine 2p peaks for both materials are shown in Figures 35 and 36 resectively. The oxygen 1s peaks for both the unreduced and reduced catalysts again showed 2 chemical enviroments but the ratio s of each having changed on comparison to catalysts 1 and 2 with the hydroxyl species being found in lower concentration, see Figures 37 and 38 respectively.

Table 5.4 a)

X.P.S. results of the unreduced 0.45% palladium chloride on cupric oxide catalyst.

Peak	K.E. (eV)	B.E.* (eV)	Assignment	Concentration
Pd $3d_{5/2}$	1148.4	337.4	$PdCl_2$	0.5%
Cu $2p_{3/2}$	551.9	933.9		
Cu $2p_{1/2}$	532.2	953.6	CuO	43.0%
Cu LMM	917.6*			
O 1s	956.1	529.7	CuO	31.4%
O 1s	954.5	531.3	OH	10.5%
Cl 2p	1287.8	198.0	Cl^-	0.8%

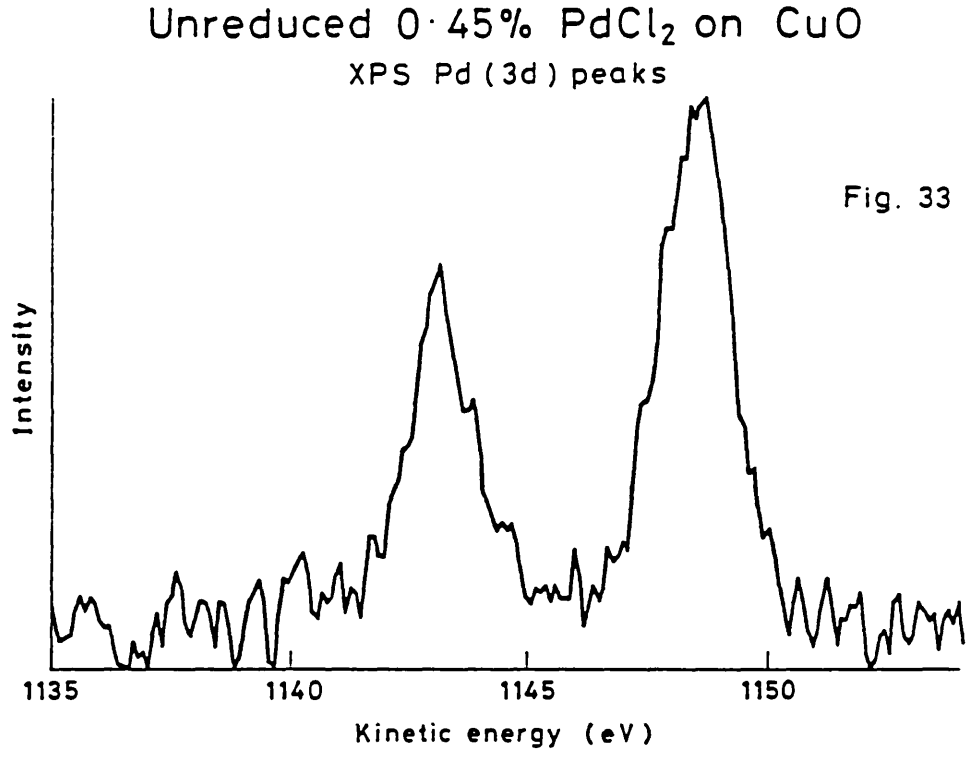

Unreduced 0·45% $PdCl_2$ on CuO
XPS Pd (3d) peaks
Intensity
1135
1140
1145
1150
Kinetic energy (eV)

Fig. 33

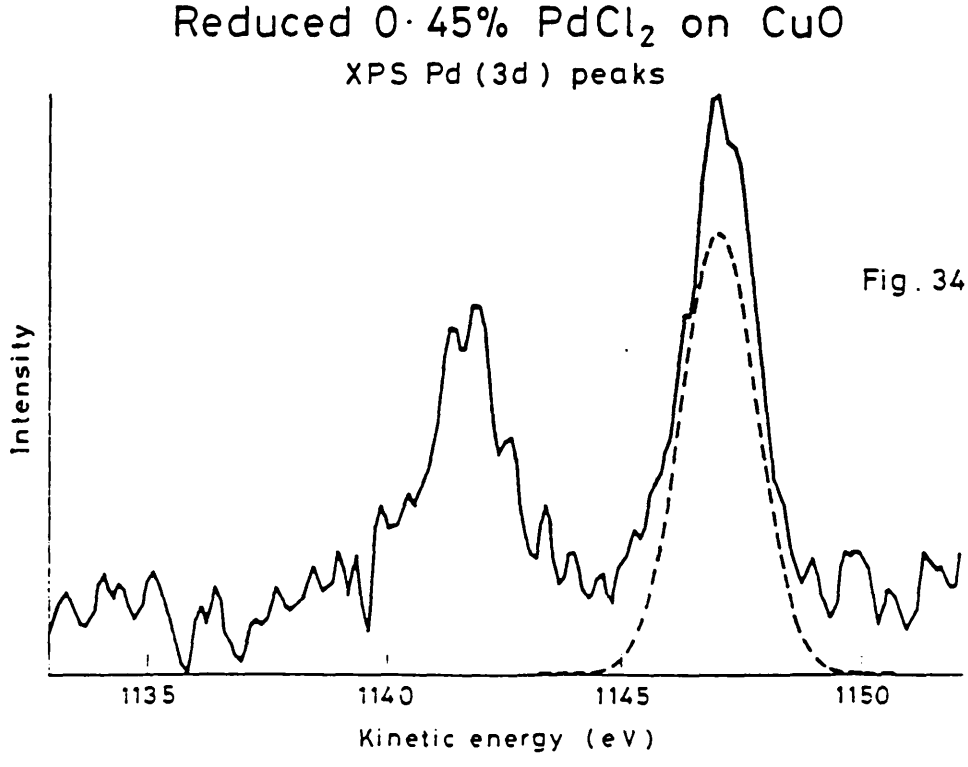

Reduced 0·45% $PdCl_2$ on CuO
XPS Pd (3d) peaks
Intensity
1135
1140
1145
1150
Kinetic energy (eV)

Fig. 34

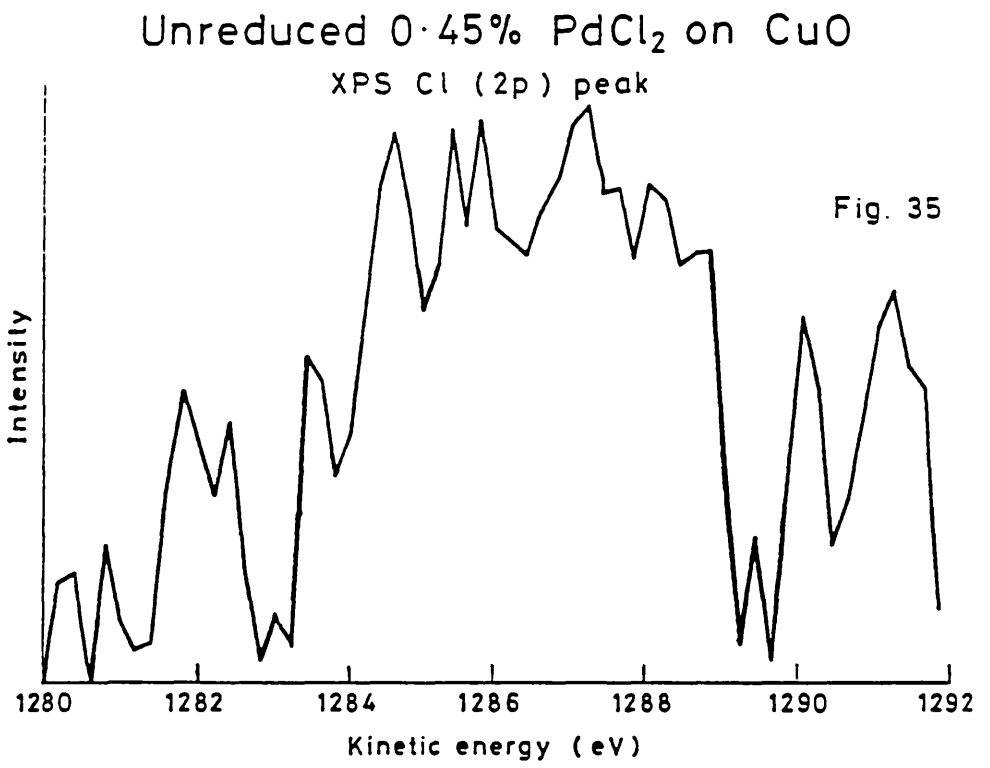

Unreduced 0·45% $PdCl_2$ on CuO
XPS Cl (2p) peak
Intensity
1280
1282
1284
1286
1288
1290
1292
Kinetic energy (eV)

Fig. 35

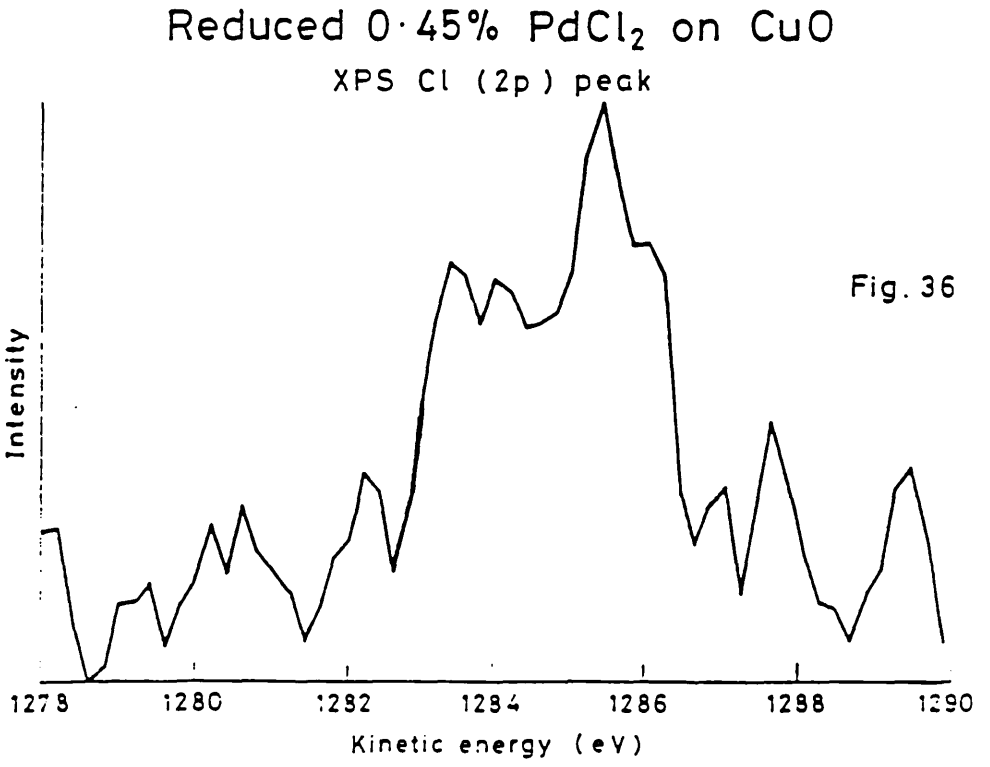

Reduced 0·45% $PdCl_2$ on CuO
XPS Cl (2p) peak
Intensity
1278
1280
1282
1284
1286
1288
1290
Kinetic energy (eV)

Fig. 36

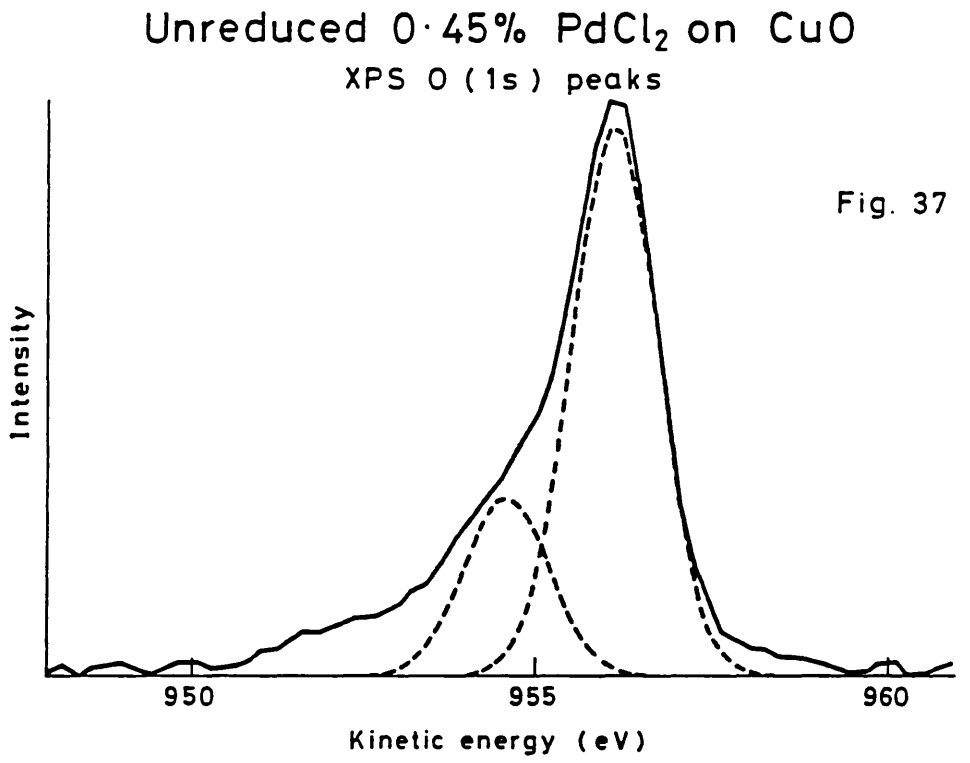

Unreduced 0·45% $PdCl_2$ on CuO
XPS O (1s) peaks
Intensity
950
955
960
Kinetic energy (eV)

Fig. 37

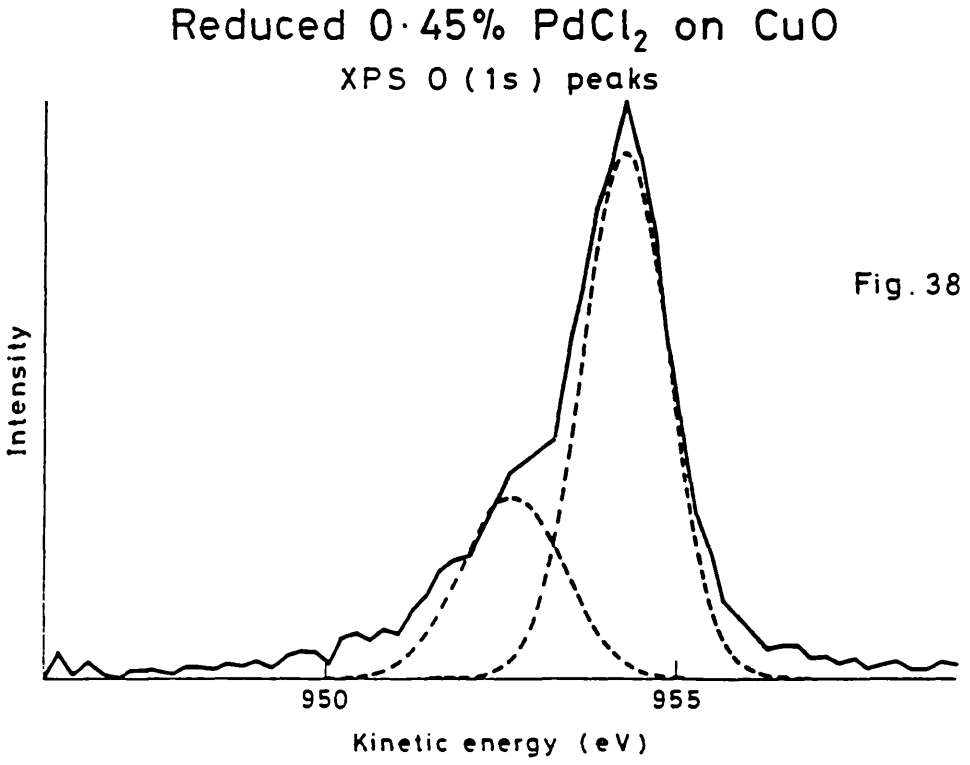

Reduced 0·45% $PdCl_2$ on CuO
XPS O (1s) peaks
Intensity
950
955
Kinetic energy (eV)

Fig. 38

Table 5.4 b)

X.P.S. results of the reduced 0.45% palladium chloride on cupric oxide catalyst.

Peak	K.E. (eV)	B.E.* (eV)	Assignment	Concentration
Pd $3d_{5/2}$	1146.9	337.1	$PdCl_2$	0.5%
Cu $2p_{3/2}$	550.0	934.0		
Cu $2p_{1/2}$	530.1	953.9	CuO	47.0%
Cu LMM	917.5*			
O 1s	954.2	529.8	CuO	30.2%
O 1s	952.6	531.4	OH	12.4%
Cl 2p	1285.4	198.6	Cl^-	8.5%

Thermogravimetric analysis of the unreduced and reduced materials this time gave identical weight loss curves. Again two decompositions were seen, the first at 320 Celsius (note a higher temperature than detected for the higher concentration palladium material) of 1.8% and the second at 390 Celsius (at a lower temperature) of 0.9%, see Figures 39 and 40. The interesting features here are the differences between the peak temperatures of the derivative curve, and the fact that the higher palladium content material gave very similar percentage weight losses for the two decompositions whereas this material gave approximately half the weight loss for the second decomposition as the first.

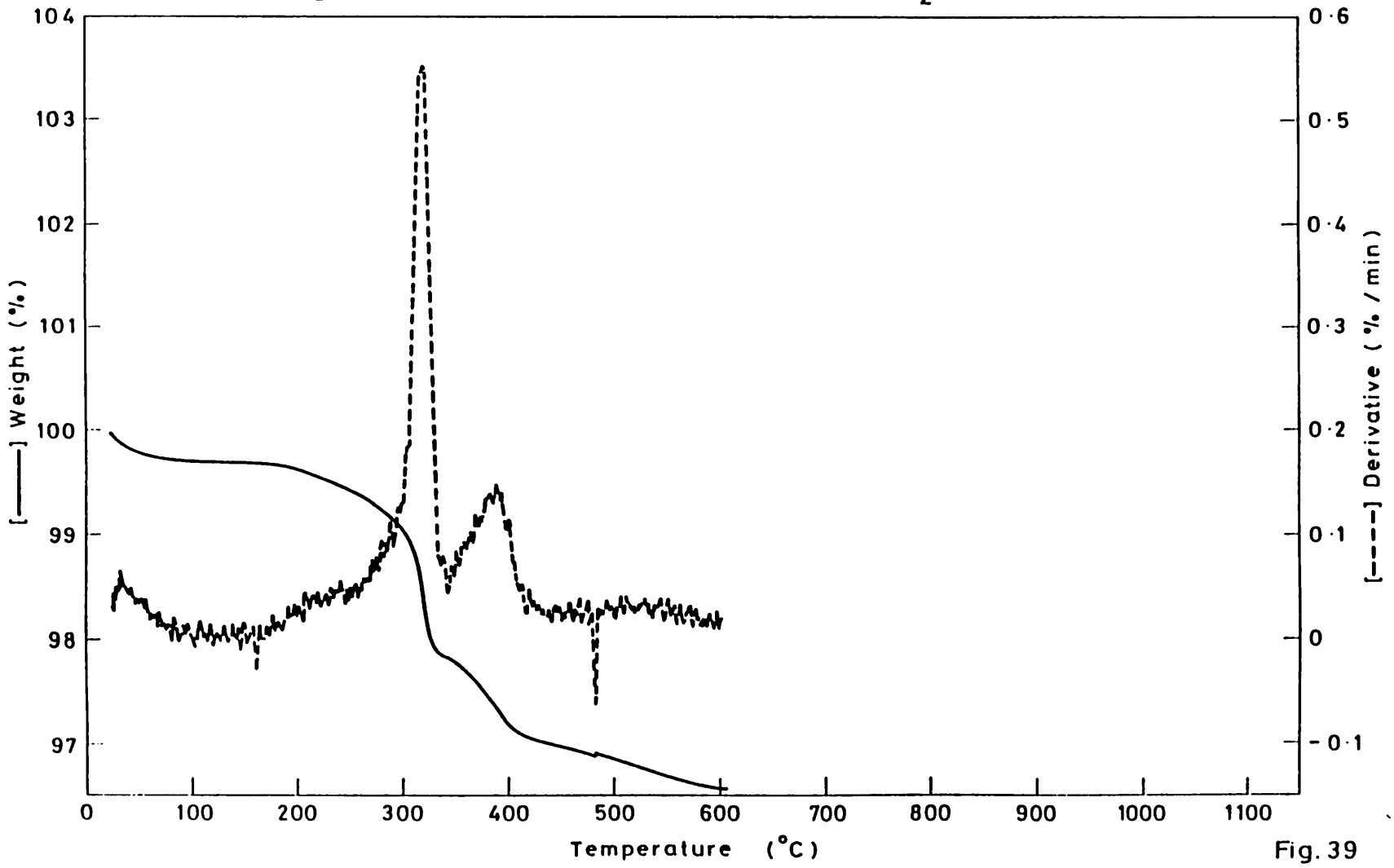

Thermogram of unreduced 0·45% $PdCl_2$ on CuO in air
104
103
102
101
100
99
98
97
[——] Weight (%)
0·6
0·5
0·4
0·3
0·2
0·1
0
-0·1
[- - - -] Derivative (% / min)
0
100
200
300
400
500
600
700
800
900
1000
1100
Temperature (°C)

Fig. 39

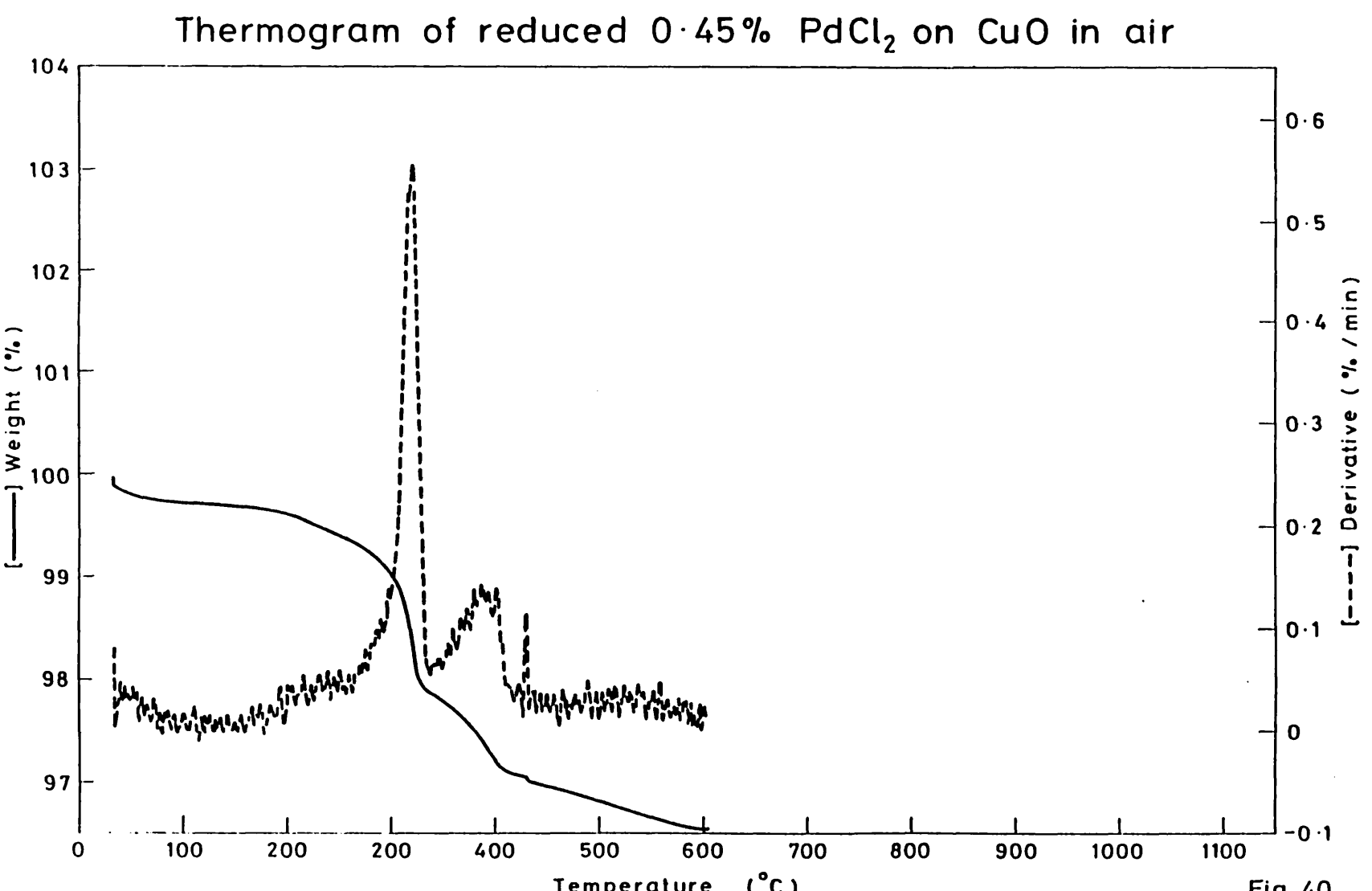

Thermogram of reduced 0·45% $PdCl_2$ on CuO in air
104
103
102
101
100
99
98
97
[——] Weight (%)
0·6
0·5
0·4
0·3
0·2
0·1
0
-0·1
[----] Derivative (% / min)
0
100
200
200
400
500
600
700
800
900
1000
1100
Temperature (°C)

Fig. 40

5.3.3 2.6% palladium nitrate on copper oxide.

Nitrogen physisorption gave B.E.T. surface area values of 23.3 and 19.3m^2/g for the unreduced and reduced materials respectively.

X-ray diffraction detected only cupric oxide for the unreduced material, see Figure 41, but the reduced material also showed a very small amount of cuprous oxide to be present, see Figure 42. No palladium species were detected for either material, suggesting the crystallite size to be very small or noncrystalline palladium species and therefore produce a very broad peak which was undetectable.

X-ray photoelectron spectroscopic analysis of the unreduced and prereduced catalysts, numbers 5 and 6, again showed both to be principally cupric oxide, see Tables 5.5 a) and b) and Figure 43 of the unreduced material. No chlorine was detected, as expected, as the preparation used the palladium (II) nitrate precursor. The palladium spectrum for the unreduced catalyst showed the presence of only one species which was identified as PdO_2, see Figure 44. However, the reduced material showed the presence of 2 species in a 1:4 ratio which were identifiable as elemental palladium and palladium (IV) oxide respectively, see Figure 45. The oxygen spectrum also showed the presence of two species in both the unreduced and prereduced catalysts, the major component being assigned as oxide (CuO) and the minor as hydroxyl, see Figures 46 and 47 respectively.

XRD pattern of unreduced 2·6% $Pd(NO_3)_2$ on CuO

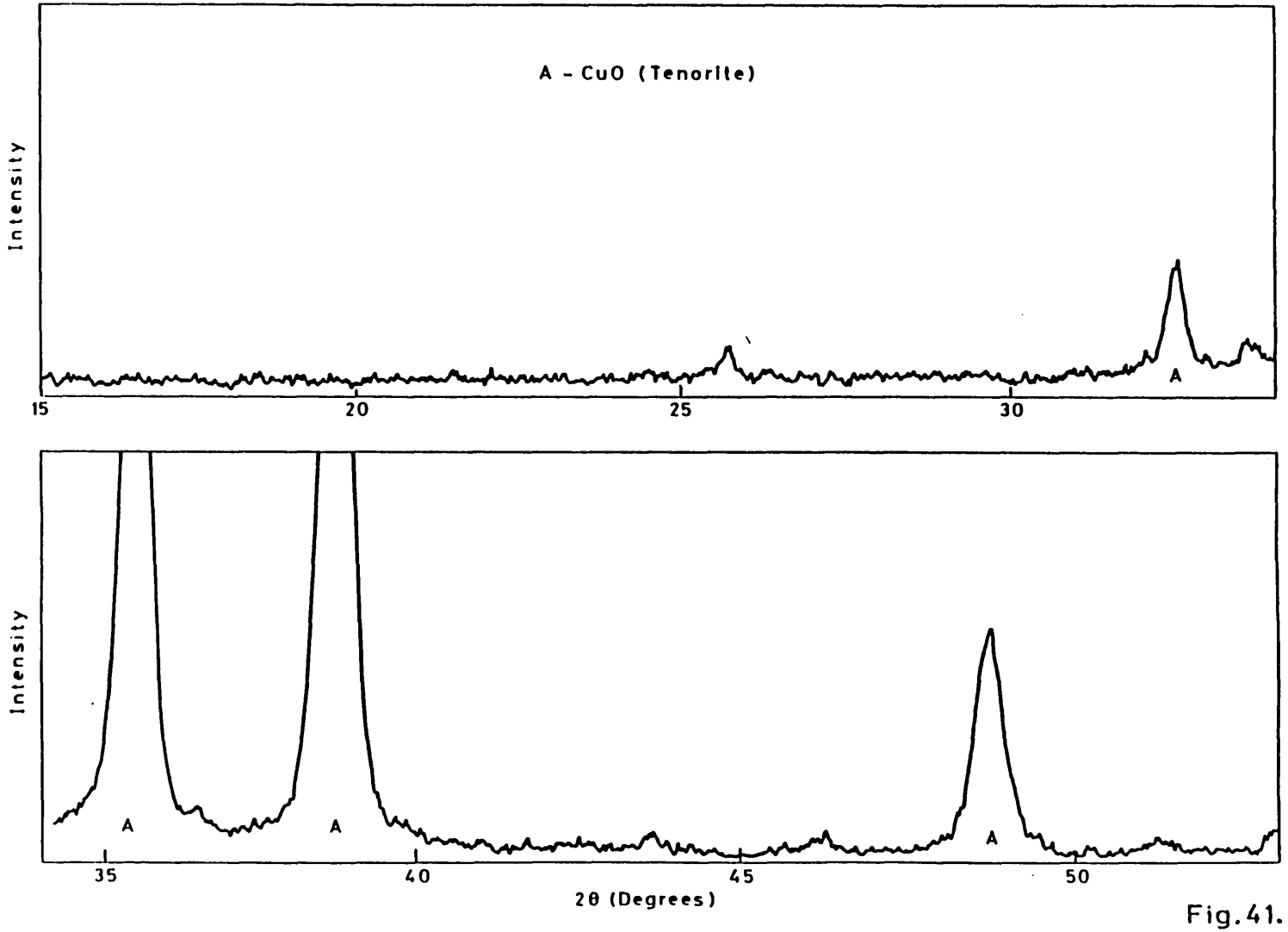


Fig. 41.

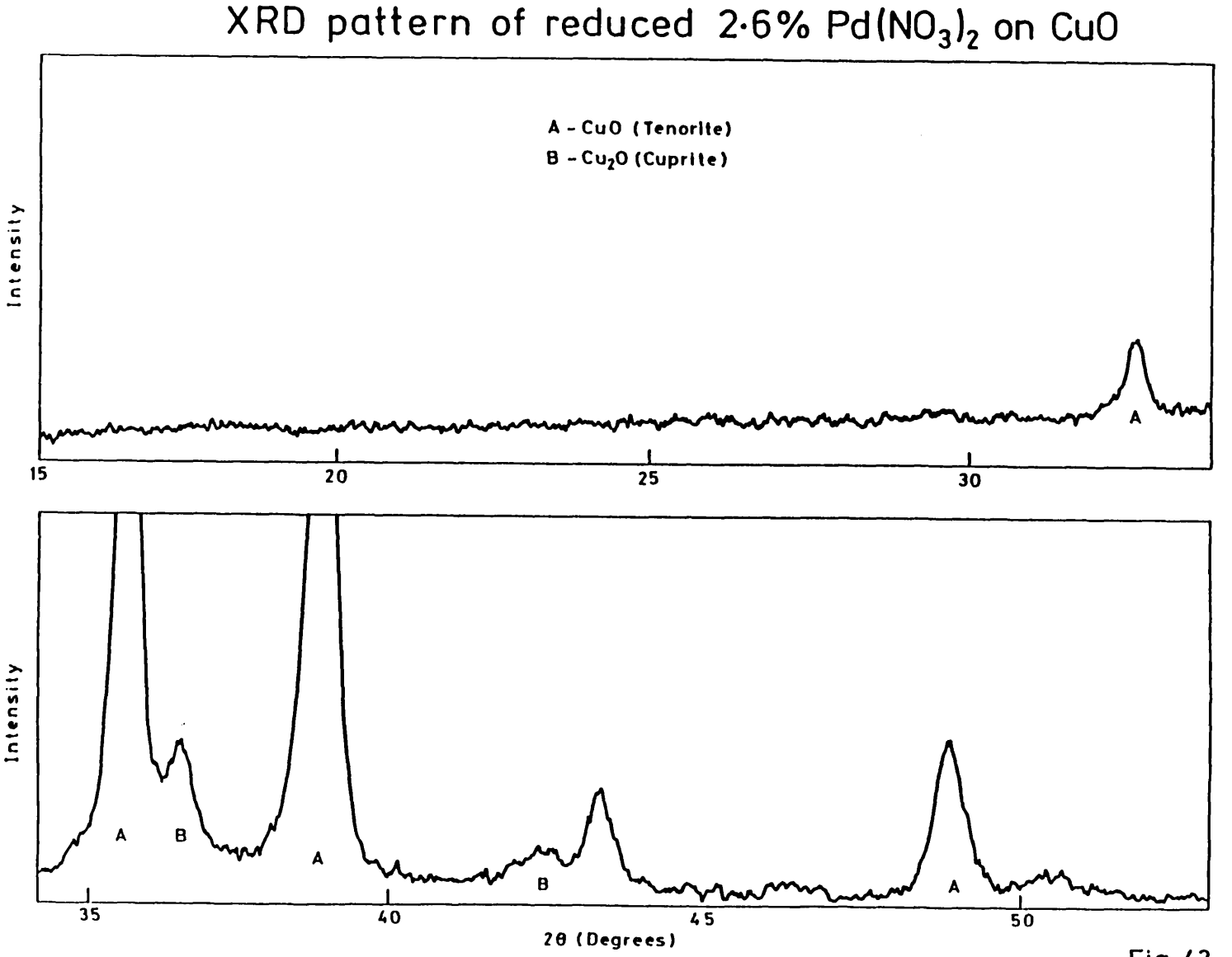

XRD pattern of reduced 2·6% $Pd(NO_3)_2$ on CuO
A - CuO (Tenorite)
B - Cu_2O (Cuprite)
Intensity
A
15
20
25
30
Intensity
A
B
A
B
A
35
40
45
50
2θ (Degrees)

Fig. 42.

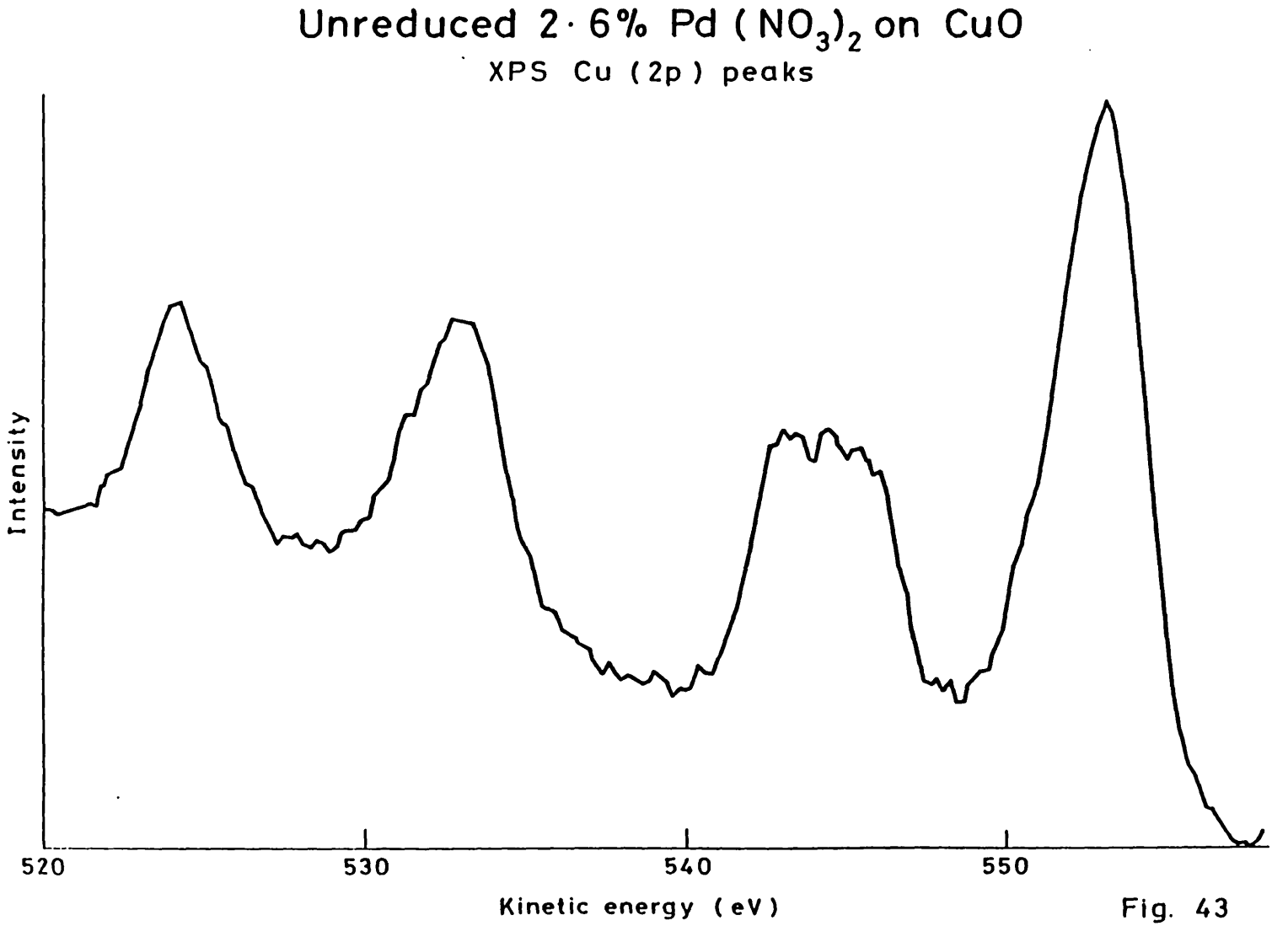

Unreduced 2·6% Pd (NO3)2 on CuO
XPS Cu (2p) peaks
Intensity
520
530
540
550
Kinetic energy (eV)

Fig. 43

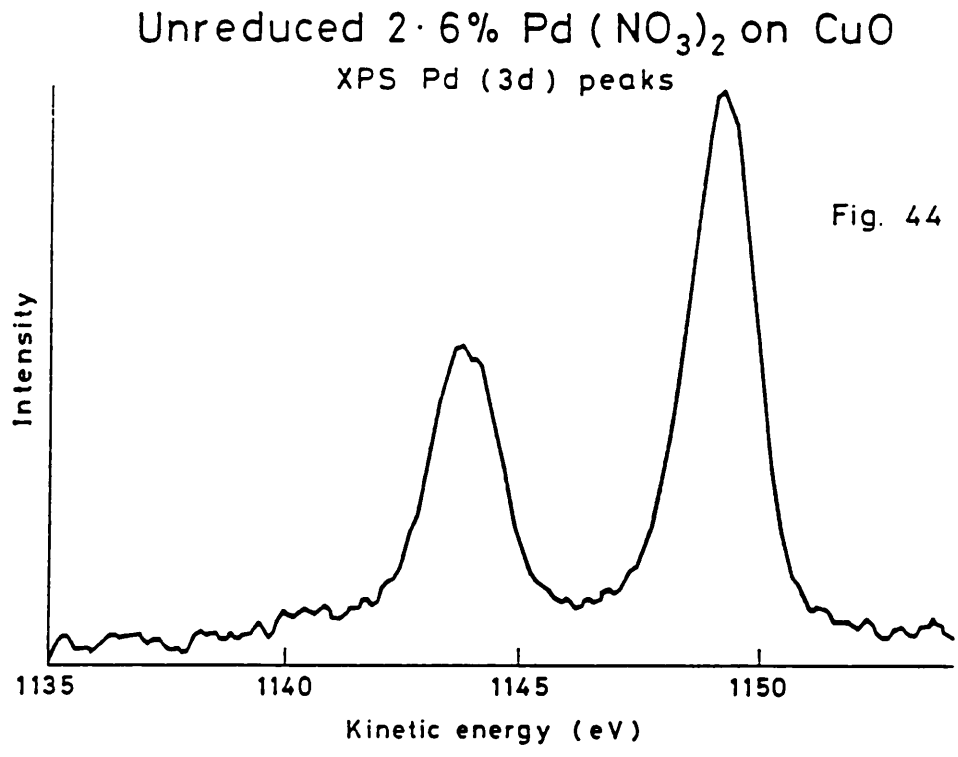

Unreduced 2·6% Pd (NO_3)$_2$ on CuO
XPS Pd (3d) peaks
Intensity
1135
1140
1145
1150
Kinetic energy (eV)

Fig. 44

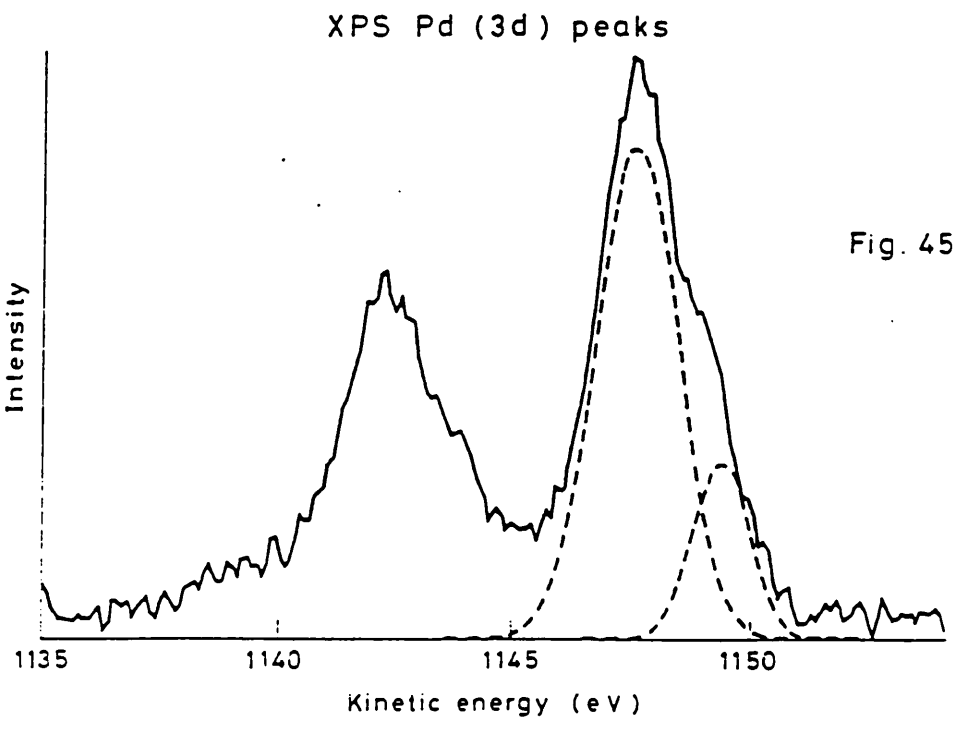

Reduced 2·6% Pd (NO_3)$_2$ on CuO
XPS Pd (3d) peaks
Intensity
1135
1140
1145
1150
Kinetic energy (eV)

Fig. 45

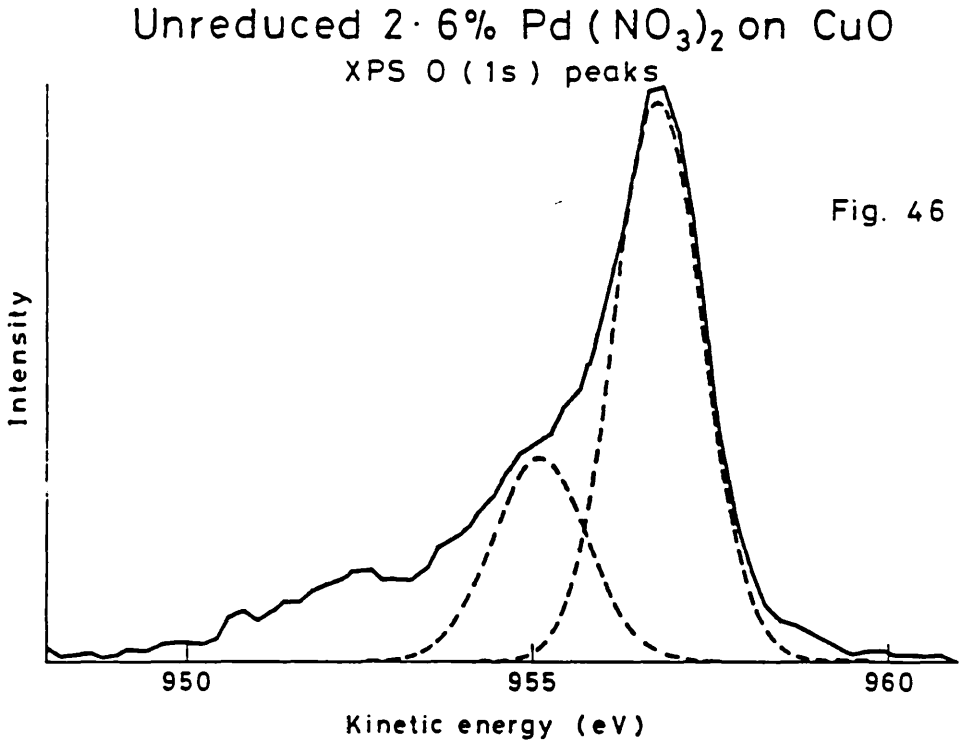

Unreduced 2·6% Pd (NO3)2 on CuO
XPS O (1s) peaks
Intensity
950
955
960
Kinetic energy (eV)

Fig. 46

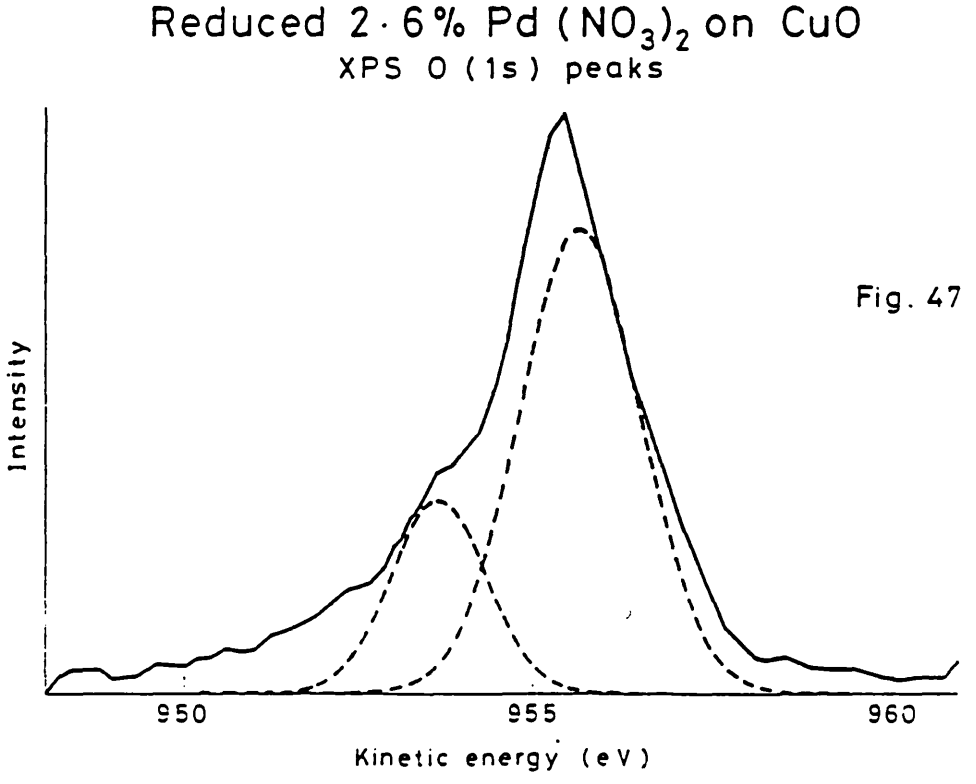

Reduced 2·6% Pd (NO3)2 on CuO
XPS O (1s) peaks
Intensity
950
955
960
Kinetic energy (eV)

Fig. 47

Table 5.5 a)

X.P.S. results of the unreduced 2.6% palladium nitrate on cupric oxide catalyst.

Peak	K.E. (eV)	B.E.* (eV)	Assignment	Concentration
Pd $3d_{5/2}$	1149.1	337.2	PdO_2	1.6%
Cu $2p_{3/2}$	552.8	933.5		
Cu $2p_{1/2}$	532.4	953.9	CuO	40.9%
Cu LMM	917.8*			
O 1s	956.7	529.6	CuO	33.8%
O 1s	955.1	531.2	OH	12.5%

Table 5.5 b)

X.P.S. results of the reduced 2.6% palladium nitrate on cupric oxide catalyst.

Peak	K.E. (eV)	B.E.* (eV)	Assignment	Concentration
Pd $3d_{5/2}$	1149.3	335.7	Pd	0.3%
Pd $3d_{5/2}$	1147.5	337.5	PdO_2	1.2%
Cu $2p_{3/2}$	551.3	933.7		
Cu $2p_{1/2}$	531.6	953.4	CuO	40.4%
Cu LMM	917.9*			
O 1s	955.6	529.4	CuO	34.7%
O 1s	953.6	531.4	OH	11.6%

Thermogravimetric analysis gave a totally different weight loss curve to the two materials prepared from palladium chloride, as expected. An initial weight loss at 40 Celsius of 0.4% probably due to loss of weakly adsorbed water was followed by a second decomposition at 200 Celsius of 1.9%, see Figure 48 of the unreduced catalyst, the reduced catalyst giving a very similar thermogram.

5.4 Discussion of Results and Conclusions.

From the results of studying the catalytic activity of the 2.6% palladium on cupric oxide (sections 5.1.1 and 5.2.1) it was shown that the material was able to catalyse the conversion of n-butane to maleic anhydride. By prereducing this material in a dilute hydrogen atmosphere at 200 Celsius an increase in the catalytic activity and selectivity was achieved despite a reduction in the overall surface area of the material. However, this did correlate with an appearence of surface elemental palladium and a reduction in the palladium chloride species compared to the unreduced material, as shown by X-ray photoelectron spectroscopy. Decreasing the amount of palladium in the catalyst (to 0.45%, by weight) further confirmed this trend, of catalytic selectivity being related to the concentration of surface elemental palladium, by showing an almost proportional reduction in the maleic anhydride selectivity to palladium species concentration. However, very little change in the n-butane conversion with respect to temperature was seen suggesting the existence of a second catalytic site which combusts the butane via a parallel route to carbon dioxide. It was also noted that none of the catalysts studied produced any carbon monoxide as a combustion product. All chlorine containing catalysts studied produced the same range of unidentified compounds shown in the chromatograms,

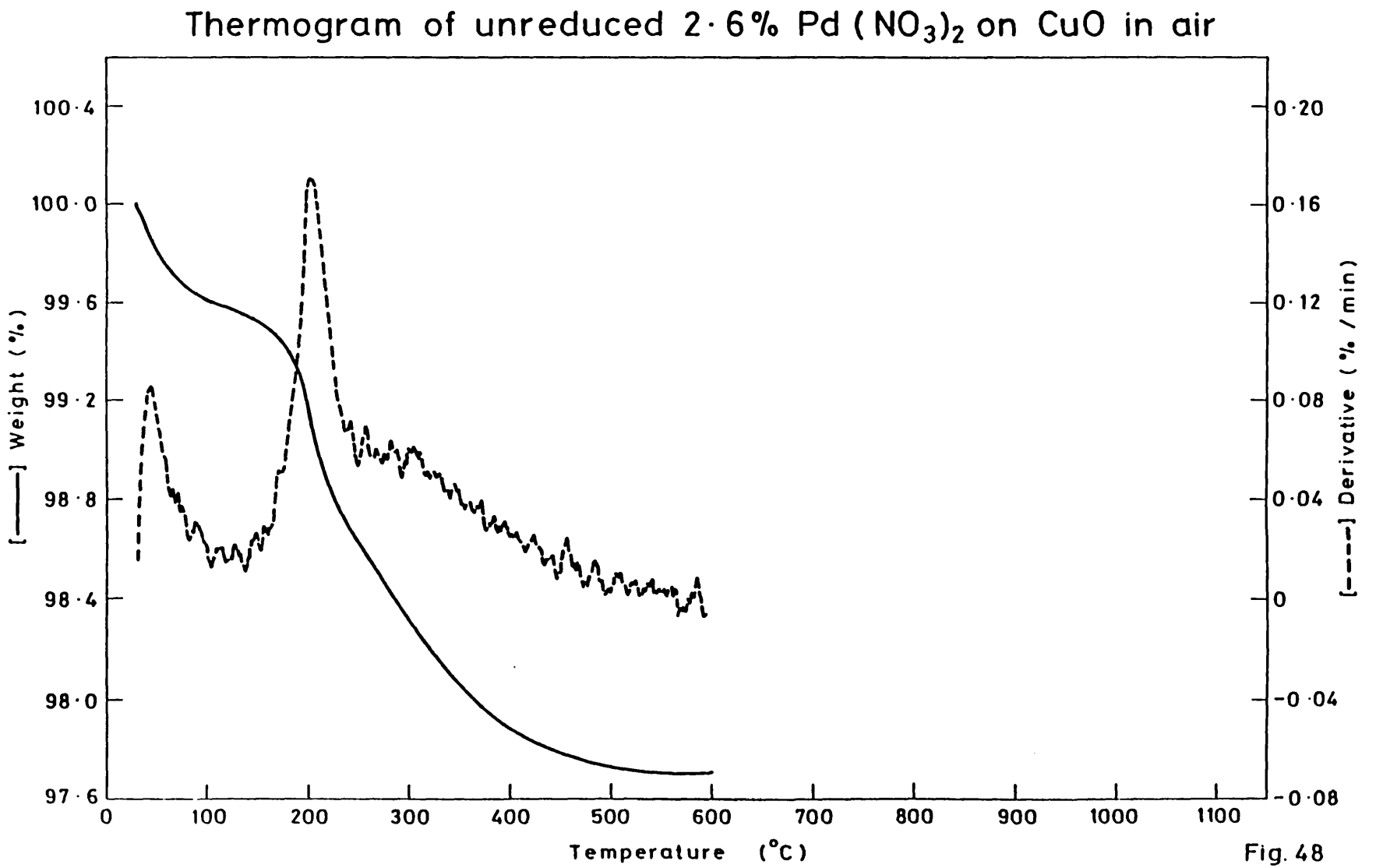

Thermogram of unreduced 2·6% Pd (NO3)2 on CuO in air
100·4
100·0
99·6
99·2
98·8
98·4
98·0
97·6
[——] Weight (%)
0·20
0·16
0·12
0·08
0·04
0
-0·04
-0·08
[- - - -] Derivative (% / min)
0
100
200
300
400
500
600
700
800
900
1000
1100
Temperature (°C)

Fig. 48

these were assumed to be reaction intermediates or byproducts, possibly chlorinated, exact identification being difficult.

In order that elemental palladium could be positively identified as providing the active sites and to investigate the effect of chlorine in the catalyst the 2.6% palladium nitrate on cupric oxide material, reduced, was studied. The results, in section 5.2.4, show that elemental palladium or palladium oxide could not be responsible for the catalysis as no maleic anhydride was detected in the product stream. This seems to contradict the idea given above that elemental palladium present on the surface of the reduced 2.6% palladium chloride catalyst could provide the active sites. Therefore, the presence of chlorine probably is necessary to moderate the catalysts oxidation activity and thus produce partially oxidised products and not just carbon dioxide. Cupric oxide alone was run to eliminate it as the active species and further highlight the necessity of the presence of chlorine. The results, as expected, showed cupric oxide to produce carbon dioxide only. The efficiency with which both cupric oxide and the palladium nitrate material combusted the n-butane was higher than the chloride containing catalysts which was shown up in the temperatures for 50% conversion of the paraffin, see Table 5.2.

X-ray diffraction analysis of the chloride containing materials showed the cupric oxide to have been chlorinated during the preparation, and a definite chlorinated copper oxide phase was identified as being present which was assigned as being copper (II) trihydroxychloride ($CuCl_2.3[Cu(OH)_2]$, known as atacamite). The presence of this material could be the active material as on reduction of the catalysts an increase in maleic anhydride yield was observed which could correspond to a retraction of the palladium species from the surface therefore exposing more of the chlorinated copper (II) lattice. The lower maleic anhydride yields for the 0.45% palladium chloride catalysts, as compared to the 2.6% palladium chloride catalysts,

could be due to the lower extent of chlorination of the cupric oxide lattice. This material is further studied in chapter 7.

CHAPTER 6

COMPARISON OF THE CATALYTIC ACTIVITY OF THE PALLADIUM/COPPER SYSTEM TO VANADIUM PHOSPHORUS OXIDES AND MOLYBDATE CATALYSTS.

The previous chapter has shown that a catalyst based upon the palladium/chlorine/cupric oxide system is active for the oxidation of n-butane to maleic anhydride. In studing these materials it is useful to compare the activities of the chosen catalysts to catalysts already known to be active for the n-butane to maleic anhydride conversion. The materials chosen for the comparative study, from the information given in the literature survey chapter, were vanadium phosphorus oxides (prepared by both the organic and aqueous routes, see section 3.1.1) which is used commercially to produce maleic anhydride, and a range of molybdates (nickel, bismuth, cobalt and iron, see section 3.1.2), which are also known to be active for the conversion of interest.

To test the activity of the chosen material at this stage the reactor system was used with the gas chromatograph set-up for rapid product analysis using method 1 (see chapter 4), as only n-butane and maleic anhydride concentration values were required. A standard reactor programme was used as described in sections 4.2.1 and 4.3.

6.1 Catalyst Preparation and Characterisation.

6.1.1 Vanadium phosphorus oxide - aqueous route[99].

Vanadium pentoxide was reduced by refluxing in a 36% hydrochloric acid solution to form a blue solution (molybdenum was also present as the trioxide, V:Mo = 1:0.003), to this reduced solution of vanadium (IV) ions phosphorus was added (as orthophosphoric acid, P:V = 1.28:1). The hydrochloric acid was then distilled off. Methanol was added to the cooled viscous mix of vanadium and phosphorus ions, in which the syrup dissolved, and xylene was added which formed an immiscible layer. The mixture was then refluxed, followed by distillation of the methanol. The xylene layer was finally decanted off to leave a blue syrup. The viscous solution was then dried in a vacuum oven under an atmosphere of dry nitrogen (0.5 atmosphere, 125 Celsius), to yield a blue green solid which was stored in a desiccator as it appeared to be hygroscopic.

X-ray diffraction identified, on comparison to the literature[10,20,23,26,27], the precursor phase present as $(VO)_2P_2O_7.2H_2O$ known as the α-phase, which is the desired precursor phase which decomposes at 380 Celsius yielding the active β- or B-phase[10].

X-ray photoelectron spectroscopy showed the average vanadium oxidation state as approximately +4 (Vanadium $2p_{3/2}$ B.E.* = 516.5 eV and Vanadium $2p_{1/2}$ B.E.* = 523.3 eV) and the surface ratio of vanadium and phosphorus to be 1:1.4 and the phosphorus to molybdenum ratio as 1:0.03. This indicated there to be a slight surface excess of phosphorus compared to the bulk, and a great surface excess of

molybdenum. This result agrees with the previously reported literature, reference 91.

Nitrogen surface area measurements gave a very low value of approximately 1 m^2/g for the precursor material.

6.1.2 Vanadium phosphorus oxide - organic route[26].

Vanadium pentoxide was suspended in a 60:40 mixture of isobutyl alcohol and benzyl alcohol and refluxed. To the cooled suspension of V(IV) ions, orthophosphoric acid dissolved in isobutyl alcohol was added to give a P:V ratio of 1.08:1, and the resulting mixture was refluxed. The green slurry that had formed was then filtered off, dried thoroughly at 150 Celsius and then slowly heated to 400 Celsius in air to convert the precursor material into the active phase.

Nitrogen physisorption measurements gave a B.E.T. surface area of 20 m^2/g. X-ray diffraction patterns, on comparison to those reported in the literature[10,19,20,23,26,27], showed the material to be a mixture of the β- and B-phases as expected and desired.

6.1.3 Bismuth molybdate, $Bi_2Mo_3O_{12}$[100].

Molybdenum trioxide was dissolved in ammonia solution to yield a solution of ammonium molybdate, to this bismuth nitrate was slowly added in dilute nitric acid to give a stoichiometric mix of bismuth and molybdenum. The resultant solution was then precipitated by the slow addition of ammonia solution to a pH of 3.0, yielding a pale yellow solid which was thoroughly washed then dried at 50 Celsius before calcining, in air, at 500 Celsius.

The B.E.T. surface area was measured as 2.4 m^2/g by nitrogen physisorption. The X-ray diffraction pattern showed the characteristic lines of monoclinic bismuth molybdate[100].

6.1.4 Bismuth molybdate plus 10% excess molybdenum trioxide[100].

The preparation of this material was identical to that of pure bismuth molybdate except 10% more than the stoichiometric amount of molybdenum was used. The excess molybdenum trioxide showed up in the X-ray diffraction pattern, but had little effect upon the B.E.T. surface area, which was 2.7 m^2/g.

6.1.5 Nickel molybdate, $NiMoO_4$, plus 15% excess molybdenum trioxide[42].

The preparation technique used was very similar to that used for bismuth molybdate. To a solution of nickel nitrate was added, slowly, a solution of ammonium heptamolybdate at a temperature of 60 Celsius. The pH of the resulting solution was then increased to 5.5 by the addition of ammonia solution. The solution was then allowed to cool to room temperature to allow full precipitation yielding a light green solid on drying. After calcination at 500 Celsius the solid had changed to yellow.

Nitrogen physisorption measurements gave a B.E.T. surface area value of 9.5 m^2/g, and the X-ray diffraction trace, on comparison to the literature[42], indicated the presence of nickel molybdate with excess molybdenum trioxide.

6.1.6 Cobalt molybdate, $CoMoO_4$, plus 15% excess molybdenum trioxide[39,42].

The method of preparation was similar to that of nickel molybdate except that the precipitate formed immediately on the addition of the ammonium heptamolybdate. The purple solid that was precipitated remained purple on calcination, but on grinding gently at room temperature it turned olive green.

Measurement of the B.E.T. surface area by nitrogen physisorption gave a value of 12.7 m^2/g. X-ray diffraction patterns of the purple and green materials showed them to be the two phases, *A* and *B*, of cobalt molybdate, the phase change reportedly occurring at 420 Celsius[39].

6.1.7 Iron (II) molybdate, $FeMoO_4$[38].

The preparation technique was again coprecipitation from a solution of iron (II) and molybdenum, the solution once mixed was held at 80 Celsius and pH 5.0 under a blanket of nitrogen to stop oxidation of the iron (II) to iron (III). The light brown precipitate was then filtered off, washed, dried and finally calcined at 400 Celsius under dry nitrogen.

The B.E.T. surface area was measured as 19.5 m^2/g, and the X-ray diffraction trace was characteristic of pure β-$FeMoO_4$[38].

6.1.8 Iron (III) molybdate, $Fe_2Mo_3O_{12}$[38].

This material was also prepared by coprecipitation, but this time from an iron (III) solution. However, accurate control of the pH was needed as above 2.2 precipitation of iron (III) hydroxide occurred, and below 2.2 polymerised

molybdenum anions are present. The precipitate obtained contains iron salts with a high Mo:Fe ratio. Calcination of this precipitate at 500 Celsius then causes these to decompose to give a mixture of $Fe_2Mo_3O_{12}$ and MoO_3.

X-ray diffraction confirmed the presence of both pseudo-orthorhombic $Fe_2Mo_3O_{12}$ and MoO_3, and nitrogen physisorption gave a B.E.T. surface area of 9.5 m^2/g.

6.2 Catalyst Activity Measurements.

6.2.1 Vanadium phosphorus oxide - aqueous route.

This catalyst produced maleic anhydride which was detected in the product stream above a catalyst temperature of 475 Celsius, no maximum in maleic anhydride production was found as the highest temperature investigated was 500 Celsius at which a yield of only 1.0% was obtained. At 500 Celsius only 25% of the n-butane had been converted and this gave a selectivity towards maleic anhydride of 3.1%, see Table 6.1. White solids were trapped out and these showed the characteristic infrared spectrum of maleic anhydride, aqueous trap washings also gave positive wet chemical tests. Despite the maleic anhydride yields being much lower than for the unreduced 2.6% palladium chloride on cupric oxide (section 5.2.1), solid maleic anhydride deposits were collected as very little water would have been produced by combustion processes during and after the maleic anhydride so hydrolysis and dissolution would not have taken place. The only reaction products detected apart

(see page 217)

from maleic anhydride were carbon monoxide, which was not found with the palladium/copper catalysts, and carbon dioxide.

6.2.2 Vanadium phosphorus oxide - organic route.

Maleic anhydride was detected in the product gas stream at catalyst temperatures above 350 Celsius. No maximum in production was detected as the highest yield, of 13%, was detected at 500 Celsius, the highest temperature used. The yield of maleic anhydride with this catalyst was significantly higher than that detected for palladium on cupric oxide (1%), however, the difference in maximum detected selectivity was much less (9.0% as opposed to 35%). A large amount of white needle shaped crystals of maleic anhydride were collected in the "U" trap, as identified by infrared spectroscopy and wet chemical analysis. Again the only products detected by G.C. apart from the maleic anhydride, were carbon monoxide and carbon dioxide.

6.2.3 Bismuth molybdates.

Both bismuth molybdates (sections 5.1.4 and 5.1.5) showed only minimal conversion efficiency towards n-butane even at 500 Celsius (10%). The catalytic material containing excess molybdenum trioxide possibly produced a small amount of maleic anhydride, as detected by wet chemical tests but too little was produced to be detected by the gas chromatograph and produce a peak large enough to be integrated or for definite identification using infrared analysis. Without excess molybdenum trioxide, maleic anhydride was not detected by the gas chromatograph

or in the product traps. The only products being detected in the chromatograms being carbon monoxide and carbon dioxide.

6.2.4 Nickel molybdate.

This material, as expected, showed some activity in the production of maleic anhydride; the maximum yield of 0.2% was detected at 500 Celsius at a n-butane conversion of 69%. The selectivity, however, was rather low (0.2%). White solids were trapped out and identified as maleic anhydride by the wet chemical tests and infrared spectroscopy. Carbon monoxide and carbon dioxide being the only other detected products.

6.2.5 Cobalt molybdate.

At 500 Celsius 44% of n-butane was converted but no maleic anhydride peak was detected in the chromatogram, only peaks for carbon monoxide and carbon dioxide were detected. However, maleic anhydride (identified by infrared spectroscopy and wet chemical tests) was collected in the "U" trap.

6.2.6 Iron molybdates.

Only slight evidence for the production of maleic anhydride was found for iron (II) molybdate (wet chemical analysis of the traps), no evidence of maleic anhydride being produced by the iron (III) molybdate material was found. At 500

Celsius with the iron (III) material only 33% of the n-butane had been converted whereas the iron (II) molybdate catalyst converted 94%.

Table 6.1

Catalyst	Maximum Maleic Anhydride Yield	Optimum Temperature	n-Butane conversion
VPO aq. prep.	1.0%	500 Celsius	25%
VPO organic prep.	13.0%	500 Celsius	99%
$BiMoO_4$	None detected.	500 Celsius	10%
$BiMoO_4$ + MoO_3	Small amount found in the cold traps.	500 Celsius	2%
$NiMoO_4$ + MoO_3	0.2%	500 Celsius	69%
$CoMoO_4$ + MoO_3	Small amount found in the cold traps.	500 Celsius	44%
$FeMoO_4$	None detected.	500 Celsius	94%
$Fe_2Mo_3O_{12}$	None detected.	500 Celsius	33%

6.2.7 Catalytic activity of other supported palladium catalysts.

As the palladium chloride / cupric oxide materials had been found to be active, a range of other supported palladium catalysts should be studied for activity towards the n-butane to maleic anhydride conversion. These materials were a family of palladium chloride on ceramic oxides. The palladium chloride materials were prepared exactly as palladium chloride on cupric oxide and in all cases the reduced

materials were used for the activity test. The support materials being alumina, magnesia, chromia, manganese dioxide, molybdenum trioxide, niobium pentoxide, tantalum pentoxide, ceria, zirconia, titania, and lanthanum trioxide. None of these materials showed any partial oxidation activity, they merely combusted the n-butane with varying ability to produce carbon oxides. Temperatures for 50% conversion of n-butane were as shown in Table 6.2 below.

Table 6.2.

Ceramic Oxide Support	T_{50} (Celsius)
Alumina (C)	325
Magnesia	475
Chromia	275
Manganese dioxide	375
Molybdenum Trioxide	400
Niobium pentoxide	425
Tantalum pentoxide	275
Ceria	375
Zirconia	300
Titania	300
Lanthanum trioxide	275

6.3 Discussion of results.

In order of decreasing maleic anhydride yield the catalysts studied were:

VPO (organic route) > Palladium chloride/cupric oxide > VPO (aqueous route) > $NiMoO_4$ > $CoMoO_4$ > $Bi_2Mo_3O_{12}$ + MoO_3 > $FeMoO_4$ > $Bi_2Mo_3O_{12}$, $Fe_2Mo_2O_{12}$.

On taking into consideration the differences in surface areas of the materials and assuming that the number of active sites to be proportional to the surface area, the maleic anhydride yield from the vanadium phosphorus oxide catalyst made by the aqueous route was comparable to that from the vanadium phosphorus catalyst made by the organic route, but a higher temperature is required to attain approximately the same turnover number, this phenomenon having been reported in the literature[10,26]. However, an even lower optimum temperature for maleic anhydride production was found for the palladium/chloride/cupric oxide catalyst than for either vanadium phosphorus oxide catalysts studied.

The order of catalytic activity with respect to maleic anhydride yields, on which the molybdate catalysts were found to fall, agreed with that published in the literature[36-42]. This series of catalysts has shown that the activity of the chosen material, palladium/chloride/cupric oxide, is comparable with the commercial vanadium phosphorus oxide catalysts and an interesting feature is that its optimum activity occurs at low temperatures. The yields of maleic anhydride were probably recorded as being lower than actually present, as it was found that stainless steel gas chromatographic columns strongly adsorb maleic anhydride (see section 4.2.2), but as only comparisons between catalysts were drawn and no absolute activity results were needed then rerunning the catalysts with glass chromatographic columns was unnecessary.

Unlike the palladium/chloride/cupric oxide catalyst none of the other catalysts studied produced any detectable quantities of unidentified products.

However, they all showed a difference to the palladium /chloride/cupric oxide catalyst in that combustion products included carbon monoxide as well as carbon dioxide, suggesting either a different reaction pathway to produce totally oxidised products or that the palladium/chloride/cupric oxide catalyst is very active for the conversion of carbon monoxide to carbon dioxide.

CHAPTER 7

INVESTIGATIONS OF COPPER HYDROXYCHLORIDE MATERIALS.

In Chapter 5 it was shown that palladium/chloride/cupric oxide catalysts are active for the selective oxidation of n-butane to maleic anhydride. Also it was found that palladium oxide or metal as well as cupric oxide are combustion catalysts only. Therefore, it was decided that the support material alone should be studied as characterisation of the active materials in chapter 5 showed that the cupric oxide support had, during preparation of the catalyst, become chlorinated, which was not surprising. X-ray diffraction analysis of the palladium/chloride/cupric oxide catalysts showed that the extent of chlorination was sufficient to produce crystalline chlorinated cupric oxide material, which was identified as copper (II) trihyroxychloride in the δ or atacamite phase.

7.1 Initial Activity Studies of the Support Material.

The preparation technique for the support material was identical to that used for the 2.6% palladium on copper oxide from palladium chloride, see section 5.1.1, which was followed exactly with the exception of the addition of the palladium chloride. The X-ray diffraction pattern of the dried, unreduced material was identical to the palladium containing species remembering that no reflections had been seen that were attributable to crystalline palladium species.

This material was then studied for catalytic activity, using the same reactor programme and gas chromatographic method as used in chapter 5 and described in section 4.2.3 as method 2. A maximumin maleic anhydride yield of 2.5% was detected

at a catalyst temperature of 375 Celsius, see Figure 49, this corresponded to an n-butane conversion of 23.2%. However, the maximum selectivity towards maleic anhydride of 19.7% was detected at 325 - 350 Celsius, as shown in Figure 50. The temperature for 50% n-butane conversion was 400 Celsius, see Figure 49. Unidentified peaks in the chromatograms were found at the same retention times in this experiment as with the 2.6% palladium (chloride) on cupric oxide material, see Figure 51.

This result shows that the support material is catalytically active for the partial oxidation of n-butane and supports the idea that none of the palladium species shown by X-ray photoelectron spectroscopy to be present on the surface of the palladium/cupric oxide catalysts, studied in chapter 5, are catalytically active for the n-butane to maleic anhydride conversion, but merely convert the n-butane to carbon dioxide and water. Support for the idea that the active material is the chlorinated cupric oxide lattice is provided by the results of this catalytic activity experiment showing a higher maleic anhydride yield and selectivity, probably due to palladium species not masking the active surface sites. Also the range of unidentified products, whether they are reaction intermediates or byproducts, found in the chromatograms were at the same retention time as those found when studing the palladium chloride on cupric oxide catalysts. The cupric oxide alone had also been shown previously to be a combustion catalyst. However, its presence in the active material along with the atacamite may be necessary, for example, as a source of lattice oxygen for insertion into the activated, dehydrogenated hydrocarbon molecule. Copper chlorides, in both valency state (I) and (II), are well known catalysts for the oxychlorination of unsaturated aliphatic and aromatic hydrocarbons[101,102,103], as well as for the polymerisation of halogenated aromatic ketones[104]. Therefore, as the actual active material and phase was uncertain initial

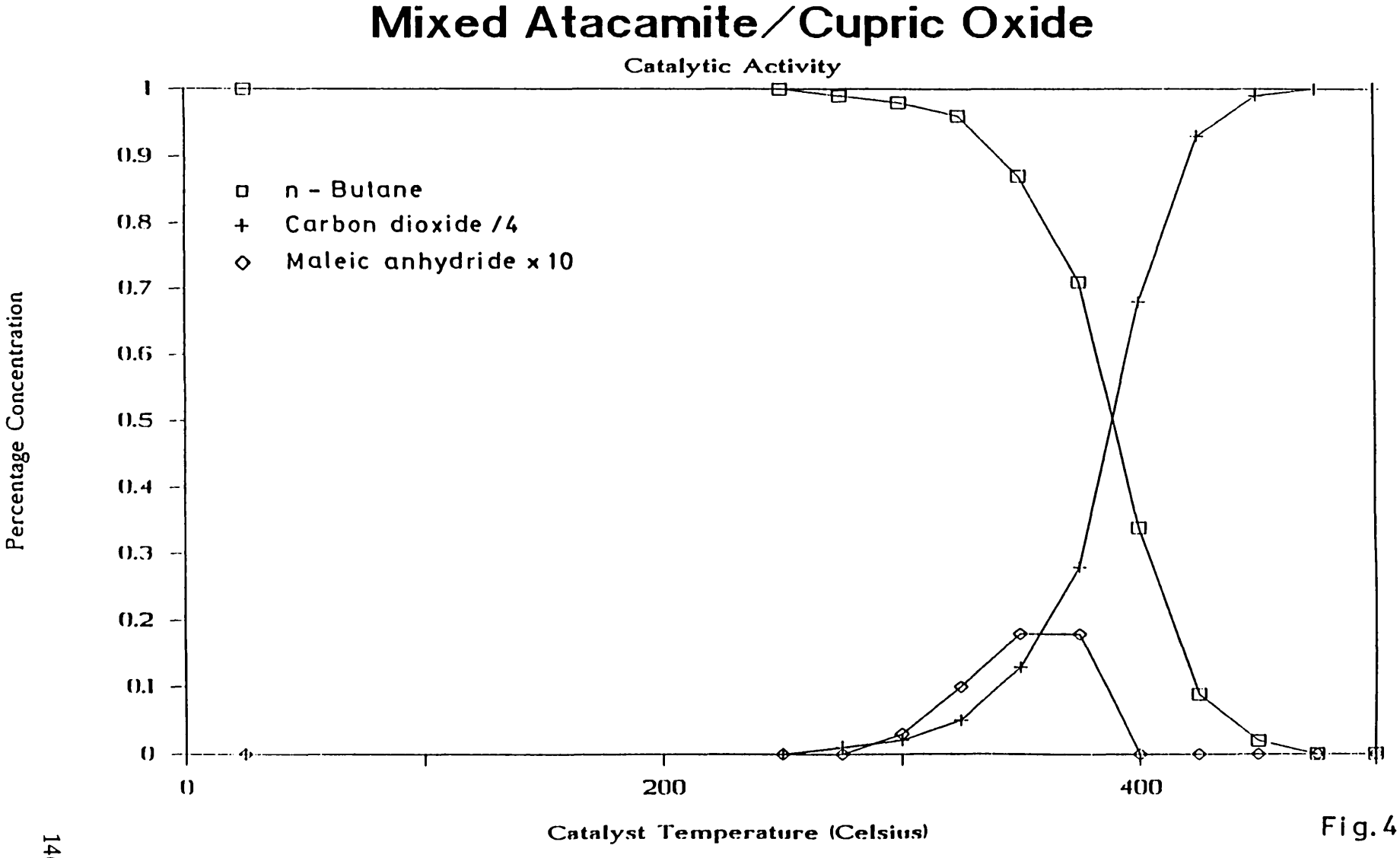

Mixed Atacamite/Cupric Oxide
Catalytic Activity
Percentage Concentration
1
0.9
0.8
0.7
0.6
0.5
0.4
0.3
0.2
0.1
0
n - Butane
Carbon dioxide /4
Maleic anhydride x 10
0
200
400
Catalyst Temperature (Celsius)

Fig.49.

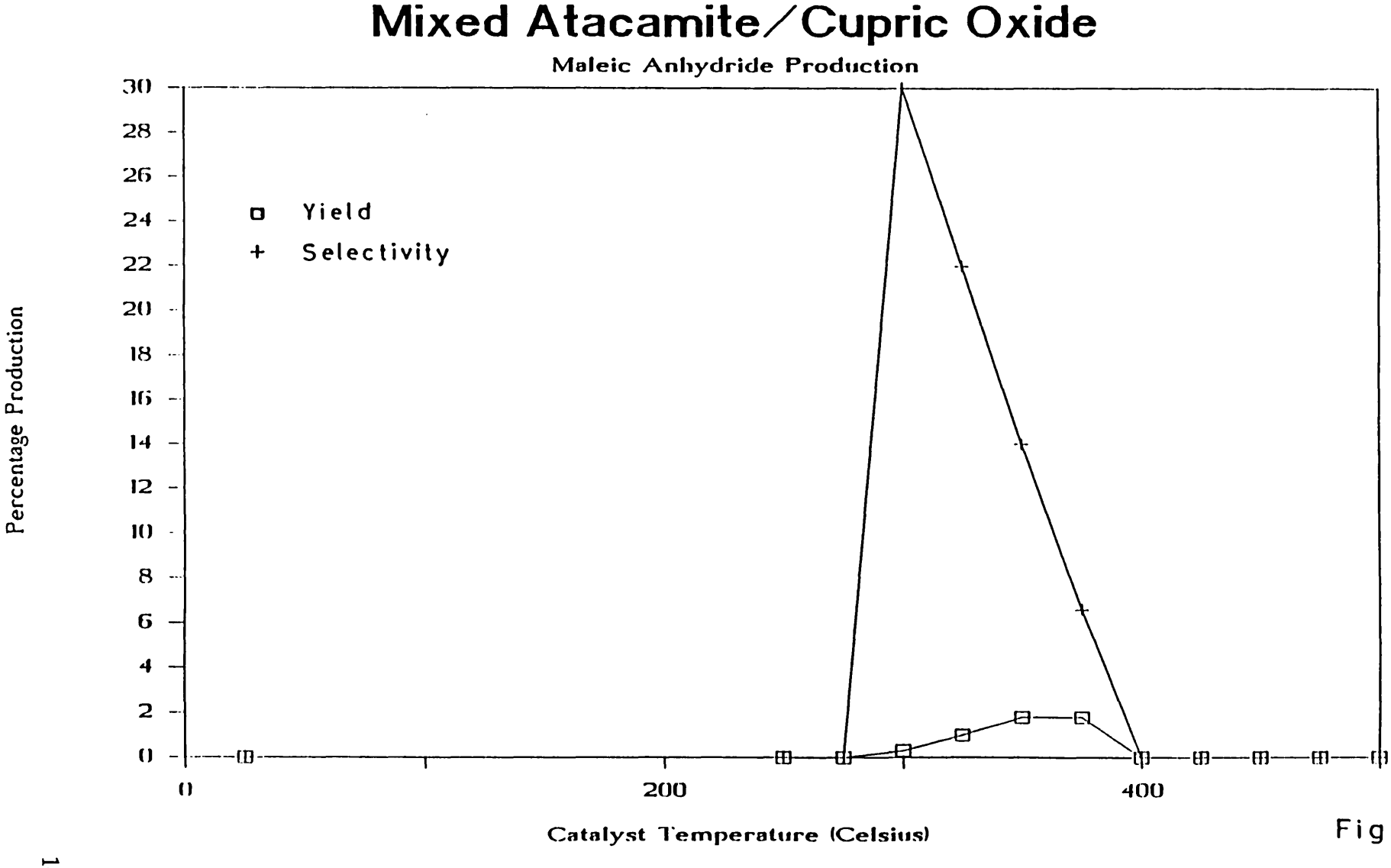

Mixed Atacamite/Cupric Oxide
Maleic Anhydride Production
Yield
Selectivity
Percentage Production
30
28
26
24
22
20
18
16
14
12
10
8
6
4
2
0
0
200
400
Catalyst Temperature (Celsius)

Fig.50.

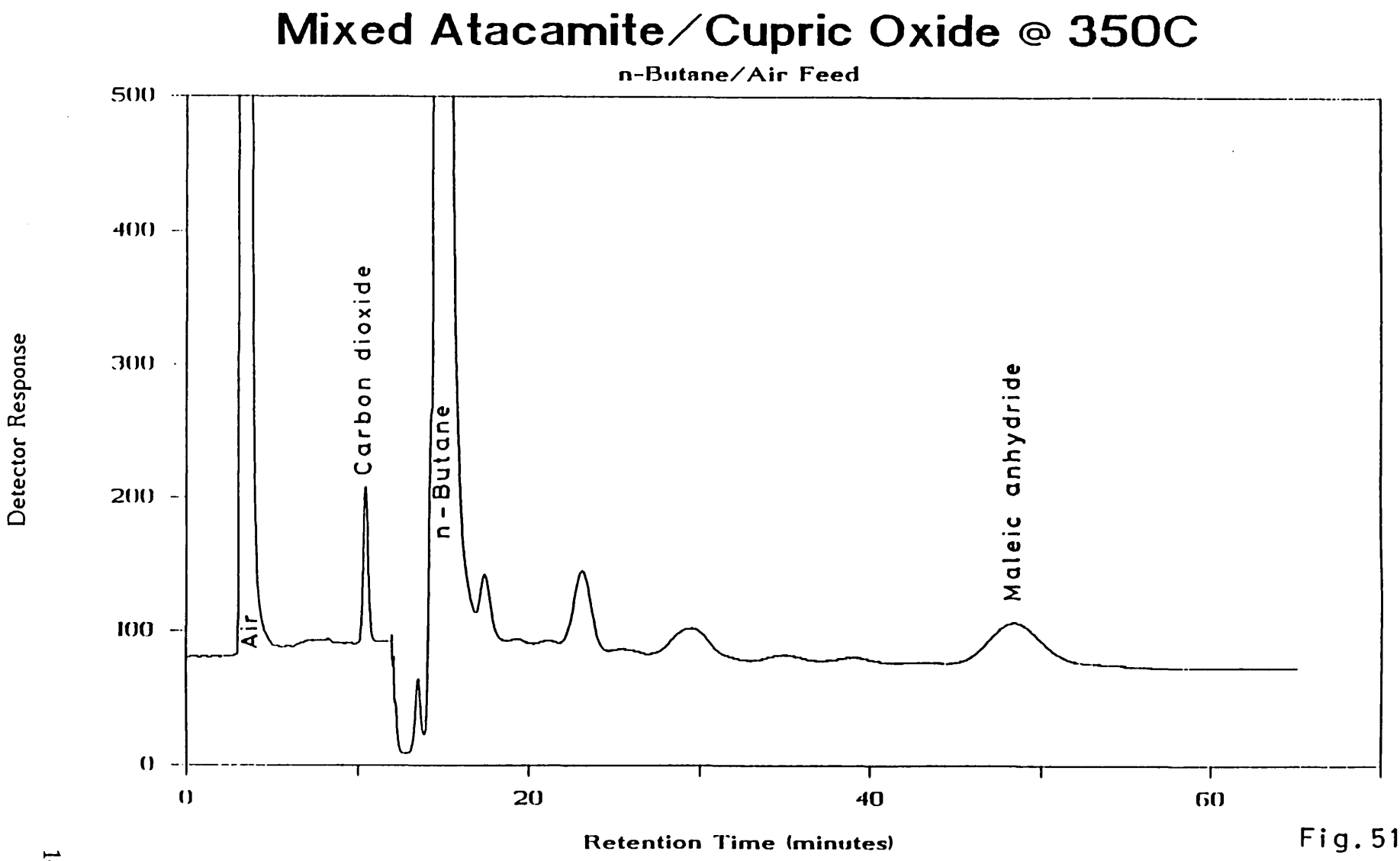

Mixed Atacamite/Cupric Oxide @ 350C
n-Butane/Air Feed
Detector Response
500
400
300
200
100
0
Air
Carbon dioxide
n-Butane
Maleic anhydride
0
20
40
60
Retention Time (minutes)

Fig. 51.

investigations to elucidate these had to be undertaken before any mechanistic studies could be started.

7.2 Atacamite.

As shown above, a mixture of atacamite and cupric oxide was active for the conversion of n-butane to maleic anhydride. However, section 5.2.5 showed cupric oxide alone only had the catalytic ability to combust n-butane. To try and elucidate whether atacamite alone is responsible for the catalytically promoted reaction, i.e. the active phase, or whether cupric oxide must be present, pure atacamite must be prepared and studied.

7.2.1 Preparation.

Atacamite, being a natural mineral found in South America, has been studied crystallographically[105-111] to reveal a framework structure, which in an idealised form is derivable from the sodium chloride structure. It also has a similarity to the spinel structure[111]. The metal atoms do not all have the same environment, one half being surrounded by 4 OH and 2 Cl and the remainder by 5 OH and 1 Cl, this being a consequence of the stoichiometry and the co-ordination numbers of Cu (6), OH (3) and Cl (3).

Preparation of atacamite, and of its other two crystal phases botallakite and paratacamite (δ, α and γ - $Cu_2(OH)_3Cl$ respectively) have been reported in the literature[107-110]. Reference 109 reports a preparation of pure atacamite by slow hydrolysis (over a period of a year) of dilute cupric chloride solutions by urea.

However, as atacamite had been identified as being formed by the action of dilute hydrochloric acid on cupric oxide a couple of preparation methods along this style were tried. The first involved warming a mixture of cupric oxide and hydrochloric acid, in a ratio calculated to give atacamite, and after 15 minutes of warming the solution at 50 Celsius the brown suspension turned grey green, the suspension was stirred and warmed for a total of 1 hour before the grey green solid was filtered off to leave a green cloudy solution which, on adding the dilute hydrochloric acid washings of the solid to it, turned blue. The solution was assumed to have dissolved atacamite as reference 112 quoted atacamite as being soluble in acidic aqueous solutions. However in hindsight, this separation and especially the addition of excess hydrochloric acid was probably wrong and resulted in the formation of cupric chloride as detected by X-ray diffraction of the evaporated solution (a green powder).

The second preparation was much closer to the original which gave a mixture of cupric oxide and atacamite. Cupric oxide and dilute hydrochloric acid were mixed and stirred in a ratio calculated to give 100% atacamite. The suspension was then dried, in an oven, at 70 Celsius. Periodically the mixture was re-stirred to mix the solid phase and the produce a suspension again. After approximately 24 hours the mixture had completely dried giving a greenish brown solid which was ground with a pestle and mortar.

7.2.2 Characterisation.

The X-ray diffraction pattern of this second material showed it to be nearly pure atacamite with a small amount of cupric chloride dihydrate to be present, see Figure 52. X-ray photoelectron spectroscopy showed the copper to exist as two

XRD pattern of pure Atacamite as prepared

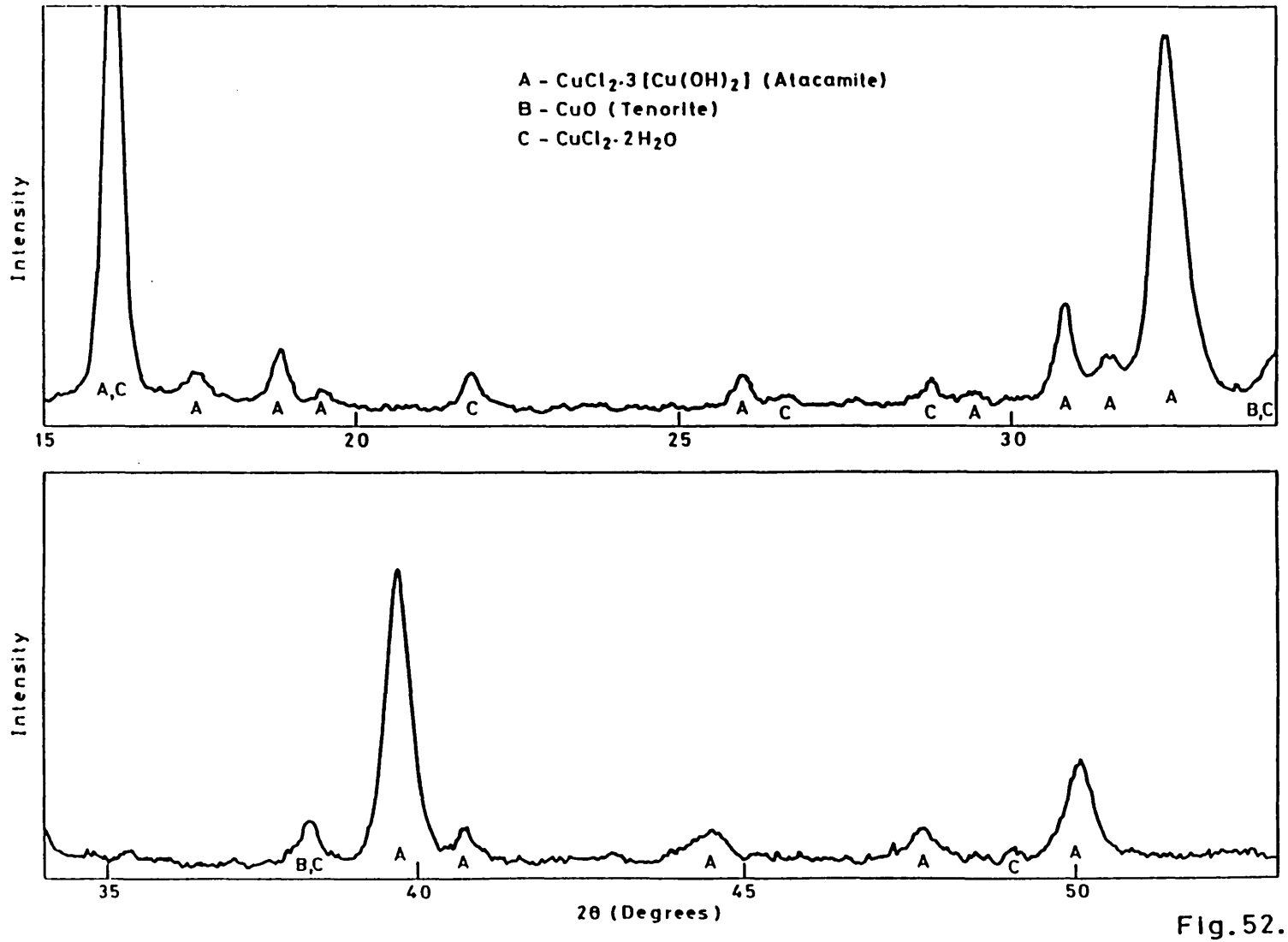


Fig.52.

species, see Figure 53, using the results of the X-ray diffraction and reference 85, the major peak was assigned as being due to the copper (II) species in atacamite and the minor was assigned as cupric chloride. The chlorine 2p peak shows one species which was assigned as being chloride. The oxygen 1s peak does show some asymmetry but too little to be accurately analysed, the peak corresponds well to an OH species, see Figure 55. Table 7.1, below, gives the compiled X.P.S. data.

Table 7.1

X.P.S. results of the pure atacamite catalyst.

Peak	K.E. (eV)	B.E.* (eV)	Assignment	Concentration
Cu $2p_{3/2}$	543.4	933.2	$CuCl_2$	7.6%
Cu $2p_{3/2}$	541.4	935.2	$CuCl_2.3[Cu(OH)_2]$	27.0%
Cu LMM	915.8*			
O 1s	944.6	532.0	OH	35.0%
Cl 2p	1277.8	198.8	Cl^-	22.8%

* *Binding energies corrected for charging using adventitious carbon (B.E. =284.4eV)*

Thermogravimetric analysis of the atacamite/cupric oxide mixed material, performed in a flowing atmosphere of dry air, shows two separate decompositions which result in a loss of weight of the sample, see Figure 56. The overall

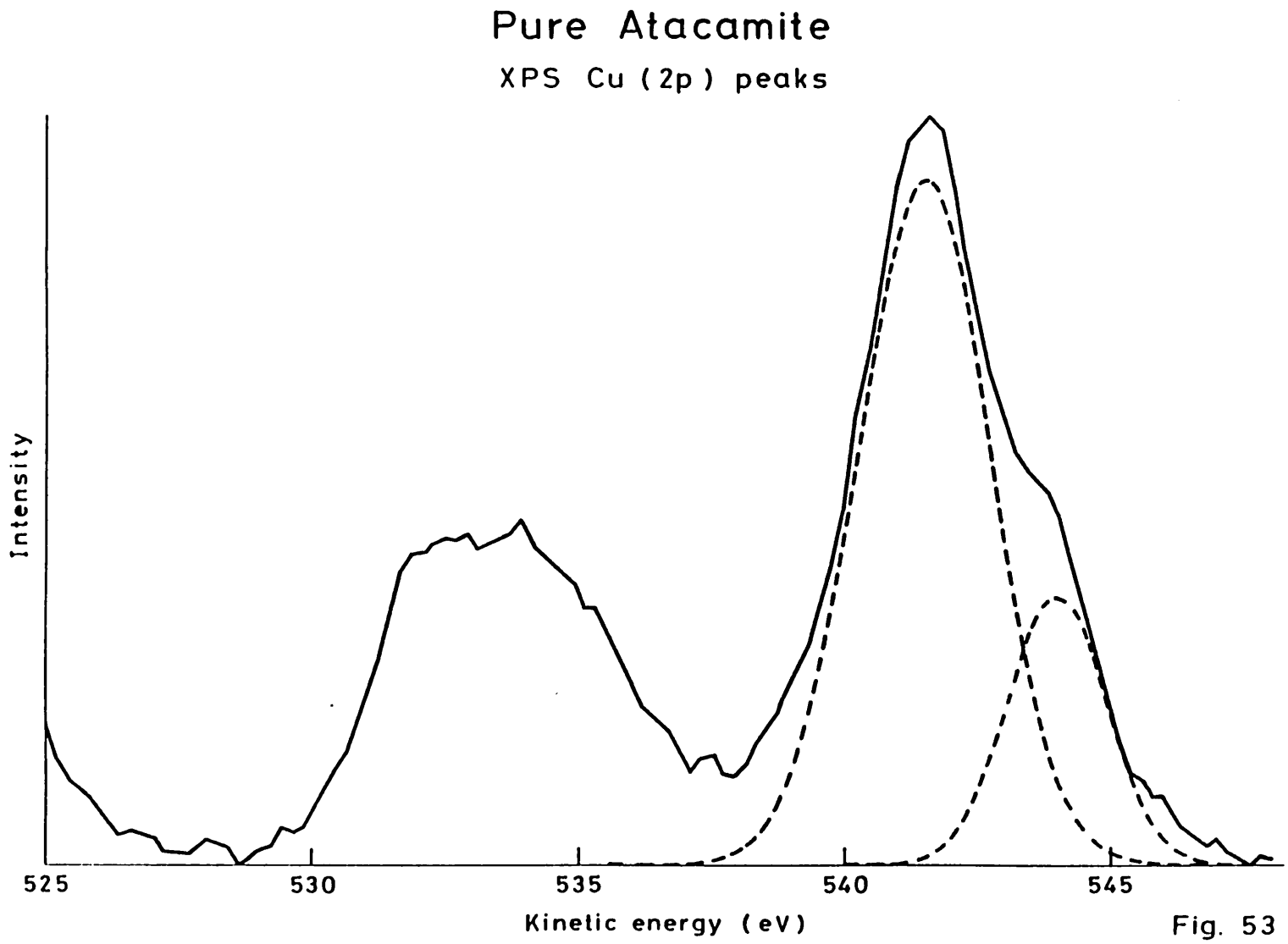

Pure Atacamite
XPS Cu (2p) peaks
Intensity
525
530
535
540
545
Kinetic energy (eV)

Fig. 53

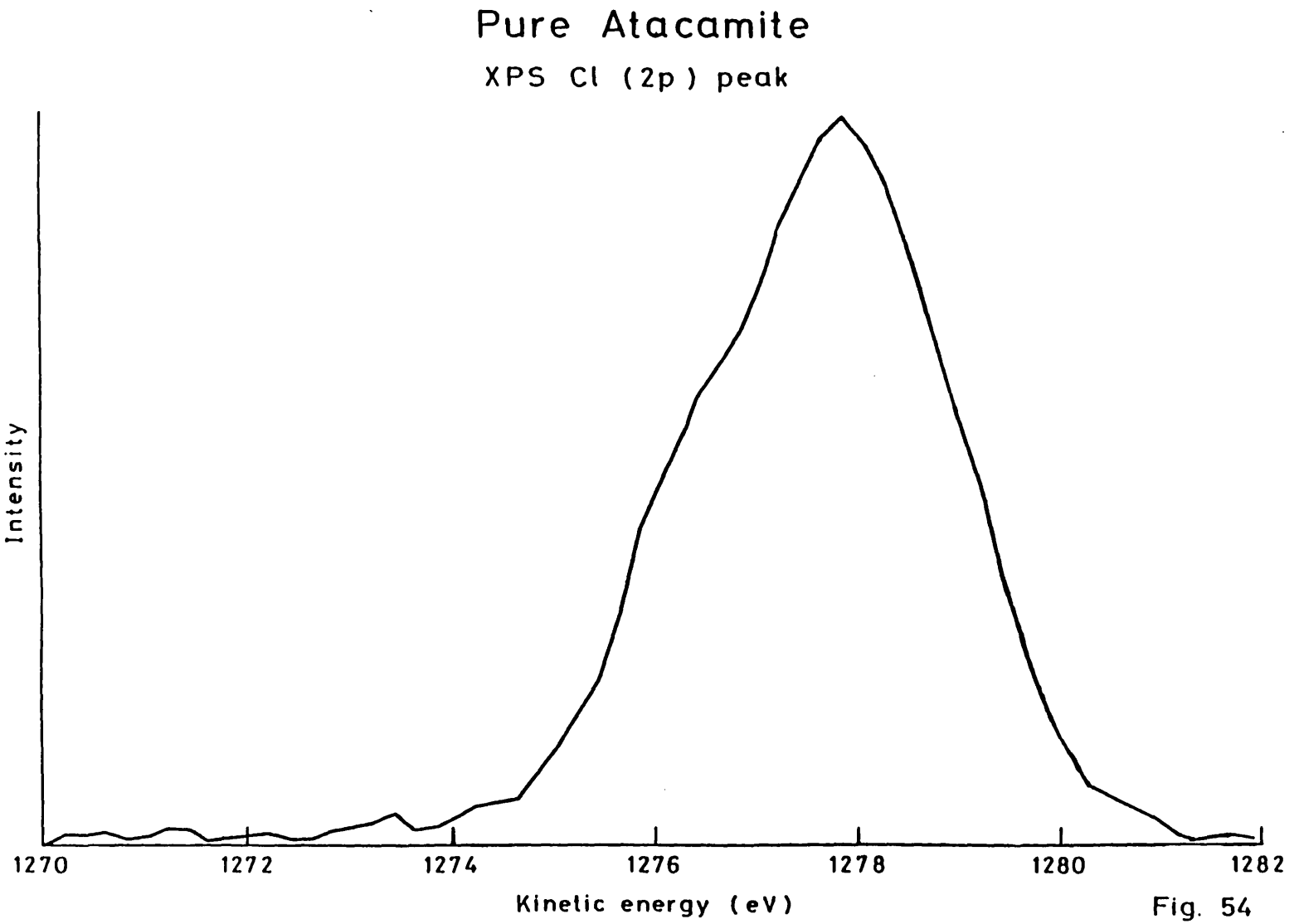

Pure Atacamite
XPS Cl (2p) peak
Intensity
1270
1272
1274
1276
1278
1280
1282
Kinetic energy (eV)

Fig. 54

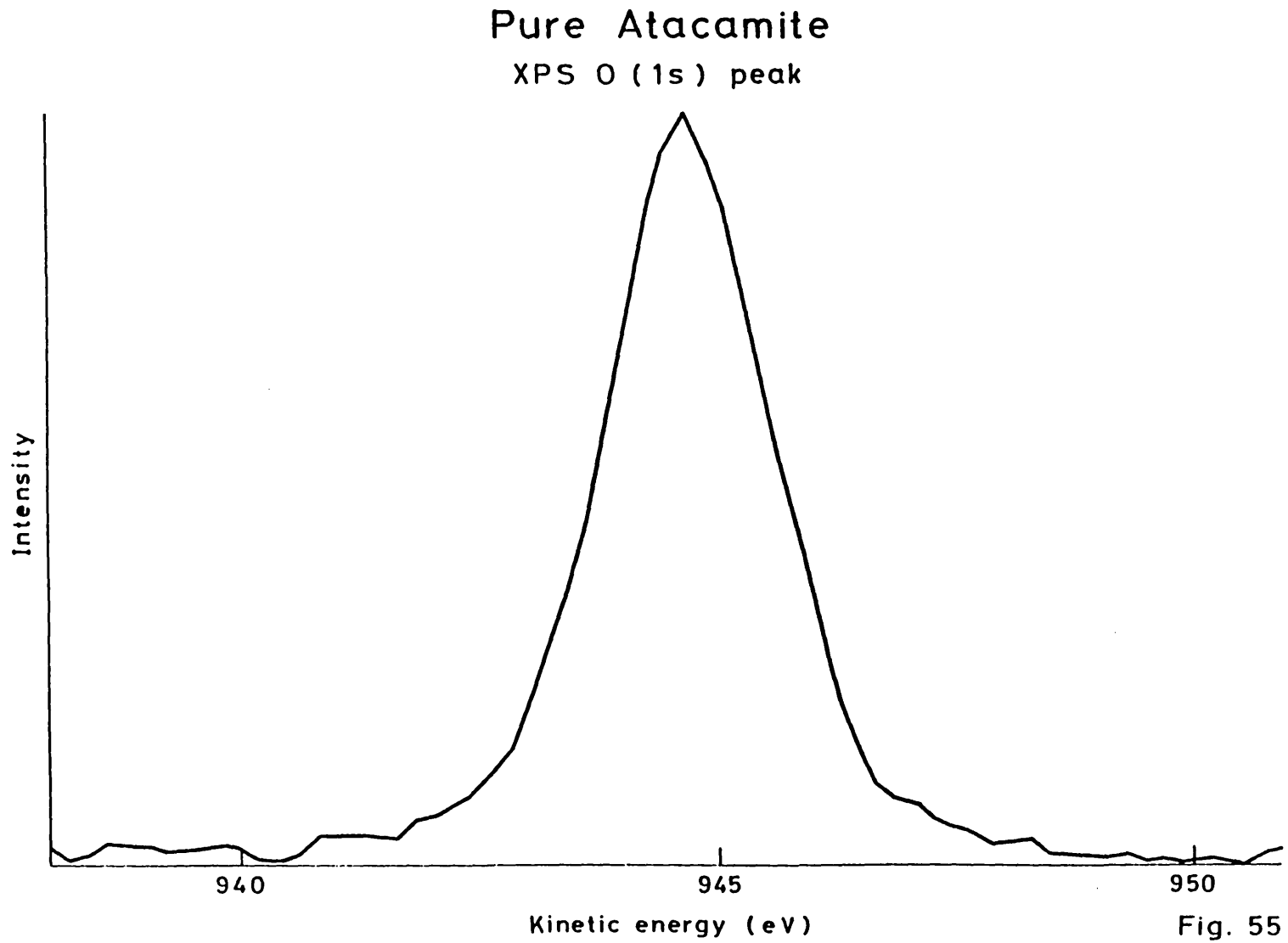

Pure Atacamite
XPS O (1s) peak
Intensity
940
945
950
Kinetic energy (eV)

Fig. 55

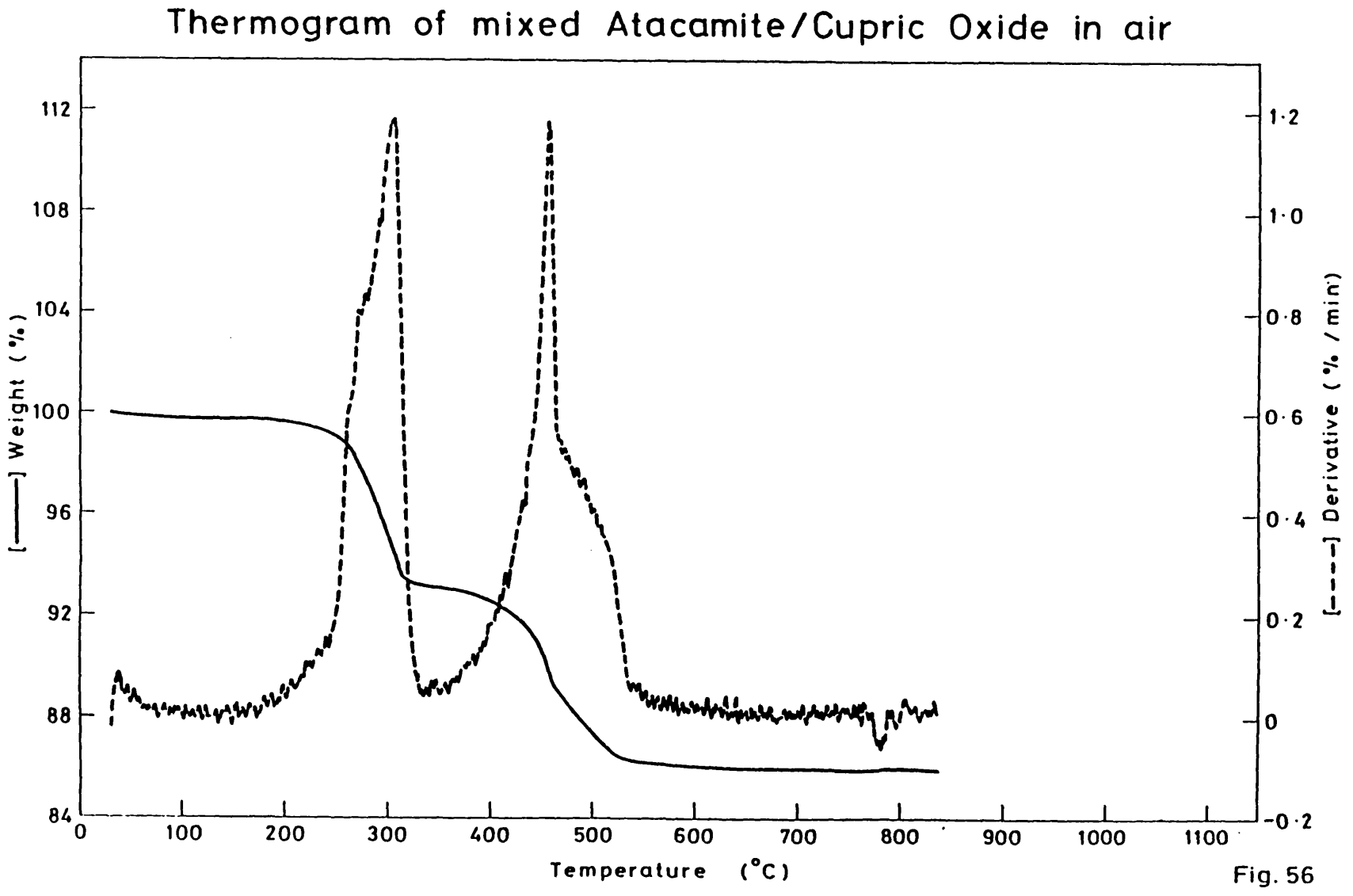

Thermogram of mixed Atacamite/Cupric Oxide in air
[——] Weight (%)
[- - - -] Derivative (% / min)
Temperature (°C)
112
108
104
100
96
92
88
84
1·2
1·0
0·8
0·6
0·4
0·2
0
-0·2
0
100
200
300
400
500
600
700
800
900
1000
1100

Fig. 56

decomposition having been identified, by X-ray diffraction (Figure 57) using a sample of the catalyst heated for 1 hour at 550 Celsius, as complete decomposition of atacamite, by loss of chlorine, to yield cupric oxide. However, on analysing the pure atacamite material, a number of decompositions were seen, see Figure 58. On close inspection of the derivative curve of the mixed material, Figure 56, it was evident that the two decompositions shown by the weight-loss versus temperature curve , at 200-350 Celsius and 400-550 Celsius, are in actual fact more than single discrete decompositions. Therefore, the curve obtained from the pure atacamite material is closer to that already obtained than initially thought. The very first decomposition, at 60 Celsius, is probably due to loss of water from the atacamite dihydrate material. The second decomposition, occurring at 200-350 Celsius was identified by taking the pure atacamite material and calcining it at 325 Celsius for 0.5 hours in air which resulted in the green atacamite turning brown. Rerunning the thermogram showed that this calcined material had lost all decompositions before 325 Celsius, see Figure 59, X-ray diffraction analysis gave a pattern which was identified as almost pure copper (II) oxychloride known as melanothallite (Cu_2OCl_2), see Figure 60.

This brown melanothallite, it was found, reverted to a green colour if left in air and thermogravimetric analysis of this green material gave an identical thermogram to that obtained from the fresh pure atacamite material indicating a reversion to atacamite probably by adsorption of atmospheric water. X-ray diffraction confirmed the reversion to atacamite by giving the characteristic diffraction pattern. The third decomposition, seen at 400 to 550 Celsius, was therefore identified as the decomposition of melanothallite, by loss of chlorine, to yield cupric oxide. The difference seen in the thermograms of the mixed and pure atacamite catalytic materials above 400 Celsius is probably the result of two

(see page 218 for the reaction scheme)

XRD pattern of mixed Atacamite / Cupric Oxide calcined at 550 Celsius

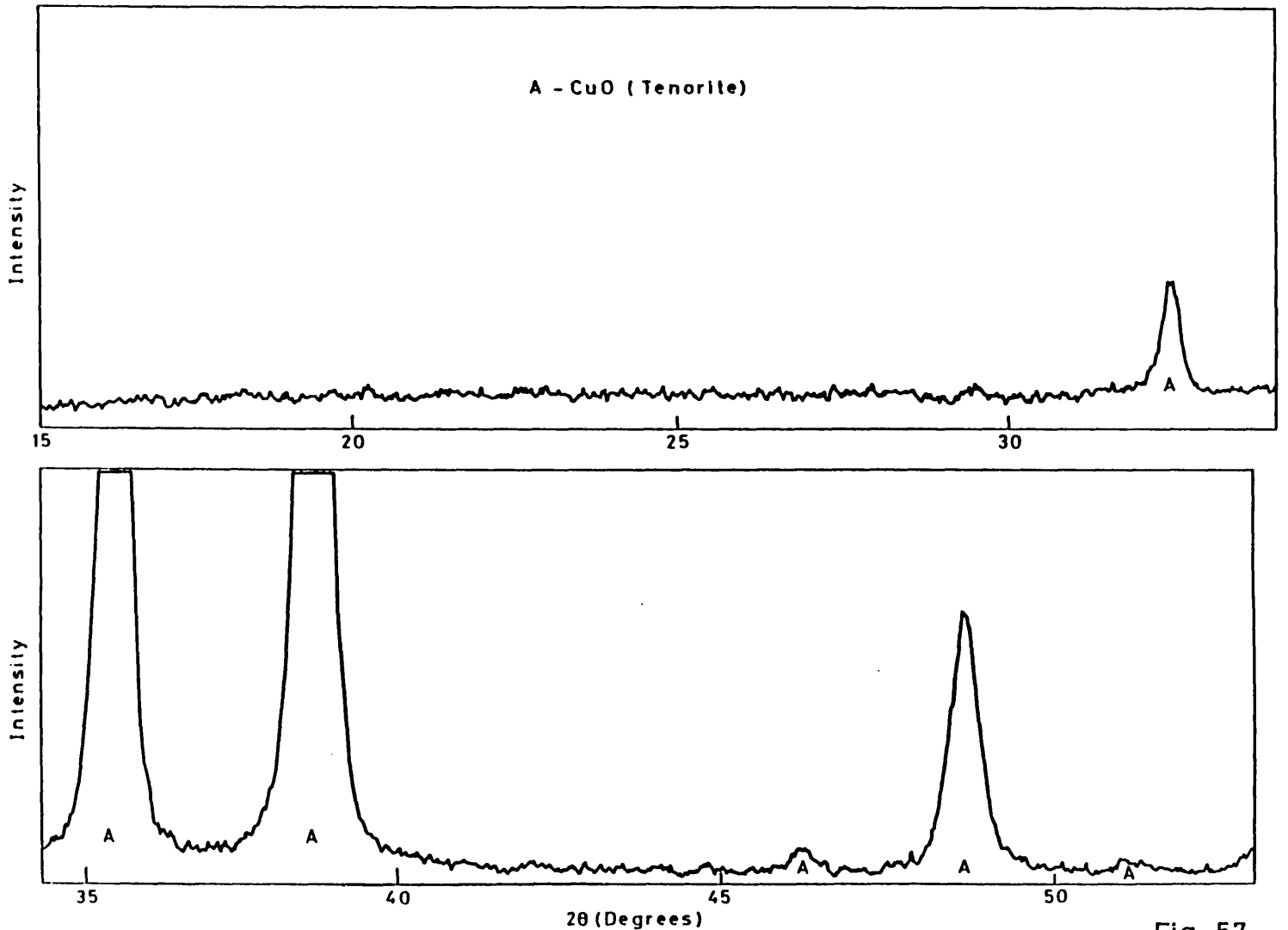


Fig. 57.

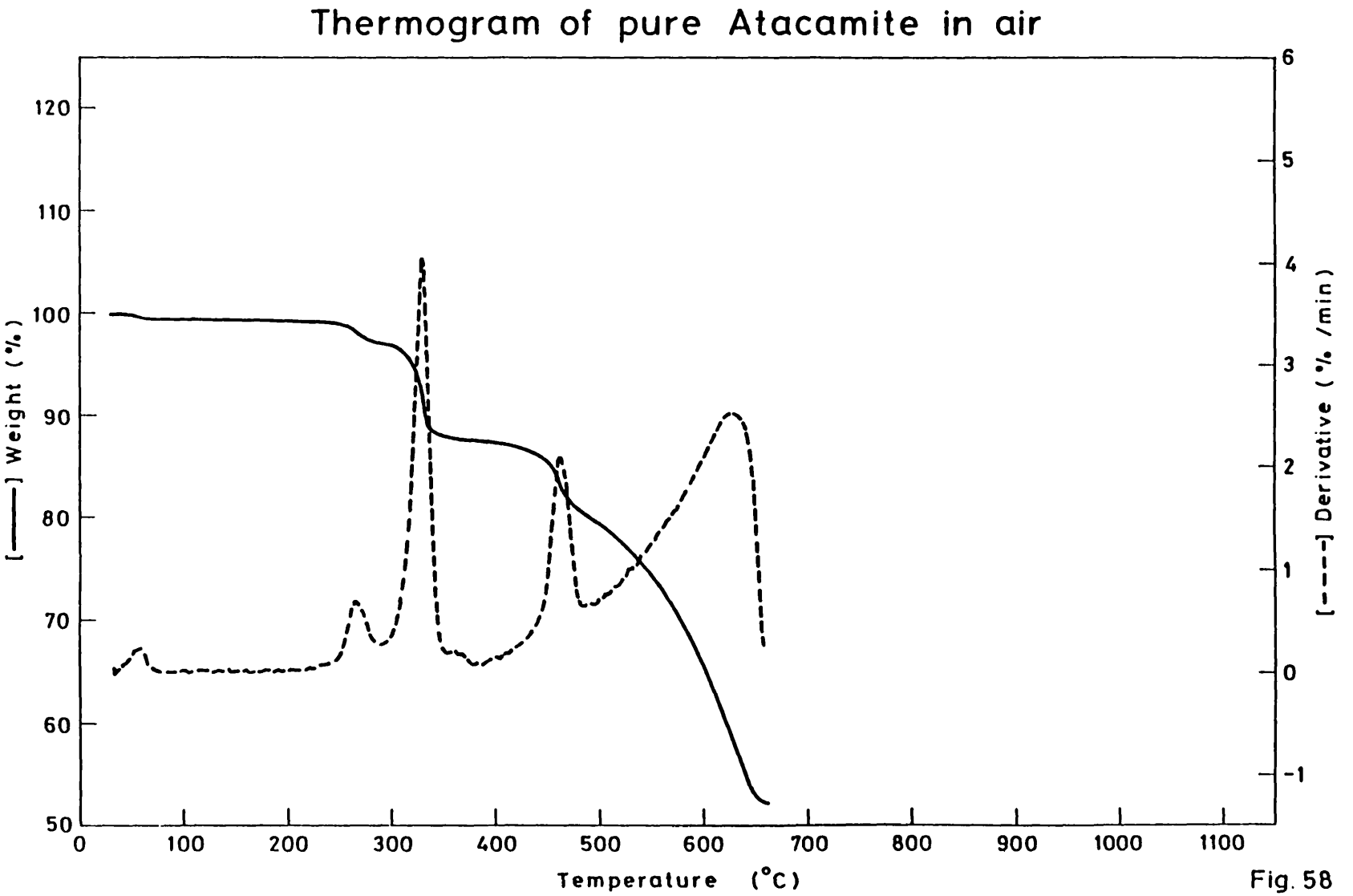

Thermogram of pure Atacamite in air
[——] Weight (%)
[----] Derivative (% /min)
Temperature (°C)
120
110
100
90
80
70
60
50
6
5
4
3
2
1
0
-1
0
100
200
300
400
500
600
700
800
900
1000
1100

Fig. 58

Thermogram of pure Atacamite after being calcined at 325C

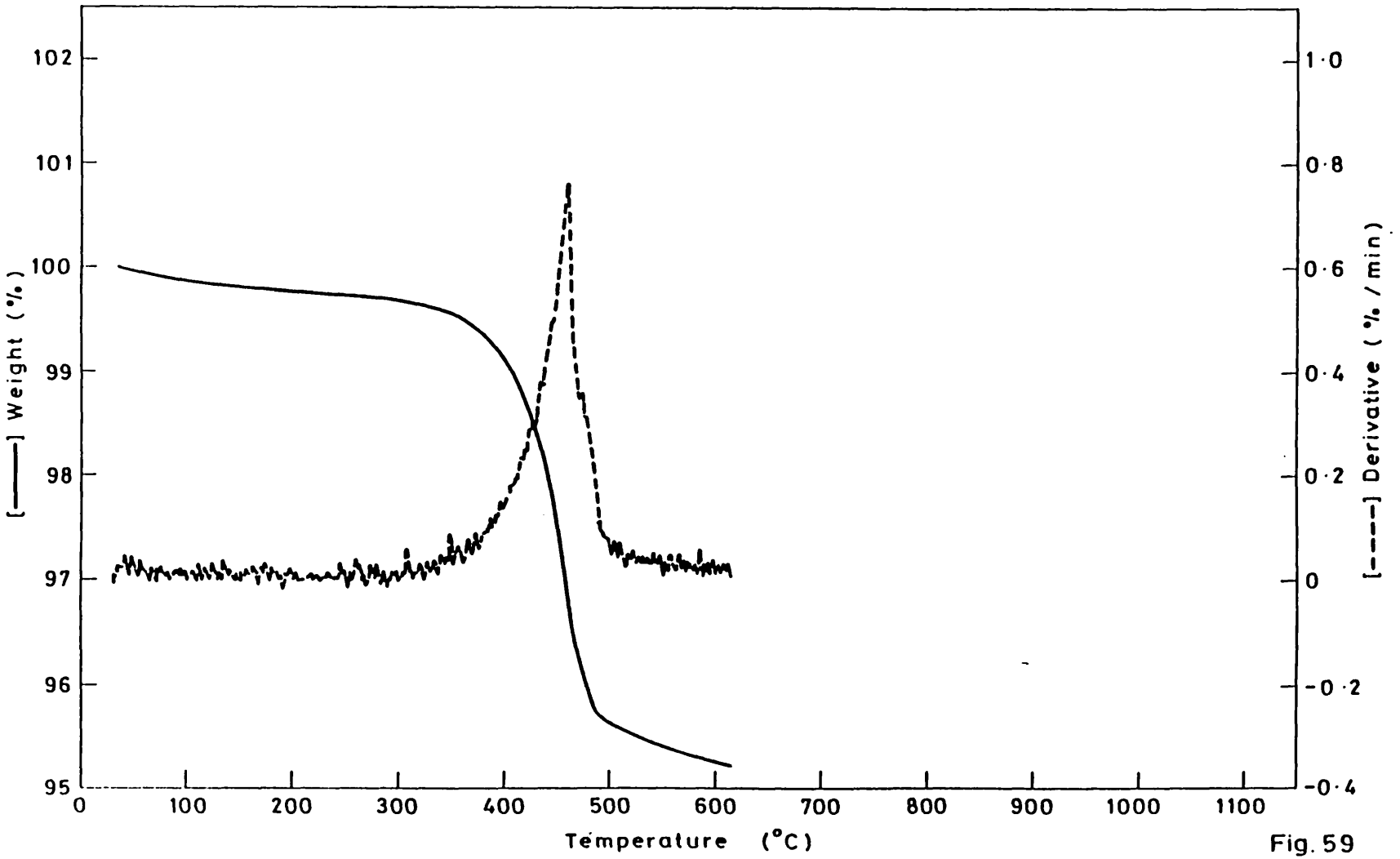


Fig. 59

XRD pattern of pure Atacamite calcined at 325 Celsius

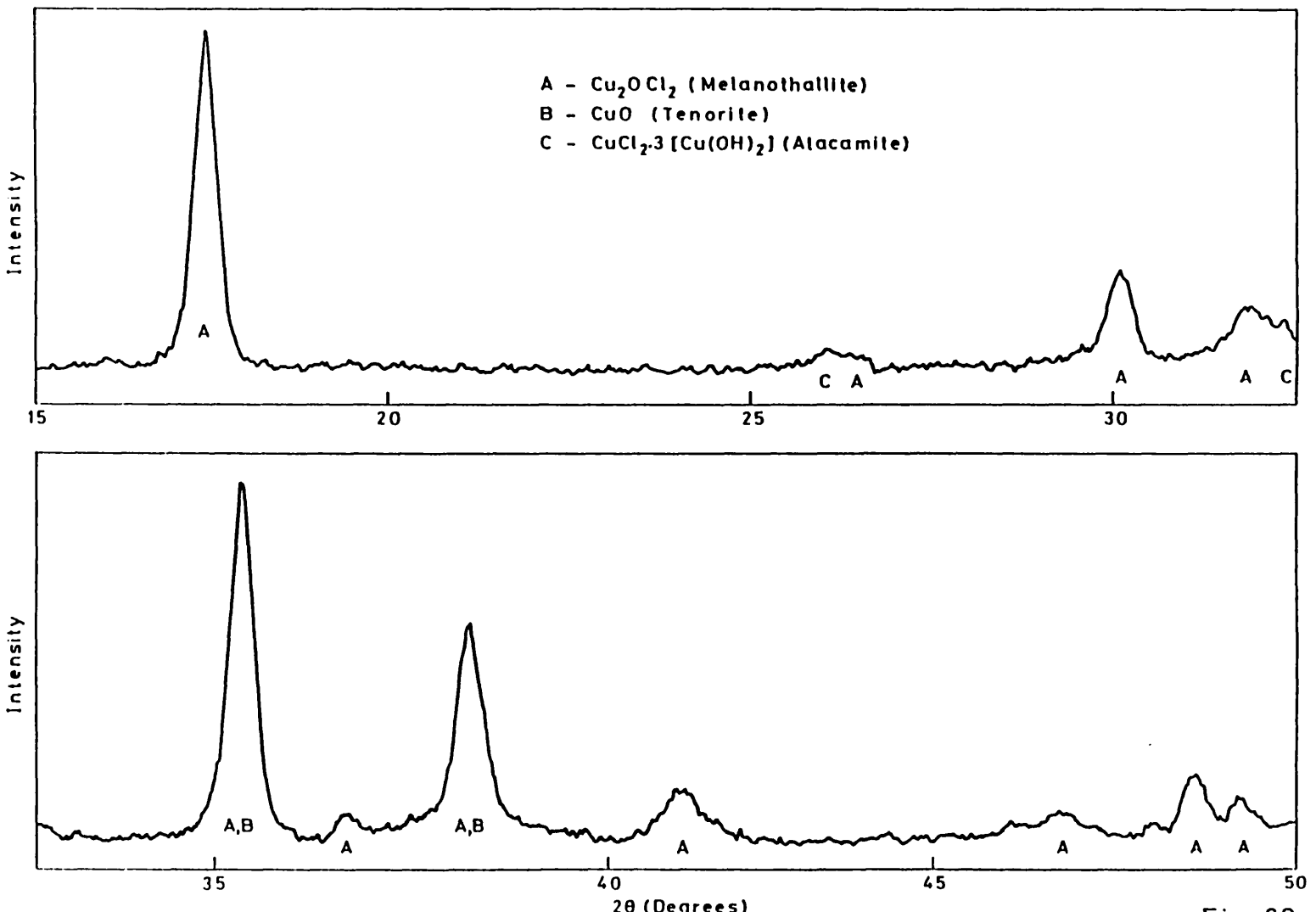


Fig. 60.

processes. The sharp derivative peaks seen in both thermograms at 460 Celsius are probably due to loss of surface chlorine due to thermal decomposition. The underlying weight loss, seem as a broad derivative peak which is shifted to higher temperature in the pure atacamite material, is due to desorption of the chlorine species again from the decomposition of the melanothallite but after it had diffused from the bulk of the material.

As the maximum of maleic anhydride production occurred at approximately 325 Celsius and maleic anhydride was first detected at about 300 Celsius it was therefore concluded that melanothallite was responsible for selectively oxidising the n-butane to maleic anhydride. Relating the activity data obtained to the thermogram explains why the partial oxidation activity rises to a maximum from 300C to 325-350C (furnace temperatures) where the melanothallite plateau occurs in the thermogram and then decreases to zero again by 400-425C where the decomposition of the melanothallite to cupric oxide occurs.

7.2.3 Catalytic activity studies.

The experimental apparatus and proceedure used to study the catalytic activity of the pure atacamite catalyst was identical to that described in chapter 4 and used in chapter 5 and previously in this chapter. A maximum in maleic anhydride yield being detected at a temperature of 400 Celsius of 11%, compared to 2.5% at 350 Celsius for the mixed atacamite/cupric oxide material (section 7.1). This maximum corresponded to a n-butane conversion of 57% and therefore a selectivity towards maleic anhydride of 20%. Figure 61 shows the variation of maleic anhydride yield, n-butane conversion and carbon dioxide production versus temperature and Figure 62 the variation of maleic anhydride yield and selectivity versus temperature.

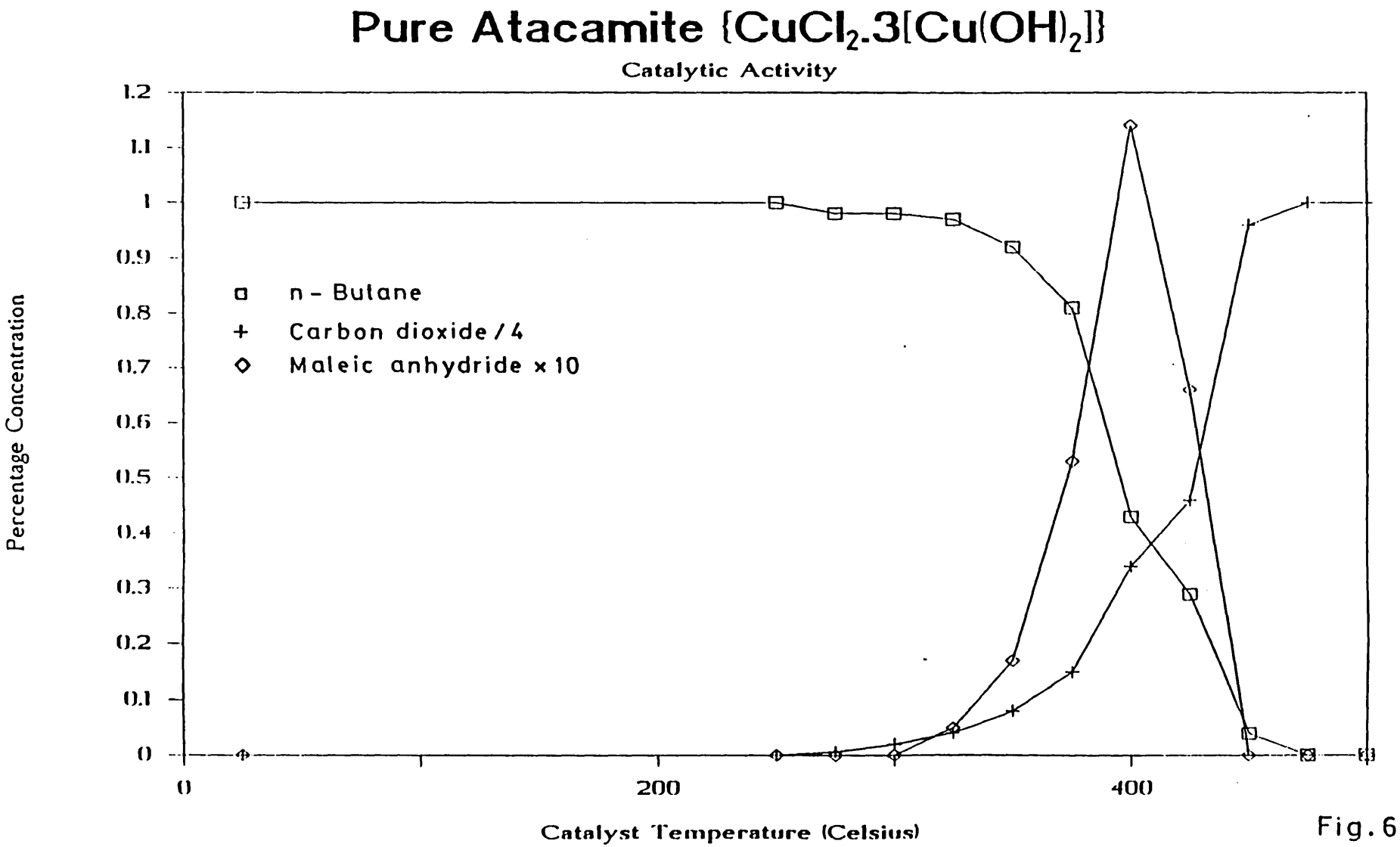

Pure Atacamite {CuCl2.3[Cu(OH)2]}
Catalytic Activity
Percentage Concentration
1.2
1.1
1
0.9
0.8
0.7
0.6
0.5
0.4
0.3
0.2
0.1
0
n - Butane
Carbon dioxide / 4
Maleic anhydride x 10
0
200
400
Catalyst Temperature (Celsius)

Fig. 61.

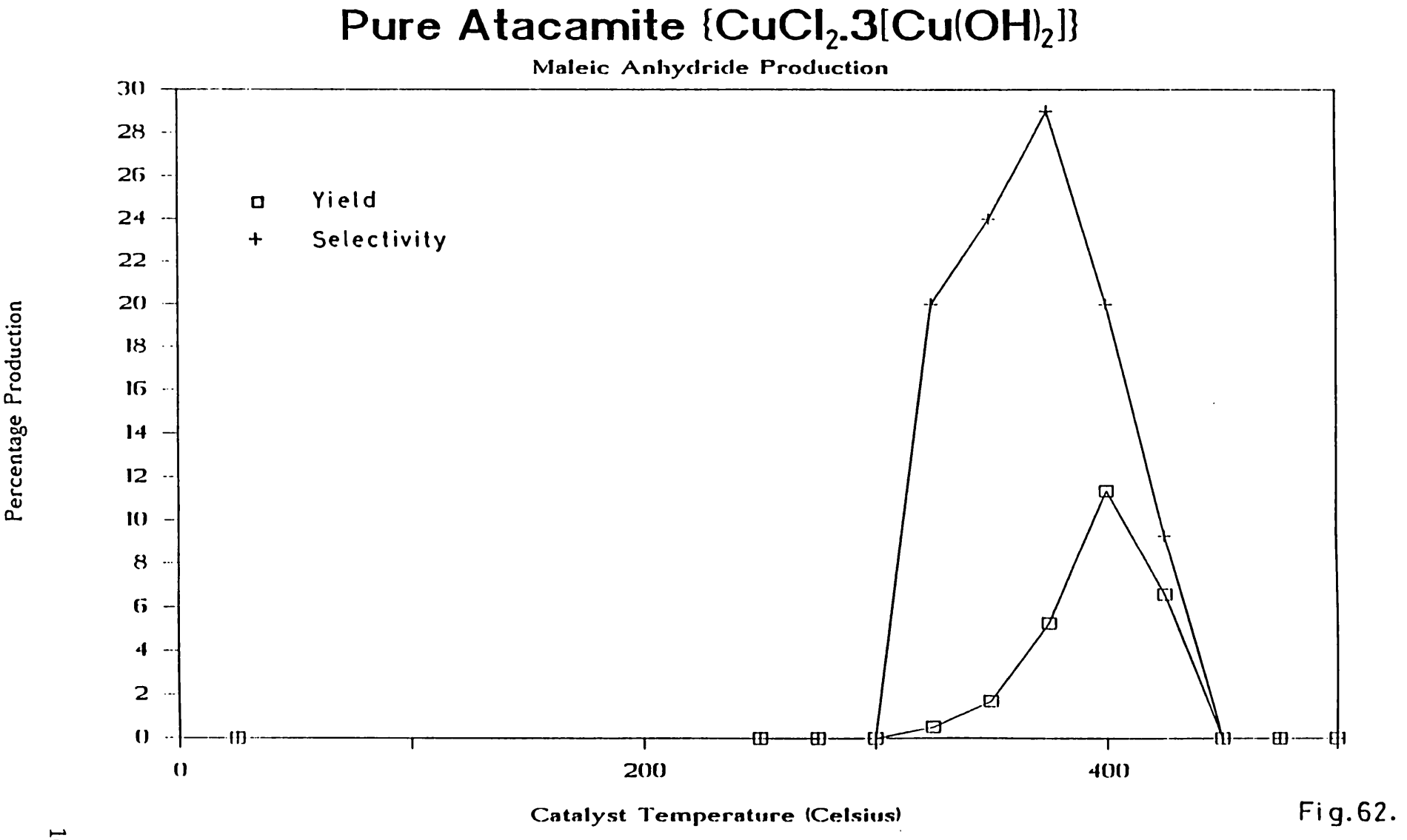

Pure Atacamite {CuCl2.3[Cu(OH)2]}
Maleic Anhydride Production
Percentage Production
Yield
Selectivity
30
28
26
24
22
20
18
16
14
12
10
8
6
4
2
0
0
200
400
Catalyst Temperature (Celsius)

Fig.62.

Again other peaks were observed in the chromatograms which correlated well, with respect to chromatographic retention times, with those observed with the palladium chloride and cupric oxide containing catalysts, these also varied in concentration as observed previously, see Figure 63 for the chromatogram obtained at 400 Celsius. This shows that the atacamite is the active material and that the presence of cupric oxide is unnecessary. The maxima for maleic anhydride yield probably occurs at a higher temperature as the decomposition of the active species, as seen in the thermograms, takes longer due to its higher concentration which agrees with the thermogravimetric studies. Also the shift in n-butane 50% conversion temperature to a higher value is probably due to the absence of the cupric oxide, which as previously shown combusts the butane.

In order to check whether a lattice oxygen content is necessary the cupric chloride produced by the first attempt to prepare atacamite was run in the reactor using standard reactor conditions used previously. However, no maleic anhydride was detected by gas chromatography or by analysis of the contents of the traps, but a wide range of unidentified peaks was seen in the chromatogram, see Figure 64, a few of these peaks did correspond to those seen for the pure atacamite material but not all. The production of these unknown organics occurred at 425-450 Celsius, at a much higher temperature than is needed to produce maleic anhydride and the associated unidentified compounds on melanothallite. Also n-butane conversion and carbon dioxide production did not occur until a higher catalyst temperature had been reached; 50% n-butane conversion temperature of 425-450 Celsius.

To complete the investigation of chloride materials, cuprous chloride was tested in an identical way for catalytic activity. Again no maleic anhydride was detected in the chromatograms or trapped out of the effluent stream. Other organics were produced but as with cupric chloride these did not occur until at least 400

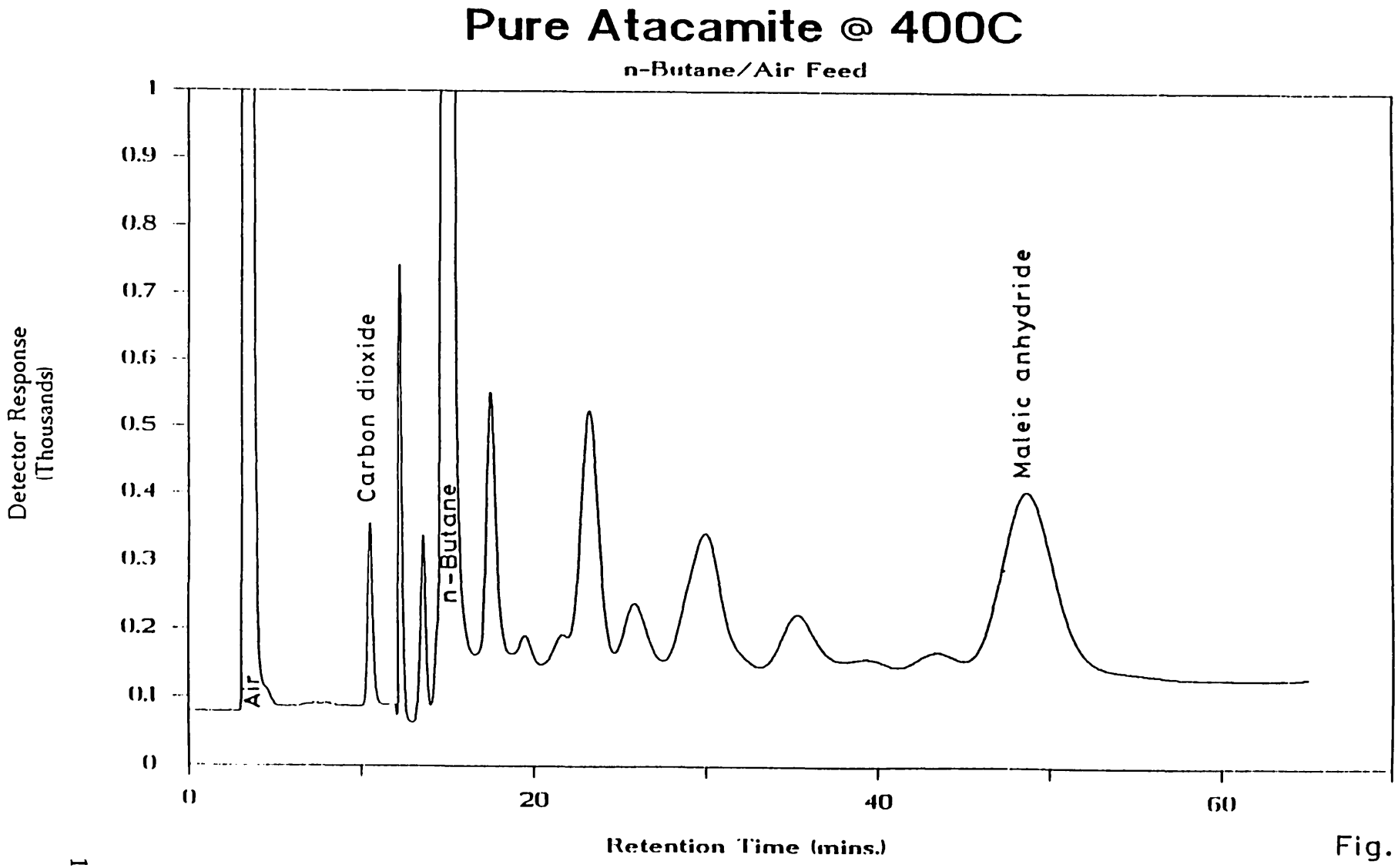

Pure Atacamite @ 400C
n-Butane/Air Feed
Detector Response
(Thousands)
1
0.9
0.8
0.7
0.6
0.5
0.4
0.3
0.2
0.1
0
Air
Carbon dioxide
n-Butane
Maleic anhydride
0
20
40
60
Retention Time (mins.)

Fig. 63.

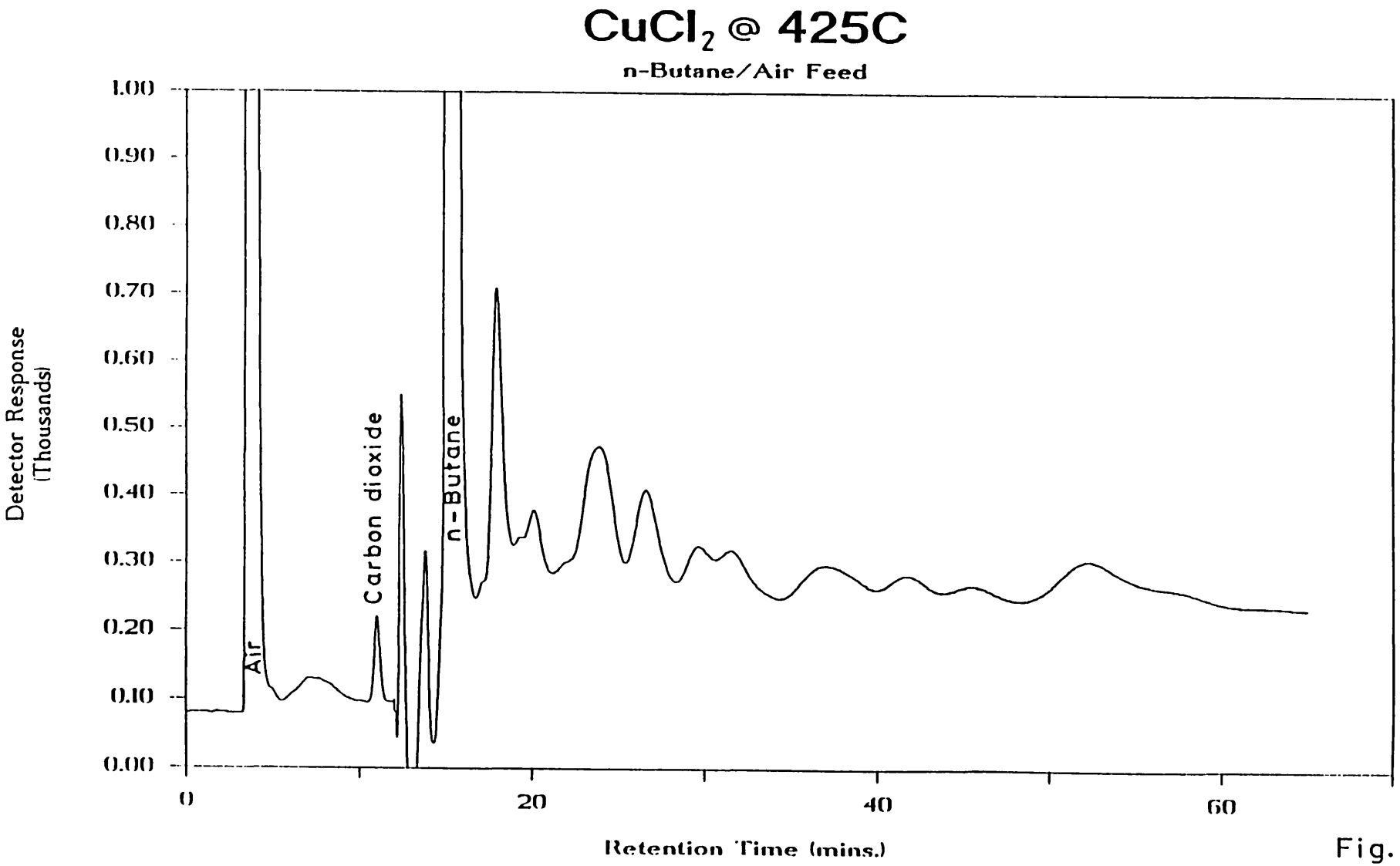

$CuCl_2$ @ 425C
n-Butane/Air Feed
Detector Response (Thousands)
1.00
0.90
0.80
0.70
0.60
0.50
0.40
0.30
0.20
0.10
0.00
Air
Carbon dioxide
n-Butane
0
20
40
60
Retention Time (mins.)

Fig. 64.

Celsius, some of these did produce chromatographic peaks at retention times corresponding to peaks seen for the atacamite materials and the cupric chloride but many were at different retention times, see Figure 65. The conversion of n-butane and production of carbon dioxide again occurred at much higher catalyst temperatures, with a temperature for 50% n-butane conversion of 475-500 Celsius. It is therefore unlikely that either cupric or cuprous chloride components of the active catalytic materials form the active sites for selective oxidation of n-butane to maleic anhydride, and that the presence of lattice oxygen is necessary.

7.3 Deactivation of the Catalytically Active Species.

A reactor run to confirm the total deactivation of the material if it is heated to a temperature of 500 Celsius was performed using the atacamite /cupric oxide mixed material. A standard catalytic activity run was performed using the standard reactor programme up to 500 Celsius as described before. The activity profiles obtained from the fresh material were identical to those obtained and reported previously in this chapter. Once the full programme was run and the material had naturally cooled to room temperature, still in the n-butane air atmosphere, the reactor programme was rerun using the same sample without exposing it to the laboratory atmosphere. The results of the chromatographic gas analysis on this second run at each temperature showed no maleic anhydride to be produced at any temperature, nor were any of the other characteristic unidentified peaks seen in the chromatograms. Post run analysis of the contents of the traps, which were cleaned between the two experiments, did not indicate the presence of maleic anhydride either. The conversion of n-butane on the second run occurred at a much lower temperature, 50% conversion of n-butane occurring at 360 Celsius as opposed to

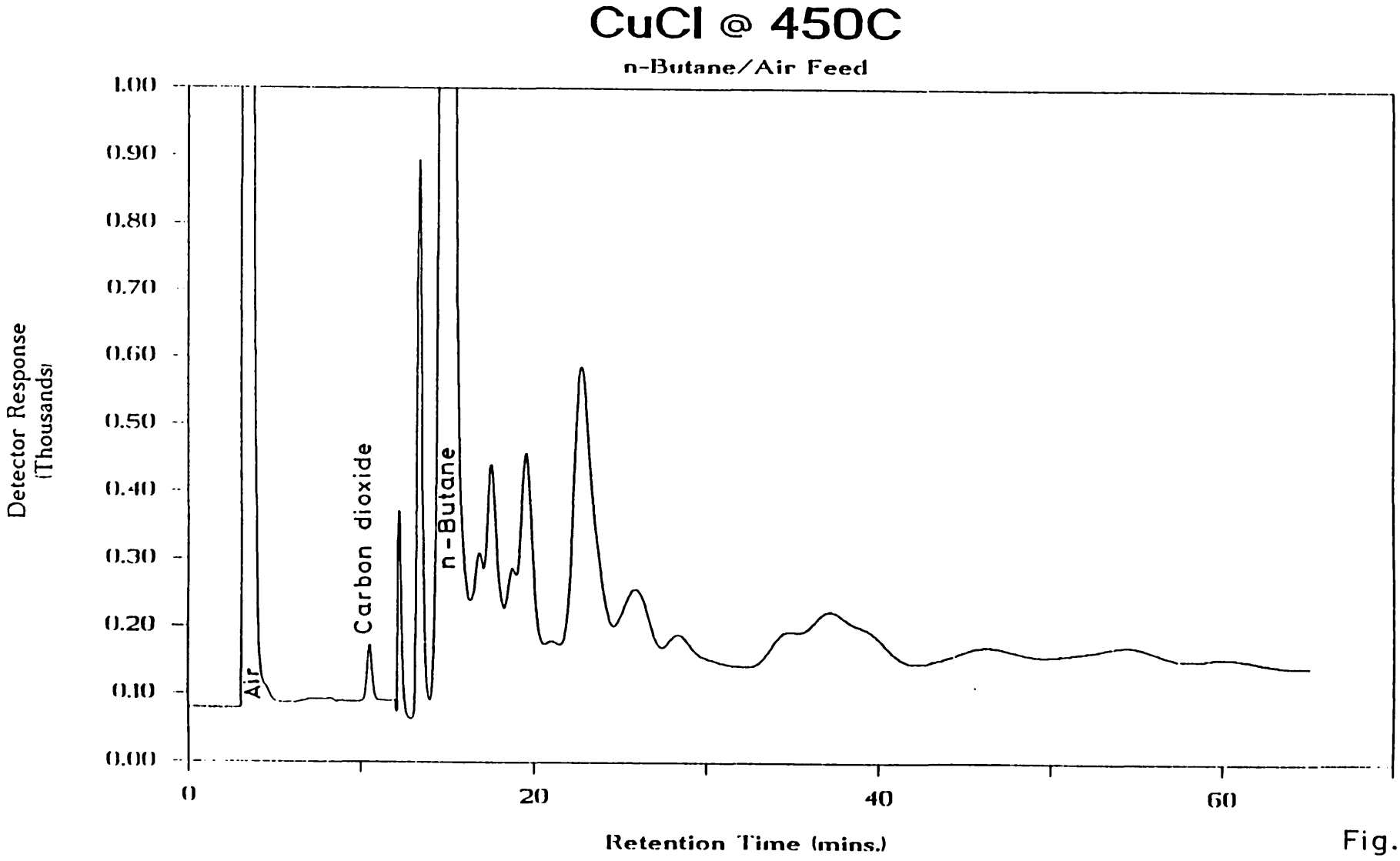

CuCl @ 450C
n-Butane/Air Feed
Detector Response (Thousands)
1.00
0.90
0.80
0.70
0.60
0.50
0.40
0.30
0.20
0.10
0.00
Air
Carbon dioxide
n-Butane
0
20
40
60
Retention Time (mins.)

Fig.65.

385 Celsius for the first run, see Figure 66, and this compares to an even lower 50% conversion temperature for pure cupric oxide of 320 Celsius as reported in section 5.2.5.

Close analysis of the thermogram curve of the pure atacamite material shows that even between 350 and 450 Celsius the material is still loosing a small amount of weight. This weight loss is probably causing deactivation of the catalytic material even under isothermal conditions. A sample of the pure atacamite material held at a constant 350 Celsius in a flowing atmosphere of 1% n-butane in air in the reactor was found to have completely deactivated after 6 hours, the first gas analysis injection being taken after 10 minutes of the isothermal period, the second injection after an elapsed time of 2.5 hours only showing a very small peak in the chromatogram attributable to maleic anhydride. The final injection after an elapsed time of 6 hours showed no maleic anhydride at all. The n-butane conversion had slightly increased also, from 7% to 9% and finally to 11%, which would agree with the formation of cupric oxide by loss of chlorine, see Figures 67, 68 and 69 of the three chromatograms taken.

Isothermal weight loss analysis, using the thermogravimetric analyser, of the pure atacamite material was then performed using a standard 40 mg of sample and a dynamic atmosphere of the desired gas, flowing at 40 ml/min with the gases being dried using a large cell of silica gel immediately before the TGA module. The samples were heated at 10 degrees per minute up to a furnace temperature of 350 Celsius then held isothermally for 600 minutes (sample temperature was 334 Celsius). In an atmosphere of synthetic air (oxygen nitrogen mix) a total of 4.65 wt.% was lost over the 10 hour isothermal period at a rate of 0.008 wt.%/min, calculated by assuming a linear weight loss with time (a slight concave curve of weight loss with time was evident), see Figure 70. In an atmosphere of pure argon a

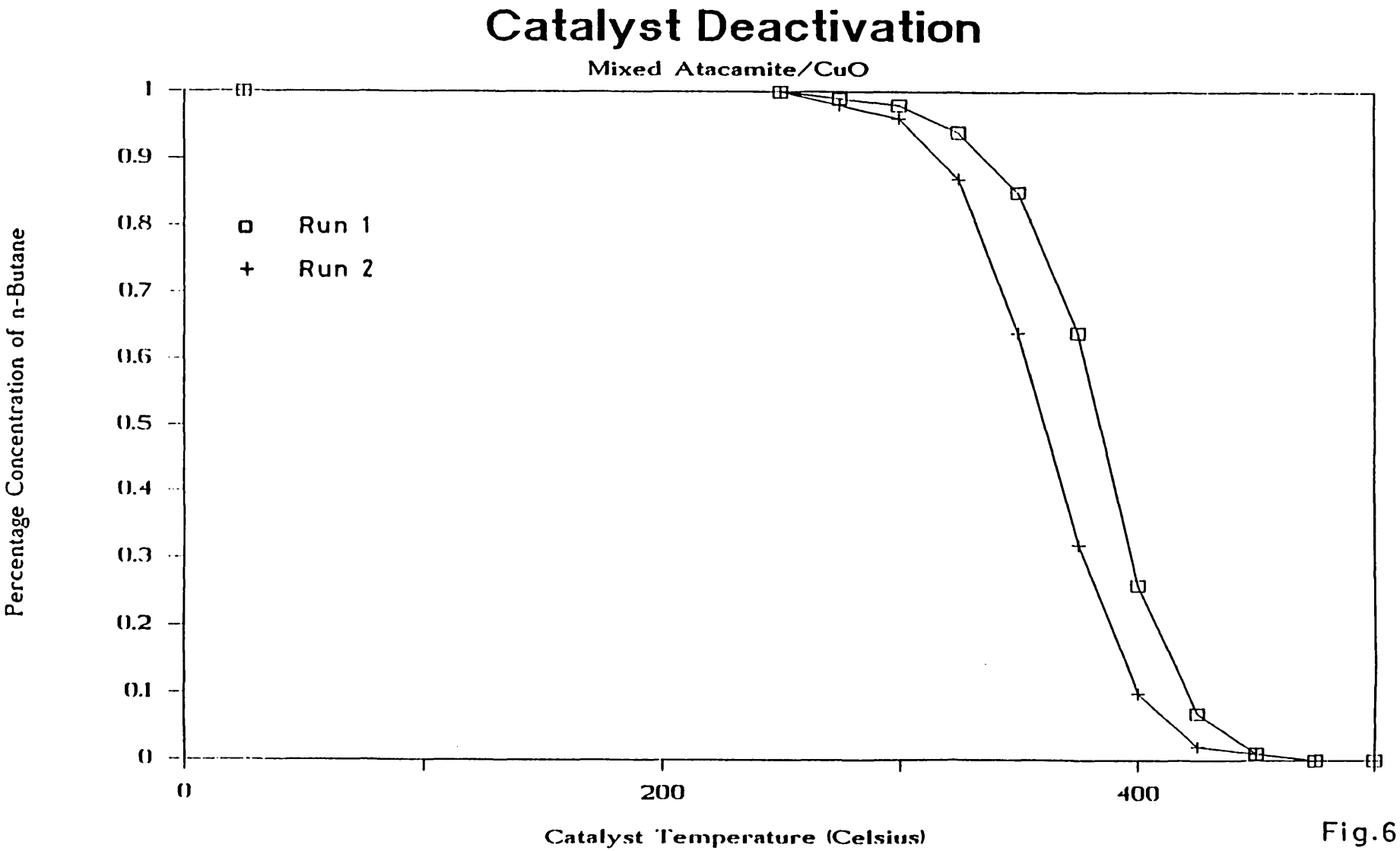

Catalyst Deactivation
Mixed Atacamite/CuO
Percentage Concentration of n-Butane
1
0.9
0.8
0.7
0.6
0.5
0.4
0.3
0.2
0.1
0
Run 1
Run 2
0
200
400
Catalyst Temperature (Celsius)

Fig.66.

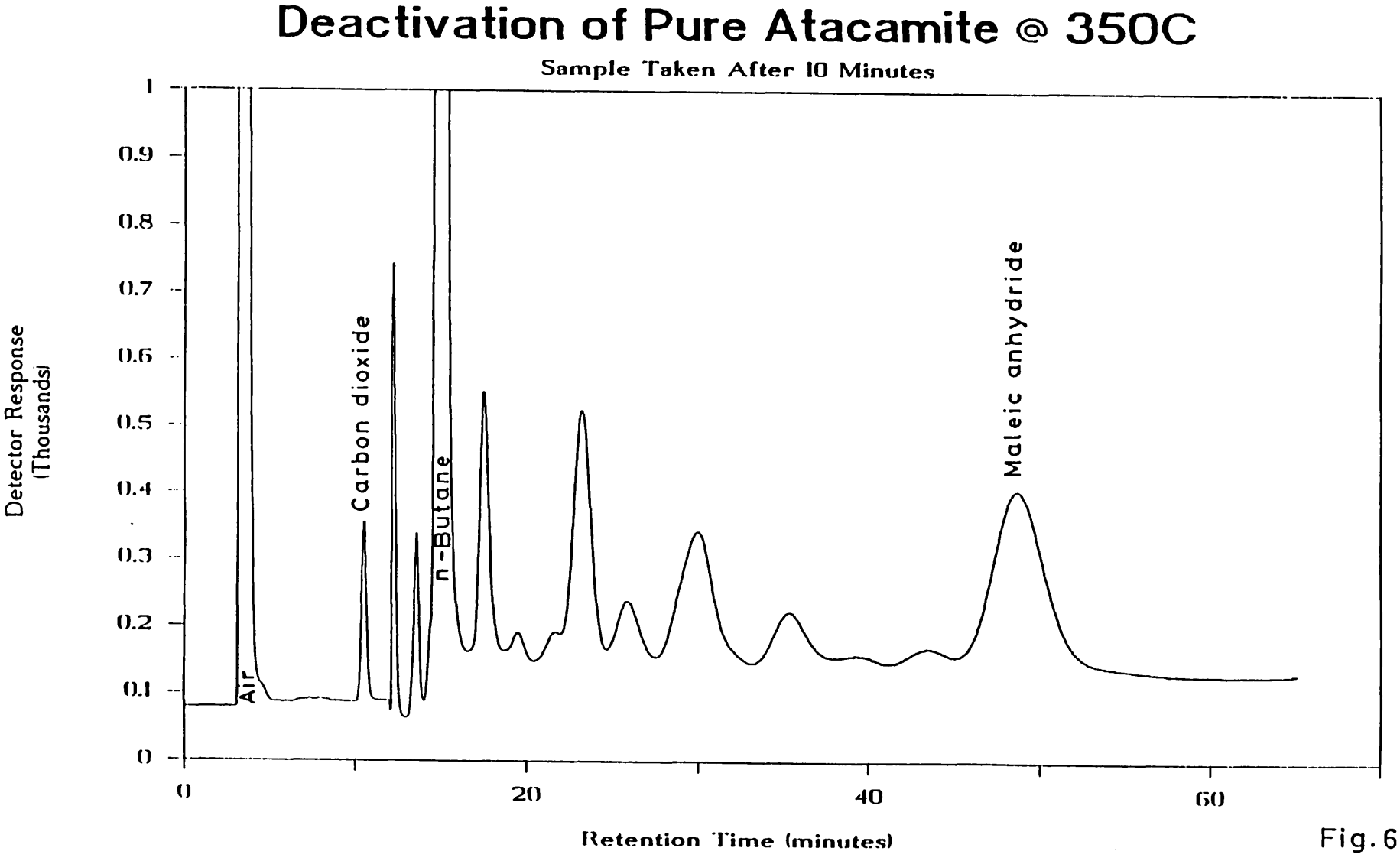

Deactivation of Pure Atacamite @ 350C
Sample Taken After 10 Minutes
Detector Response
(Thousands)
1
0.9
0.8
0.7
0.6
0.5
0.4
0.3
0.2
0.1
0
Air
Carbon dioxide
n-Butane
Maleic anhydride
0
20
40
60
Retention Time (minutes)

Fig. 67.

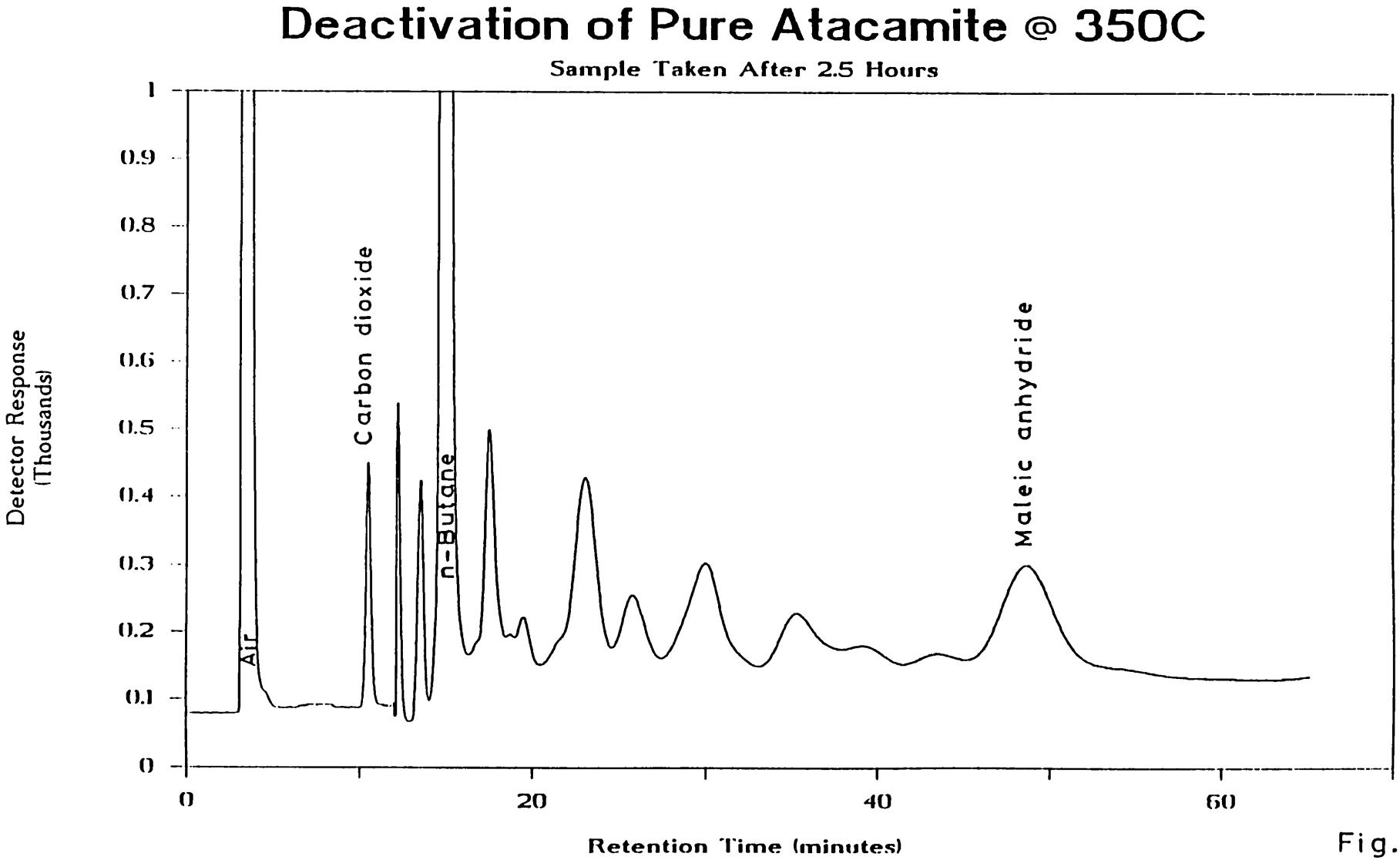

Deactivation of Pure Atacamite @ 350C
Sample Taken After 2.5 Hours
Detector Response (Thousands)
1
0.9
0.8
0.7
0.6
0.5
0.4
0.3
0.2
0.1
0
Air
Carbon dioxide
n-Butane
Maleic anhydride
0
20
40
60
Retention Time (minutes)

Fig. 68.

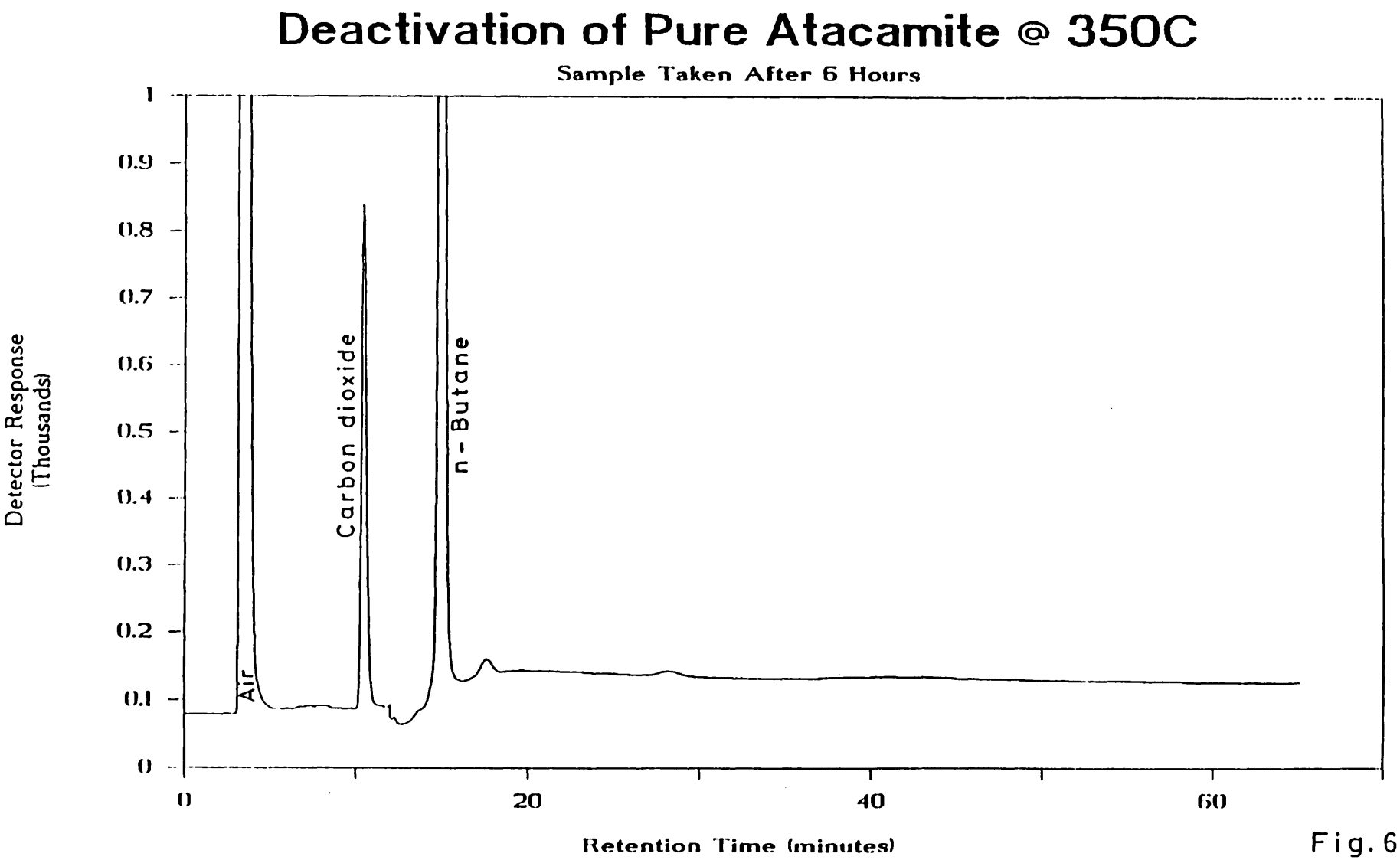

Deactivation of Pure Atacamite @ 350C
Sample Taken After 6 Hours
Detector Response (Thousands)
1
0.9
0.8
0.7
0.6
0.5
0.4
0.3
0.2
0.1
0
Air
Carbon dioxide
n-Butane
0
20
40
60
Retention Time (minutes)

Fig. 69.

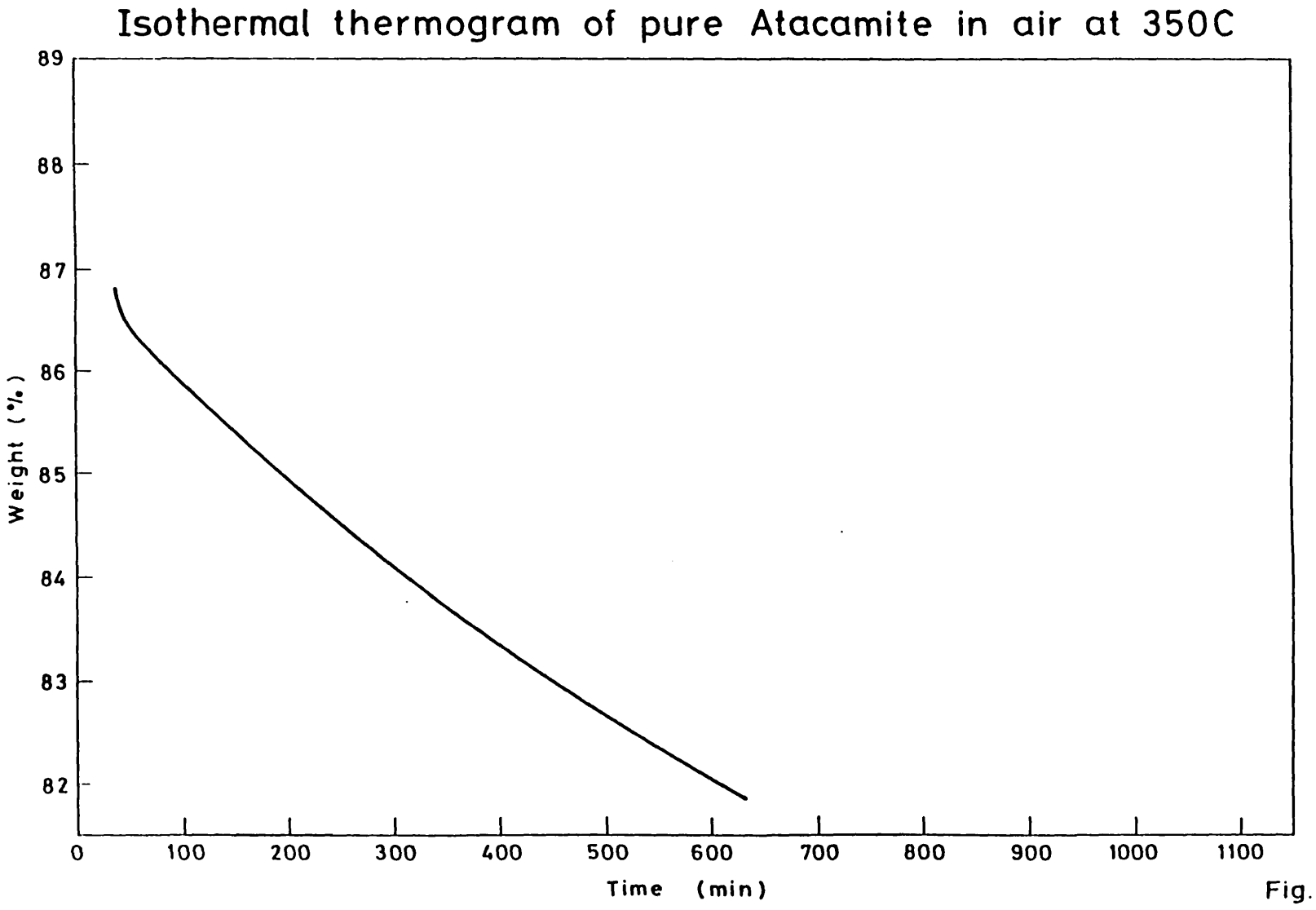

Isothermal thermogram of pure Atacamite in air at 350C
Weight (%)
89
88
87
86
85
84
83
82
0
100
200
300
400
500
600
700
800
900
1000
1100
Time (min)

Fig. 70

total of 5.9 wt.% was lost at a rate of 0.010 wt.%/min., this gave a reference corresponding to thermal decomposition and desorption of chlorine, probably molecular. Unlike the thermogram taken in an atmosphere of air adsorption of oxygen to form cupric oxide, as identified by post run X-ray diffraction analysis as described earlier, could not occur with an atmosphere of argon, it is more likely that formation of copper (I) oxide occurred, see Figure 71. However, using a purge gas of 1% n-butane in synthetic air, as used as the reactant gas in the reactor catalytic activity studies, the total weight loss over the isothermal period was recorded as 10.35% at a rate of 0.018 wt.%/min, see Figure 72, indicating that the n-butane was probably partaking in the chlorine stripping process either to produce chlorinated hydrocarbons, possibly the unidentified peaks in the chromatograms obtained from the reactor studies, or hydrogen chloride by the chlorine partaking in the activation of the paraffin and subsequent dehydrogenation.

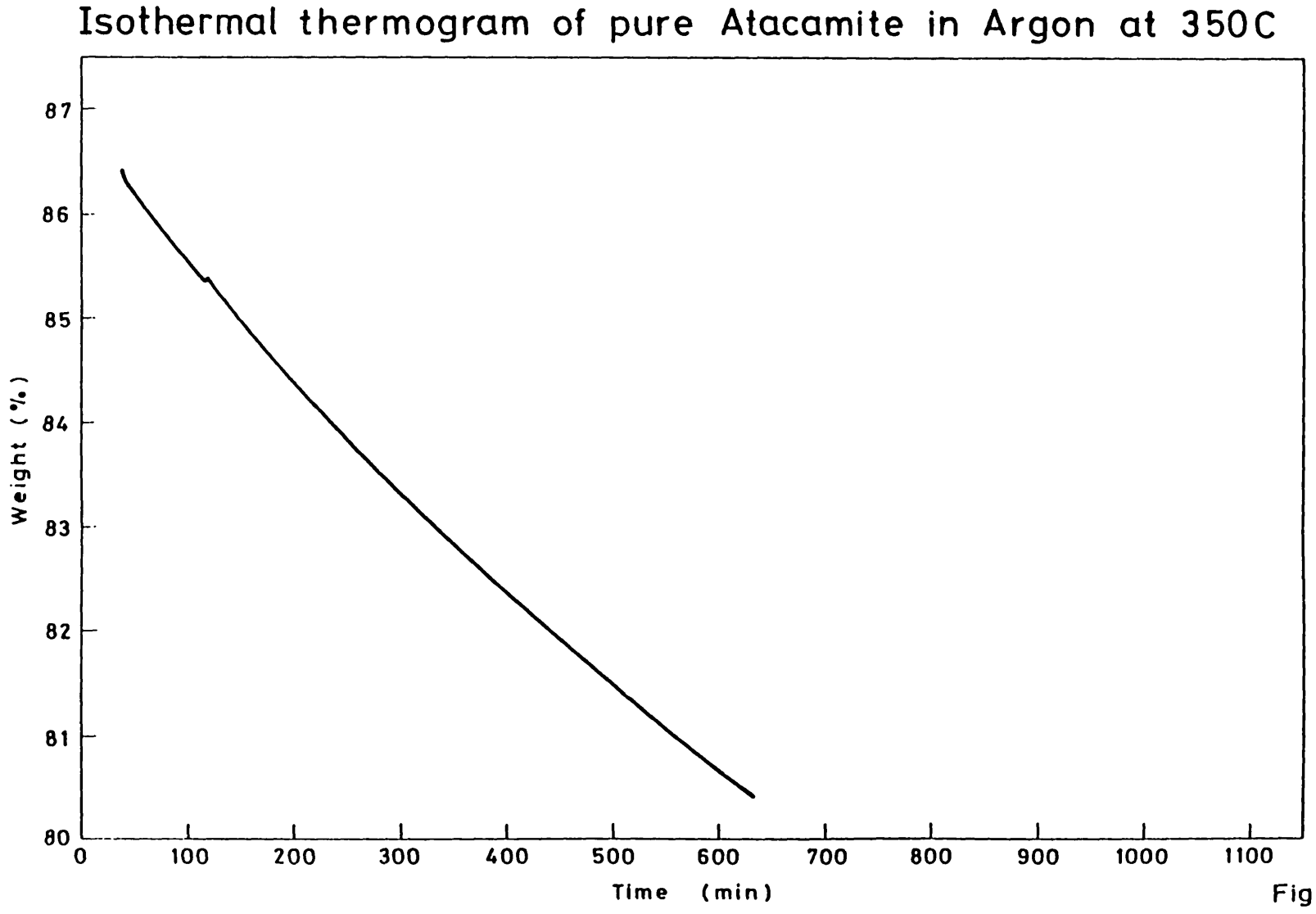

Isothermal thermogram of pure Atacamite in Argon at 350C
Weight (%)
87
86
85
84
83
82
81
80
0
100
200
300
400
500
600
700
800
900
1000
1100
Time (min)

Fig. 71

Isothermal thermogram of pure Atacamite in 1% n-Butane/air at 350C

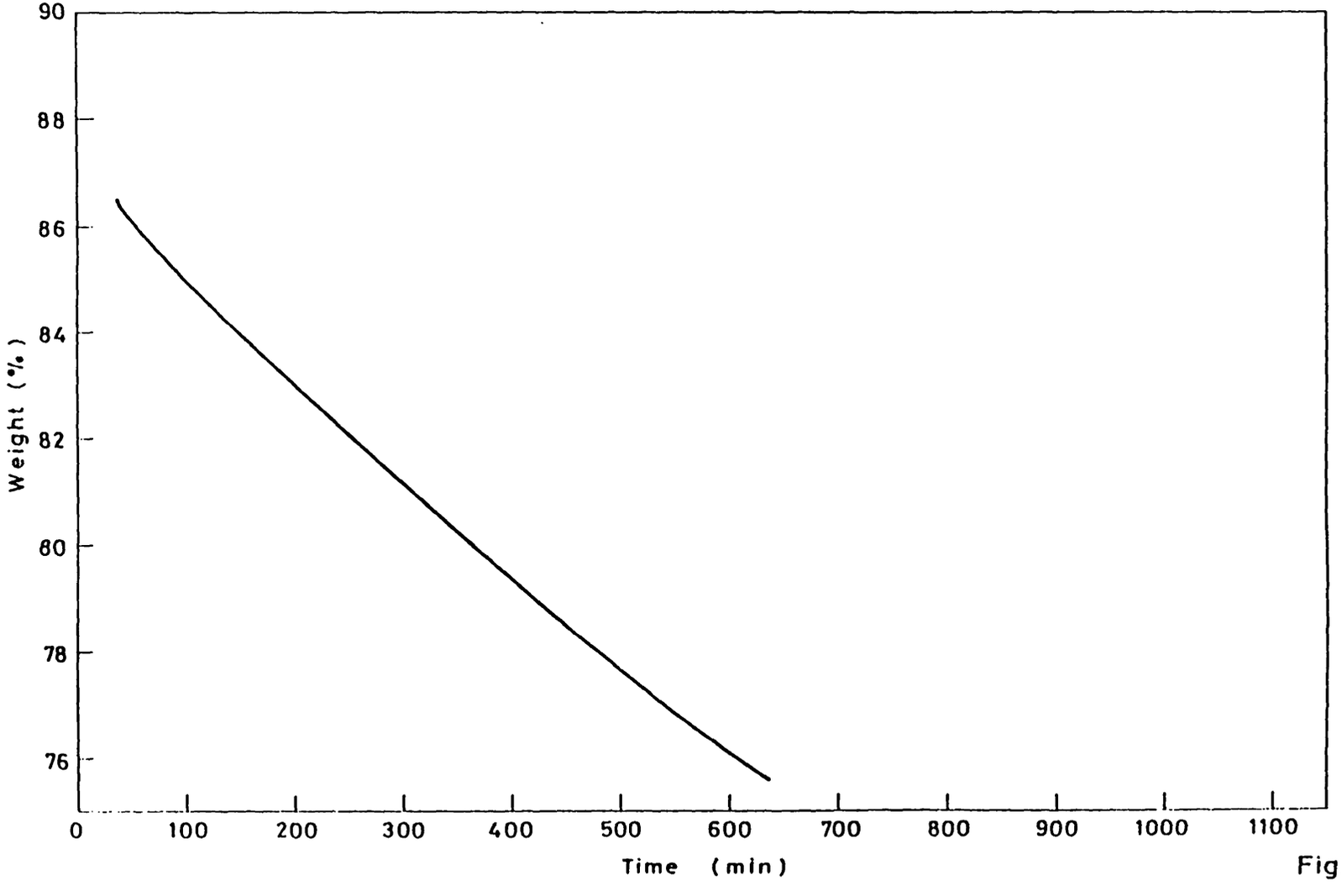


Fig. 72

CHAPTER 8.

MECHANISTIC INVESTIGATIONS

The results of the previous chapter have proved that the palladium species on the surface of the copper (II) lattice are not partaking in the catalysis of the n-butane to maleic anhydride conversion, and as shown previously the presence of elemental palladium or palladium oxide actually catalyses the combustion of n-butane to carbon dioxide and water. The presence of copper (II) oxide either alone or in combination with the identified active phase, melanothallite, also has been shown to totally oxidise the hydrocarbon feed to carbon dioxide and water. The active material, a copper (II) oxychloride, in the melanothallite phase was prepared by the chlorination of cupric oxide, by the action of dilute hydrochloric acid on cupric oxide, to produce the precursor, copper (II) trihydroxychloride, in the δ or atacamite phase. The precursor material decomposes at approximately 300 Celsius to yield the catalytically active melanothallite phase of copper (II) oxychloride (Cu_2OCl_2). This material, however, is thermally unstable and even at a catalyst temperature of 325 Celsius a deactivation is seen in a loss of yield and selectivity towards maleic anhydride. This was identified as thermal decomposition of the melanothallite and desorption of chlorine resulting in a reversion to cupric oxide. The presence of n-butane in the feedstream was found to increase the rate of chlorine stripping from the catalyst, presumably by the chlorine reacting with the hydrocarbon and producing chlorinated products. On studying the catalysts containing melanothallite in the microreactor, at temperatures where maleic anhydride is produced a number of other compounds were detected in the

product stream by gas chromatography. These unidentified products are probably reaction intermediates or byproducts and the identification of them would give an invaluable insight into the mechanistic pathway of the reaction. The only logical method of identifying them is using gas chromatography with detection, and therefore identification, of the separated products by mass spectroscopy.

8.1 Product Gas Analysis Using Gas Chromatography - Mass Spectroscopy.

In an attempt to identify the unknown peaks in the chromatogram, and from that possibly gain an insight into the reaction pathway, product gas analysis using Gas Chromatograph - Mass Spectroscopy was performed. Due to the configuration of the on-line gas chromatograph which uses packed columns and a lack of availability of a suitable mass spectrometer it was decided that a trap for the products would have to be used for the collection of a sample of the product gases followed by transfer to and injection onto a separate, dedicated G.C.-M.S. system. A two-way switchable valve was placed in the heated tubing carrying gases from the reactor, the exact positioning was between the valve oven used for injecting hot samples into the gas chromatograph and before the cold traps. The valve was used to divert the flow of gases from passing straight through the traps to flow through a short adsorbent column. The adsorbent column, 0.25 inches diameter and 3 inches long, contained a porous polymer adsorbent known as Tenax, which had been preconditioned and sealed. Both the two-way valve and the Tenax column were kept at room temperature, the valve for construction and operational reasons and the Tenax column for obvious adsorption reasons. Three Tenax columns were available to take samples over three different time periods and therefore loadings.

The catalyst reactor was loaded with 0.50 g of the cupric oxide / atacamite mixed material and purged with 1% n-butane in synthetic air. To confirm that the reactor had been thoroughly purged a sample was taken at room temperature and analysed by the gas chromatograph. Once the gas chromatograph had "come ready" again the reactor programme was started causing the reactor temperature to be ramped up to 350 Celsius and held at 350 Celsius for the duration of the experiment. After 10 minutes at 350 Celsius an injection was taken for analysis by the on-line gas chromatograph, after a further minute the two-way valve was switched to load the first Tenax column with a sample for a period of 10 minutes after this time the valve was reset and the Tenax column removed and very promptly sealed. The second Tenax column was then installed and the valve once again switched to load a product stream sample onto the Tenax column for a period of 1 hour, after which time the valve was reset and the column removed and sealed as before. Next a sample of the gas stream was injected into the on-line gas chromatograph to ensure a standard product stream was still being produced. One minute after this sample had been taken the third Tenax column was loaded with a sample for a period of 30 minutes. After this had been taken the reactor was allowed to cool to room temperature again. Analysis of the chromatograms obtained by the on-line gas chromatograph confirmed that throughout the experiment the expected range of products, maleic anhydride included, were being produced.

The samples held on the Tenax column were desorbed at 250 Celsius for 15 minutes with reverse gas flow into a liquid nitrogen trap. The trapped sample was then flash heated at 250 Celsius onto the front of a capillary column in a Perkin-Elmer Sigma 3 gas chromatograph. The column was held at 20 Celsius for 1 minute then ramped at 6°/min. to 300 Celsius. Species eluting from the column were fed into a Finnigan Mat 1020 mass spectrometer scanning for masses above 35

atomic mass units. Post run identification of the species was done by computer library matching.

The Tenax column that had been loaded for ten minutes, number one, was found to be slightly overloaded resulting in a little too much product being present for clean separation of the species using the gas chromatograph. The first peak to be eluted from the chromatogram contained a mixture of n-butane, hydrogen chloride, carbon dioxide and possibly butenes. The rest of the chromatogram contained mainly chlorinated organics including CH_2Cl_2, $CHCl_3$, CCl_4, C_2HCl_3 and C_2Cl_4 mainly, and also a range of C1, C2, C3, C4 and C6 chlorinated organics often unsaturated and a range of oxychlorinated organics. Maleic anhydride was not detected. However, maleic acid was detected as part of a peak eluting after 15.3 minutes and therefore was difficult to unequivocally identify. The hydrolysis of maleic anhydride readily occurring under conditions of moist air which was produced by the partial and total oxidation reactions. The small quantities of hydrocarbons and oxycompounds detected was probably due to a number of factors, one being the fact that the switching valve and Tenax column were at room temperature, therefore, condensation of many species would have occurred. Secondly the Tenax column was overloaded, so many species would have been swept through the column and the chlorinated organics which adsorb strongly to the Tenax would be preferentially retained. Thirdly, also due to the column overload, signal swamping was a problem for accurate analysis and identification of the species present. A list of identified species is contained in appendix B.

Confirmation of the production of maleic anhydride was not the purpose of this experiment as it had already been identified by pyroprobe injection of known maleic anhydride standards in the calibration of the flame ionisation detector of two gas chromatograph set-ups and by comparison with chromatograms obtained from

samples taken from product streams from vanadium phosphorus oxide catalysts. Identification of a number of unknown product species, possibly not all, had been achieved but relating these to individual peaks in the chromatogram from the on-line gas chromatograph was not possible. However, identification of the presence of hydrogen chloride, chlorinated and oxychlorinated organics in the product stream shows that the chlorine in the copper oxychloride lattice does partake in the reaction. Due to the presence of hydrogen chloride in the product gas stream abstraction of hydrogen atoms from the n-butane in the initial activation and/or dehydrogenation steps by surface chloride is highly probable. This formation of hydrogen chloride also backs up the findings of the thermogravimetic studies of the deactivation by loss of chlorine reported in the previous chapter, where the rate of weight loss of a sample of the catalyst doubled when 1% n-butane in air was used as the flowing atmosphere instead of just air or pure argon.

8.2 Catalytic Activity with n-Butene Feeds.

This set of experiments was designed to throw light on the reaction pathway from n-butane to maleic anhydride. The findings of research[10] into the reaction mechanisms on vanadium phosphorus oxide materials, see section 3.1.1, was found to be initial activation of the n-butane to either 1-butene or cis-2-butene, then further dehydrogenation to 1,3-butadiene before oxygen insertion to form furan and finally maleic anhydride. Therefore, four reactant gas mixtures were tested each containing 1% (by volume) of a hydrocarbon in synthetic air, the hydrocarbons being n-butane, 1-butene, cis-2-butene and 1,3-butadiene.

The atacamite / cupric oxide mixed material was used as the catalyst and as this had been shown previously to be deactivated with time on stream a slight

change was made to the reactor control programme to minimise this. Instead of waiting until 10 minutes before the end of the 2 hour isothermal temperature step before taking an injection for analysis on the gas chromatograph, the injection was taken just 10 minutes from the start of the temperature step. After loading the catalytic reactor with 0.50g of the catalyst the reactor system was purged with the desired hydrocarbon / air gas mixture. Thorough purging was ensured by taking a sample at room temperature and analysing it in the gas chromatograph.

The first observation made of the four experiments with different feed hydrocarbons was that, as expected, the olefins were converted at much lower temperatures than n-butane, see Figures 73, 74 and 75 for the hydrocarbon conversions versus temperature for 1-butene, cis-2-butene and 1,3-butadiene respectively and Figure 49 for the comparison to that obtained from a n-butane feed. The temperature for 50% conversion of the hydrocarbon was 400 Celsius and 275-300 Celsius respectively for the n-butane and olefin feeds, and no difference was observable between the olefins using the current reactor control programme with 25 Celsius steps. The greatest variation was noted in the temperature for approximately 100% hydrocarbon conversions, with temperatures for n-butane, 1-butene, cis-2-butene and 1,3-butadiene being 450, 375-400, 350-375 and 350 Celsius respectively. However these values could be just a function of mass transport, but as the catalyst is non-porous and identical volumetric flow rates and catalyst forms were used and diffusion rates for the four hydrocarbons would not be expected to be very different it is reasonable to expect the observed variation to be in the rates of catalytic combustion to form carbon dioxide.

The appearance of carbon dioxide in relation to maleic anhydride also showed an interesting trend which is that with all the hydrocarbon feeds, both saturated and unsaturated, carbon dioxide appears at approximately the same

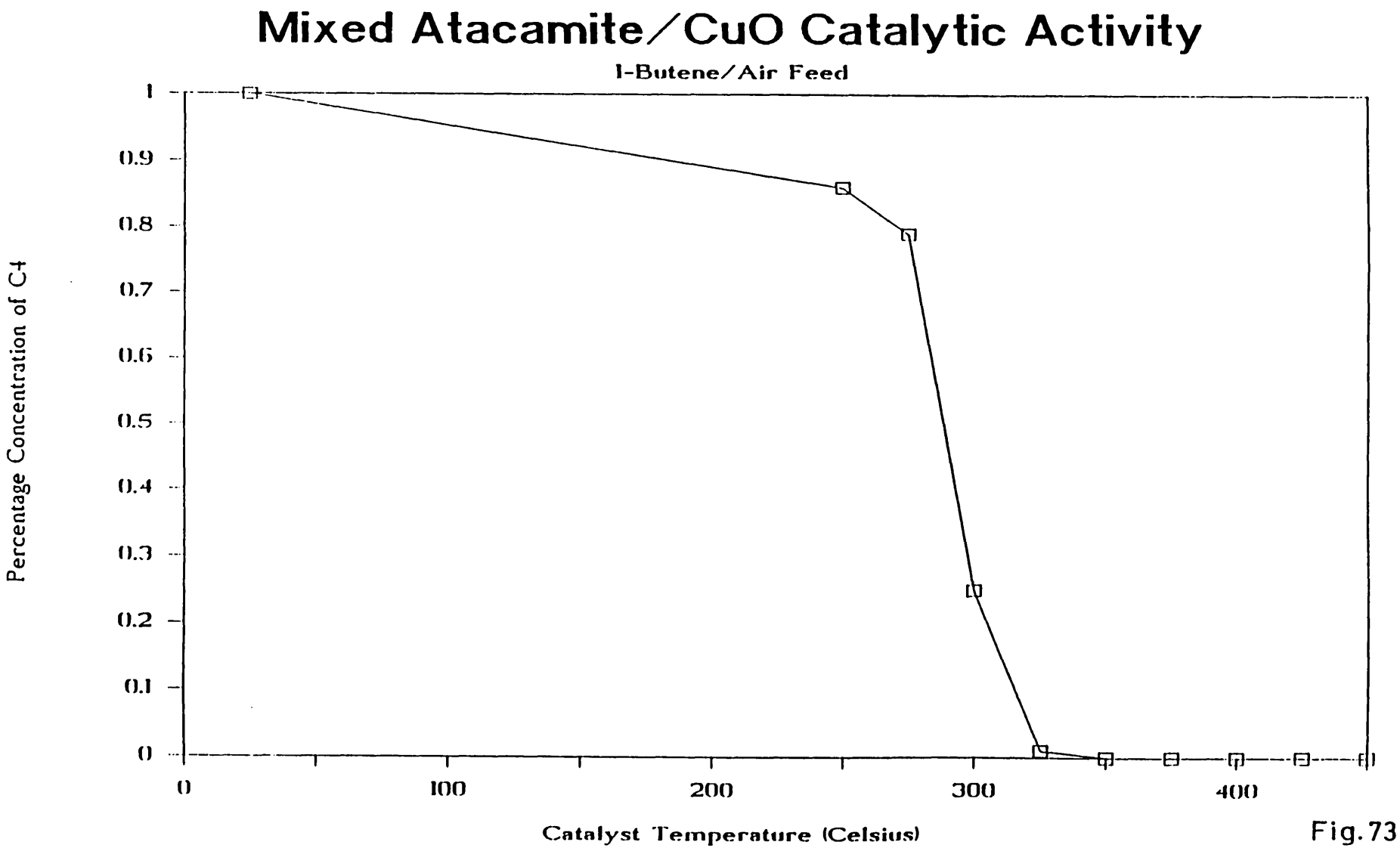

Mixed Atacamite/CuO Catalytic Activity
1-Butene/Air Feed
Percentage Concentration of C4
1
0.9
0.8
0.7
0.6
0.5
0.4
0.3
0.2
0.1
0
0
100
200
300
400
Catalyst Temperature (Celsius)

Fig.73.

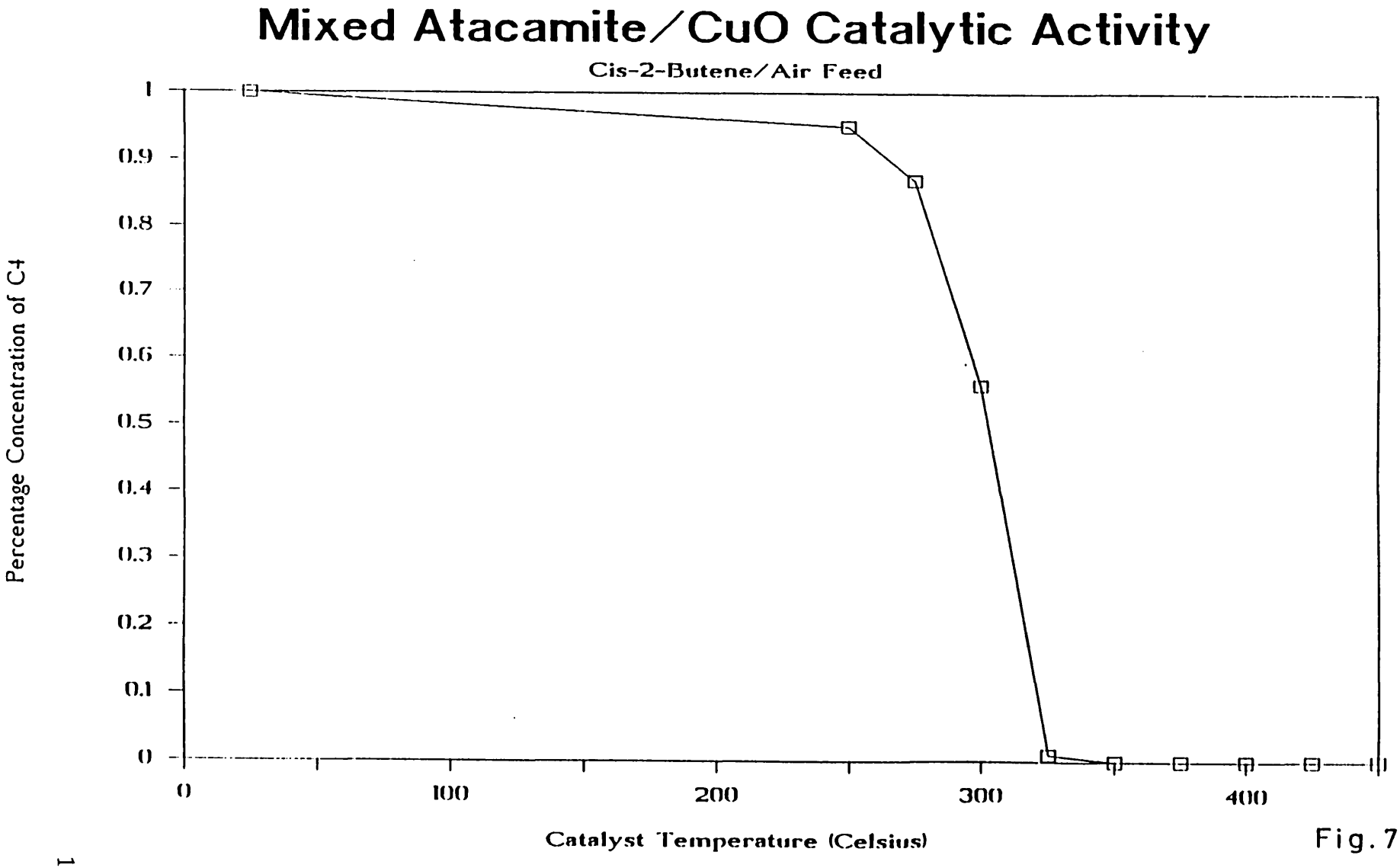

Mixed Atacamite/CuO Catalytic Activity
Cis-2-Butene/Air Feed
Percentage Concentration of C4
1
0.9
0.8
0.7
0.6
0.5
0.4
0.3
0.2
0.1
0
0
100
200
300
400
Catalyst Temperature (Celsius)

Fig. 74.

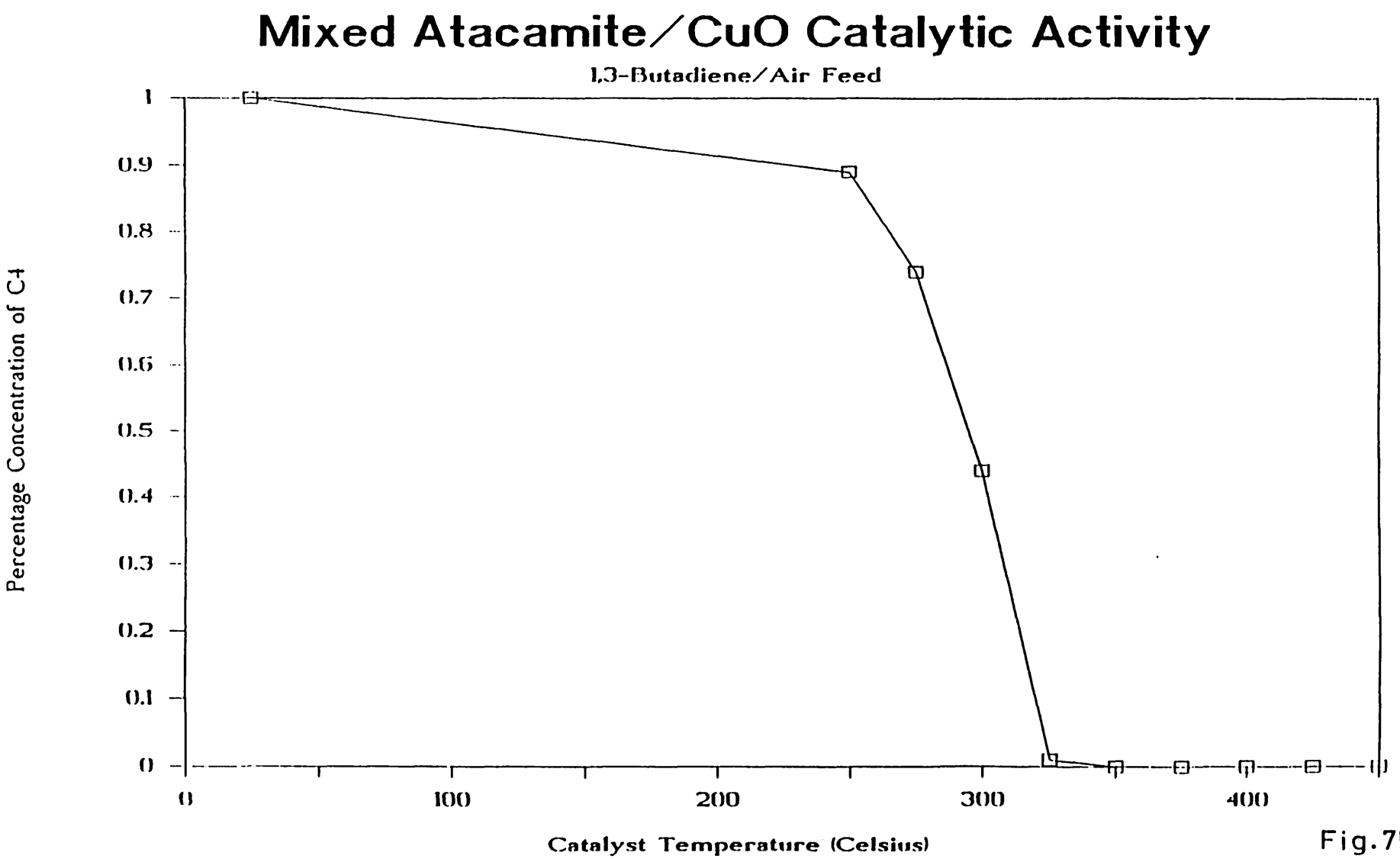

Mixed Atacamite/CuO Catalytic Activity
1,3-Butadiene/Air Feed
Percentage Concentration of C4
1
0.9
0.8
0.7
0.6
0.5
0.4
0.3
0.2
0.1
0
0
100
200
300
400
Catalyst Temperature (Celsius)

Fig.75.

temperature as maleic anhydride and the other reaction products. This result suggests that at low temperatures, parallel combustion of n-butane, and the other C4 hydrocarbons tested, is minimal and that the production of carbon dioxide is probably by sequential oxidation, i.e. further oxidation of maleic anhydride. This was also the finding of research into combustion processes occurring on vanadium phosphorus oxide catalysts[29]. Although maleic anhydride yields with olefin feeds, all maximising at about 10 nmol. in the sample taken, are comparable to that obtained with an n-butane feed, the concentration of the reaction intermediates and byproducts shown by the chromatogram is greatly enhanced when the unsaturated hydrocarbons were used suggesting a lower selectivity towards maleic anhydride, although this could not be accurately determined as an accurate calibration of the unidentified chlorocompounds response on the F.I.D. was not made.

On comparing the chromatograms obtained at each temperature step for each of the feed gases a definite trend was observable in the unidentified peaks of the chromatogram for the peaks between retention times of 19 and 35 minutes. The trend was only seen for olefin feeds, n-butane feeds gave a very reproducible chromatogram with only peak intensities varying. This trend is best seen in the chromatograms obtained at 250, 275 and 300 Celsius with cis-2-butene as the feed, see Figures 76, 77 and 78, where the peak at 22.7 minutes, peak a, decreases with increasing temperature whilst that at 25.0 minutes, peak b, increases, and this second peak matches the trend seen in maleic anhydride production. This trend is also seen for 1-butene and 1,3-butadiene feeds with the "cross-over", peaks a and b at approximately the same area, seen at 275 Celsius for cis-2-butene, 250 Celsius for 1-butene and 250 Celsius for 1,3-butadiene. The experiment using n-butane saw, as before, maleic anhydride appear at 300 Celsius and reach a maximum at 375 Celsius before declining to zero again by 425 Celsius along with all the unidentified

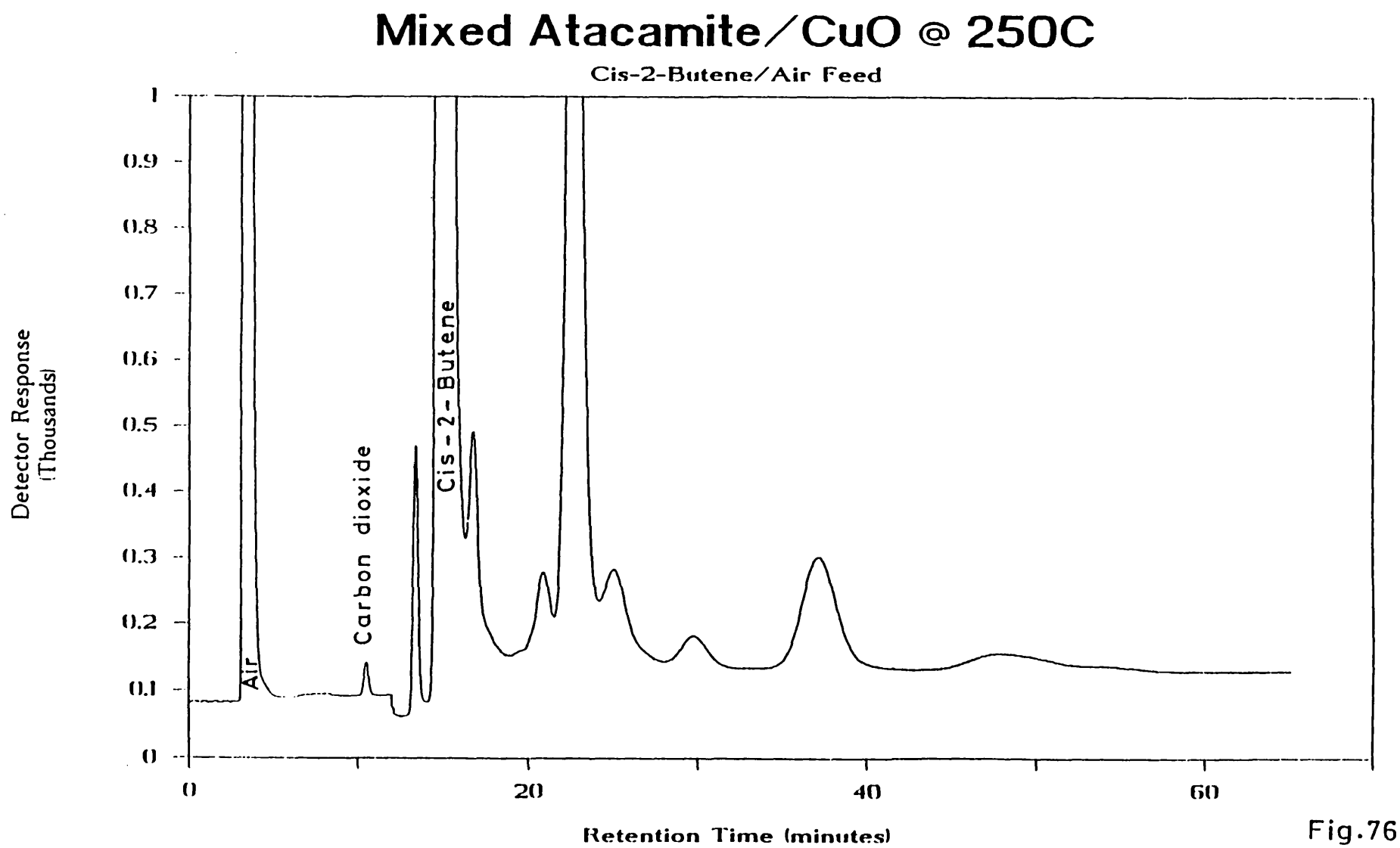

Mixed Atacamite/CuO @ 250C
Cis-2-Butene/Air Feed
Detector Response (Thousands)
1
0.9
0.8
0.7
0.6
0.5
0.4
0.3
0.2
0.1
0
Air
Carbon dioxide
Cis-2-Butene
0
20
40
60
Retention Time (minutes)

Fig.76.

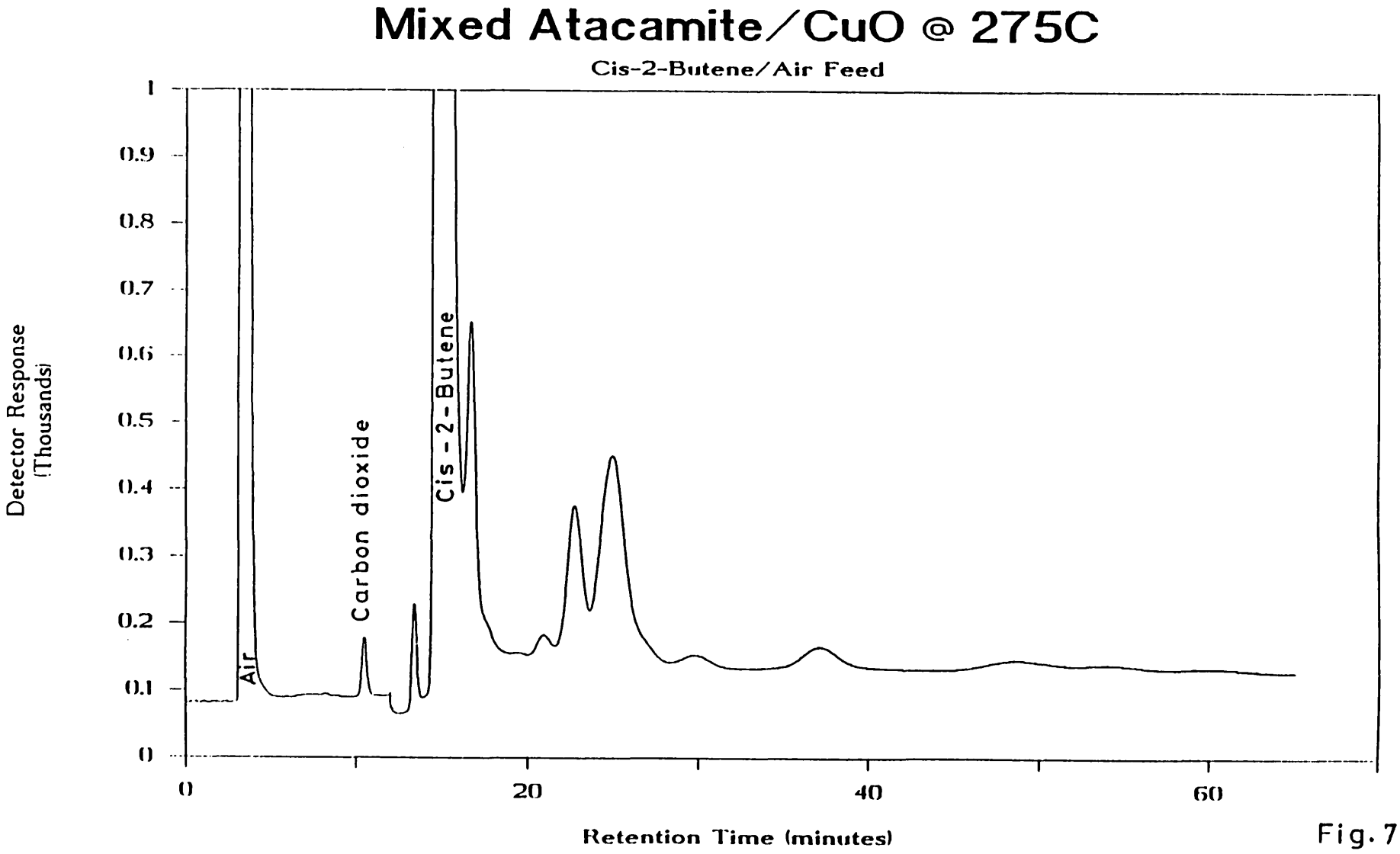

Mixed Atacamite/CuO @ 275C
Cis-2-Butene/Air Feed
Detector Response (Thousands)
1
0.9
0.8
0.7
0.6
0.5
0.4
0.3
0.2
0.1
0
Air
Carbon dioxide
Cis-2-Butene
0
20
40
60
Retention Time (minutes)

Fig. 77.

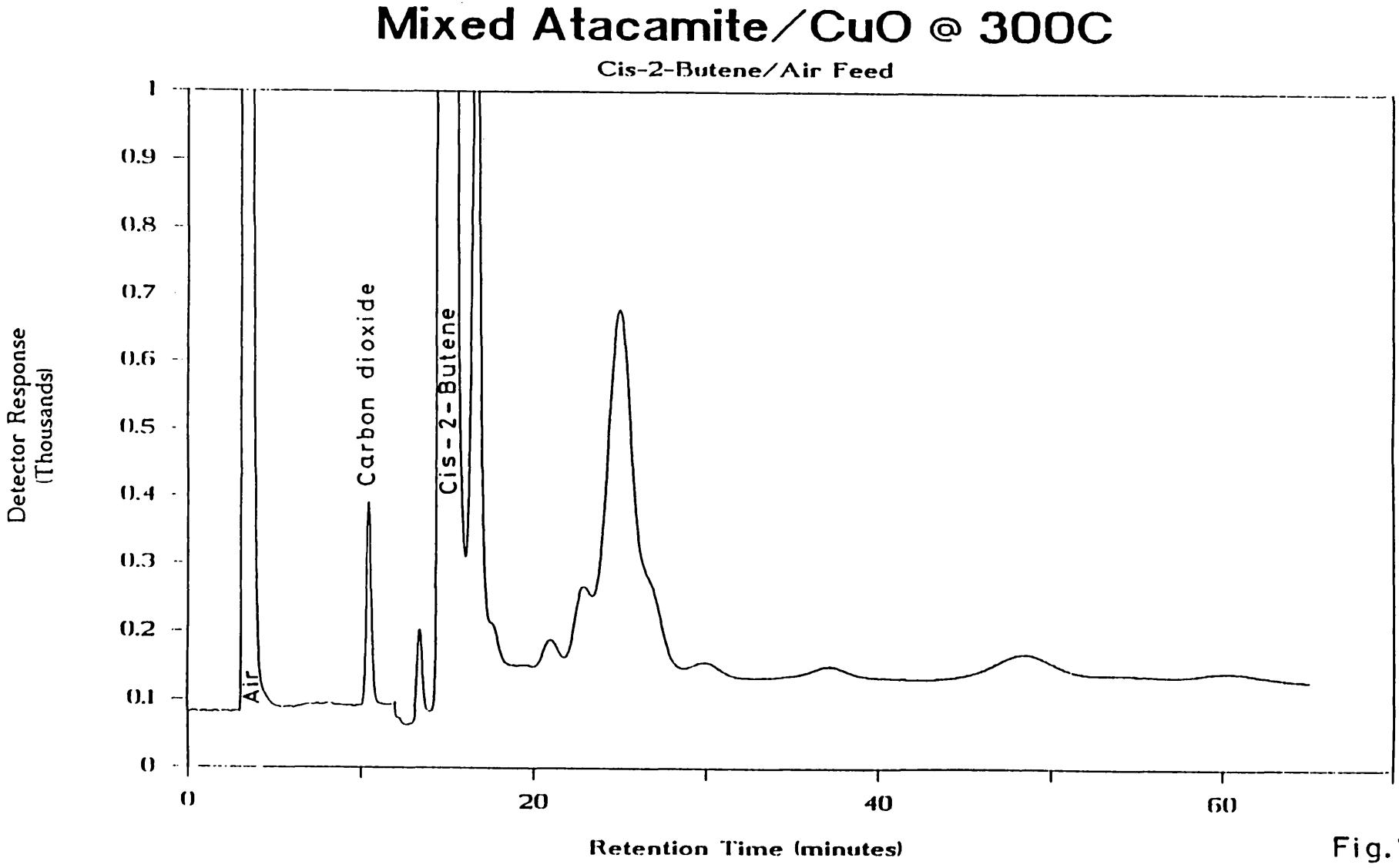

Mixed Atacamite/CuO @ 300C
Cis-2-Butene/Air Feed
Detector Response (Thousands)
1
0.9
0.8
0.7
0.6
0.5
0.4
0.3
0.2
0.1
0
Air
Carbon dioxide
Cis-2-Butene
0
20
40
60
Retention Time (minutes)

Fig.78.

chromatographic peaks. The retention times of all the peaks in the chromatogram were reproducible to less than 0.2 minutes, and an example chromatogram obtained with a n-butane feed is shown in Figure 79. Also from Figure 79, it can be seen that the peaks that vary for olefin feeds do not occur in the chromatograms obtained with n-butane feed, only the two peaks that occur immediately either side of the feed hydrocarbon peak are seen in the chromatograms from the four different gases. This difference in the chlorocompounds detected suggests a different reaction pathway exists for olefin feeds compared to the paraffin feed.

The difference in olefin feeds and paraffin feeds with respect to the greater yield of unidentified peaks in the chromatogram, which the earlier experiment using G.C. - M.S. indicates as probably chlorinated organics, indicates that removal of surface chlorine by formation of hydrogen chloride in the activation / dehydrogenation step results in less available surface chlorine for the formation of chlorocompounds. The much lower 50% conversion temperatures for the three olefin feeds with respect to the paraffin feed indicates a very much higher activation energy for n-butane oxidation, as expected since the rate limiting step in many, if not all, paraffin oxidations is the initial activation for chemisorption which for paraffins involves carbon-hydrogen bond fission. Olefins can be chemisorbed without any bond fission and therefore is a much lower energy barrier process. The difference in the chromatograms obtained for olefin and paraffin feeds, mainly between retention times 19 and 35 minutes, may indicate that a different mechanism is in operation to that observed on vanadium phosphorus oxide catalysts, however, this would require further investigation to fully determine this.

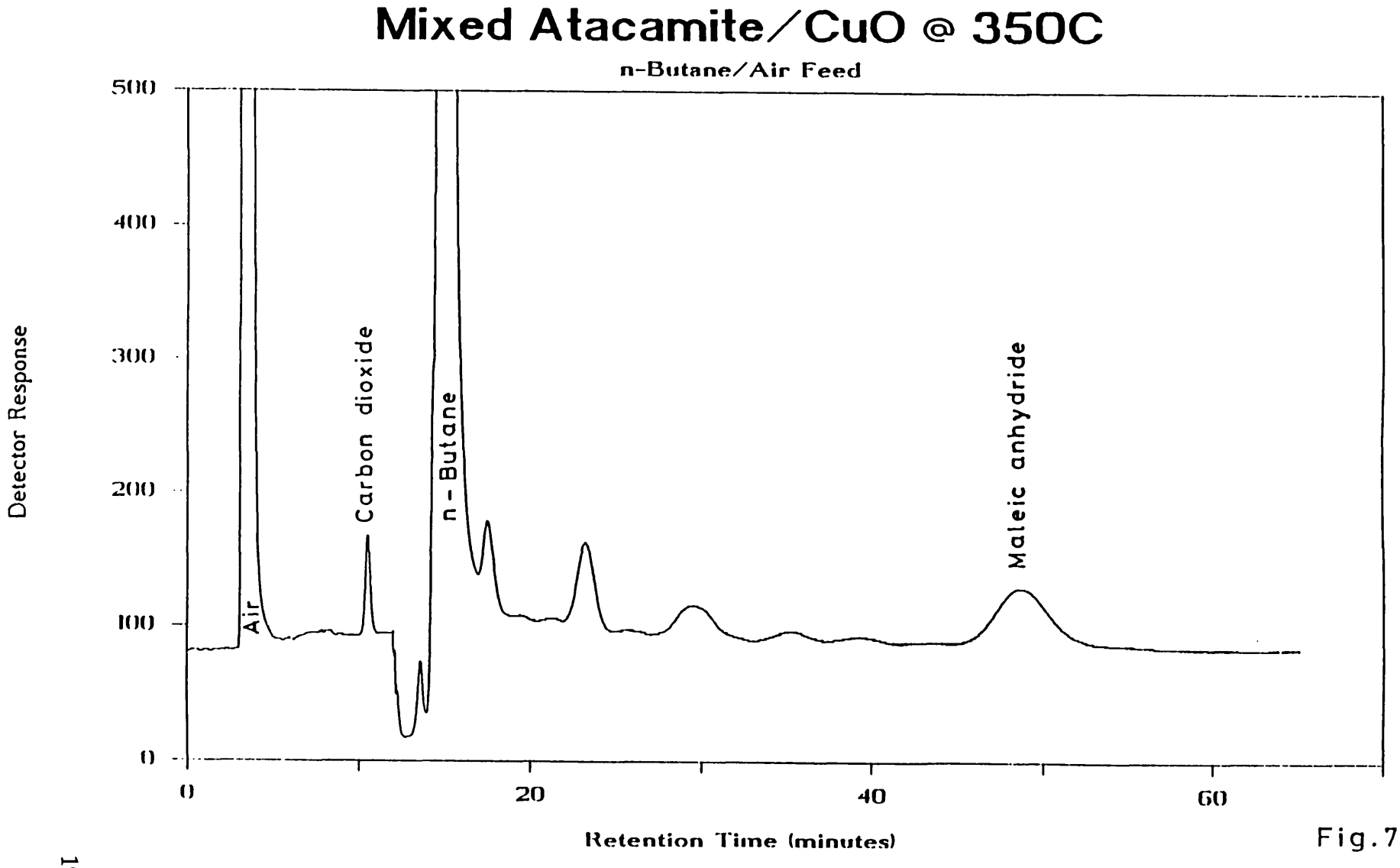

Mixed Atacamite/CuO @ 350C
n-Butane/Air Feed
Detector Response
500
400
300
200
100
0
Air
Carbon dioxide
n-Butane
Maleic anhydride
0
20
40
60
Retention Time (minutes)

Fig.79.

8.3 Catalytic Activity in the Absence of Oxygen in the Feed Gas.

In an attempt to elucidate whether the oxygen used for dehydrogenation and/or oxygen insertion was lattice oxygen or chemisorbed oxygen the following experiment was performed using a hydrocarbon feed at approximately the same partial pressure as used for the experiments using a n-butane in air feed. To this end, the hydrocarbon feed was diluted with an inert "carrier" gas. The hydrocarbon used was cis-2-butene as this molecule had shown good yields of maleic anhydride when used in synthetic air, see previous section. This gas was available in a helium carrier at 0.75% (by volume) from earlier tests on the gas chromatographic set-up experiments, section 4.2.3. Pure atacamite was used, 0.50g, and identical space velocities that had been previously used were reproduced, approximately 1300 hr^{-1}. Empirical calculations using stoichiometric ratio s showed that the lattice oxygen contained in the quantity of atacamite used would be exhausted in just over 25 minutes assuming 100% hydrocarbon conversion was achieved and that only carbon dioxide was produced. With this figure in mind, the reactor control programme was designed so that the reactor temperature was ramped quickly to 250 Celsius where it was held for the duration of the experiment and after 10 minutes at 250 Celsius, a time well short of the calculated lattice oxygen supply time, an injection was taken to be analysed by gas chromatography. A second injection was taken after 3 hours at 250 Celsius to get a product distribution after presumably all the available lattice oxygen and probably chlorine had been used up.

After loading the catalyst into the reactor thorough purging of the system was performed and checked by gas chromatographic analysis for nitrogen/oxygen from a sample taken at room temperature. When the gas chromatograph had reached the "ready" state again, the reactor control programme was started. The injection taken

after 10 minutes of the isothermal period showed that no maleic anhydride was being produced, see Figure 80 for the chromatogram obtained. However, on comparing the chromatogram obtained to that obtained for the cis-2-butene in air at the same temperature, Figure 76, very few of the peaks corresponded. Also in the absence of oxygen in the feedstock the conversion of cis-2-butene was much higher at the same reaction temperature for the sample taken 10 minutes into the isothermal period, 50% as opposed to 17%, this again could be a function of the different catalytic material being used, but such a dramatic change in this way would not have been expected as cupric oxide is a better combustion catalyst than atacamite, at least for n-butane. Pure atacamite giving a 43% conversion for n-butane in air feeds at 400 Celsius whereas the mixed material gave a 51% conversion under the same reaction conditions. Despite the difference in hydrocarbon conversion and the greater concentration of the unidentified species in the product stream, carbon dioxide was observable in the chromatogram at approximately the same concentration as observed when oxygen was present in the feedstream at the same catalyst temperature. The second injection, taken after a total time at 250 Celsius of 3 hours, showed a cis-2-butene conversion of only 2% and as can be seen from the chromatogram, Figure 81, all the unidentified intermediates / byproducts had very nearly disappeared. This shows that all the available lattice oxygen and chlorine had been removed by either thermal desorption or reactive abstraction by the hydrocarbon. The remaining material probably consisted of reduced copper oxides probably in the +1 oxidation state.

These results show that chemisorbed oxygen from the gas stream plays a critical role in the reaction and is probably responsible for the provision of oxygen atoms for insertion into the dehydrogenated C4 hydrocarbon to produce maleic anhydride. However, the presence, or absence, of gas phase molecular oxygen seems

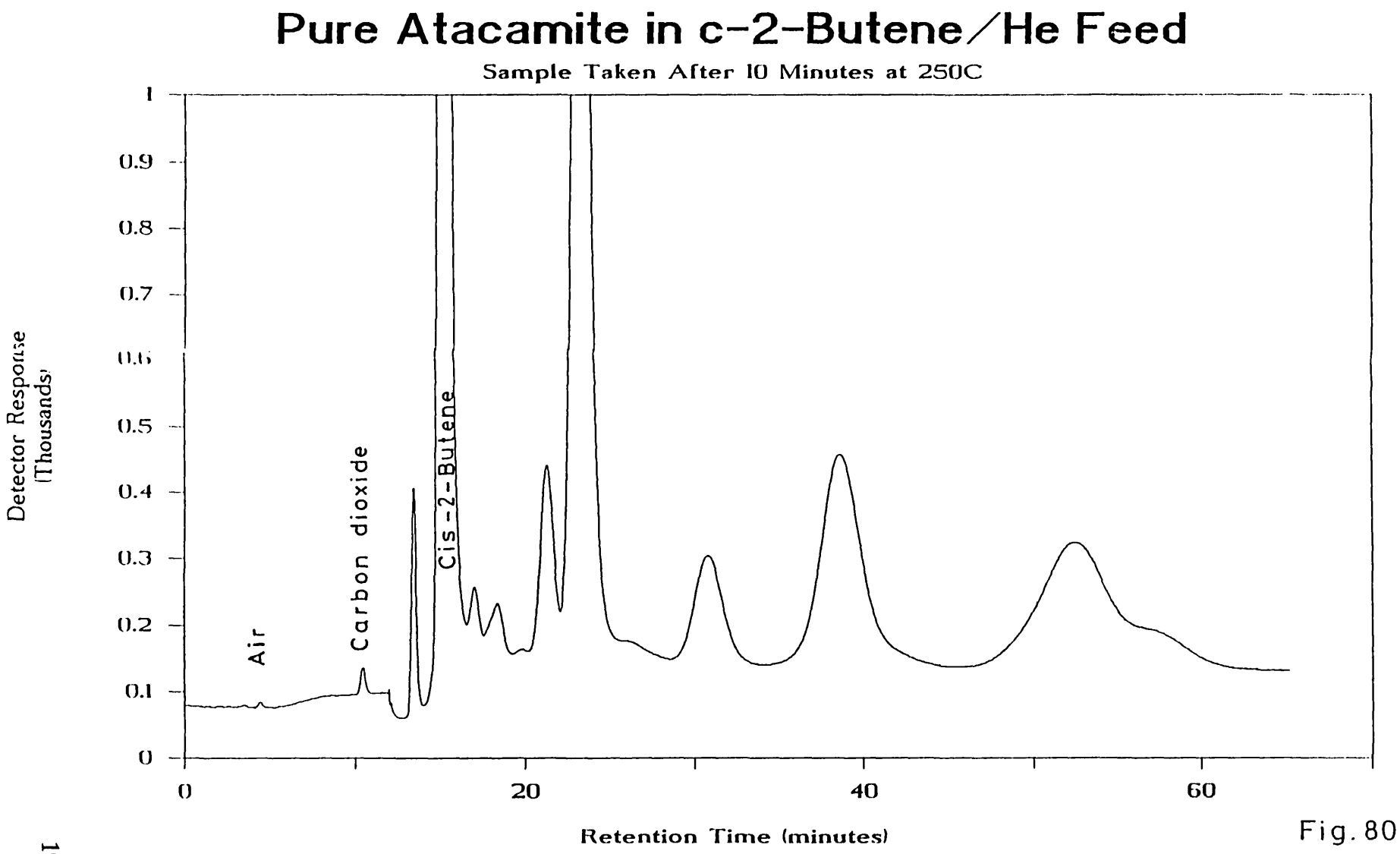

Pure Atacamite in c-2-Butene/He Feed
Sample Taken After 10 Minutes at 250C
Detector Response (Thousands)
1
0.9
0.8
0.7
0.6
0.5
0.4
0.3
0.2
0.1
0
Air
Carbon dioxide
Cis-2-Butene
0
20
40
60
Retention Time (minutes)

Fig. 80.

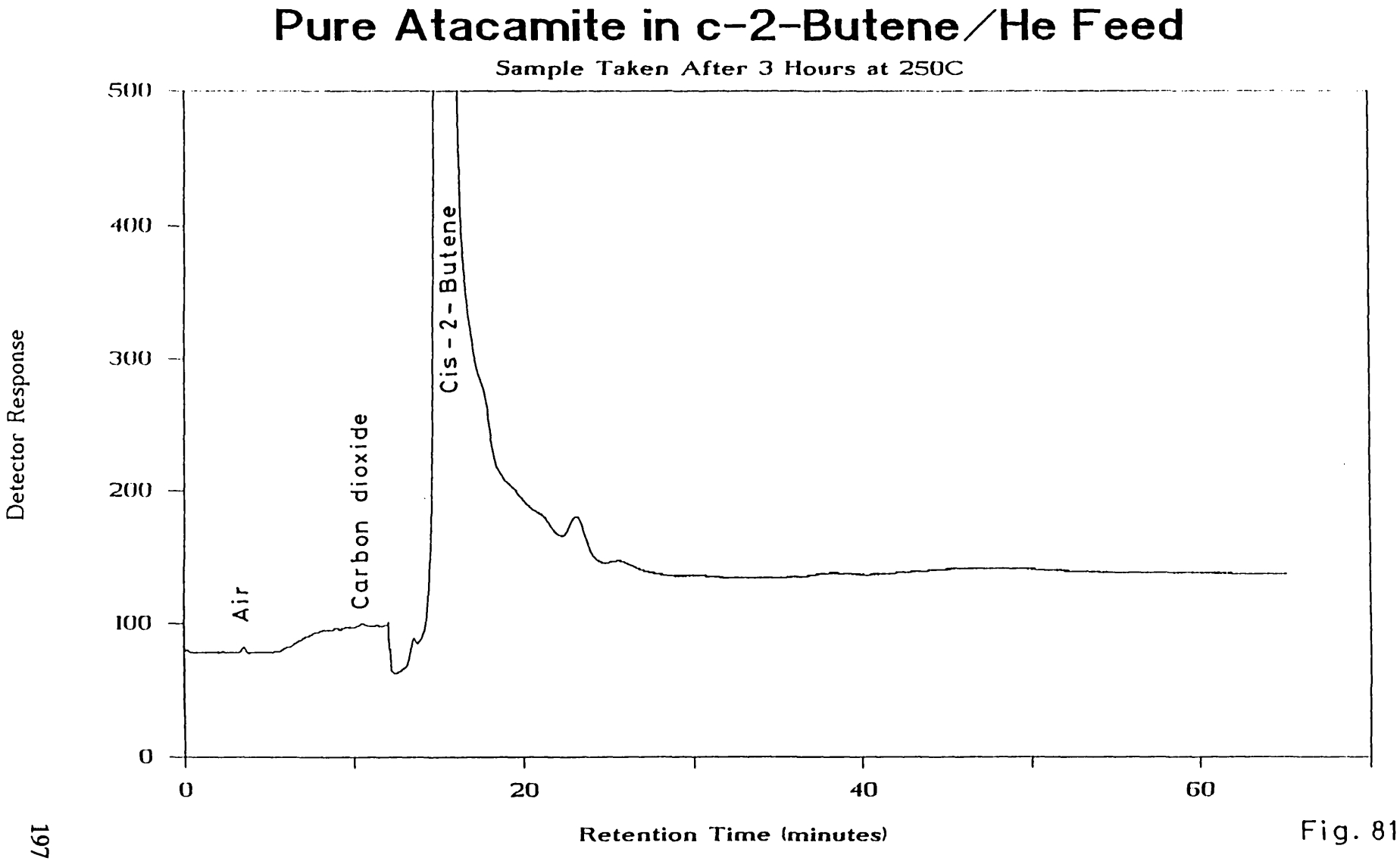

Pure Atacamite in c-2-Butene/He Feed
Sample Taken After 3 Hours at 250C
Detector Response
500
400
300
200
100
0
Air
Carbon dioxide
Cis - 2 - Butene
0
20
40
60
Retention Time (minutes)

Fig. 81.

to have very little effect upon the rate of production of carbon dioxide and therefore it seems reasonable to assume that carbon dioxide is formed from lattice oxygen (O^{2-}). However, in the long term absence of oxygen, as shown by the second injection taken at 250 Celsius, the lattice oxygen must be replaced by chemisorbed oxygen from the gas phase to maintain this reaction. To further substantiate these findings and further investigate the effect of oxygen would require a study using a range of oxygen partial pressures along with kinetic information for the production of various species and also the use of "labelled" oxygen for the lattice and/or the gas feed and possibly oxygen/hydrocarbon cycling to identify the oxygen species ($O_{(ads)}$, $O_{2\,(ads)}^{-}$ or $O_{2(ads)}$) responsible for the partial oxidation of the n-butane.

CHAPTER 9

CONCLUSIONS

The objectives of the research, described in this thesis, were to study the properties of a catalytic system based upon palladium and copper for the selective oxidation of n-butane, a readily available saturated hydrocarbon, to maleic anhydride, a commercially very important cyclic anhydride with many uses. The conversion being scientifically interesting as it includes paraffin activation, dehydrogenation, oxygen insertion to form functional groups and finally desorption of a partially oxidised product. Chapters 2 and 3 both indicated that palladium and copper might provide an interesting system for study as they are known to be catalytically active for a range of selective hydrocarbon oxidation reactions particularly the homogeneous catalytic conversion of ethylene to acetaldehyde which uses a palladium chloride/cupric chloride couple, and is known as the Wacker Process.

9.1 Investigations of the Palladium/Copper System.

Due to the close analogy between the system chosen for study and the Wacker catalyst the materials initially prepared were made by the impregnation of palladium chloride onto cupric oxide. This material was made with two different loadings of palladium, the first, 2.6% palladium, was chosen to give approximately a monolayer of elemental palladium over the cupric oxide support when reduced, and the second, 0.45% palladium, was chosen to give approximately a monolayer of square planar $PdCl_4^{2-}$ ions on the surface of the cupric oxide. On studying these

materials, in both the unreduced and reduced forms, for catalytic activity with a n-butane in air feed it was found, as shown in chapter 5, that prereducing the catalyst caused an increase in the yield and selectivity towards maleic anhydride. A higher yield and selectivity was also found for the higher palladium content catalyst. On characterising these materials it appeared that this increase in catalytic activity was associated with the presence of elemental palladium. It was also noted that the cupric oxide lattice had become chlorinated during the preparation and had formed a crystalline copper (II) trihydroxychloride known as atacamite. The prereduced 2.6% palladium chloride on cupric oxide catalyst, the one showing greatest activity, showed also that the prereduction had not completely reduced all of the palladium chloride, and that if the material was calcined at 550 Celsius the chlorinated copper lattice reverted to cupric oxide.

However, on studying a material made using palladium(II) nitrate / cupric oxide at 2.6% palladium loading, which was prereduced to give a cupric oxide supported elemental palladium, no partial oxidation catalytic activity was detected and carbon dioxide was the only reaction product. This material also gave a much higher n-butane conversion at each temperature step analysed than the chlorine containing materials. Characterisation of this material showed the presence of both elemental palladium and palladium oxide on the surface. Therefore, the presence of chlorine must be necessary to limit the oxidation process.

These findings do not correlate with the material being a heterogeneous analogue of the Wacker catalyst where the reaction rate expression has been found to be:[81]

$$r = \frac{k[Pd^{2+}][C_2H_4]}{[Cl^-][H^+]}$$

where the rate of reaction increases with Pd^{2+} concentration and decreases with Cl^- concentration. However, the prepared catalyst may have been expected to work as recent studies on a heterogeneous analogue to the Wacker catalyst[113] using a eutectic melt of cuprous chloride and potassium chloride with palladous chloride supported on silica to form the $PdCl_2/CuCl_2$ catalyst in a stable CuCl/KCl eutectic melt "solvent" has shown the same rate equation.

The identified presence of atacamite in the active chloride containing materials could, however, be envisaged as providing the active centres. The higher palladium content materials, and therefore higher chloride content, showed a greater bulk concentration of atacamite, and reduction of these materials which resulted in greater yields and selectivities towards maleic anhydride production could correspond to a retraction of the palladium species and a consequential exposure of more of the atacamite surface.

9.2 Investigations of Copper Hydroxychloride Materials.

The initial studies of the catalytic performance of the material prepared in the same way as the 2.6% $PdCl_2$ on CuO catalysts with the omission of the palladium salt, showed that indeed the presence of the palladium chloride species played no part in the selective oxidation process and by its presence lowered the maleic anhydride yield probably by blocking some of the otherwise available active copper sites. Close inspection of the chromatograms obtained from both the palladium containing and pure copper oxychloride catalysts showed the catalytic reaction on both materials to be the same.

Preparations, by an identical method using calculated ratios of cupric oxide and hydrochloric acid, of the pure atacamite materials, which was confirmed by

X-ray diffraction, X-ray photoelectron spectroscopy and thermal analysis, showed that the active material was a chlorinated copper oxide lattice. Thermogravimetric analysis and X-ray diffraction identified the active material as being copper (II) oxychloride (Cu_2OCl_2, known as melanothallite) which has a crystal structure very close to that of atacamite. Interconversion by loss and gain of water to form hydroxyl groups was found to readily occur.

Studies of the catalytic activity of the prepared pure atacamite, on comparison to the results obtained from the initial preparations, showed the effect of the presence of cupric oxide was to lower selectivities by increasing the combustion of n-butane to carbon dioxide. However, an oxide content in the lattice was shown to be necessary in forming the desired oxygenate, maleic anhydride, by studying cupric and cuprous chlorides for the n-butane conversion. Neither chloride produced any detectable quantities of maleic anhydride.

These catalytic materials were found to be active for a period of less than 6 hours, after which time the selectivity towards maleic anhydride had reached zero in favour of the combustion reaction. Analysis of this deactivation using thermogravimetry and X-ray diffraction showed it to be due to decomposition of the melanothallite, by loss of chlorine, to yield cupric oxide which had been identified earlier as a combustion catalyst only. The decomposition/deactivation process was shown to be due to thermal desorption of the chlorine but in the presence of n-butane the decomposition rate was increased probably by chlorine stripping and formation of chlorinated organics as reaction by-products and/or hydrogen chloride by the chlorine partaking in the paraffin activation and dehydrogenation steps.

9.3 Investigations of the Reaction Mechanism on Copper Oxychloride.

Having identified the material active for the partial oxidation of n-butane to maleic anhydride in this study, a number of experiments were conducted to investigate the reaction mechanism occurring. The chromatograms that were obtained from the active palladium containing catalysts and the melanothallite materials all showed a typical characteristic set of peaks of the reaction feed, air and n-butane, and at reaction temperatures around 350 Celsius products including carbon dioxide, maleic anhydride and a range of unidentified reaction intermediates or by-products. Identification of the other reaction products, but not actual relation to peaks seen from the on-line gas chromatograph, was performed by gas chromatography - mass spectroscopy of trapped samples. These products were identified as hydrogen chloride, butenes, chlorinated and oxychlorinated organics often unsaturated. The presence of hydrogen chloride indicates that surface chloride groups are probably responsible for initial hydrogen abstraction, and therefore paraffin activation for chemisorption, and/or subsequent oxidative dehydrogenation, chlorine being well known to facilitate hydrogen abstraction from hydrocarbons. The other products, a wide range of chlorinated and oxychlorinated organics are most probably by-products and along with the formation of hydrogen chloride are probably responsible for the observed enhanced deactivation of the catalyst by chlorine stripping.

The mechanistic pathway identified as occurring on the vanadium phosphorus oxide catalyst proceeds by initial n-butane activation by dehydrogenation yielding a butene (1-butene or cis-2-butene) chemisorbed onto the catalyst surface, and then further dehydrogenation to produce a surface 1,3-butadiene species before oxygen insertion. If such a pathway was occurring on

the surface of melanothallite using 1-butene, cis-2-butene or 1,3-butadiene feeds would produce maleic anhydride and probably a similar range of reaction by-products. On investigating hydrocarbon/air feeds of the the above olefins, maleic anhydride was detected in the product stream but at a much lower temperature than from n-butane feed. This was to be expected as overcoming the highly energetic process of paraffin activation for chemisorption is not necessary. However, the range of reaction by-products detected were significantly different, as described in section 8.2, with only a few chromatographic peaks being found at the same retention times. This throws doubt on the mechanistic pathway being the same for the two catalyst systems.

The final experiment performed was to investigate the effect of an absence of oxygen from the feed gas. Cis-2-butene in helium was used as the reactant gas and analysis of the chromatograms, one taken shortly after reaching a suitable reaction temperature and a second after a number of hours at temperature, showed that without gaseous oxygen present in the gas stream no maleic anhydride was formed. However, the first injection did show that carbon dioxide was being formed at similar levels to when gaseous oxygen is present also that very few of the by-products formed were the same and that in the absence of a molecular oxygen feed the butene conversion was higher. The second injection, taken after 3 hours at temperature, showed the butene to be practically unconverted, probably as the catalyst had been fully reduced to a lower oxidation state, and only very small amounts of by-products or carbon dioxide were being formed. These results show that (chemisorbed) oxygen plays a very critical role in producing oxygenated organics either in dehydrogenation or oxygen insertion steps. However, the experiments performed with cupric and cuprous oxides show that a certain concentration of lattice oxygen is necessary for activity. Chemisorbed oxygen also seems to suppress

hydrocarbon conversion rates, probably by occupying some of the active sites. However, carbon dioxide is still produced at similar rates in the presence or absence of gaseous oxygen which suggests that lattice oxygen is responsible for combustion, and this is undoubtedly by a parallel route to that produces the partially oxidised species.

Further study of this catalytically active material would, for the sake of experimental ease, require the problem of deactivation over such a short period of time to be overcome. This could probably be achieved by either the addition of a chlorine containing species to the feedstream or addition of a component to the catalyst, during preparation, to stabilise it. The former method being the most promising if the conclusions drawn earlier of the chlorine being necessary of initial paraffin activation by formation of hydrogen chloride is found by further work to be correct, however, stabilisation of the catalyst by lattice modifications would be preferable and would reveal whether chlorine has to be liberated from the solid catalyst in order for it to function effectively. Obviously for simplicity and catalyst longevity modification of the catalyst lattice to minimise loss of constitutional chlorine is desirable. However, if this stabilisation resulted in total deactivation of the catalyst because chlorine participation in for example hydrogen abstraction forming hydrogen chloride cannot take place, addition of a controlled amount of a chlorine containing species to the reactant feedstream may prove to be the more suitable alternative.

Studies on a bismuth oxychloride material for the partial oxidation of methane have revealed the usefulness of oxychlorides for the partial oxidation of hydrocarbons with the chlorine helping in the catalytic reaction by initial hydrogen abstraction, in this system stabilisation of the catalyst was achieved by lattice modifications[114]. A major help to studying this catalyst system would also be to use

an on-line gas chromatograph with mass spectroscopic detection and identification of the products.

In summary, the research described in this thesis has identified a new material that is active for the partial oxidation of n-butane to maleic anhydride, that is copper (II) oxychloride known as melanothallite. The identification of this material further reveals the usefulness of oxychlorides for the partial oxidation of hydrocarbons. Studies of this material have provided a good insight into the chemistry of the catalyst and the reaction mechanism occurring.

REFERENCES.

1. D.B. Dadyburjor, S.S. Jewur and E. Ruckenstein, Catal. Rev. -Sci. Eng., 19(2)293 (1979).
2. W.R. Patterson, Catalysis and Chemical Processes, 251 (1981).
3. T.P. Moser, PhD Thesis, "Model Vanadium-Phosphorus-Oxygen Catalysts for the Selective Oxidation of C_4 Hydrocarbons to Maleic Anhydride", Ames Laboratory, Iowa State University, (1987).
4. Yu. Kruchinin, Yu. Mishchenko, P. Nechiporuk and A. Gel'bshtein, Kinet. Katal. (english translation), 25(2), 328 (1984).
5. D.J. Hucknall, Selective Oxidation of Hydrocarbons, Academic Press, (1974).
6. L.Y. Margolis, Adv. Catalysis, 14, 429 (1963).
7. H.H. Kung, Ind. Eng. Chem. Prod. Res. Dev., 25, 171 (1986).
8. R. Higgins and P. Hayden, Catalysis, 1, 168 (1977).
9. R.L. Varma and D.N. Saraf, Ind. Eng. Chem. Prod. Res. Dev., 18(1), 7 (1979).
10. B.K. Hodnett, Catal. Rev. -Sci. Eng., 27(3), 373 (1985).
11. K. Wohlfahrt and G. Emig, Hydrocarbon Processing, 83 (1980).
12. A.A. Balandin, Adv. Catal., 19, 1 (1969).
13. Th. Wolkenstein, Adv. Catal., 12, 189 (1960).
14. D.A. Dowden and D. Wells, Actes du 2^e Congres International de Catalse, Paris, 2, 1489 (1960); Pub. Editions Technip (1961).
15. D.A. Dowden, Proc. 4th Internat. Congr. Catal., Moscow, 163 (1968); Akad. Kiado., Budapest (1971).
16. P. Mars and D.W. Van Krevelen, Chem. Eng. Sci. Suppl., 3, 41 (1954).
17. G.A. Somorjai, Adv. Catal., 26, 1 (1977)

18. D.L. Trimm, Design of Industrial Catalysts, Elsevier, 1980.

19. G. Busca, F. Cavani, G. Centi and F. Trifiro, J. Catal., 99, 400 (1986).

20. G. Bergeret, J.P. Broyer, M. David, P. Gallezot, J.C. Volta and G. Hecquet, J. Chem. Soc. Chem. Commun., 825 (1986).

21. M. Ai, J. Catal., 100, 336 (1986).

22. G. Busca, G. Centi and F. Trifiro, J. Am. Chem. Soc., 107, 7757 (1985).

23. G. Busca, G. Centi, F. Trifiro and V. Lorenzelli, J. Phys. Chem., 90, 1337 (1986).

24. A. Escardino, C. Sola and F. Ruiz, An. Quim, 69(3), 385 (1973).

25. A. Escardino, C. Sola and F. Ruiz, An. Quim, 69(11), 1157 (1973).

26. F. Cavani, G. Centi and F. Trifiro, Applied Catalysis, 9, 191 (1984).

27. F. Garbassi, J.C.J. Bart, F. Mantino and G. Petrini, Applied Catalysis, 16, 271 (1985).

28. R.W. Wenig, PhD Thesis, "Vanadium-Phosphorus-Oxygen Industrial Catalysts for C_4 Hydrocarbon Selective Oxidation to Maleic Anhydride", Ames Laboratory, Iowa State University, (1987).

29. T.P. Moser, R.W. Wenig and G.L. Schrader, Applied Catalysis, 34, 39 (1987).

30. G. Centi, F. Trifiro, G. Busca, J.R. Ebner and J.T. Gleaves, Proceedings of the Ninth International Congress on Catalysis, Calgary, V4, 1538 (1988).

31. G.L. Schrader, T.P. Moser and M.E. Lashier, Proceedings of the Ninth International Congress on Catalysis, Calgary, V4, 1624 (1988).

32. M. Blanchard and J.C. Delgrange, C. r. hebd. Seanc. Acad. Sci., Paris, C262, 1231 (1966).

33. M. Blanchard, G. Longuet, G.K. Boreskov, V.S. Muzykantov and G.I. Panov, Bull. Soc. Chim. Fr., 814 (1971).

34. J.C. Delgrange and M. Blanchard, Bull. Soc. Chim. Fr., 1093 (1971).

35. M. Blanchard, H. Delplace and J.C. Delgrange, C. r. hebd. Seanc. Acad. Sci., Paris, C269, 1016 (1969).

36. M. Ai and S. Suzuki, Bull. Chem. Soc. Jpn., 44, 3081 (1971).

37. M. Ai and S. Suzuki, Bull. Chem. Soc. Jpn., 46, 1208 (1973).

38. I. Pasquon, F. Trifiro and G. Caputo, La Chemica E L'Industria, 55(2), 168 (1973).

39. J. Haber, J. Less-Common Metals, 36, 277 (1974).

40. F. Trifiro, G. Caputo and P.L. Villa, Journal of the Less-Common Metals, 36, 305 (1974).

41. J.S. Jung, E. Bordes and P. Cortine, Adsorption and Catalysis on Oxide Surfaces, Elsevier Science Publishers, Amsterdam, (1985).

42. U. Ozkan and G.L. Schrader, J. Catal., 95, 120 (1985), Parts I, II and III.

43. H.B. Charman, R.M. Dell and S.S. Teale, Trans. Faraday Soc., 59, 453 (1963).

44. R.B. Grant, C.A.J. Harbach, R.M. Lambert and S.A. Tan, Faraday Symp. Chem. Soc., 21, paper 8 (1986).

45. G.R. Schultze and H. Tiele, Erdoel Khole, 5, 552 (1952).

46. W. Herzog, Ber. Bunsenges. Phys. Chem., 74, 216 (1970).

47. R.A. van Santen, J. Moolhuysen and W.M. Sachlter, J. Catal., 65, 478 (1980).

48. H.R. Gerberich, N.W. Cant and W.K. Hall, J. Catal., 16, 204 (1970).

49. C. Kemball and W.R. Patterson, Proc. R. Soc., A270, 219 (1962).

50. N.W. Cant and W.K. Hall, J. Catal., 16, 204 (1970).

51. A. Mitsutani, K. Tanaka and M. Yano, Kogyo Kagaku Zasshi, 68, 1219 (1965); Chem Abstr., 65, 3732e.

52. Y. Ishii and I. Matsuura, Technol. Rep. Kansai Univ. N°. 10, 47 (1969).

53. R.J. Sampson and D. Shooter, Oxid Combust Rev., 1, 225 (1965).

54. H.H. Voge and C.R. Adams, Adv. Catalysis, 17, 151 (1967).

55. C.R. Adams, Chemy. Ind., 52, 1644 (1970).

56. K.P. Zhdanova, A.A. Filippova and N.I. Popova, Propl. Kinet. Katal., 12, 211 (1968).

57. L.L. Holbrook and H. Wise, J. Catal., 20, 367 (1971).

58. J.L. Callahan, R.K. Grasselli, E.C. Millberger and H.A. Strecker, Ind. Eng. Chem. Prod. Res. Dev., 9, 134 (1970).

59. C.C. McCain, G. Gough and G.W. Godin, Nature, 198, 989 (1963).

60. C.R. Adams and T.J. Jennings, J. Catal., 3, 549 (1964).

61. G.W. Godin and C.C. McCain, Proc. Int. Symp. on Catalytic Oxidation, Imperial College, London, July 1970, The Chemical Society, London, (1970).

62. C.C. McCain and G.W. Godin, Nature, 202, 692 (1964).

63. L. Ya Margolis, J. Catal., 21, 93 (1971).

64. W.R. Grace and Co., Br. Pat. 1 112 638, (1968).

65. R. Krabetz, C.H. Willersinn, H. Engelbach, H. Wistuba, U. Herbert and W. Frey, Ger. Offen. 2 056 614, (1972).

66. J. Buiten, J. Catal., 10, 188 (1968).

67. Y. Moro-oka, S. Tan and A. Ozaki, J. Catal., 12, 291 (1968).

68. H.H. Voge and C.Z. Morgan, Ind. Eng. Chem. Prod. Res. Dev., 11, 454 (1972).

69. V.K. Skarchenko, N.S. Kruglikova, S.P. Kuz'yenenko, I. Ya Tyuryaev and E.E. Golubova, Neft. Gazov. Prom., 5, 46 (1966); Chem. Abstr., 64, 4922e.

70. Ph.A. Batist, B.C. Lippens and G.C.A. Schuit, J. Catal., 5, 55 (1966).

71. Ph.A. Batist, C.J. Kapeijns, B.C. Lippens and G.C.A. Schuit, 7, 33 (1967).

72. I. Matsuura and G.C.A. Schuit, J. Catal., 20, 19 (1971).

73. V.P. Shchukin, S.A. Ven'yaminov and G.K. Boreskov, Kinet. Katal., 11, 1236 (1970) - English Translation.

74. V.P. Shchukin, S.A. Ven'yaminov and G.K. Boreskov, Kinet. Katal., 12, 547 (1971) - English Translation.

75. M.M. Aleiva, K.V. Adzhamov, G.M. Shikhalizade and A.A. Vartimov, Uch. Zap. Azerb. Inst. Nefti. Khim., 9, 79 (1971); Chem. Abstr., 77, 156825y.

76. R.S. Cichowski, U.S. Pat. 3 660 514 (1972); J.W. Davidson, U.S. Pat. 3 660 513 (1972).

77. Ya.B. Gorokhovatskii, A.I. Pyatnitskaya, A.N. Korol', E.N. Popova and E.V. Rozhkova, Kinet. Katal., 9, 81 (1968).

78. C.R. Adams, Proc. 3rd Int. Congr. on Catalysis, I, 240, Amsterdam (1964); Pub. North-Holland Pub. Co. (1965).

79. N.S. Butt and A. Fish, J. Catal., 5, 494 (1966).

80. C.R. Adams, Ind. Engng. Chem., 61, 30 (1969).

81. B.C. Gates, J.R. Katzer and G.C.A. Schuit, Chemistry of Catalytic Processes, McGraw-Hill, New York, 1979.

82. J. Schmit et al, Angew Chem., 71, 176 (1959).

83. J. Schmit, Chemistry and Industry, 52 (1962).

84. W.R. Patterson, Catalysis and Chemical Processes, 265 (1981).

85. M. Kolb, E. Bratz and K. Dailer, Journal of Molecular Catalysis, 2, 399 (1977).

86. S. Brunauer, P.H. Emmett and E. Teller, J. Am. Chem. Soc., 60, 309 (1938).

87. G.S. Faass, Masters Thesis, Georgia Institute of Technology, Atlanta, GA. (1981).

88. E.P. Barrett, L.G. Joyner and P.P Halenda, J. Am. Chem. Soc., 73, 373 (1951).

89. J.B. Tobin et al, Applications of Surface Science, 16, 441 (1983).

90. Wagner, Riggs, Davis, Molder and Moulenburg (eds.), Handbook of X-ray Photoelectron Spectroscopy, Perkin-Elmer Corp., 1979.

91. W.E. Moddeman, W.C. Bowling, D.C. Carter and D.R. Grove, Surface and Interfacial Analysis, II, 317 (1988).

92. G.I. Straguzzi, K.B. Bischoff, T.A. Kock and G.C.A. Schuit, J. Catal., 104, 47 (1987).

93. G. Centi, G. Fornasari and F. Trifiro, Ind. Eng. Chem. Prod. Res. Dev., 24, 32 (1985).

94. T.P. Moser and G.L. Schrader, J. Catal., 92, 216 (1985).

95. P.S. Drew and M.J. Haynes, A.E.R.E. Report M3187, (1981).

96. E. van der Heide, M. de Wind, A.W. Gerritsen and J.J.F. Scholten, Proc. 9th Int. Congr. Catal. Calgary, **4**, 1648 (1988).

97. Vandenberg et al (eds.), An Infrared Spectroscopy Atlas for the Coatings Industry, Fed. of Soc. for Coatings Tech., (1980).

98. J.M. Thomas and W.J. Thomas, Introduction to the Principles of Heterogeneous Catalysis, Academic Press, (1967).

99. C.A. Udovich and R.C. Edwards, U.S. Pat. 4 510 259, (1983).

100. J.D. Burrington and R.K. Grasselli, J. Catal., 59, 79 (1979).

101. R. Vetrivel, K.V. Rao, K. Seshan, K.R. Krishmurthy and T.S.R. Prasada Rao, Proc. 9th Int. Congr. Catal., Calgary, 4, 1766 (1988).

102. A.M. Potapov, Neftekhimiya, 26(2), 235 (1986); Chem. Abs. 105-23767.

103. I.G. Solomonik et al, Izu. Acad. Nauk SSSR, Ser. Khim., 11, 243 (1984); Chem. Abs. 102-33283.

104. J.A. Daniels, Euro. Pat. 182 648, ICI (1986).

105. H. Brasser and J. Toussaint, Bull. Soc. Roy. Sci. Liege, 11, 55 (1942).

106. A.F. Wells, Acta Cryst., 2, 175 (1949).

107. Y. Itaka, S. Locchi and H.R. Oswald, Helvetica Chimica Acta, 44, 2095 (1961).

108. H.R. Oswald, Y. Itaka, S. Locchi and A. Ludi, Helvetica Chimica Acta, 44, 2103 (1961).

109. H.R. Oswald and W. Feitknecht, Helvetica Chimica Acta, 47, 272 (1964).

110. L.W Levy, A.M. Goreaud and M. Goreaud, Bull. Soc. Chim. Fr., 8-9, 2789 (1970).

111. J.B. Parise and B.G. Hyde, Acta Cryst., C42, 1277 (1986).

112. Handbook of Chemistry and Physics, Chemical Rubber Company Press, 63rd Ed., B98 (1982-83).

113. V. Rao and R. Datta, J. Catal., 114, 337 (1988).

114. J.M. Thomas, W. Ueda, J. Williams and K.D.M. Harris, Faraday Discussion Meeting, Liverpool, (1989).

Appendix A.

Gas Chromatograph Control Method

Injector temperature	100 C.
Zone temperatures	220 C.
Auxillary temperature	220 C.
Carrier flows	60 mL/min.
Initial oven temperture	70 C.

Run time 0 mins. hot wire detector on.

Isothermal time	5 mins.
Oven ramp rate	30 C/min.
Oven temperature	160 C.
Isothermal time	4 mins.

Run time 12 mins. column valve switch.

Run time 12.14 mins. hot wire detector off.

Run time 12.15 mins. flame ionisation detector on.

Oven ramp rate	40 C/min.
Oven temperature	200 C.
Isothermal time	55 mins.

End run, valve reset, flame ionisation detector off.

CLAS Data Collection and Processing Method

Data end collection time 65 mins.

Data collection rate 0.320 seconds per data point (code 6).

Baseline sensitivity code 25

Area sensitivity code 150

Calibration using peak areas.

Timed Events:

00.00 Skim algorithm on to skim CO peak off air peak.

11.70 Force base point after CO_2 peak.

11.75 Peak detector off for valve switch and detector switch.

12.70 Peak detector on.

12.75 Bunch data factor 2 for n-butane peak.

26.00 Bunch data factor 8 for maleic anhydride peak.

Peak Calibrations:

Air	03.18 min	
CO	04.46 min	1.4324E-02 nmol/area unit.
CO_2	10.60 min	6.9706E-03 nmol/area unit.
C_4H_{10}	14.93 min	1.5938E-05 nmol/area unit.
M.A.	50.49 min	5.8270E-05 nmol/area unit.

Appendix B

List of species detected by G.C.-M.S.

CO_2

C_4H_{10}

C_4H_8

HCl

HOOCCHCHCOOH

$CHCl_3$, CCL_4.

C_2H_3Cl, $C_2H_2Cl_2$, C_2HCl_3, C_2Cl_4, $C_2H_4Cl_2$, $C_2H_3Cl_3$, $C_2H_2Cl_4$, C_2HCl_5, C_2Cl_6.

$C_3H_4Cl_2$.

$C_4H_5Cl_3$.

C_6H_5Cl, $C_6H_4Cl_2$, C_6Cl_6.

CCl_3CHO, CCl_3OH.

Some of these species may be fragmentation species formed in the mass spectrometer.

Infrared Spectrum of White Solid from VPO Catalyst - Section 6.2.1

